



Rheological behaviour of Bambara groundnut starch-soluble dietary fibre nanocomposite for delivering active compounds in food systems

Yvonne Maphosa

Thesis submitted in fulfilment of the requirements for the degree

Doctor of Food Science and Technology

in the Faculty of Applied Sciences

at the Cape Peninsula University of Technology

Supervisor: Professor V.A Jideani

Co-supervisor: Professor D. Ikhu-Omoregbe

Bellville Campus

DECLARATION

I, **Yvonne Maphosa**, declare that the contents of this dissertation/thesis represent my own unaided work, and that the dissertation/thesis has not previously been submitted for academic examination towards any qualification. Furthermore, it represents my own opinions and not necessarily those of the Cape Peninsula University of Technology.

Signed

Date

ABSTRACT

This aim of this study was to assess the effect of Bambara groundnut (BGN) (*Vigna subterranea* (L.) Verdc) starch-soluble dietary fibre nanocomposite (STASOL) on the functional, physicochemical and rheological properties of orange oil beverage emulsions. STASOL was composed of 11.5% Bambara groundnut starch (BGNS) and 88.5% Bambara groundnut soluble dietary fibre (BGN-SDF). STASOL had a mean particle size of 74.01 nm and conductivity of -57.3 mV which qualified it as a nanocomposite and a very stable compound, respectively. STASOL and BGN-SDF were amorphous in nature while BGNS was crystalline, showing strong peaks at 15, 17 and 23° (2 θ), thus classifying it as type C starch. STASOL, BGN-SDF and BGNS had functional groups in the regions 3600-2900, 1641.71, 1200-900, 1300-800 cm⁻¹ which were attributed to the vibrations of C-H and OH, C=O and OH, C-C and C-H-O as well as C-O and C-C bonds, respectively. BGNS had smooth, oval structures while BGN-SDF and STASOL exhibited irregular, polygonal morphologies. STASOL was the most thermally stable biopolymer suggesting its suitability for high-temperature food applications. STASOL was high in carbohydrates (78.69%) and proteins (6.96%), low in fat (0.84) and had a considerable amount of ash (4.88%). BGNS, BGN-SDF and STASOL showed significant ($p = 0.00$) differences in solubility with BGNS being insoluble in water. The emulsion activity index (EAI) and emulsion stability index (ESI) of BGNS, BGN-SDF and STASOL were 23.25 and 23.33%, 85.71 and 87.13%, 90.65 and 87.49%, respectively. The significantly ($p = 0.000$) higher EAI and ESI of STASOL suggested its suitability as a stabiliser in emulsions. The oil binding capacities of BGNS, BGN-SDF and STASOL differed significantly ($p = 0.000$) and were 1.13, 3.78 and 1.61 g/g, respectively. STASOL had a substantial amount of antioxidant compounds with 1.45 μ mol AAE/g ferric reducing antioxidant power and 0.46 mg GAE/g. Colour characteristics described all studied biopolymers as light (L*), reddish (+a*) and yellowish (+b*). The mean initial backscattering (BS_{AVO}) of STASOL stabilised emulsions was in the range 50.73-70.47% for emulsions composed of 14:30:56 and 20:30:50 (STASOL:oil:water), respectively. The turbiscan stability index (TSI) of the emulsions ranged from 0.0005 to 0.1000 for formulation 11 (20:30:50 STASOL:oil:water) and formulation 5 (8:42:50 STASOL:oil:water), respectively. Low TSI values indicate a low probability of phase separation. The hysteresis loop area (HLA) of emulsions ranged from 2.04 Pas⁻¹ [Formulation 10 (12:34:54 STASOL:oil:water)] to 43.09 Pas⁻¹ [Formulation 2 (20:30:50 STASOL:oil:water)]. The first-order stress decay with a zero equilibrium stress value and Herschel-Bulkley models were the best predictors of time-dependent and time-independent rheological flow behaviour, respectively. The most stable emulsion system was characterised by the highest STASOL (20%), lowest orange oil (30%) and lowest water (50%) concentrations and had the highest BS_{AVO}, lowest TSI and highest HLA. All emulsions were non-Newtonian, time-dependent,

thixotropic, shear-thinning and possessed yield stress. Both temperature and time largely affected the extent of destabilisation, with emulsions stored at 5 and 45°C showing the least and most destabilisation over time, respectively. The viscosity of emulsions stored at 5°C started significantly ($p = 0.000$) decreasing after the 9th day while that of emulsions stored at 20 and 45°C significantly ($p = 0.000$) decreased after the 3rd day. Emulsions stored at 5 and 45°C for 20 days were the most and least stable, respectively. STASOL stabilised emulsions should be refrigerated to prolong their shelf life.

CONTENTS

Chapter	Page
Declaration	ii
Abstract	iii
Contents	v
Acknowledgements	xvi
Dedication	xviii
Glossary	xix

CHAPTER ONE: MOTIVATION AND DESIGN OF THE STUDY

1.1	Introduction	1
1.2	Statement of the Research Problem	2
1.3	Objectives of the Research	3
1.3.1	Broad objective	3
1.3.2	Specific objectives	3
1.4	Hypotheses	4
1.5	Delineation of the Research	4
1.6	Significance of the Research	4
1.7	Expected Outcomes, Results and Contributions of the Research	5
1.8	Thesis Overview	6
	References	9

CHAPTER TWO: LITERATURE REVIEW

2.1	Bambara groundnut dietary fibres	12
2.1.1	Active compounds in soluble dietary fibres	14
2.2	Starch	14
2.3	Composites	16
2.3.1	Synthesis of composites	17
1.	Free radical grafting	17
2.	Acid hydrolysis	18
3.	Self-assembly	18
4.	Crosslinking	18
5.	Complex coacervation	19
6.	Mechanical treatments	19
7.	Thermal treatments	19
2.3.2	Analytical techniques used to characterise and verify composites	19
1.	Fourier transform infrared spectroscopy	19

2.	Thermal characterisation techniques	20
3.	Powder X-ray diffraction	21
4.	Scanning electron microscopy	21
5.	Fluorescence spectroscopy	22
2.4	Emulsions	22
2.4.1	Beverage emulsions	23
2.4.2	Emulsion stability	23
2.4.3	Emulsion stabilisers	26
2.5	Biopolymers in food systems	26
2.5.1	Polysaccharide conjugates in emulsions	28
2.6	Biopolymer complexation and phase behaviour	30
2.7	Phase separation mechanisms	30
2.7.1	Associative phase separation	31
2.7.2	Segregative phase separation	32
2.8	Rheology	33
2.8.1	Rheological models	35
1.	Power law model	35
2.	Herschel-Bulkley model	36
3.	Bingham plastic model	36
4.	Casson model	36
5.	Ellis fluid model	37
6.	Weltman model	37
7.	First-order stress decay with a zero equilibrium stress value model	37
8.	Hysteresis loop area	38
2.9	Conclusions	38
	References	38

CHAPTER THREE: PHASE BEHAVIOUR OF BAMBARA GROUNDNUT (VIGNA SUBTERRANEA [L.] VERDC) STARCH-SOLUBLE DIETARY FIBRE NANOCOMPOSITE

	Abstract	51
3.1	Introduction	52
3.2	Materials and Methods	53
3.2.1	Source of materials and equipment	53
3.2.2	Extraction of Bambara groundnut soluble dietary fibre and starch	53
3.2.3	Phase behaviour study of Bambara groundnut starch and Bambara groundnut soluble dietary fibre	56
3.2.4	Production of starch-soluble dietary fibre nanocomposite	56

3.2.5	Verification of starch-soluble dietary fibre nanocomposite	57
1.	Conductivity and particle size determination of Bambara groundnut starch, soluble dietary fibre and starch-soluble dietary fibre nanocomposite	57
2.	Functional groups of Bambara groundnut starch, soluble dietary fibre and starch-soluble dietary fibre nanocomposite	58
3.	Crystallinity of Bambara groundnut starch, soluble dietary fibre and starch-soluble dietary fibre nanocomposite	58
4.	Morphology and microstructure of Bambara groundnut starch, soluble dietary fibre and starch-soluble dietary fibre nanocomposite	58
5.	Fluorescence analysis of Bambara groundnut starch, soluble dietary fibre and starch-soluble dietary fibre nanocomposite	58
3.2.6	Thermal analysis of Bambara groundnut starch, soluble dietary fibre and starch-soluble dietary fibre nanocomposite	59
1.	Differential scanning calorimetry	59
2.	Thermogravimetric analysis	59
3.2.7	Data analysis	59
3.3	Results and Discussion	60
3.3.1	Yield of Bambara groundnut starch, soluble dietary fibre and starch-soluble dietary fibre nanocomposite	60
1.	Yield of Bambara groundnut starch	60
2.	Yield of Bambara groundnut soluble dietary fibre and Bambara groundnut starch-fibre nanocomposite	61
3.3.2	Predicted formation mechanism for starch-soluble dietary fibre nanocomposite	62
3.3.3	Phase behaviour of various Bambara groundnut starch and Bambara groundnut soluble dietary fibre concentrations in solution	63
3.3.4	Particle size and conductivity of Bambara groundnut starch, soluble dietary fibre and starch-soluble dietary fibre nanocomposite	68
1.	Particle sizes of Bambara groundnut starch, soluble dietary fibre and starch-soluble dietary fibre nanocomposite	68
2.	Conductivity of Bambara groundnut starch, soluble dietary fibre and starch-soluble dietary fibre nanocomposite	69
3.3.5	Functional groups of Bambara groundnut starch, soluble dietary fibre and starch-soluble dietary fibre nanocomposite	70

	1. Native Bambara groundnut starch	71
	2. Bambara groundnut soluble dietary fibre	71
	3. Bambara groundnut starch-soluble dietary fibre nanocomposite	75
3.3.6	Crystallinity of Bambara groundnut starch, soluble dietary fibre and starch-soluble dietary fibre nanocomposite	78
	1. X-ray diffraction patterns of Bambara groundnut starch	79
	2. X-ray diffraction patterns of Bambara groundnut soluble dietary fibre and starch-soluble dietary fibre nanocomposite	79
3.3.7	Microstructure and morphology of Bambara groundnut starch, soluble dietary fibre and starch-soluble dietary fibre nanocomposite	80
3.3.8	Fluorescence spectra of Bambara groundnut starch, soluble dietary fibre and starch-soluble dietary fibre nanocomposite	82
3.3.9	Thermal properties of Bambara groundnut starch, soluble dietary fibre and starch-soluble dietary fibre nanocomposite	83
	1. Thermal properties of Bambara groundnut starch, soluble dietary fibre and starch-soluble dietary fibre nanocomposite using differential scanning calorimetry	83
	2. Thermal properties of Bambara groundnut starch, soluble dietary fibre and starch-soluble dietary fibre nanocomposite using thermogravimetric analysis	87
3.3.10	Choice of chemicals for a greener method	90
	1. Hydrogen peroxide	91
	2. Ascorbic acid	91
	3. Ethanol	92
3.4	Conclusions	92
	References	92

CHAPTER FOUR: FUNCTIONAL AND ANTIOXIDANT PROPERTIES OF BAMBARA GROUNDNUT (*VIGNA SUBTERRANEA* [L.] VERDC.) STARCH-SOLUBLE DIETARY FIBRE NANOCOMPOSITE

	Abstract	99
4.1	Introduction	100
4.2	Materials and Methods	101
4.2.1	Source of materials and equipment	101
4.2.2	Pasting properties of Bambara groundnut starch, soluble dietary fibre and starch-soluble dietary fibre nanocomposite	101
4.2.3	Colour characteristics of Bambara groundnut starch, soluble	101

	dietary fibre and starch-soluble dietary fibre nanocomposite	
4.2.4	Chemical analysis of Bambara groundnut starch, soluble dietary fibre and starch-soluble dietary fibre nanocomposite	103
4.2.5	Determination of elemental content of Bambara groundnut starch, soluble dietary fibre and starch-soluble dietary fibre nanocomposite by inductively coupled plasma-optical emission spectrometry (ICP-OES)	103
4.2.6	Hydration properties of Bambara groundnut starch, soluble dietary fibre and starch-soluble dietary fibre nanocomposite	104
	1. Water absorption capacity	104
	2. Solubility index	104
4.2.7	Oil binding capacity of Bambara groundnut starch, soluble dietary fibre and starch-soluble dietary fibre nanocomposite	104
4.2.8	Emulsion activity and stability of Bambara groundnut starch, soluble dietary fibre and starch-soluble dietary fibre nanocomposite	105
4.2.9	Antioxidant properties of Bambara groundnut starch, soluble dietary fibre and starch-soluble dietary fibre nanocomposite	105
	1. Determination of total phenolic compounds	105
	2. Determination of ferric reducing antioxidant power	105
4.2.10	Determination of glucose in Bambara groundnut starch, soluble dietary fibre and starch-soluble dietary fibre nanocomposite	106
4.2.11	Phenolic profiling of Bambara groundnut starch, soluble dietary fibre and starch-soluble dietary fibre nanocomposite	106
4.2.12	Data analysis	107
4.3	Results and Discussion	107
4.3.1	Pasting properties of Bambara groundnut starch, soluble dietary fibre and starch-soluble dietary fibre nanocomposite by rapid visco analysis	107
	1. Peak viscosity	107
	2. Trough viscosity	111
	3. Final viscosity	111
	4. Breakdown viscosity	112
	5. Setback viscosity	112
	6. Pasting temperature	113
	7. Peak time	114
4.3.2	Colour characteristics of Bambara groundnut starch, soluble dietary fibre and starch-soluble dietary fibre nanocomposite	114

1.	Colour differences	116
4.3.3	Chemical composition of Bambara groundnut starch, soluble dietary fibre and starch-soluble dietary fibre nanocomposite	117
4.3.4	Determination of Bambara groundnut starch, soluble dietary fibre and starch-soluble dietary fibre nanocomposite elemental content by inductively coupled plasma-optical emission spectrometry (ICP-OES)	119
4.3.5	Hydration properties of Bambara groundnut starch, soluble dietary fibre and starch-soluble dietary fibre nanocomposite	121
1.	Solubility index	121
2.	Water absorption capacity	123
4.3.6	Oil binding properties of Bambara groundnut starch, soluble dietary fibre and starch-soluble dietary fibre nanocomposite	124
4.3.7	Emulsion activity and stability indexes of Bambara groundnut starch, soluble dietary fibre and starch-soluble dietary fibre nanocomposite	125
4.3.8	Glucose composition of Bambara groundnut starch, soluble dietary fibre and starch-soluble dietary fibre nanocomposite	126
4.3.9	Antioxidant properties of Bambara groundnut starch, soluble dietary fibre and starch-soluble dietary fibre nanocomposite	126
4.3.10	Polyphenolic compounds in Bambara groundnut starch, soluble dietary fibre and starch-soluble dietary fibre nanocomposite	129
4.4	Conclusions	130
	References	131

CHAPTER FIVE: RHEOLOGICAL AND STABILITY PROPERTIES OF BAMBARA GROUNDNUT STARCH-SOLUBLE DIETARY FIBRE NANOCOMPOSITE STABILISED EMULSION

	Abstract	139
5.1	Introduction	140
5.2	Materials and Methods	141
5.2.1	Effects of emulsion components and concentrations on emulsion stability	143
5.2.2	Preparation of beverage emulsions	144
5.2.3	Emulsion stability evaluation	144
5.2.4	Rheological measurements of emulsions	145
1.	Time-dependent rheological measurements	145
2.	Time-independent rheological measurements	146

5.2.5	Modelling the effect of Bambara groundnut starch-soluble dietary fibre nanocomposite, orange oil and water on emulsion stability and rheology	146
5.2.6	Data analysis	147
5.3	Results and Discussion	148
5.3.1	Effect of Bambara groundnut starch-soluble dietary fibre nanocomposite, orange oil and water concentrations on initial backscattering of STASOL stabilised emulsions	148
5.3.2	Effect of emulsion components on Turbiscan stability index	154
5.3.3	Time-dependent rheological properties of STASOL stabilised emulsions	158
	1. Hysteresis loop area	158
	2. Effect of constant shear decay on apparent viscosity of STASOL stabilised emulsions	164
5.3.4	Time-dependent rheological models	166
	1. First-order stress decay with a zero equilibrium stress value	166
	2. Weltman model	168
	3. Comparison of the time dependent rheological models used in the predicting STASOL stabilised emulsions behaviour	170
5.3.5	Time-independent rheological properties of STASOL stabilised emulsions	170
	1. Apparent viscosity of STASOL stabilised emulsions at different shear rates	170
5.3.6	Time-independent rheological models	172
	1. Power law model	172
	2. Herschel-Bulkley model	175
	3. Bingham plastic model	177
	4. Casson Model	177
	5. Comparison of the time-independent rheological models used in predicting STASOL stabilised emulsions behaviour	180
5.4	Conclusions	182
	References	182

CHAPTER SIX: EFFECT OF STORAGE TIME AND TEMPERATURE ON THE STABILITY AND RHEOLOGICAL PROPERTIES OF BAMBARA GROUNDNUT STARCH-SOLUBLE DIETARY FIBRE NANOCOMPOSITE STABILISED EMULSION

	Abstract	189
6.1	Introduction	190

6.2	Materials and Methods	191
6.2.1	Preparation of STASOL stabilised beverage emulsions	191
6.2.2	Effect of storage time and temperature on the rheological properties of STASOL stabilised emulsions	191
6.2.3	Effect of storage time and temperature on the stability of STASOL stabilised emulsions	191
1.	Turbiscan stability analysis	191
2.	Creaming stability	191
6.2.4	Turbidity loss rate of STASOL stabilised emulsions	193
6.2.5	Effect of storage time and temperature on pH of STASOL stabilised emulsions	193
6.2.6	Effect of storage time and temperature on the microstructure of STASOL stabilised emulsions	193
6.2.7	Effect of storage time and temperature on the droplet sizes of STASOL stabilised emulsions	194
6.2.8	Data analysis	194
6.3	Results and Discussion	194
6.3.1	Effect of storage time and temperature on stability of STASOL stabilised emulsions	194
1.	Turbiscan stability of STASOL stabilised emulsions	195
2.	Creaming stability of STASOL stabilised emulsions	198
6.3.2	Turbidity loss rate of STASOL stabilised emulsions	200
6.3.3	Effect of storage time and temperature on the pH of STASOL stabilised emulsions	201
6.3.4	Effect of STASOL and orange oil on droplet size and microstructure of STASOL stabilised emulsions	202
6.3.5	Effect of storage time and temperature on hysteresis loop area	205
6.3.6	Effect of storage time and temperature on minimum apparent viscosity	207
6.4	Conclusions	209
	References	210

CHAPTER SEVEN: GENERAL SUMMARY AND CONCLUSIONS

7.1	General Summary and Conclusions	214
7.2	Future Studies and Recommendations	218
7.3	Research Outputs	218
	References	218

LIST OF FIGURES

Figure		Page
1.1	Thesis overview	8
2.1	A) Bambara groundnut seeds. B) Bambara groundnut soluble dietary fibre	12
2.2	Structure of amylose and amylopectin in starch	15
2.3	Mechanisms of emulsion destabilisation	24
2.4	Possible mode of interaction between polysaccharides and proteins	29
2.5	Phase separation diagram of a protein-polysaccharide mixture	31
2.6	Phase behaviour of mixed biopolymer solutions	32
2.7	Different rheological behaviours	33
2.8	Rheometer	34
3.1	Outline of chapter 3	54
3.2	Isolation of Bambara groundnut STASOL	55
3.3	Pictorial representation of BGNS, BGN-SDF and STASOL	60
3.4	Mechanism of radical scavenging activity of ascorbic acid	62
3.5	Possible modes of interaction between BGNS and BGN-SDF	66
3.6	Changes in the backscattering (BS) profile (%) as a function of sample height with varying BGNS:BGN-SDF ratios	67
3.7	Particle sizes of BGNS, BGN-SDF and STASOL	68
3.8	Zeta potential of BGNS, BGN-SDF and STASOL	69
3.9	FTIR spectra of native Bambara groundnut starch (BGNS)	72
3.10	FTIR spectra of Bambara groundnut soluble dietary fibre (BGN-SDF)	74
3.11	FTIR spectra of Bambara groundnut starch-soluble dietary fibre nanocomposite (STASOL)	76
3.12	FTIR spectra of BGNS, BGN-SDF and STASOL	77
3.13	Powder X-Ray diffraction patterns of BGNS, BGN-SDF and STASOL.	78
3.14	Microstructure of BGNS, BGN-SDF and STASOL	81
3.15	Fluorescence spectra of BGNS, BGN-SDF and STASOL	81
3.16	Thermal properties of BGNS, BGN-SDF and STASOL using differential scanning calorimetry (DSC)	87
3.17	Thermal properties of BGNS, BGN-SDF and STASOL using TGA	89
4.1	Outline of chapter 4	102
4.2	Pasting properties of A) Bambara groundnut starch; B) Bambara groundnut soluble dietary fibre; C) Bambara groundnut starch-soluble dietary fibre nanocomposite (STASOL)	110
4.3	Mineral composition of BGNS, BGN-SDF and STASOL.	120
5.1	Outline of Chapter 5	142

5.2	Backscattering profiles of STASOL stabilised emulsions	151
5.3	Mixture response surface (left) and Piepel graph (right) for the effect of (A) Bambara groundnut starch-soluble dietary fibre nanocomposite (STASOL), (B) orange oil and (C) water concentrations on the backscattering of STASOL stabilised emulsions	154
5.4	Mixture response surface (left) and Piepel graph (right) for the effect of (A) Bambara groundnut starch-soluble dietary fibre nanocomposite (STASOL), (B) orange oil and (C) water concentrations on the Turbiscan stability index (TSI) of STASOL stabilised emulsions	157
5.5	Hysteresis loop areas obtained for Bambara groundnut starch-soluble dietary fibre nanocomposite (STASOL) stabilised emulsions	162
5.6	Mixture response surface (left) and Piepel graph (right) for the effect of (A) Bambara groundnut starch-soluble dietary fibre nanocomposite (STASOL), (B) orange oil and (C) water concentrations on the hysteresis loop areas of STASOL stabilised emulsions	164
5.7	Apparent viscosity vs shearing time of Bambara groundnut starch-soluble dietary fibre nanocomposite (STASOL)	165
5.8	Effect of STASOL:oil:water concentrations on the apparent viscosity of beverage emulsions at different shear rates	171
6.1	Outline of Chapter 6	192
6.2	STASOL stabilised emulsions stored at (a) 5°C, (b) 20°C and (c) 45°C on day 3	194
6.3	Changes in the backscattering profile as a function of sample height of emulsions stored at 5°C for 20 days	196
6.4	Variation in backscattering in the 20-40 mm zone monitored over 20 days for samples stored at 5, 20 and 45°C	197
6.5	Turbidity loss of STASOL stabilised emulsions stored at 5, 20 and 45°C for 20 days	200
6.6	Change in pH of emulsions stored at 5, 20 and 45°C for 20 days	201
6.7	Microstructures of STASOL stabilised emulsions stored at 5, 20 and 45°C for 20 days	203
6.8	Droplet sizes of STASOL stabilised emulsions stored at 5, 20 and 45°C for 20 days	204
6.9	Hysteresis loop areas of STASOL stabilised emulsions stored at (a) 5°C, (b) 20°C and (c) 45°C for 20 days	208
6.10	Apparent viscosity of STASOL stabilised emulsions stored at 5, 20 and 5°C for 20 days	209

LIST OF TABLES

Table		Page
2.1	Physicochemical properties of Bambara groundnut soluble and insoluble dietary fibres	13
2.2	Chemical composition of Bambara groundnut starches	16
2.3	Classification of different types of emulsions	22
2.4	Polymer-polysaccharide complexes	28
3.1	Phase behaviour analysis of BGNS and BGN-SDF	56
3.2	Process variables and levels used for 2 ² augmented factorial design	58
3.3	Visual representation of phase separation between BGNS and BGN-SDF	64
3.4	Backscattering of BGNS and BGN-SDF combinations	65
3.5	FTIR spectra of BGNS, BGN-SDF and STASOL	73
3.6	Thermal properties of BGNS, BGN-SDF and STASOL using differential scanning calorimetry	84
3.7	Thermal properties of BGNS, BGN-SDF and STASOL using TGA	88
3.8	Effects of modification methods on the functional properties of starch	90
4.1	Pasting properties of BGNS, BGN-SDF and STASOL	108
4.2	Colour attributes of BGNS, BGN-SDF and STASOL	115
4.3	Colour difference among BGNS, BGN-SDF and STASOL	116
4.4	Chemical composition of BGNS, BGN-SDF and STASOL	118
4.5	Physicochemical properties of BGNS, BGN-SDF and STASOL	122
4.6	Glucose composition of BGNS, BGN-SDF and STASOL	126
4.7	Phenolic composition of BGNS, BGN-SDF and STASOL	128
4.8	Antioxidant properties of BGNS, BGN-SDF and STASOL	129
5.1	Randomised D-optimal exchange mixture design for STASOL stabilised emulsion	143
5.2	Effect of STASOL, orange oil and water fractions on initial backscattering of STASOL stabilised emulsions	148
5.3	ANOVA for reduced special quartic mixture model for backscattering	153
5.4	Effect of STASOL, water and orange oil fractions on Turbiscan stability index of STASOL stabilised emulsions	155
5.5	ANOVA for linear mixture model for Turbiscan stability index	156
5.6	Effect of STASOL, orange oil and water fractions on the hysteresis loop area of STASOL stabilised emulsions	159
5.7	ANOVA for quadratic mixture model of hysteresis loop area	163
5.8	First-order stress decay with a zero equilibrium stress value for STASOL stabilised emulsions	167

5.9	Weltman model parameters for STASOL stabilised emulsions	169
5.10	Effect of STASOL, orange oil and water fractions on the apparent viscosity of STASOL stabilised emulsions	173
5.11	Power law model parameters for STASOL stabilised emulsions	174
5.12	Herschel-Buckley model parameters for STASOL stabilised emulsions	176
5.13	Bingham plastic model parameters for STASOL stabilised emulsions	178
5.14	Casson model parameters for STASOL stabilised emulsions	179
5.15	Comparison of the four rheological models used in predicting STASOL stabilised emulsions behaviour	181
6.1	Creaming stability index for samples stored at 5, 20 and 45°C for 20 days	198
6.2	Effect of storage time and temperature on Power law parameters and hysteresis loop area of emulsion	206

Language and style used in this thesis are in accordance with the requirements of the *International Journal of Food Science*. This thesis represents a compilation of manuscripts where each chapter is an individual entity and some repetition between chapters has, therefore, been unavoidable.

ACKNOWLEDGEMENTS

I would like to extend my sincere gratitude to the following people and institutions that formed an integral part of the completion of this research study:

- Professor Victoria A. Jideani, my Supervisor and Senior Lecturer at the Cape Peninsula University of Technology, for being my source of inspiration and for her endless support and guidance throughout the duration of this study.
- Professor Daniel Ikhu-Omoregbe, my co-supervisor and head of department of the Chemical Engineering Department of the Cape Peninsula University of Technology, for his endless support and guidance throughout the duration of this study.
- Mr Fanie Rautenbach, Laboratory Manager in the Oxidative Stress Research Centre at the Cape Peninsula University of Technology, for his assistance with the polyphenolics and antioxidant analyses.
- Mr Owen Wilson, Senior Technician in the Department of Food Technology at the Cape Peninsula University of Technology for assistance with procurement of chemicals and consumables.
- Dr Pardon Nyamukamba, Senior Technologist at the Technology Station in Clothing and Textile, for assistance with differential scanning calorimetry and thermogravimetric analyses.
- Dr. Oladayo Adeyi, at the Michael Okpara University of Agriculture, Umudike, Nigeria for assistance with rheology and emulsion analyses.
- Mr Ndumiso Mshicileli, Manager at the AgriFood Technology Station, for assistance with specialised instrumentation and chemical analyses.
- Stellenbosch University for assistance with equipment for scanning electron microscopy, monomers and phenolic profiling.
- The Vice Chancellor's Prestigious Award, for financial assistance towards tuition and residence fees.
- The ETDP SETA postgraduate bursary, for financial assistance towards tuition, stationery and residence fees.
- Cape Peninsula University of Technology University Research Funding (URF) and National Research funding (NRF), for financial assistance towards the research running and conference costs.
- The Departments of Food Science and Technology, Chemical Engineering and Oxidative Stress of the Cape Peninsula University of Technology, for the equipment used in this study.

- The laboratory technicians in the Departments of Food Science and Technology, for assistance with laboratory bookings.
- The Cereals and Legumes Biopolymer Research for Food Security research group for the moral and technical support.
- My friends and colleagues, Zolelwa Hardy, Nontobeko Gulu and Oladayo Adeyi, for assistance and support throughout my PhD journey.

DEDICATION

Dedicated to my mother, Lesia Maphosa, for being such a phenomenal woman, for always loving and encouraging me, for guiding me and always pushing me to be the best I can be. No words can ever express how much I love you, mom. My father, Patrick David Maphosa, thank you for being a wonderful father. You taught me so much and I'm forever grateful. I love you dad. My siblings, Mildred Mabuza, Dr. Lancelot Maphosa, Dr Emmanuel Maphosa, Lilian Maphosa and Howard Ndabezihle Maphosa. I cannot imagine going through life without you. I love you all sincerely. Thank you for being my role models, support structure and for being proud of me. Thank you for being my family. My wonderful brother Tatenda John Maphosa, thank you for loving me the way you do. I hope you know I love you even more. I couldn't have asked for a better brother. My beautiful nieces and nephews, you make me a proud aunt. Professor Victoria A. Jideani thank you for being a wonderful supervisor. You have held my hand since undergraduate and have never let go. Even when I don't believe in myself, you keep me afloat. Thank you for your kindness, guidance and beautiful soul. May the Lord almighty increase you. My dear friend, Dr Oladayo Adeyi, words can not express my gratitude. Thank you for the love, support and encouragement. To my lovely sisters-in-law, you are the sisters God knew I needed. Thank you for being part of my life and for always showing up for me. I love you. To all my friends, thank you for the endless love and support. I truly appreciate you. And above all, to God Almighty, for loving me and keeping me, it is by His grace that I finished this work. In Him I live, move and have my being.

GLOSSARY

Acronym	Definition/Explanation
ANOVA	Analysis of variance
AOAC	Association of official analytical chemists
BGN	Bambara groundnut
BGNS	Bambara groundnut starch
BGN-SDF	Bambara groundnut soluble dietary fibre
BS	Backscattering
BS _{AVO}	Initial backscattering
CI	Creaming index
CV	Coefficient of variation
DF	Degrees of freedom
DSC	Differential scanning calorimetry
EAI	Emulsion activity index
ESI	Emulsion stability index
FRAP	Ferric reducing antioxidant power
FTIR	Fourier transform infrared
GAE	Gallic acid equivalents
HE	Total height of emulsion in the tubes
HS	Height of the serum layer
HLA	Hysteresis loop area
ICP-OES	Inductively coupled plasma-optical emission spectrometry
MANOVA	Multivariate analysis of variance
OBC	Oil binding capacity
RMSE	Root mean squared error
RVA	Rapid visco analyser
SE	Standard error
SEM	Scanning electron microscope
SI	Solubility index
SSE	Sum of squares
SST	Total corrected sum of squares
STASOL	Bambara groundnut starch- soluble dietary fibre nanocomposite
TGA	Thermogravimetric analysis
TSI	Turbiscan stability index
XRD	X-Ray diffraction
WAC	Water holding capacity
Y _c	Calculated value for each data point

Y_m	Measured value
R^2	Coefficient of determination
n	Flow behaviour index
K	Consistency co-efficient
$\dot{\gamma}$	Shear rate
τ	Shear stress
τ_o	Yield stress
τ_{yB}	Bingham yield stress
K_B	Bingham plastic viscosity
μ	Apparent viscosity
μ_0	Zero shear viscosity
t	Shearing time
L^*	Lightness
$+a^*$	Redness
$-a^*$	Greenness
$+b^*$	Yellowness
$-b^*$	Blueness
C^*	Chroma
h^*	Hue
x_i	Average value of the scattered light intensity at each time
x_{BS}	Average of x_i - The average value of the scattered light intensity at each time
n	Number of scans

CHAPTER ONE

MOTIVATION AND DESIGN OF THE STUDY

1.1 Introduction

The study of biopolymers as food additives has received interest in the food emulsion industry (Mackie, 2004; McClements *et al.*, 2007; Bandyopadhyay *et al.*, 2012; Evans *et al.*, 2013). Biopolymers stabilise emulsions either by modifying the rheological properties of the continuous phase or by providing a steric barrier at the oil/water interface, or a combination of both (Adeyi, 2014). As such, biopolymers retard droplet movement within an emulsion system, thereby reducing the rate of destabilisation by coalescence and flocculation (Maphosa *et al.*, 2017). Rheological properties hugely influence sensory characteristics, stability, nutritive properties as well as convenience aspects such as pumping and filling (Fischer & Windhab, 2011). Rheological data and theoretical models are useful for process and/or product optimisation (Fischer & Windhab, 2011). They also allow for the prediction of the stability of the product, the phenomenon of destabilisation as well as the shelf life of an emulsion (Adeyi *et al.*, 2014; Maphosa *et al.*, 2017).

Biopolymers are commonly conjugated to form composites with desirable characteristics. Composites are recyclable, transparent and low weight functionalised molecules that possess the characteristics of the grafted molecules as well as the natural polymer (Spizzirri *et al.*, 2010). They consist of two types of components; the matrix which supports and protects the filler, and the filler which reinforces the matrix. Furthermore, composites tend to have superior physical and chemical properties at low concentrations (Kim *et al.*, 2015). Nanocomposites are composites filled with nanosized rigid particles and have at least one of the phases with a particle size of less than 100 nm (Kim *et al.*, 2015).

Recent trends have seen the conjugation of biopolymers into composites and applying them in different branches of engineering and food industries (Spizzirri *et al.*, 2010; Kim *et al.*, 2015). Although polymer-polysaccharide and polysaccharide-polysaccharide composites have been widely studied (Mackie, 2004; Sanchez & Patino, 2005; McClements *et al.*, 2007; Bandyopadhyay *et al.*, 2012; Evans *et al.*, 2013; Liu *et al.*, 2015), they are still one of the most difficult topics to understand (Doublier *et al.*, 2000; Bandyopadhyay *et al.*, 2012). Biopolymer complexes are generally non-toxic, relatively stable, nutritional beneficial, biocompatible, biodegradable and have a low cost (Yu *et al.*, 2014; Yin *et al.*, 2015). As such, they are largely preferred in the food industry.

Starch is frequently used in composites (Winarti *et al.*, 2014; Yu *et al.*, 2014; Hasanvand *et al.*, 2015). However, its industrial utilisation is limited because of its many undesirable properties (Ashogbon & Akintayo, 2013; Winarti *et al.*, 2014; Wang *et al.*, 2015). These

undesirable characteristics are mitigated by modification (Ashogbon & Akintayo, 2014). Starch from legumes such as Bambara groundnut (BGN) (*Vigna subterranea* (L.) Verdc.) has not been extensively researched for use in food systems. Bambara groundnut has a starch composition of 22-50% (Yao *et al.*, 2015; Oyeyinka *et al.*, 2016), with an amylose content of 21-35% (Sirivongpaisal, 2008). This starch content is comparable to that of the commonly used potato (15-23%) and maize [24-25%] (Oyeyinka *et al.*, 2016) starch sources. The increasing demand for starch by the food industry due to decreased cereal production as a result of climate change (Gammans *et al.*, 2017), makes BGN starch (BGNS) a potential and sustainable alternative.

One way of mitigating the undesirable properties of BGNS involves its modification by complexing it with a more robust biopolymer. Biopolymers such as soluble dietary fibre (SDF) can be grafted onto a starch matrix to increase the stoutness of starch while maintaining the active compound delivery capabilities of SDF. Both starch and SDF find use as fortifiers, stabilisers, thickeners and fat replacers in food systems (Rosell *et al.*, 2009; Dhingra *et al.*, 2012; Hasanvand *et al.*, 2015).

Bambara groundnut is an excellent raw material for the extraction of dietary fibres (Diedericks & Jideani, 2014; Maphosa, 2016). Bambara groundnut SDF is rich in bioactive compounds, namely, uronic acids (11.8%) and hydrolysable polyphenols [20 mg/g Gallic acid equivalent (GAE)], with crucial physiological and functional benefits (Chhabra, 2012; Maphosa & Jideani, 2016). Uronic acids and hydrolysable polyphenols are absent in starch but present in BGN-SDF, therefore the conjugation of these two polysaccharides would deliver these active compounds from BGN-SDF to BGNS and later to the emulsion system that the nanocomposite would be incorporated in. Moreover, the low modulus, strength and heat resistance of starch could be reinforced by SDF, forming a stable and robust complex.

As such, nanocomposites made from BGNS and BGN-SDF would find use in delivering active compounds to food systems as well as in emulsion stabilisation. The employment of such a nanocomposite in a food system would produce a product with a relatively "greener" label as all components used will be natural.

1.2 Statement of the Research Problem

Bambara groundnut is a source of soluble dietary fibre (SDF) (17%, dry mass) and starch (50%, dry mass) (Yao *et al.*, 2015), making it a great source of the two polysaccharides (Maphosa, 2016). Bambara groundnut SDF possesses high oil binding capabilities (2.78-4.03 g oil/g sample) making it useful in emulsion stabilisation. It stabilises emulsions by retarding droplet movement hence reducing the rate of coalescence and flocculation (Maphosa *et al.*, 2017). Both BGN-SDF and BGNS have not been extensively researched and currently have no reported use in food products in the market. The industrial utilisation of native starch is limited

because of the inherent undesirable attributes that render it unstable (Wang *et al.*, 2015). These attributes include its tendency to easily gelatinise (converting the semi-crystalline structure to amorphous phase), retrograde and undergo syneresis, as well as instability to various temperatures, shear and pH (Winarti *et al.*, 2014; Ashogbon & Akintayo, 2014).

Bambara groundnut SDF on the other hand is rich in polyphenols, uronic acids and is a prebiotic (Maphosa, 2016). However, a large amount of SDF (30%) is needed to achieve desirable emulsion stability (Maphosa, 2016). Such a high amount would be too costly for use in products. As such, complexing these two polysaccharides, BGNS and BGN-SDF, to form a robust nanocomposite will not only provide a novel ingredient and emulsion stabiliser but will mitigate the limitations of starch and allow the use of lower amounts of BGN-SDF. Furthermore, BGN-SDF will deliver bioactive compounds to the food system.

The study of nanocomposites as food ingredients is very limited and their study has the potential to revolutionise the food industry. Nanocomposites have improved physical properties and may be used as nutrients or bioactive compound delivery systems thereby enriching the products they are incorporated in (Yu *et al.*, 2014; Yin *et al.*, 2015; Kim *et al.*, 2015). Currently, the focus is on the employment of nanocomposites in edible packaging films (Bandyopadhyay *et al.*, 2012). However, there is limited knowledge on nanocomposite food polymers and nothing is known of Bambara groundnut starch-soluble dietary fibre nanocomposite (STASOL). Furthermore, it is important to establish how stabilisers affect the rheology and stability of food emulsions. While the rheology of polysaccharides in emulsion systems has been studied (Gabriel *et al.*, 2013; Adeyi *et al.*, 2014; Maphosa *et al.*, 2017), nothing is known about the effect of STASOL on the rheological characteristics of beverage emulsions. Investigating the effect of STASOL on the physicochemical, functional, rheological and stability properties of beverage emulsions will address this knowledge gap.

1.3 Objectives of the Research

1.3.1 Broad objective

The broad objective of this research was to assess the effect of Bambara groundnut starch-soluble dietary fibre nanocomposite (STASOL) on the rheological, functional and physicochemical properties of beverage emulsion systems.

1.3.2 Specific objectives

The specific objectives of this research were to:

1. Synthesise and characterise the physicochemical properties of STASOL extracted from the BGN black-eye variety.

2. Establish the optimum quantity of STASOL for a stable orange oil beverage emulsion using a mixture design.
3. Characterise and model the rheological and stability properties of STASOL stabilised orange oil beverage emulsions.
4. Establish the relationship between emulsion stability and rheological properties of STASOL stabilised orange oil beverage emulsions.
5. Model the shelf life stability and rheological properties of STASOL stabilised orange oil beverage emulsions.
6. Investigate the effect of storage temperature and time on the stability and rheological properties of STASOL stabilised orange oil beverage emulsions.

1.4 Hypotheses

The hypotheses that were tested in this research were:

1. BGNS and BGN-SDF will be successfully complexed to form STASOL, a nanocomposite with desirable physicochemical and functional properties.
2. STASOL will significantly affect the rheological and stability properties of orange oil beverage emulsions.
3. The rheological behaviour of STASOL stabilised orange oil beverage emulsions will be effectively described using rheological models.
4. STASOL stabilised orange oil beverage emulsions will have desirable shelf life stability and rheological properties.

1.5 Delineation of the Research

The delimitations of this research were that:

1. Only starch and SDF from the BGN black-eye variety were studied.
2. Only one emulsion system (beverage emulsions) was studied.

1.6 Significance of the Research

This project ties with human resource development, bio-economy, food security as well as reduction of poverty and malnutrition. The growing demand in the food and beverage industries for new alternatives to emulsion stabilisers has encouraged research into natural emulsifiers and stabilisers (Gabriel *et al.*, 2013; Ashogbon & Akintayo, 2014). This is a response to consumer demand for natural food components. The production of STASOL will introduce an innovative, natural, biocompatible, biodegradable, affordable and readily available emulsion stabiliser to the food industry. Furthermore, the nanocomposite will have certain therapeutic and prebiotic properties as its constituents are rich in polyphenols and uronic acids (Maphosa & Jideani,

2016). This study will facilitate the increased use of nanotechnology in the beverage industry. The formation, characteristics and behaviour of STASOL in beverage emulsions will be understood. Furthermore, revealing the physicochemical, emulsion stabilising and thickening properties of STASOL will contribute vastly in addressing consumer demands for natural additives.

The use of STASOL will increase the energy and dietary fibre content of the emulsion systems. The successful commercialisation of BGN components (BGNS and BGN-SDF) would, consequently, lead to a higher demand for this legume. This in turn will encourage farmers to produce higher yields of BGN thereby empowering local farmers and creating employment opportunities. Increasing the production of BGN as well as making the knowledge of BGN-SDF and BGNS functions and properties available will lead to the exportation of the legume, benefiting the country as a whole by increasing exports and Gross Domestic Product (GDP). Bambara groundnut, an orphan crop, has been labelled a “poor man’s” legume cultivated mostly at the household level by women, especially in sub-Saharan Africa. Hence, an increase in its production would play a role in women empowerment as well as improving the socio-economic status of female farmers. Additionally, successfully commercialising BGN would play a role in increasing food security as well as in alleviating malnutrition.

Furthermore, including BGN-SDF in foods will increase the dietary fibre content of the systems helping curb low fibre intakes. The inclusion of starch in foods increases their energy value. Hence, the high fibre-high energy beverage emulsion stabilised with STASOL would find an important role in feeding programmes and thus in alleviating malnutrition and poverty.

As such, the application of STASOL in a beverage emulsion will not only increase the market value of BGN but will also significantly improve the overall quality of emulsions. This research will also lead to the completion of a doctoral degree which positively impacts the postgraduate output of the Cape Peninsula University of Technology thereby impacting human capacity building.

1.7 Expected Outcomes, Results and Contributions of the Research

The outcomes of this research will give insight into the application of nanocomposites in food systems. They will also provide the food industry with a natural, non-toxic, cheaper and readily available natural alternative emulsion stabiliser. The effect of STASOL on the emulsion systems will provide knowledge of the nature, behaviour and other functions that these complexes could be exposed to. Results of the stabilising and rheological effects of STASOL will improve understanding of the phenomena by which the emulsions destabilise, thereby allowing this problem to be tackled in advance. Rheological assessments are expected to offer information

on the nature of STASOL, its effect on time-dependent and time-independent properties in beverage emulsions as well as its behaviour when subjected to varying stresses and over time.

From this work, two chapters have been published in InTech Books; *The role of legumes in human nutrition* published in Functional Food (2017) and *Factors affecting the stability of emulsions stabilised by biopolymers* published in Science and Technology behind Nanoemulsions (2018). Also, a patent titled *Bambara groundnut starch and soluble dietary fibre (STASOL)* was filed in 2020 and findings from this study were presented at the 13th International Congress on Engineering and Food (ICEF13) held in Melbourne, Australia on 23-26 September 2019. The attainment of a Doctoral degree in Food Science and Technology is also expected from this study.

1.8 Thesis Overview

This thesis comprises six chapters and is structured in article format with each chapter presented as a standalone study (Figure 1.1). Chapter one gives the motivation and design of the study; stating the research problem, broad and specific objectives, hypotheses, delineation of the study, the significance of the research as well as expected outcomes, results and contributions of the research.

Chapter two is the literature review. A background on BGN soluble and insoluble dietary fibres is given. Physicochemical and functional properties, as well as industrial applications of starch, are outlined. Furthermore, the different synthesis and verification methods, as well as application and uses of composites, are discussed. The classification, stability and destabilisation mechanisms of emulsions are critically discussed, with emphasis on the application of nanocomposites in the food industry, beverage emulsions and stabilisation of emulsions using biopolymers. Biopolymers and their phase behaviour, complexing, separation mechanisms, their effects on different food emulsion systems and prospects are also discussed. Finally, the importance of rheological knowledge as well as various rheological models commonly applied in describing rheological data are reviewed.

Chapter three details the conjugation and verification of BGNS and BGNS from the black-eye BGN variety to produce STASOL. Phase behaviour studies were carried out to determine the optimum starch:soluble dietary fibre ratio for the formation of a stable nanocomposite. Fourier transform infrared (FTIR), powder X-ray diffraction (XRD), scanning electron microscopy (SEM), zeta potential, differential scanning calorimetry (DSC), thermogravimetric analysis (TGA) and fluorescence spectroscopy analyses were used as STASOL verification methods.

Chapter four looks into the pasting properties, colour characteristics, chemical composition, hydration properties, oil binding capacity (OBC), emulsion activity index (EAI),

emulsion stability index (ESI), total antioxidant properties, monomers and phenolic compounds. The pasting properties that were measured are peak viscosity, trough viscosity, breakdown and final viscosities as well as setback, pasting temperature and peak time.

Chapter five focuses on finding the best combination of STASOL, orange oil and water using a randomised D-optimal exchange mixture design. The optimum ratio was applied in the production of a STASOL stabilised orange oil beverage emulsion. Emulsion stability and rheological properties were evaluated using the Turbiscan and rheometer, respectively. The time-dependent and time-independent characteristics of the emulsions were studied and described using several rheological models.

Chapter six focuses on the stability and rheological behaviour of STASOL stabilised orange oil beverage emulsion over 20 days at 5, 20 and 45°C. The changes in the rheology of the emulsions were assessed using a rheometer while stability was assessed using the Turbiscan, turbidity loss, pH as well as optically assessing creaming index studies.

Chapter seven gives a summary of the research and general conclusions of the study.

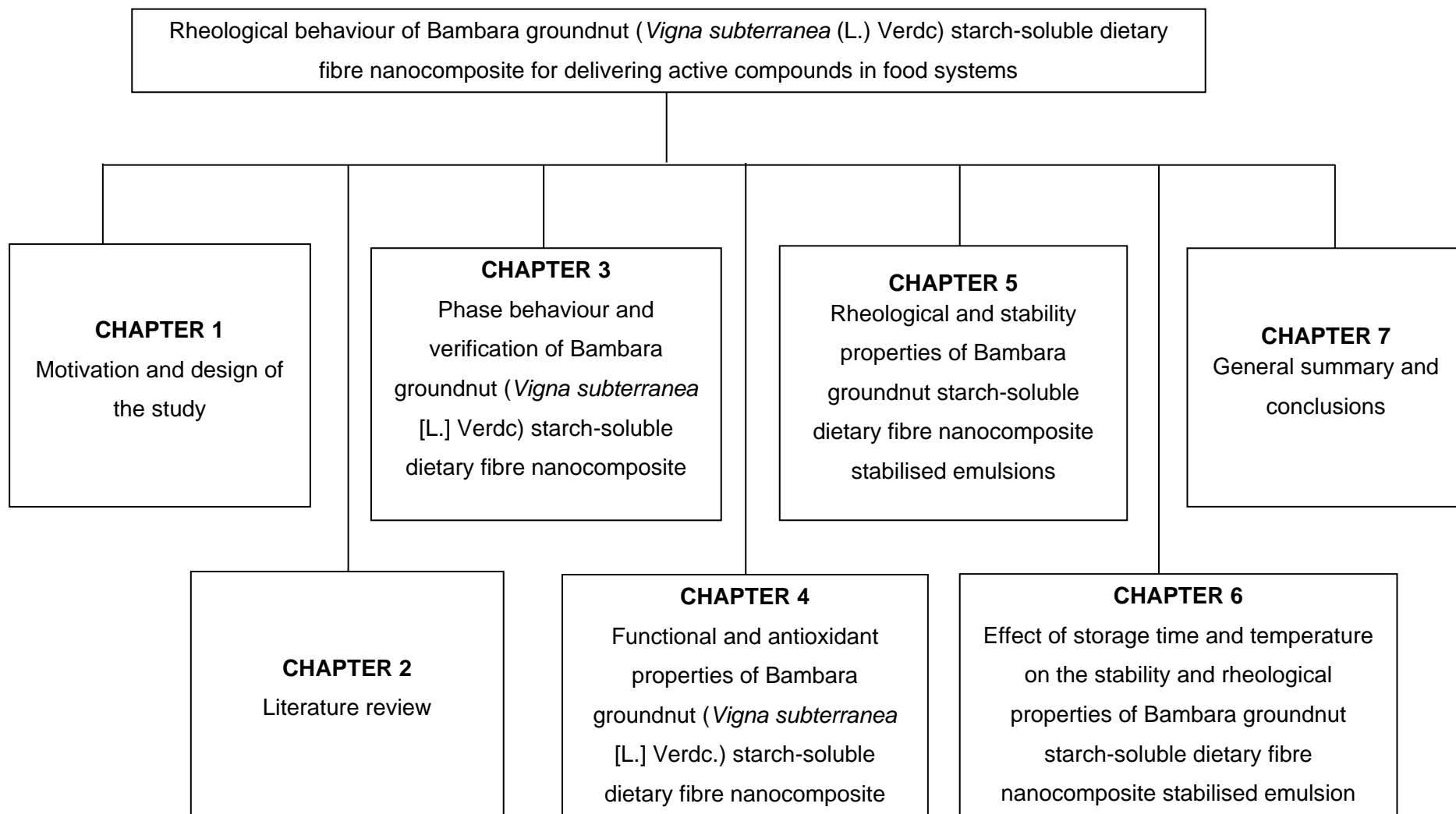


Figure 1.1 Thesis overview.

References

- Adeyi, O. (2014). Effect of Bambara Groundnut flour on the stability and rheological properties of oil-in-water emulsion. PhD Thesis, Cape Peninsula University of Technology.
- Adeyi, O., Ikhu-Omoregbe, D. & Jideani, V. (2014). Emulsion stability and steady shear characteristics of concentrated oil-in-water emulsion stabilized by gelatinized bambara groundnut flour. *Asian Journal of Chemistry*, **26**, 4995-5002.
- Ashogbon, A.O. & Akintayo, E.T. Morphological and functional properties of starches from cereal and legume: A comparative study. *International Journal of Biotechnology and Food Science*, **1(4)**, 72-83.
- Bandyopadhyay, P., Ghosh, A.K. & Ghosh, C. (2012). Recent developments on polyphenol–protein interactions: Effects on tea and coffee taste, antioxidant properties and the digestive system. *Food & Function*, **3(6)**, 592-605.
- Chhabra, N. (2012). Uronic acid pathway. In: *Biochemistry for Medics*. Medical College, Mauritius.
- Dhingra, D., Michael, M., Rajput, H. & Patil, R.T. (2012). Dietary fibre in foods: a review. *Journal of Food Science and Technology*, **49(3)**, 255-266.
- Diedericks, C.F. & Jideani, V.A. (2014). Nutritional, therapeutic, and prophylactic properties of *Vigna subterranea* and *Moringa oleifera*. In: *Antioxidant-Antidiabetic Agents and Human Health*. (Edited by O. Oguntibeju). Pp 187. Croatia: InTech.
- Doublier, J.L., Garnier, C., Renard, D. & Sanchez, C. (2000). Protein-polysaccharide interactions. *Current Opinion in Colloid and Interface Science*, **5(3-4)**, 202-214.
- Evans, M., Ratcliffe, I. & Williams, P.A. (2013). Emulsion stabilisation using polysaccharide-protein complexes. *Current Opinion in Colloid & Interface Science*, **18(4)**, 272-282.
- Fischer, P. & Windhab, E.J. (2011). Rheology of food materials. *Current Opinions in Colloid and Interface Science*, **16**, 36-40.
- Gabriel, E.G., Jideani, V.A. & Ikhu-Omoregbe, D.I.O. (2013). Investigation of the emulsifying properties of Bambara groundnut flour and starch. *International Journal of Biological, Veterinary, Agricultural and Food Engineering*, **7(11)**, 724-732.
- Gammans, M., Merel, P. & Ortiz-Bobea, A. Negative impacts of climate change on cereal yields: statistical evidence from France. *Environmental Research Letters*, **12(5)**, 054007.
- Hasanvand, E., Fathi, M., Bassiri, A., Javanmard, M. & Abbaszadeh, R. (2015). Novel starch based nanocarrier for Vitamin D fortification of milk: Production and characterization. *Food and Bioproducts Processing*, **96**, 264-277.
- Kim, R.J., Kim, Y., Choi, N. & Lee, I. (2015). Polymerization shrinkage, modulus, and shrinkage stress related to tooth-restoration interfacial debonding in bulk-fill composites. *Journal of Dentistry*, **43(4)**, 430-439.

- Liu, Y., Chen, W., Chen, C. & Zhang, J. (2015). Physicochemical property of starch-soluble dietary fiber conjugates and their resistance to enzymatic hydrolysis. *International Journal of Food Properties*, **18**, 2457-2471.
- Mackie, A. (2004). Structure of adsorbed layers of mixtures of protein and surfactants. *Current Opinion in Colloid and Interface Science*, **9**, 357-361.
- Maphosa, Y. (2016). Characterisation of Bambara groundnut (*Vigna Subterranea* (L.) Verdc.) non-starch polysaccharides from wet milling as prebiotics. Master of Technology Thesis, Cape Peninsula University of Technology.
- Maphosa, Y. & Jideani, V.A. (2016). Physicochemical characteristics of Bambara groundnut dietary fibres extracted using wet milling. *South African Journal of Science*, **112(1/2)**, 1-8.
- Maphosa Y, Jideani VA. & Adeyi O. (2017). Effect of soluble dietary fibres from Bambara groundnut varieties on the stability of orange oil beverage emulsion. *African Journal of Science, Technology, Innovation and Development*, **9(1)**, 69-76.
- McClements, D.J., Decker, E.A. & Weiss, J. (2007). Emulsion-based delivery systems for lipophilic bioactive components. *Journal of Food Science*, **72(8)**, 109-124.
- Oyeyinka, S.A., Singh, S., Ma, Y. & Amonsou, E.O. (2016). Effect of high-pressure homogenization on structural, thermal and rheological properties of Bambara starch complexed with different fatty acids. *Royal Society of Chemistry*, **6**, 80174-80180.
- Rosell, C.M., Santos, E. & Collar, C. (2009). Physico-chemical properties of commercial fibres from different sources: A comparative approach. *Food Research International*, **42**, 176-184.
- Sanchez, C.C. & Patino, J.M.R. (2005). Interfacial, foaming and emulsifying characteristics of sodium caseinate as influenced by protein concentration in solution. *Food Hydrocolloids*, **19(3)**, 407-416.
- Sirivongpaisal, P. (2008). Structure and functional properties of starch and flour from bambarra groundnut. *Songklanakarin Journal of Science and Technology*, **30**, 51-56.
- Spizzirri, U.G., Parisi, O.I., Iemma, F., Cirillo, G., Puoci, F. & Curcio, M. (2010). Antioxidant polysaccharide conjugates for food application by eco-friendly grafting procedure. *Carbohydrate Polymers*, **79(2)**, 333-340.
- Wang, S., Wang, J., Zhang, W., Li, C., Yu, J. & Wang, S. (2015). Molecular order and functional properties of starches from three waxy wheat varieties grown in China. *Food Chemistry*, **181**, 43-50.
- Winarti, C., Sunarti, T., Mangunwidjaja, D. & Richana, N. (2014). Preparation of arrowroot starch nanoparticles by butanol-complex precipitation, and its as bioactive encapsulation matrix. *International Food Research Journal*, **21(6)**, 2207-2213.
- Yao, D.N., Kouassi, K.N., Erba, D., Scazzina, F., Pellegrini, N. & Casiraghi, M.C. (2015). Nutritive evaluation of the Bambara groundnut Ci12 landrace [*Vigna subterranea* (L.)

- Verdc. (*Fabaceae*)] produced in Côte d'Ivoire. *International Journal of Molecular Science*, **16**, 21428-21441.
- Yin, B., Zhang, R. & Yao, P. (2015). Influence of pea protein aggregates on the structure and stability of pea protein/soybean polysaccharide complex emulsions. *Molecules*, **20**, 5165-5183.
- Yu, Y., Huang, X. & Yu, W. (2014). High Performance of Bamboo-Based Fiber Composites from Long Bamboo Fiber Bundles and Phenolic Resins. *Journal of Applied Polymer Science*, **131**(12), 1-8.

CHAPTER TWO

LITERATURE REVIEW

2.1 Bambara groundnut dietary fibres

Bambara groundnut (BGN) (*Vigna subterranea* (L). Verdc) is an orphan leguminous crop commonly grown by low-income female farmers in sub-Saharan Africa (Jideani & Mpotokwane, 2009; Bamshaiye *et al.*, 2011; Diedericks & Jideani, 2015; Yao *et al.*, 2015). It is the third most important legume, after *Arachis hypogaea* (groundnuts) and *Vigna unguiculata* (cowpea), in terms of consumption and socioeconomic status (Murevanhema & Jideani, 2015). Several researchers have reported BGN as a complete food, containing carbohydrates (49-65%) (Murevanhema & Jideani, 2015), dietary fibre (17.7-24.3%) (Maphosa & Jideani, 2016), protein (15-25%) (Mayes *et al.*, 2019) fat (4.5-7.4%) (Diedericks & Jideani, 2015), ash (0.1-0.5%) (Kaptso *et al.*, 2014) and essential amino acids (Murevanhema & Jideani, 2015). This makes it suitable for complementing cereals, which have lysine as a limiting amino acid. Bambara groundnut is drought, disease and pest resistant, with the capability of thriving under nutrient-deficient soils. This legume also has nitrogen-fixing properties thereby contributing immensely to soil fertility and crop rotation (Mayes *et al.*, 2019). As such, BGN is important both agronomically and nutritionally.

Diedericks (2014) reported five main types of BGN seeds; brown, red, cream, black, and speckled. The cream variety is further categorised into black-eye, brown-eye and no-eye. Bambara groundnut seeds are shown in Figure 2.1.



Figure 2.1 (a) Bambara groundnut seeds, (b) Bambara groundnut soluble dietary fibre.

Bambara groundnut is rich in SDFs that have important physicochemical and physiological functions. The South African Foodstuffs, Cosmetics and Disinfectants Act, 1972 (Revised on 1 March 2010) states that a food product is high in dietary fibre if it contains more than 6% dietary fibre. Therefore, BGN, with a composition of 17.7-24.3% SDF, can be considered high in dietary fibre (Gulu, 2018). Bambara groundnut SDFs are characterised by high oil binding capacities, hydrolysable polyphenolics, monomers and uronic acids as shown in Table 2.1 (Maphosa & Jideani, 2016).

Table 2.1 Physicochemical properties of Bambara groundnut soluble dietary fibres

Physicochemical property	Quantity
Oil binding capacity (g oil/g dry)	2.78-4.03
Bulk density (g/mL)	0.5-0.6
Direct density (g/mL)	0.05-0.11
Hydrolysable polyphenols (mg/g GAE)	6.89-20.86
Tannins (mg/g)	<1
Total sugars (%)	31.2-44.8
Uronic acids (%)	10.6-11.5
Lightness (L*)	71.0-74.0
Redness/Greenness (a*)	1.7-2.5
Yellowness/Blueness (b*)	13.8-15.6
Thermal stability (Peak temperature) (°C)	358.36-361.51
Volume surface mean diameter (d _{3,2}) (µm)	73.05-116.24
Equivalent volume-mean diameter (d _{4,3}) (µm)	74.74-124.30

Adapted from: Maphosa (2016)

As such, BGN-SDFs can be effectively used as binders or fat replacers in high-fat foods such as meat and meat products as well as serve as emulsion stabilisers (Slavin 2013). Physiologically, BGN-SDF would be of importance in the absorption of bile acid resulting in the reduction of cholesterol and consequently cholesterol-related illnesses (Tosh & Yada, 2010). Also, BGN-SDFs were reported to have high thermal stability, with thermographs showing final degradation at temperatures above 230°C (Maphosa, 2016). This makes them appropriate for possible use as ingredients in high-temperature processes such as extrusion and baking. Maphosa *et al.* (2017) reported the effect of four varieties of BGN-SDFs on the stability of orange oil beverage emulsions and concluded that the BGN-SDF from the black-eye variety, at a concentration of 30%, was the most suitable stabiliser.

2.1.1 Active compounds of soluble dietary fibres

Hydrolysable polyphenols present in BGN-SDFs are suggestive of the presence of antioxidant properties. This renders BGN-SDFs suitable for application as natural antioxidants in foods, protecting the system from superoxide and hydroxyl free radicals as well as lipid peroxidation, hence increasing their shelf life (Elleuch *et al.*, 2011). Antioxidants are beneficial physiologically as they lessen the risk of conditions such as arteriosclerosis as well as work against degenerative diseases such as some cancers. Uronic acids in SDFs suggest the presence of pectin, a thickening agent that increases the thickness of systems (Saha & Bhattacharya, 2010). Thickening agents stabilise systems by increasing their viscosity thereby retarding droplet movement. Furthermore, uronic acids chelate with some waste compounds in the body, thus aiding their elimination (Chhabra, 2012; Vazquez *et al.*, 2013).

Bambara groundnut SDF was concluded to be prebiotic by Maphosa (2016). As such, it could be predicted that BGN-SDF would support the growth of probiotics in the colon. Bifidobacteria constitute a large proportion of the microflora in the intestines of infants (Maphosa, 2016) suggesting that BGN-SDF would be a valuable ingredient in infant food products. The prebiotic properties of BGN-SDF can be employed in the production of various foods to impart health benefits (Verma & Banerjee, 2010).

Dietary fibre is fermented by probiotics in the human colon producing short-chain fatty acids (SCFAs) (Martin-Pelaez, 2008). The SCFAs help in the elimination of toxic compounds and bile acids from the body as well as regulate and promote the health of the colon (Verma & Banerjee, 2010). Therefore, dietary fibre helps in preventing health conditions such as diabetes and coronary heart infections (Martin-Pelaez, 2008).

2.2 Starch

Starch serves as an energy reserve in many plants (Oyeyinka & Oyeyinka, 2017). It is produced from glucose during photosynthesis and consists of glucopyranose units bonded in α -linkages (Song, 2011). In nature, starch appears in two forms; amylose (15-30%) and amylopectin (70-85%), with the former existing as a linear chain of glucose units in α 1,4 linkages (Figure 2.2) and with a molecular weight of 10^5 - 10^6 g/mol (Song, 2011). Amylopectin is highly branched with α 1,4 glucan chains interlinked by α 1,6 linkages (Figure 2.2) and has a molecular weight of 10^7 - 10^9 g/mol.

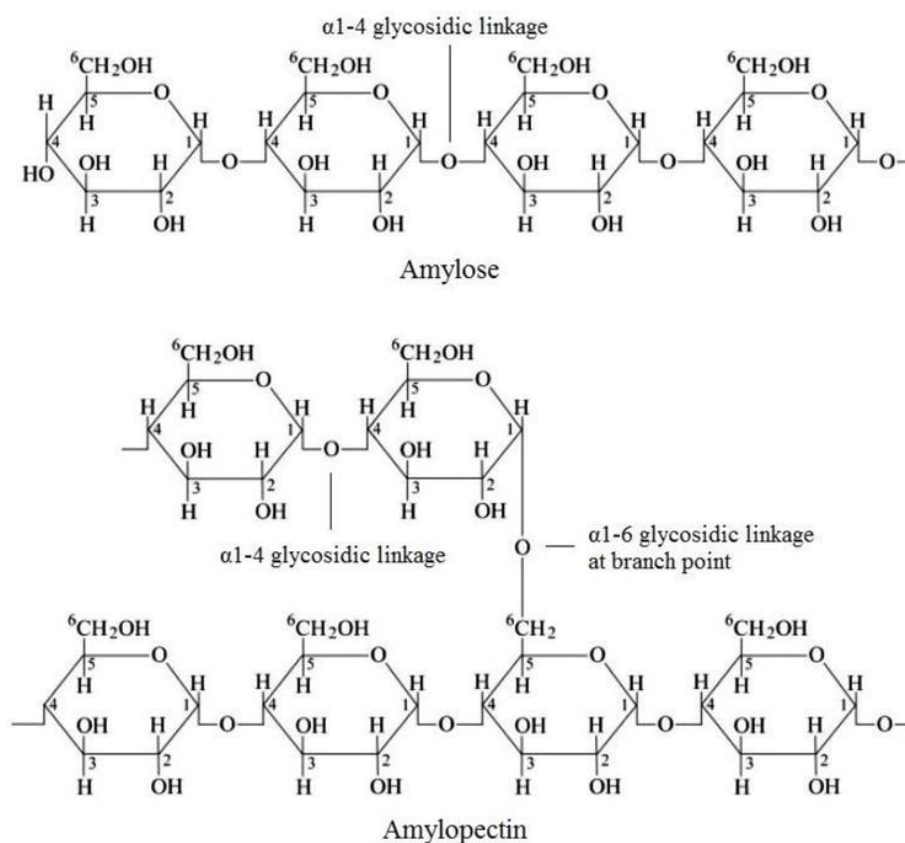


Figure 2.2 Structure of amylose and amylopectin in starch (Nawaz *et al.*, 2020).

In food applications, starch finds use as a thickener, emulsion stabiliser, flowing aid, encapsulating agent and gelling agent (Gulu, 2018) and in non-food applications, it finds use in adhesives, fermentation, papermaking additives, coatings, cosmetics, fillers and serves as a carrier material in pharmaceuticals (Oyeyinka *et al.*, 2015). Starch is a good energy source as it is digested into glucose units which are then used by body cells for energy (Kim *et al.*, 2015). As a natural polymer, starch is attractive because it is biodegradable, non-toxic, non-immunogenic, biocompatible, economic and has good chemical reactivity (Spizzirri *et al.*, 2010; Song, 2011). Bambara groundnut consists of 50% starch (Yao *et al.*, 2015) of which 20-35% is amylose (Kaptso *et al.*, 2014; Oyeyinka *et al.*, 2015; Gulu *et al.*, 2019). The starch content of BGN is comparable to that of potato (15-23%) and maize (24-25%) (Oyeyinka *et al.*, 2016) which are widely used as starch sources in the food industry. With the increasing demand for starch due to decreased cereal production following climate changes (Gammans *et al.*, 2017), BGN starch has potential as an alternative.

Several morphologies of Bambara groundnut starch (BGNS) particles have been reported. It has been described as round, oval and elliptical with non-ruptured smooth surfaces (Sirivongpaisal, 2008; Gulu *et al.*, 2019), oval or irregularly shaped (Oyeyinka *et al.*, 2015), polygonal shaped (Oyeyinka *et al.*, 2016) and spherical for starch from the black BGN

variety (Kaptso *et al.*, 2014). The morphology of BGNS is commonly studied using scanning electron microscopy (SEM) and sometimes light microscopy (Adebowale *et al.*, 2002; Oyeyinka & Oyeyinka, 2017). Variations in morphology are dependent on cultivar, the growth stage of plant, variety, environmental factors, extraction methods as well as purity of the starch (Oyeyinka & Oyeyinka, 2017). The chemical properties of BGNS studied by various researchers are presented in Table 2.2.

Table 2.2 Chemical composition of Bambara groundnut starches

Moisture (%)	Ash (%)	Protein (%)	Fat (%)	Reference
12.80	0.10	0.90	0.10	Kaptso <i>et al.</i> (2014)
14.11	0.21	1.77	2.59	Afolabi <i>et al.</i> (2018)
9.10	0.10	0.30	0.10	Oyeyinka & Oyeyinka (2017)
8.90	0.30	0.30	0.20	Oyeyinka & Oyeyinka (2017)
-	0.47	0.61	0.44	Sirivongpaisal (2008)
9.30	0.20	0.40	0.10	Oyeyinka & Oyeyinka (2017)
8.50	0.20	0.80	0.40	Oyeyinka & Oyeyinka (2017)
8.60	0.20	0.60	0.10	Oyeyinka & Oyeyinka (2017)
12.30	0.20	1.10	0.10	Kaptso <i>et al.</i> (2014)

The industrial utilisation of native starch is very restricted because of its undesirable characteristics such as gelatinisation, retrogradation, the tendency to syneresis as well as instability to elevated temperatures, shear and pH (Ashogbon & Akintayo, 2014; Winarti *et al.*, 2014; Wang *et al.*, 2015). As such, several methods are commonly employed to modify starch so it can be suitable for food applications (Ashogbon & Akintayo, 2014). Starch modification techniques can be broadly grouped into physical, enzymatic and chemical methods (Neelam *et al.*, 2012 Gulu, 2018).

2.3 Composites

Consumer concerns about food quality and health have shifted the focus of researchers towards the use of composites and nanocomposites in food systems (Singh *et al.*, 2017). Composites are functionalised molecules that consist of two types of components, the matrix and the filler. The matrix protects the filler while the filler reinforces the matrix (Spizzirri *et al.*, 2010). Nanocomposites are polymeric composites filled with nanosized rigid particles (Kim *et al.*, 2015). Compared to simple composites, nanocomposites are more superior in terms of mechanical and thermal properties, recyclability and they have a relatively low weight (Kim

et al., 2015; Singh *et al.*, 2017). Furthermore, nanoparticle-based materials have high solubility, viscosity, aggregation, gelation, foaming and stability which can be applied in areas like macromolecular purification, microencapsulation, food formulations and synthesis of biomaterials (Schmitt *et al.*, 1998, Ye, 2008). They are preferred because of their safety, stability, nutritional benefits, biocompatibility, biodegradability and relatively low cost (Yin *et al.*, 2015).

Nanocomposites are divided into two categories, namely, food nanostructured ingredients and food nanosensing ingredients (Singh *et al.*, 2017). Nanostructured ingredients have a wide range of functions in food manufacturing where they can be used as additives, carriers of active compounds, anti-caking agents, antimicrobial agents as well as fillers for improving the robustness of packaging materials (Roselli *et al.*, 2003). Nanosensing ingredients are employed to improve food quality, safety, sensory and shelf life of foodstuffs (Singh *et al.*, 2017).

Polymer-polymer composites have been studied by various researchers (Bos & van Vliet, 2001; Benichou *et al.*, 2002; Dickinson, 2003; McClements *et al.*, 2007, Mackie, 2009; Evans *et al.*, 2013) yet they remain one of the most challenging topics to understand (Doublier *et al.*, 2000).

2.3.1 Synthesis of composites

Several methods can be employed in the formation of composites. These include complex coacervation, desolvation, reactive extrusion, crosslinking, free radical-induced grafting, acid hydrolysis and self-assembling (Bhattacharya & Misra, 2004; Spizzirri *et al.*, 2010; Song *et al.*, 2012; Winarti *et al.*, 2014; Yu *et al.*, 2014). The choice of method is dependent on factors such as source of polymer, physicochemical stability, employed active agent and the desired end use of composite (Yang *et al.*, 2015). Some of the methods used in the formation of composites are discussed in the following sections.

1. Free radical grafting

Grafting is a method of modifying natural or synthetic polymeric materials to improve their physicochemical properties by covalently binding monomers onto a polymer chain (Bhattacharya & Misra, 2004). Free radical grafting as described by Spizzirri *et al.* (2010) involves the employment of an ascorbic acid/hydrogen peroxide redox pair as an initiator system. This redox system generates free radicals that react with monomers forming copolymers. Hydrogen peroxide oxidises ascorbic acid-forming hydroxyl and ascorbate radical intermediates (Spizzirri *et al.*, 2010). When added to polysaccharides, the ascorbic acid/hydrogen peroxide pair catalyses the activation of the polysaccharide chains towards radical reaction. The initiator system produces hydroxyl radicals that extract H⁺ atoms from the polysaccharide's OH⁻ groups (Gulu, 2018). This leaves the polysaccharide chain

exposed allowing other reaction groups to form self-aggregates by forming intra- and inter-molecular associations.

2. *Acid hydrolysis*

Acid hydrolysis involves the use of acids such as hydrochloric and sulphuric acids. This method requires a neutralising step using a base such as sodium hydroxide and a washing step (Winarti *et al.*, 2014). Acid hydrolysis is widely used because it is simple and easy to control (Kim *et al.*, 2015). The drawback of acid hydrolysis is the possibility of acid residue in the composites.

3. *Self-assembly*

Self-assembly is an aqueous procedure important in the creation of materials with a controlled nanostructure. This procedure is desirable as it does not involve the use of any harsh solvents or reaction conditions (Yang *et al.*, 2015). Ethanol is commonly employed to initiate self-assembly. It is mostly used on water-soluble polymers modified by hydrophobic groups such as alkyl and deoxycholic acid. When polymeric amphiphiles are dissolved in water, they spontaneously form intra- and inter-molecular associations between hydrophobic moieties. The nanostructure formed as a result of self-assembly is capable of trapping various proteins and other hydrophobic substances (Yang *et al.*, 2015).

4. *Crosslinking*

Polysaccharides possessing carboxylic groups on their molecular chains can bind with bivalent calcium ions to form nanoparticles. The use of sodium trimetaphosphate in crosslinking starch and soluble dietary fibre was reported by Liu *et al.* (2015). The researchers successfully conjugated soluble dietary fibre and starch granules and reported improved physicochemical properties in the resultant composites. Soluble dietary fibre binds to starch either by reacting with the 2, 3 and 6 OH groups of glucose molecules or by linking to the amorphous part of starch derived from destructured starch granules (Liu *et al.*, 2015). In the former, soluble dietary fibre would form a protective layer around the starch thereby forming a composite of high resistance and strength and in the latter, a highly homogenous but low strength nanocomposite would be formed.

5. *Complex coacervation*

Complex coacervation is a process where two aqueous solutions of polymers with opposite charges are mixed (Yang *et al.*, 2015). The coacervation effect can be induced by the addition of agents such as alcohols and salts. An example is the addition of ethanol to a solution containing two polymers followed by crosslinking with polyethylene glycol-di-aldehyde in silver nitrate solution (Berthold *et al.*, 1996). Particles with sizes between 1.5-2.5

μm can be obtained using this method. The drawbacks of complex coacervation are that the use of a potential toxic desolvating agent requires a purification step hence making the method costly (Yang *et al.*, 2015). Furthermore, there is a possibility of toxic residue in the composites.

6. *Mechanical treatments*

Homogenisation and/or thermal treatments can be used in the preparation of polysaccharide composites. This method involves the mixing of polysaccharides on a dry basis at different ratios, adding water then stirring at 200 rpm for 24 hours at room temperature to enable complete hydration (Russ *et al.*, 2016).

7. *Thermal treatments*

Thermal treatments can be used with other methods or on their own. When used on their own, they involve the preparation of a film solution by dissolving two polysaccharides in water, stirring at 40°C followed by the addition of glycerol. The resultant mixture is heated at high temperatures coupled with continuous stirring to allow for the complete gelatinisation of starch (Saber *et al.*, 2016).

2.3.2 Analytical techniques used to characterise and verify composites

Several techniques are used in the characterisation and verification of biopolymer composites. These include but are not limited to Fourier transform infrared spectroscopy (FTIR), differential scanning calorimetry (DSC), thermogravimetric analysis (TGA), scanning electron microscopy (SEM), fluorescence spectroscopy and powder X-ray diffraction (XRD). All these six analytical techniques were carried out in this study to confirm the successful grafting of BGN-SDF onto BGNS. Most researchers usually make use of only one or two methods to characterise modified starch (Gulu, 2018); however, in this research study, six methods were used for more conclusive results.

1. *Fourier transform infrared spectroscopy*

Fourier transform infrared spectroscopy (FTIR) assesses the functional groups present in a sample and produces data in the form of infrared spectra (IR) observed as peaks (Kasran, 2013). This technique provides information based on the physicochemical composition of a sample (Oyeyinka & Oyeyinka, 2017). In this research study, this technique was used to confirm the presence of carbon, hydrogen and oxygen which make up the bulk composition of starch, soluble dietary fibre and the new composite formed from the conjugation of the two biopolymers. The successful formation of a new composite would be demonstrated by a shift of the spectral peaks, the formation of new absorption peaks or the disappearance of existing peaks (Gulu, 2018).

2. *Thermal characterisation techniques*

The study of the thermal behaviour of materials is significant in understanding the behaviour of a material when subjected to different temperatures (Gill *et al.*, 2010). The information obtained from thermal studies gives insight into the performance of a material and allows for the prediction of the behaviour of the material when exposed to elevated temperatures.

Differential scanning calorimetry assesses the heat stability of materials by studying the changes in their physical properties against temperature and time (Maphosa, 2016). In DSC, a sample is placed in a pan and placed directly above a constantan disc and the adsorption of heat by the sample is measured by a chromel-alumel thermocouple (Liu, 2015). The difference in temperature across the reference chromel wafers and the sample measures heat flow and the thermal behaviour of the material is observed as peaks. The data reveals the onset, maximum and end of each peak (Zhang & Wang, 2013). Negative enthalpy changes of reaction (ΔH) indicate exothermic reactions, meaning the samples release energy as they combust and are therefore charred instead of volatilised when they degrade. Positive enthalpy changes of reaction (ΔH) indicate endothermic reactions, meaning the samples absorb energy as they combust (Yang *et al.*, 2007). The high thermal stability of material is indicative of the presence of strong intra- and inter-molecular bonds (Tarasov, 2012).

Thermogravimetric analysis (TGA) measures the change in mass of a sample as a function of temperature or time (Groenewoud, 2001). The data obtained provides information about the composition of material as well as phase transitions, absorption, adsorption, desorption, thermal decomposition, oxidation and/or reduction (Rajisha *et al.*, 2011). A thermogravimetric analyser continuously measures the mass of a sample while the temperature changes over time (Anon., 2000). Mass, temperature and time are considered base measurements in TGA. Data is presented in the form of a thermograph plotted as mass against temperature (Rajisha *et al.*, 2011). The thermogravimetric analysis gives the stable temperature range of a material beyond which the material will degrade (Tarasov, 2012).

3. *Powder X-ray diffraction*

Powder XRD is used to determine starch crystallinity (Gulu, 2018). According to XRD patterns, starch crystallinity can be described as Type A, B or C (Wang *et al.*, 2015). The A- and B- types differ in their level of hydration as well as in the manner in which the double helices formed from short chains within the amylopectin molecule are arranged (Gulu, 2018). Type C consists of a mixture of type A and B polymorphs with peaks at 15, 17 and 23° (Sandhu & Lim, 2008). Type A starch exhibits peaks at 15, 23 and 27° and is tightly packed with water molecules between each double helix. Type B is less closely packed, has more

water molecules in the central cavity and exhibits peaks at 5, 6 and 17° (Oyeyinka *et al.*, 2015). Type C starch can be further classified as C_A-type (closer to A-type), C_B-type (closer to B-type) and C_C-type (typical C-type) depending on the ratio of A- and B-type allomorphs. The crystallinity patterns of C_A- and C_B-type starches resemble that of C_C-type, but exhibit a shoulder peak at about 18° 2 θ . A strong singlet peak is exhibited at 23° 2 θ for C_A-type starch while two shoulder peaks at about 22° and 24° 2 θ for C_B-type starch are common (Kaptso *et al.*, 2014). Type C crystallinity is typical for legume starches (Hoover *et al.*, 2010) and has been reported for BGN starch (Afolabi, 2012; Oyeyinka *et al.*, 2015). However, type A crystallinity in BGN starch has also been reported by some researchers (Sirivongpaisal, 2008). Literature suggests that BGN starch is more likely to be type C than type A because it is a legume and type A is typical for cereal starches (Gulu, 2018).

4. *Scanning electron microscopy*

Scanning electron microscopy gives the morphology and microstructure of biopolymers and proves useful in studying the physicochemical properties, purity and integrity of biopolymer granules (Diedericks, 2014). Typical leguminous starch is round, oval and exhibits elliptical shapes with smooth, unruptured surfaces (Adebowale *et al.*, 2002; Sirivongpaisal, 2008; Kaptso *et al.*, 2014; Oyeyinka *et al.*, 2015). Fractured surfaces are an indication of impurities in extracted starches (Sirivongpaisal, 2008; Oyeyinka *et al.*, 2015; Gulu, 2018). Oval and irregularly shaped as well as polygonal and spherical shaped BGN starch granules have also been reported in the literature (Kaptso *et al.*, 2014; Oyenyika & Oyenyika, 2017; Enyidi & Onyenakazi, 2019). Variances in shapes and sizes of starch granules are attributed to different cultivars, growth stage at harvest, environmental factors as well as milling, extraction and purification methods (Sirivongpaisal, 2008; Kaptso *et al.*, 2014; Oyeyinka *et al.*, 2015; Oyeyinka *et al.*, 2016). Non-starch polysaccharides like dietary fibre commonly exhibit irregular and polygonal morphologies (Diedericks, 2014; Maphosa & Jideani, 2016). Morphologies similar to those of BGN starch have been reported for pea starch (Dalgetty & Baik, 2003; Elleuch *et al.*, 2011). Other studies on starches have reported round, polygonal shapes with heterogeneous sizes for yellow sorghum (Olayinka *et al.*, 2015), a mixture of oval, spherical and ellipsoid granules for yellow ginger (Zhang *et al.*, 2011) as well as oval and round granules with heterogeneous sizes for Jack bean starch (Lawal & Adebowale, 2005).

5. *Fluorescence spectroscopy*

Fluorescence spectroscopy involves the absorption and fluorescence of wavelengths and the subsequent collection of the excitation and emission spectra. It is a non-destructive analytical technique that provides information on the presence of fluorescent molecules (Skoog *et al.*, 2006). Intrinsic emission fluorescence spectroscopy is a reliable procedure

that can be used to accurately reveal the conformational changes in modified starches (He *et al.*, 2006). The method is precise, rapid, does not require the use of special reagents or incubations and is highly sensitive and specific with low detection limits (Skoog *et al.*, 2006).

2.4 Emulsions

An emulsion is a colloid that consists of two immiscible liquids, usually oil and water, with one of the liquids dispersed in the other (Robins *et al.*, 2002; McClements *et al.*, 2007). Emulsions consist of two phases; a dispersed and a continuous phase, with the former consisting of the particles that make up the droplets and the latter being the surrounding liquid in which the droplets are dispersed (Robins *et al.*, 2002). They can be categorised according to the relative spatial distribution of the oil and aqueous phases, the nature of the emulsifying agent or the arrangement of the system as shown in Table 2.3.

Table 2.3 Classification of different types of emulsions

Nature of emulsifier	System organisation	Reference
Non-ionic surfactants	Oil-in-water, water-in-oil	Ghosh & Rousseau (2012)
Ionic surfactants	Macro-emulsions	Zhang <i>et al.</i> (2011)
Mixture of surfactants	Micro-emulsions	Benichou <i>et al.</i> (2002)
Non-ionic polymers	Bilayer droplets	Mao & Miao (2015)
Polyelectrolytes	Multiple emulsions	Singh & Kumar (2014)
Mixture of polymers and surfactants	Mixed emulsions	Zhang <i>et al.</i> (2011)
Solid particles	Pickering emulsion	Tadros (2013)
Liquid crystalline phases	Glassy emulsion	Tadros (2013)

Examples of types of emulsions include oil-in-water (O/W), water-in-oil (W/O), macro-emulsions, micro-emulsions, bilayer droplets, multiple emulsions, mixed emulsions, pickering emulsions and glassy emulsions (McClements *et al.*, 2007, Ghosh & Rousseau, 2012; Tadros, 2013, Singh & Kumar, 2014). The most common emulsions are O/W and W/O emulsions, with the former being more popular than the latter (Williams, 2001). Many food products such as butter (W/O), margarine (O/W), mayonnaise (O/W), salad dressings (O/W), vinaigrettes (O/W), homogenised milk (O/W), beverages (O/W) and ice cream (O/W) consist partly or fully of emulsions (Piorkowski & McClements, 2014). Emulsions can be further classified according to droplet size into three categories, namely, conventional emulsions (d

> 200 nm), microemulsions ($d < 100$ nm) and nanoemulsions ($d < 200$ nm) (Given, 2009; Zhang & McClements, 2016).

2.4.1 Beverage emulsions

Beverage emulsions are one of the most produced and profitable drinks worldwide (Piorkowski & McClements, 2014). Beverage emulsions are described as flavour emulsions if they contain lipophilic compounds such as lime and orange terpenes to provide aroma and taste and as cloud emulsions, if they contain flavourless vegetable oil and provide turbidity (Shachman, 2004). Beverage emulsion production is a two-step process. Firstly, a beverage concentrate (3-30 wt% oil) is manufactured then diluted to make the final product (<0.1 wt% oil). In the production of beverage emulsions, high energy or low energy homogenisation methods are commonly employed (Given, 2009). High energy homogenisation methods involve mixing all the aqueous ingredients and the oil ingredients separately, then applying thermal or mechanical energy to both systems to facilitate dissolution and dispersion (Maphosa, 2016). The aqueous and oil mixtures are then mixed using high shear mixers and homogenised to further reduce droplet size ($d = 0.1-1$ nm). On the other hand, low energy homogenisation methods involve mixing all the aqueous and oil ingredients and converting the mixture into an emulsion either by phase inversion or spontaneous emulsification (Piorkowski & McClements, 2014).

2.4.2 Emulsion stability

Emulsion stability refers to the ability of the different phases of an emulsion to remain mixed together (Maphosa *et al.*, 2017) and to resist changes to its structure while maintaining its physicochemical properties over a while (Dickinson, 2009; Eltayeb *et al.*, 2011; Fasinu *et al.*, 2015; Mubaiwa *et al.*, 2018). The extent of emulsion stability is determined by various factors such as particle size, particle size distribution, density between the dispersed and continuous phases as well as the chemical integrity of the dispersed phase (Given, 2009). The stability of an emulsion determines its shelf-life (Anon., 2011).

Emulsions are thermodynamically unstable systems (Ghosh & Rousseau, 2011) due to different densities between the oil and aqueous phases and the unfavourable contact between oil and water molecules (Kerkhofs *et al.*, 2011; Maphosa *et al.*, 2017). The major challenge faced by formulators is maintaining the stability of beverage emulsions because of their very dilute nature (Daniells, 2010). Phenomena such as flocculation, coalescence, Ostwald ripening, creaming, phase inversion, oxidation and degradation are responsible for the destabilisation of emulsions (Zhang, 2011) as illustrated in Figure 2.3.

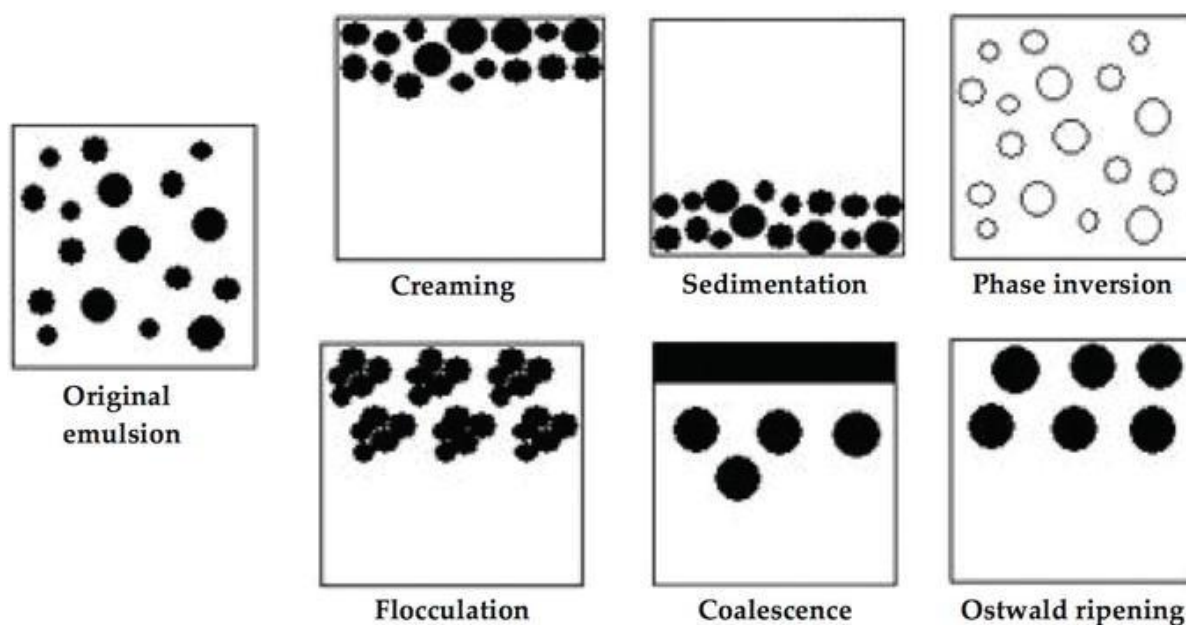


Figure 2.3 Mechanisms of emulsion destabilisation (McClements, 2005).

Flocculation is the process where droplets in an emulsion are attracted to each other and form flocs without the rupture of the stabilising layer at the interface (Adeyi, 2014; Mao & Miao, 2015). Droplet flocculation occurs due to gravitational force, centrifugation, Brownian forces as well as when the repulsive energy is less than van der Waals energy (Payet & Terentjev, 2008). This phenomenon is undesirable as it promotes creaming and reduces clouding due to larger particle sizes as well as promotes coalescence due to droplets being brought closer together (Chanamai & McClements, 2000).

Creaming (upward) and sedimentation (downward) occur as a consequence of gravitational separation (Mao & Miao, 2015). These occur when emulsion droplets merge together forming bigger droplets or when the droplets rise to the surface of the emulsion due to buoyancy. This is usually a result of gravitational force, when the density of the dispersed phase is less than the density of the continuous phase (Zhang, 2011; Tadros, 2013). This phenomenon usually results in a separated emulsion with a droplet-rich cream layer and a droplet-depleted watery layer (Mao & Miao, 2015).

Creaming is usually a precursor of coalescence and is followed by phase separation. It occurs gradually and at different rates depending on the emulsion. As it progresses, the emulsion eventually loses its stability. Its extent in O/W emulsions can be described using the creaming index (Anon., 2011). The creaming index gives insight into the extent of droplet aggregation that has occurred, as such, a higher creaming index means more droplets have agglomerated (Onsaard *et al.*, 2006). Creaming can be measured by visual observation or by optical imaging and can be reduced by adding a thickener to the continuous phase (Adeyi, 2014). Coalescence is the process where droplets come into contact, merge and create

larger droplets. With time, this reduces the stability of the emulsion (Adeyi, 2014). Ostwald ripening is a phenomenon where larger droplets expand at the expense of smaller ones and is largely affected by the solubility of the dispersed phase in the continuous phase (Jiao & Burgess, 2003; Zhang, 2011). These mechanisms of destabilisation occur due to the nature and concentration of emulsifier or stabiliser, pH of the system, ionic strength, temperature, homogenisation parameters and interaction of the dispersed with the continuous phase (McClements, 2005; Sjoblom, 2006).

Substances such as emulsifiers, stabilisers, weighting agents, ripening inhibitors and texture modifiers (thickeners and gelling agents) are introduced to increase the kinetic stability of emulsion systems for longer periods (Shachman, 2004; Payet & Terentjev, 2008; Kerkhofs *et al.*, 2011). To produce a fine emulsion, large droplets are broken down into smaller ones by the application of intense mechanical energy (Dickinson, 2009). For food emulsions, this is commonly accomplished using high-speed mixers, colloid mills or high-pressure valve homogenisers (Dickinson, 2009). From a thermodynamic level, the emulsification process is very inefficient as most of the energy applied is dissipated as heat. The final droplet size of an emulsion is largely determined by the time taken to cover the interface with the emulsifier (Dickinson, 2003). A slow emulsification rate results in the small droplets formed during emulsification coalescing or flocculating.

Various tests and instrumentation for characterising and predicting the stability of emulsions have been developed over the years. These give data on the change in droplet size and concentration with time and subsequently on the extent of stability and destabilisation phenomena (Gabriel *et al.*, 2013; Maphosa, 2016). The Turbiscan was employed in this study. This instrument is based on the principle of light scattering in which a monochromatic beam of near infrared light is directed through an emulsion placed in a vertical flat-bottomed glass tube. The Turbiscan is fitted with a transmission detector, which receives light passing through the sample and a backscattering detector, which receives light reflected by the sample (Diedericks, 2014). The amount of transmitted or backscattered light is measured as a function of the height of the emulsion (Adeyi, 2004). The data obtained from the Turbiscan studies gives information on the changes in droplet concentrations along the height of the emulsion and is used to determine creaming and/or sedimentation/flocculation. Creaming is generally observed as a change in backscattering flux at the bottom and top of the sample and is observed as a peak in delta backscattering curves between 0-20 mm. Flocculation, coalescence and/or sedimentation are observed as a decrease in backscattering over the entire height of the sample in the optimum zone of 20-50 mm (Alvarez-Cerimedo *et al.*, 2010).

2.4.3 Emulsion stabilisers

Stabilisers are a group of additives that are capable of stabilising emulsions by forming a fine film coating around individual oil droplets thereby increasing their density as well as increasing the viscosity of the aqueous phase (Weiss, 2005). In this manner, they reduce the rate of creaming and the ultimate destabilisation of the system (Shachman, 2004). Stabilisers are usually hydrophilic in nature and include modified starch, pectin, gum Arabic, gum tragacanth, xanthan gum and carrageenan. They may be classified either as emulsifiers or texture modifiers depending on their mode of action (Yang & Lai, 2003). Furthermore, texture modifiers can also be divided into two categories, namely, thickening agents and gelling agents, depending on their mode of operation and the rheological characteristics of their solutions (Stern *et al.*, 2001). Thickening agents increase the viscosity of emulsions, whereas gelling agents form a gel in the continuous phase of emulsions. Therefore, stabilisers enhance emulsion stability by retarding the movement of the droplets (Kerkhofs *et al.*, 2011).

Emulsifiers are surface active molecules that adsorb to the surface of freshly formed droplets of an oil-water interface during homogenisation, forming a protective membrane that prevents the droplets from aggregating (Zhang, 2011). As such, emulsifiers act as surface-modifying substances at the interface between each droplet and the continuous phase (Robins *et al.*, 2002). They are amphiphilic in nature; possessing both hydrophilic portions that align with the aqueous phase and hydrophobic portions that align with the lipid phase (Cottrell & van Peij, 2014). In this manner, they act as surface-modifying substances at the interface between each droplet and the continuous phase (Robins *et al.*, 2002). Emulsifiers form a close-packed layer at the interface with a low interfacial tension. This results in an emulsion with a small droplet size distribution, stabilised by the fluid Gibbs-Marangoni mechanism or weak electrostatic repulsion (Robins *et al.*, 2002; Dickinson, 2008).

2.5 Biopolymers in food systems

Biopolymers are long chain molecules composed of monomers covalently bonded together to form larger structures. They can be divided into three groups, namely, polysaccharides, polypeptides and polynucleotides (Mohan *et al.*, 2016). Polysaccharides that have been studied include dietary fibre, starch, dextran, maltodextrin, pectin and carboxymethylcellulose (CMC) as well as many other hydrocolloids (Dickinson, 2009). Although polymer-polymer complexes have been studied by various researchers (Bos & van Vliet, 2001; Benichou *et al.*, 2002; Dickinson, 2003; Mackie, 2009; Sanchez & Patino, 2005; McClements *et al.*, 2007; Bandyopadhyay *et al.*, 2012; Evans *et al.*, 2013), they still remain one of the most challenging topics to understand (Bandyopadhyay *et al.*, 2012; Doublier *et al.*, 2000). These complexes are preferred in the food industry because of their sustainability, non-toxicity, non-immunogenicity, biocompatibility, good chemical reactivity, relatively low cost (Spizzirri *et al.*,

2010; Song, 2011), stability, nutritional benefits, biodegradability (Yin *et al.*, 2015) as well as their generally-recognised-as-safe (GRAS) status. Furthermore, the replacement of synthetic stabilisers with natural biopolymers gives products a 'cleaner' label.

Biopolymers are inherently present in food systems and they play a major role in food structure and stability (Gao *et al.*, 2017). In emulsions, they exhibit various modes of action that reduce the rate of coalescence and creaming (Kerkhofs *et al.*, 2011). Before a biopolymer hybrid can be applied as a stabiliser, it is of utmost importance to understand the interaction between the individual polymers, their phase behaviours as well as their interaction with the system (Jia *et al.*, 2014). An understanding of the science behind the phase behaviour of a biopolymer system helps the formulator in designing and controlling the microstructure of the product (Jia *et al.*, 2014). Furthermore, since the phase morphology and interactions in polymeric mixtures largely influence the technological and functional properties of materials, having this knowledge beforehand is vital in predicting the behaviour of the product during processing, handling and distribution (Yang *et al.*, 2013; Hanazawa & Murray, 2014).

Biopolymers such as polysaccharides and proteins are widely employed as functional ingredients in emulsion systems (Bandyopadhyay *et al.*, 2012). Most biopolymers have the ability to stabilise emulsions, but only a few possess emulsifying properties (Evans *et al.*, 2013). Being an emulsifier requires extensive surface activity at the oil-water interface, which is absent in most biopolymers such as polysaccharides (Dickinson, 2009). The most commonly used polysaccharides in food include gum Arabic, modified starch, modified cellulose, pectin and galactomannans (Cottrell & van Peij, 2014, Castellani *et al.*, 2010; Lim & Baik, 2011). The effectiveness of biopolymers as stabilisers is highly dependent on concentration and rate of adsorption (de Souza & Rojas, 2012). At low concentrations, the biopolymer may fail to cover the entire surface of droplets, resulting in coalescence and consequent destabilisation (Zhao *et al.*, 2015).

Biopolymers stabilise emulsions either by modification of the rheological properties of the bulk phase or adsorption at the oil-water interface, thereby providing a steric or an electrosteric barrier, or a combination of the two effects (Koocheki *et al.*, 2009). Proteins, on the other hand, have been reported to stabilise emulsions by forming a viscoelastic adsorbed layer on the oil droplets, which forms a physical barrier, hindering the contact of droplets, thus reducing coalescence and flocculation (Robins *et al.*, 2002; Guzey & McClements, 2006).

2.5.1 Polysaccharide conjugates in emulsions

There is growing interest in harvesting the combined beneficial attributes of biopolymers as emulsifiers and stabilisers (Dickinson, 2009; Koocheki *et al.*, 2009). Some polysaccharide-

polysaccharide and polymer-polysaccharide conjugates that have been studied are given in Table 2.4.

Table 2.4 Polymer-polysaccharide complexes

Polysaccharide	Polymer	Reference
Dextran	Soybean protein	Bouyer <i>et al.</i> (2012)
Soybean polysaccharide	Pea protein	Yin <i>et al.</i> (2015)
Dextran	Whey protein	Dickinson (2009)
Carboxymethylcellulose	Egg yolk protein	Lim & Baik (2011)
Pectin	Whey protein	Dickinson (2009)
Gum Arabic	Flaxseed protein	De Kruif & Tuinier (2001).
Pectin	Pea protein	Jimenez-Castano <i>et al.</i> (2007)
Soluble dietary fibre	Starch	Liu <i>et al.</i> (2015)
Soybean polysaccharide	Pea protein	Yin <i>et al.</i> (2015)
Gum Arabic	Flaxseed protein	Diftis <i>et al.</i> (2005)
Dextran	Whey protein	Flanagan & Singh (2006)
Pea starch	Guar gum	Saberi <i>et al.</i> (2016)
Carboxymethylcellulose	Ovalbumin	Jia <i>et al.</i> (2014)
Wheat starch	Whey protein	Yang <i>et al.</i> (2013)
Xanthan	Whey protein	Oliver <i>et al.</i> (2006)
Pectin	Gelatin	Oliver <i>et al.</i> (2006)
Starch	Gelatin	Oliver <i>et al.</i> (2006)
Sugar beet pectin	Gum Arabic	Gao <i>et al.</i> (2017)

Many emulsions constitute polysaccharide-protein combinations (Ron & Rosenberg, 2002). These biopolymers are excellent ingredients in food emulsions as they alter the rheological characteristics of the system through their gelling networking system (McClements, 2005; (Rodriguez Patino & Pilosof, 2011). Polysaccharides, mostly being hydrophilic, tend to remain dispersed within the aqueous phase, increasing thickening and gelling. Although some polysaccharides can adsorb at a globule surface, most stabilise emulsions by increasing the viscosity of the continuous phase, thus impeding droplet movement (Bouyer *et al.*, 2012). The combination of the properties of biopolymers under appropriate conditions leads to improved physicochemical and functional properties (Bouyer *et al.*, 2012).

Figure 2.4 shows a representation of the possible mode of interaction between polysaccharides and proteins.

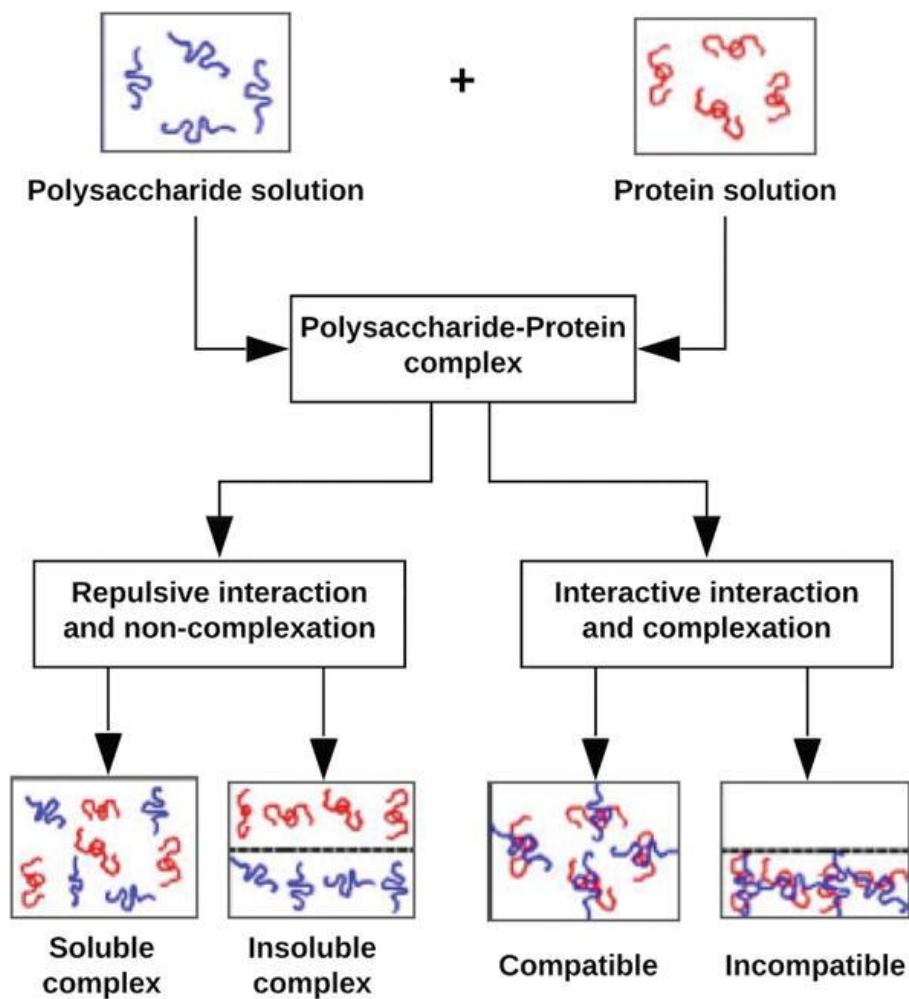


Figure 2.4 Possible mode of interaction between polysaccharides and proteins.

Polysaccharides such as xanthan, when used in emulsion systems, control texture and stability. They influence pseudoplastic flow at low concentrations as well as retard the rate of creaming and/or sedimentation of particles under inert or low shear conditions yet allow production processes such as pumping and filling under high shear (Hanazawa & Murray, 2014).

2.6 Biopolymer complexation and phase behaviour

The covalent linkage of polysaccharides to other polymers can be obtained using chemical (Diftis *et al.*, 2005), enzymatic (Flanagan & Singh, 2006) or thermal treatments (Oliver *et al.*, 2006). Thermal treatment is the most commonly used of the techniques and involves exposing a dry mixture of the biopolymers to heat (Oliver *et al.*, 2006). This heat-induced complexing has been reported to improve solubility and stability under undesirable medium

conditions such as high temperatures, low pH and high ionic strength (Oliver *et al.*, 2006). Mixtures of biopolymers in aqueous media influence the phase behaviour of the system, influencing the overall structural and textural properties and ultimately their stability (Mession *et al.*, 2012). Such mixtures display one of three equilibrium states; miscibility, complex coacervation or thermodynamic incompatibility (Jia *et al.*, 2014). Miscibility occurs when the two biopolymers are co-soluble and are compatible (Mession *et al.*, 2012). Complex coacervation and thermodynamic incompatibility occur at high biopolymer concentration and the former occurs when the net attraction between the biopolymers is attractive while the latter occurs when the net charge is repulsive (Jia *et al.*, 2014; Hanazawa & Murray, 2014).

There are five stages of structural transition involved in the formation of a protein-polysaccharide complex (Gao *et al.*, 2017). These are (1) stable region of mixed individual soluble polymers; (2) stable region of intra-molecular soluble complexes; (3) a partially stable region of inter-molecular soluble complexes; (4) an unstable region of intermolecular insoluble complexes; and (5) a second stable region of mixed individual soluble polymers. Inter-molecular forces are formed between proteins and anionic polysaccharides when these biopolymers carry opposite charges and occur more efficiently when the pH is below the Isoelectric point (pI) of the protein (Mession *et al.*, 2012). A mixture of biopolymers exhibits different phase behaviours with synergistic or antagonistic action, resulting in compatible and incompatible complexes, respectively (Gao *et al.*, 2017).

2.7 Phase separation mechanisms

Phase separation is a phenomenon where biopolymer mixtures are thermodynamically incompatible and therefore separate into distinct phases (Jia *et al.*, 2014; Hanazawa *et al.*, 2014). Initial phase separation in biopolymer systems results in one phase staying continuous while the other remains dispersed through it in the form of discontinuous inclusions (Fitzsimons *et al.*, 2008; Yang *et al.*, 2013). Phase separation is dependent on medium conditions such as pH, ionic strength as well as nature and concentration of biopolymers (Hanazawa & Murray, 2014). At equilibrium, the biopolymer mixture separates into a lower and upper phase, each rich in one of the biopolymers (Mession *et al.*, 2012).

If two biopolymers are used in an emulsion system but do not interact with each other, they exist either in a single-phase system or in a phase-separated system (Evans *et al.*, 2013). In a single-phase system, the two biopolymers exist separately, distributed throughout the medium, while in a phase-separated system, the biopolymers exist as two distinct phases. Phase separation of biopolymer mixtures can be associative or segregative (Tolstoguzov, 2006; Fang *et al.*, 2006; Jha *et al.*, 2014) and can be quantitatively described using phase diagrams, such as the binodal curve (Figure 2.5). The binodal curve separates the region of co-solubility from that of phase separation.

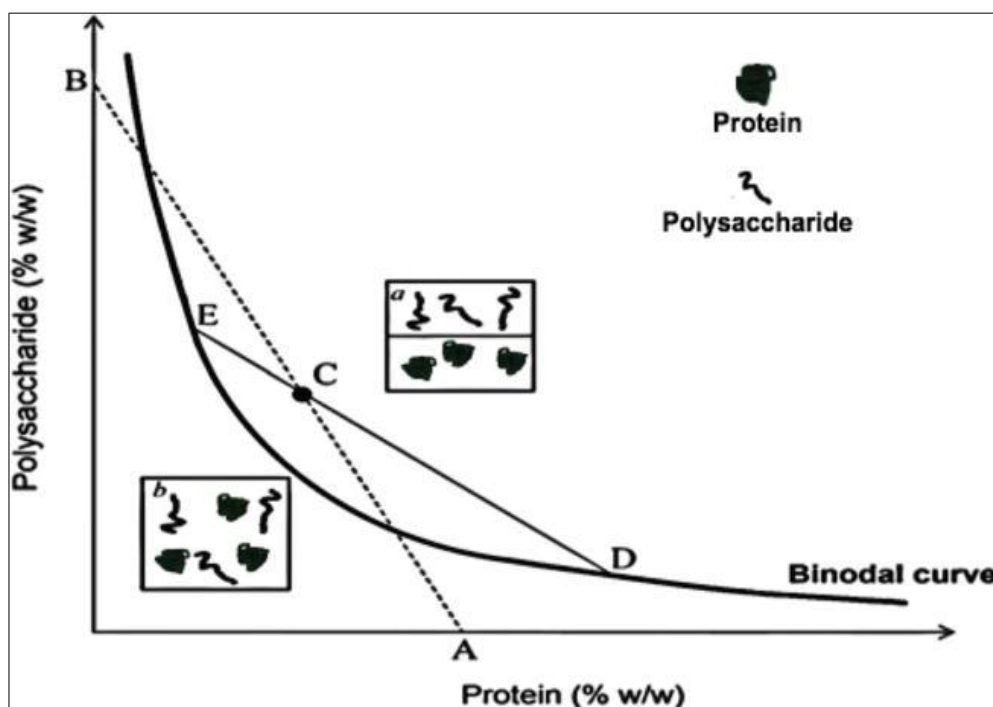


Figure 2.5 Phase separation diagram of a protein-polysaccharide mixture adapted from Maphosa & Jideani (2018).

A: protein; B: polysaccharide; C: initial mixture of protein and polysaccharide; D: composition of protein-rich phase; E: composition of polysaccharide-rich phase; a: distinct separation of phases; and b: biopolymers co-existing but mutually excluding each other.

The separation of the mixture occurs above a certain critical concentration as illustrated in Figure 2.5, below which the biopolymers co-exist in a single-phase and above which a distinct separation of phases is observed (Mohan *et al.*, 2016).

2.7.1 Associative phase separation

Associative phase separation occurs if the two biopolymers are oppositely charged, such as an ionic polysaccharide and a protein, leading to electrostatic attraction and consequently resulting in separation into two clear coacervate/precipitate and supernatant phases (Gao *et al.*, 2017). Essentially, associative phase separation involves the formation of two distinct phases, one very rich in both biopolymers and the other with very small amounts of the biopolymers. The biopolymer rich phase is formed when the soluble biopolymer complexes interact and form neutral aggregates which eventually sediment and form a precipitate (Mohan *et al.*, 2016). Associative phase separation can be reversible or irreversible, depending on the strength of bonds formed. In complexes where one polymer is negatively

charged and the other positively charged, strong electrostatic complexes are formed which may be irreversible. Reversible complexes are formed between negatively charged biopolymers and a negatively charged biopolymer or a biopolymer carrying nearly a zero charge (Maphosa & Jideani, 2017).

2.7.2 Segregative phase separation

Segregative phase separation occurs between two biopolymers carrying a similar charge, two neutral biopolymers or one charged biopolymer and a neutral biopolymer (Maphosa & Jideani, 2017). This leads to electrostatic repulsion or steric exclusion, resulting in mutual exclusion of each polymer from the vicinity of the other and consequently resulting in the two biopolymers separating into two distinct phases (Jha *et al.*, 2014; Gao *et al.*, 2017). This separation mechanism is commonly observed in semi-dilute or concentrated mixed emulsions (Mohan *et al.*, 2016). The mechanism of polysaccharide-polysaccharide separation is presented in Figure 2.6.

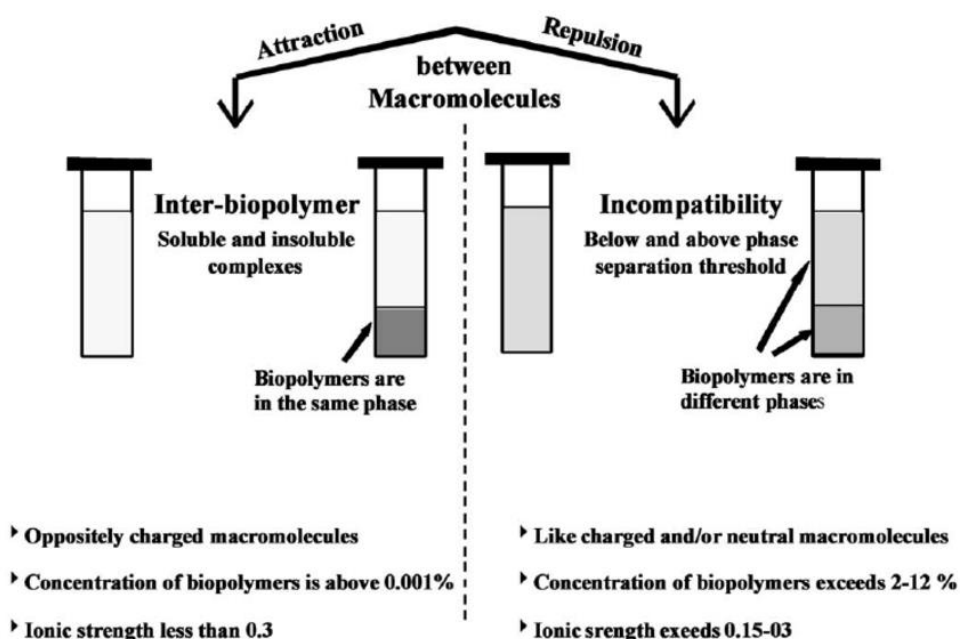


Figure 2.6 Phase behaviour of mixed biopolymer solutions (Tolstoguzov, 2003).

An example of a system that would undergo segregative phase separation is one consisting of gum Arabic and sugar beet pectin. Both hydrocolloids are negatively charged and would therefore repel each other, resulting in separation into two layers (Gao *et al.*, 2017). A mixture of neutral soluble dietary fibre and modified starch in which the OH^- groups have been exposed following the abstraction of H^+ by a redox pair (ascorbic acid/hydrogen peroxide) would experience segregative phase separation. At sufficiently high

concentrations, mixing two similarly charged or uncharged biopolymers may lead to phase separation due to restrictions in the freedom of orientation of the biopolymer molecules Tolstoguzov (2006). An advantage of phase separation is its potential in producing functional components. Molecular fractionation of gum Arabic, when complexed with protein, has been previously reported (Mao & Miao, 2015). The researchers hypothesised that phase separation was responsible for the molecular fractionation and could therefore be used to obtain purified functional components from polydisperse hydrocolloids.

2.8 Rheology

Rheology is the study of the deformation and flow of matter under stress (Maphosa, 2016). In food systems, viscosity is one of the most important parameters of rheology (Sahin & Sumnu, 2006). Materials exhibit Newtonian or non-Newtonian flow behaviour in response to applied shear stress or shear rate (Partal & Ma Franco, 2006). Figure 2.7 illustrates different behaviours of rheological systems.

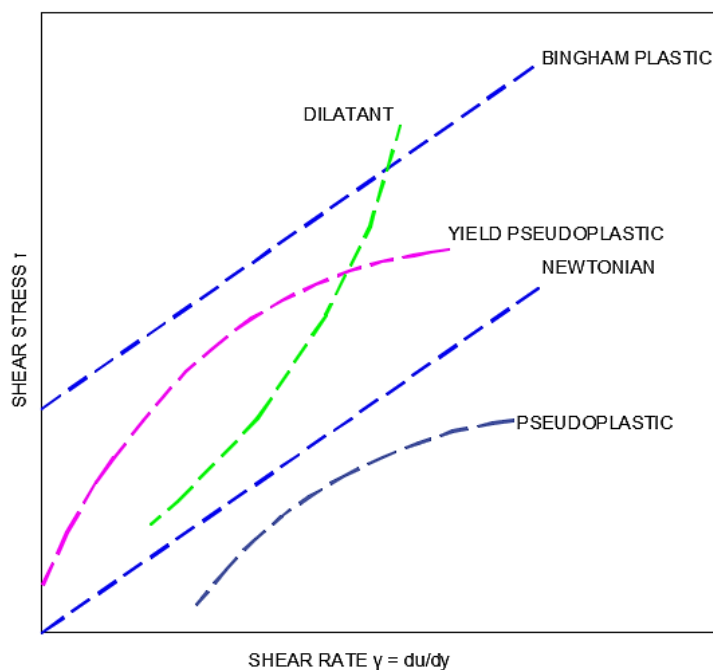


Figure 2.7 Different rheological behaviours (Kelly, 2019).

A Newtonian system is an ideal system where shear stress is directly related to shear rate. In such a system, the viscosity remains constant and reversible under conditions of shear (Chhabra & Richardson, 2008). Newtonian behaviour is observed in systems such as gases, water, glycerol, chloroform as well as true solutions like sugar syrups. The majority of systems exhibit non-Newtonian behaviour (Chhabra & Richardson, 2008). Most non-Newtonian fluids display apparent viscosity, a shear-rate dependent type of viscosity (Partal

& Ma Franco, 2006). When apparent viscosity increases with increasing shear rate, the material is described as shear-thickening and if it decreases with increasing shear rate, the material is described as shear-thinning (Partal & Ma Franco, 2006). At very high or low shear rates, many non-Newtonian systems mimic Newtonian behaviour. Rheology is commonly assessed using a rheometer, such as the one shown in Figure 2.8.



Figure 2.8 Rheometer (Anton Paar, 2020).

A rheometer contains the material of interest in a controlled environment, in a geometric configuration, and measures wide ranges of stress and strain (Muntz, 2017). The study of rheology is used in the food industry for the characterisation of ingredients and finished products (Tabilo-Munizaga & Barbosa-Canovas, 2005). The results help manufacturers predict the acceptability, processing and handling of food products (Given, 2009). The rheological and flow properties of food products can be used to describe and predict their stability and textural properties (Gallegos *et al.*, 2004; Fischer & Windhab, 2011) as well as convenience aspects of food products such as mixing and filling (Fischer & Windhab, 2011). Food engineering is more concerned with process vs rheology relationships and makes use of rheological data for process and/or product optimisation (Fischer & Windhab, 2011).

Hydrocolloids such as gum Arabic, larch, tragacanth, guar, xanthan, starch, galactomannans, locust bean gum, BGN flour and BGN dietary fibres have been researched

for use in stabilising food emulsions (Chanamai & McClements, 2000; Yadav *et al.*, 2007; Acton, 2012; Gharibzahedi *et al.*, 2012; Cheong *et al.*, 2014; Adeyi, 2014).

2.8.1 Rheological models

The development of models that can be applied in the prediction of various linear and non-linear viscoelastic properties of materials is of importance (Baig *et al.*, 2006). There is no single model that can accurately explain the complicated phenomena involved in describing the flow behaviour of fluids (Baig *et al.*, 2006; Adeyi, 2014). A rheological model can be defined as a mathematical formula that is used in the description of rheological data in a basic diagram. The shear-thinning flow behaviour of simple systems studied over a small shear range can be effectively modelled using Power Law (Izidoro *et al.*, 2009) and Herschel Bulkley model (Ikhu-Omoregbe & Bushi, 2008). Over a large shear range, dispersions deviate from these relationships and exhibit complex behaviours which can be described using models such as the Ellis fluid model (Lorenzo *et al.*, 2008), Cross model (Roberts *et al.*, 2001) and Sisko model (Brewer *et al.*, 2016). Some rheological models are briefly discussed in the following sections.

1. Power law model

The Power law or Oswald de Waele model (equation 2.1) is a simple, constitutive mathematical equation that describes the behaviour of many non-Newtonian fluids (Balhoff, 2005; Adeyi, 2014).

$$\tau = Ky^n. \quad \text{Equation 2.1}$$

Where: n : flow behaviour index which indicates the tendency of a fluid to shear-thinning; K : consistency co-efficient; y : shear rate and τ : shear stress.

A plot of the logarithm of shear stress against the logarithm of shear rate produces a straight line with a slope equal to the flow behaviour index (n) and an intercept equal to $\log K$ (consistency coefficient) (Adeyi, 2014). If the flow behaviour index is lower than 1, the fluid is predicted to be shear thinning (Balhoff, 2005).

2. Herschel-Bulkley model

The Herschel-Bulkley model (Equation 2.2) is a non-linear model similar to the Power Law, only with yield stress added (Feys *et al.*, 2007). The Herschel-Bulkley model was developed to address the inaccurate results given by the Power Law model at very low shear rates (Khalil & Jan, 2012). The Herschel-Bulkley model is expressed by Feys *et al.* (2007).

$$\tau = \tau_o + Ky^n \quad \text{Equation 2.2.}$$

Where: $\dot{\gamma}$: shear rate; τ : shear stress; τ_o : yield stress; K : consistency coefficient and n : flow behaviour index. The exponent n indicates shear-thinning if $n < 1$ and shear thickening if $n > 1$ (Feys *et al.*, 2007). If the yield stress of a sample is known from an independent experiment, K and n can be determined from linear regression of $\log (\tau - \tau_o)$ versus $\log \dot{\gamma}$ as the intercept and slope, respectively. Alternatively, non-linear regression techniques can be used to estimate τ_o , K and n (Rao & Cooley, 1983).

3. Bingham plastic model

Fluids that obey the Bingham model (Equation 2.3) are referred to as Bingham fluids (Zengeni, 2016). These fluids usually have critical stress below which they do not flow. They tend to exhibit linear shear stress-shear rate behaviour after an initial shear stress threshold has been attained.

$$\tau = \tau_{yB} + K_B \dot{\gamma} \quad \text{Equation 2.3.}$$

Where: τ : shear stress; τ_{yB} : Bingham yield stress; K_B : Bingham plastic viscosity and $\dot{\gamma}$: shear rate.

4. Casson model

Casson model (Equation 2.4) is a non-Newtonian fluid model with yield stress and has been widely used for modelling certain non-Newtonian fluid behaviour (Siddiqui *et al.*, 2015). A Casson fluid is a shear-thinning liquid assumed to have an infinite viscosity at zero rates of shear, yield stress below which no flow occurs and a zero viscosity at an infinite rate of shear (Mukhopadhyay *et al.*, 2013). The Casson model has two parameters, namely, the Casson yield stress (τ_o) and the Casson plastic viscosity (K).

$$\tau^{1/2} = \tau_o^{1/2} + (K \dot{\gamma})^{1/2} \quad \text{Equation 2.4.}$$

Where: τ : shear stress; K : Casson plastic viscosity; $\dot{\gamma}$: shear rate of shear strain and τ_o : yield stress.

5. Ellis fluid model

The Ellis fluid model (Equation 2.5) describes Power Law fluids at high shear rates and Newtonian fluids at low shear rates. It is the model of choice when describing polymeric systems as it gives better results than the Power Law model (Adeyi, 2014). At high shear rates, the Ellis model reduces to a Power Law model while at low shear rates, it reduces to a Newtonian model (Balhoff, 2005).

$$\mu = \frac{\mu_0}{\{(1 + (A\mu_0\tau^{\alpha-1}))\}} \quad \text{Equation 2.5.}$$

Where: μ : apparent viscosity at given shear stress (τ); μ_0 : zero shear viscosity and A and α are adjustable parameters.

6. *Weltman model*

The Weltman model (Equation 2.6) is used to describe the time-dependent behaviour of systems at different shear rates. Parameters A and B represent the initial shear stress of the emulsions and the time coefficient of thixotropic structural breakdown, respectively (Koocheki *et al.*, 2009). A negative B value indicates how fast the shear stress decreases from the initial value to the final equilibrium (Adeyi, 2014).

$$\tau = A + B \ln(t) \quad \text{Equation 2.6}$$

Where: τ : shear stress; t : shearing time; and A and B are constants representing the initial shear stress and the time coefficient of thixotropic breakdown, respectively.

7. *First-order stress decay with a zero equilibrium stress value model*

The first-order stress decay with a zero equilibrium stress value model (Equation 2.7) can be used to describe the data of shear stress decay time.

$$\tau = \tau_0 e^{-kt} \quad \text{Equation 2.7}$$

Where: τ : shear stress; t : shearing time; τ_0 : initial shear stress value and k : breakdown rate constant.

8. *Hysteresis loop area*

The hysteresis loop area is the zone between the upstream and downstream data of shear stress vs shear rate experiments (Koocheki *et al.*, 2009). The hysteresis loop area model is calculated using equation 2.8.

$$\int_{\gamma_1}^{\gamma_2} K \gamma^n - \int_{\gamma_1}^{\gamma_2} K' \gamma^{n'} \quad \text{Equation 2.8}$$

Where: K and K' : consistency coefficients; n and n' : flow behaviour indices for upward and downward measurements, respectively and γ : shear rate or shear strain.

2.9 Conclusions

The high starch and soluble dietary fibre composition of BGN makes it a promising alternative source of polysaccharides. This would reduce the pressure on crops such as potatoes and maize that are commonly used in the food industry as sources of starch. The inclusion of BGN-SDFs in foodstuffs could play a major role in alleviating dietary fibre deficiencies, production of healthy food as well as increase the market value of BGN. This would result in BGN playing a role in lessening malnutrition and increasing food security. Biopolymer nanocomposites play a significant role in emulsion stabilisation and have a huge potential of replacing synthetic stabilisers in food emulsions, thus allowing for the development of products with 'clean' labels. The inclusion of biopolymers and nanocomposites in emulsions not only increases their stability but also positively impacts the nutritional value, shelf life, texture and mouthfeel of the final product. Grafting BGN-SDF onto BGNS would mitigate the inherent undesirable properties of native starch while delivering active compounds to the final product. Studying the rheological and stability characteristics of emulsions is important in predicting their destabilisation phenomena, shelf life and behaviour during handling and processing.

References

- Acton, A. (2012) Beverage emulsions as functions of main emulsion components. In: *Issues in Food production, Processing and Preparation*. Atlanta: Scholarly Editions.
- Adeyi, O. (2014). Effect of Bambara Groundnut flour on the stability and rheological properties of oil-in-water emulsion. PhD Thesis, Cape Peninsula University of Technology.
- Afolabi, T.A. (2012). Synthesis and physicochemical properties of carboxymethylated bambara groundnut (*Voandzeia subterranea*) starch. *International Journal of Food Science and Technology*, **47**, 445-451.
- Afolabi, T. A., Opara, A. O., Kareem, S. O., & Oladoyinbo, F. O. (2017). In vitro digestibility of hydrothermally modified *Bambara* groundnut (*Vigna subterranean* (L.) starch and flour. *Food Science & Nutrition*, **6(1)**, 36-46.
- Alvarez-Cerimedo, M.S., Iriart, C.H., Candal, R.J. & Herrera, M.L. (2010). Structure of lipid emulsions formulated with sodium caseinate. *Food Research International*, **43(5)**, 1482-1493.
- Anonymous. (2000). Thermogravimetric Analysis (TGA). Perkin Elmer. https://www.perkinelmer.com/lab-solutions/resources/docs/faq_beginners-guide-to-thermogravimetric-analysis_009380c_01.pdf. Accessed: 10 May 2020.

- Anonymous. (2011). Emulsion Stability and Testing. In: *Particle Sciences: Drug and Development Services*, **2**, 1-2.
- Anton Paar. (2020). Rheometer. <https://www.anton-paar.com/corp-en/products/group/rheometer/>. Accessed: 20 April 2020.
- Ashogbon, A.O. & Akintayo, E.T. Morphological and functional properties of starches from cereal and legume: A comparative study. *International Journal of Biotechnology and Food Science*, **1**(4), 72-83.
- Baig, C., Jiang, B., Edwards, B.J., Keffer, D.J. & Cochran, H.D. (2006). A comparison of simple rheological models and simulation data of n-hexadecane under shear and elongational flows. *Journal of Rheology*, **50**, 625-640.
- Balhoff, M. (2005). Modelling the flow of non-Newtonian fluids in packed beds at the pore scale. PhD Thesis: Chemical Engineering. Louisiana State University and Agricultural and Mechanical College.
- Bamshaiye, O.M., Adegbola, J.A. & Bamishaiye, E.I. (2011). Bambara groundnut: An underutilized nut in Africa. *Advances in Agricultural Biotechnology*, **1**, 60-72.
- Bandyopadhyay, P., Ghosh, A.K. & Ghosh, C. (2012). Recent developments on polyphenol–protein interactions: Effects on tea and coffee taste, antioxidant properties and the digestive system. *Food & Function*, **3**(6), 592-605.
- Benichou, A., Aserin, A. & Garti, N. (2002). Double emulsions stabilized by new molecular recognition hybrids of natural polymers. *Polymers for Advanced Technologies*, **13**(1012), 1019-1031.
- Berthold, A., Cremer, K. & Kreuter, J. (1996). Preparation and characterization of chitosan microspheres as drug carrier for prednisolone sodium phosphate as model for anti-inflammatory drugs. *Journal of Controlled Release*, **39**(1), 17-25.
- Bhattacharya, A. & Misra, B.N. (2004). Grafting: A versatile means to modify polymers: Techniques, factors and applications. *Progress in Polymer Science (Oxford)*, **29**, 767-814.
- Bos, M.A. & Van Vliet, T. (2001). Interfacial rheological properties of adsorbed protein layers and surfactants: A review. *Advances in Colloid and Interface Science*. **91**, 437-471.
- Bouyer, E., Mekhloufi, G., Rosilio, V., Grossiord, J.L. & Agnely, F. (2012). Proteins, polysaccharides, and their complexes used as stabilizers for emulsions: Alternatives to synthetic surfactants in the pharmaceutical field? *International Journal of Pharmaceutics*, **436**, 359-378.
- Brewer, D.R., Franco, J.M. & Garcia-Zapateiro, L.A. (2016). Rheological properties of oil-in-water emulsions prepared with oil and protein isolates from sesame (*Sesamum Indicum*). *Food Science and Technology*, **36**(1), 64-69.
- Castellani, O., Guibert, D., Al-Assaf, S., Axelos, M., Phillips, G.O. & Anton, M. (2010). Hydrocolloids with emulsifying capacity - Emulsifying properties and interfacial

- characteristics of conventional (*Acacia senegal* (L.) Willd. Var. *senegal*) and matured *Acacia Senegal*. *Food Hydrocolloids*, **24(2-3)**, 193-199.
- Chanamai, R. & McClements, D.J. (2000). Impact of weighting agents and sucrose on gravitational separation of beverage emulsions. *Journal of Agricultural and Food Chemistry*, **48(11)**, 5561-5565.
- Cheong, K.W., Tan, C.P., Mirhosseini, H., Joanne-Kam, W.Y., Hamid, N.S.A. & Basri, M. (2014). The effect of prime emulsion components as a function of headspace concentration of soursop flavor compounds. *Chemistry Central Journal*, **8(23)**, 1-11.
- Chhabra, N. (2012). Uronic Acid pathway. In: *Biochemistry for Medics*. Medical College, Mauritius.
- Chhabra, R.P. & Richardson, J.F. (eds) (2008). Non-Newtonian fluid behaviour. In: *Non-Newtonian flow and applied rheology: Engineering Applications*. 2nd ed. Pp. 1-5. Oxford: Butterworth-Heinemann Publications.
- Cottrell, T. & van Peij, J. (2014). Emulsifiers in Food Technology. 2nd ed. Emulsifiers in Food Technology. Pp. 73-92.
- Dalgetty, D.D. & Baik, B. (2003). Isolation and characterisation of cotyledon fibres from Peas, Lentils, and Chickpeas. *American Association of Cereal Chemists*, **80(3)**, 310-315.
- Daniells, S. (2010). The science of beverage emulsions. In: *Food Navigator*. <http://www.foodnavigator.com/Science/The-science-of-beverage-emulsions>. Accessed: 16 May 2020.
- De Kruif, C.G. & Tuinier, R. (2001). Polysaccharide protein interactions. *Food Hydrocolloids*, **15(4-6)**, 555-563.
- De Souza, C.J.F. & Rojas, E.E.G. (2012). Emulsion of systems containing egg yolk, polysaccharides and vegetable oil. *Ciencia E Agrotecnologia*, **36(5)**, 543-550.
- Dickinson, E. (2003). Hydrocolloids at interfaces and the influence on the properties of dispersed systems. *Food Hydrocolloids*, **17**, 25-39.
- Dickinson, E. (2008). Interfacial structure and stability of food emulsions as affected by protein-polysaccharide interactions. *Soft Matter*, **4**, 932-942.
- Dickinson, E. (2009) Hydrocolloids as emulsifiers and emulsion stabilizers. *Food Hydrocolloids*. **23(6)**, 1473-1482.
- Diedericks, C.F. (2014). Functional properties of Bambara groundnut (*Vigna Subterranea* (L) Verdc.) non-starch polysaccharides in model and food systems. Master of Technology: Food Technology Thesis, Cape Peninsula University of Technology.
- Diederecks, C.F. V.A. & Jideani, V.A. (2014). Nutritional, Therapeutic and Prophylactic Properties of *Vigna subterranea* and *Moringa oleifera*. *The Journal of Food Science and Technology*, **52(7)**, 4078-4089.
- Diedericks, C. & Jideani, V. (2015). Physicochemical and Functional Properties of Insoluble Dietary Fiber Isolated from Bambara Groundnut (*Vigna subterranea* [L.] Verdc.). *Journal*

- of *Food Science*, **80(9)**, 1933-1944.
- Diftis, N.G., Biliaderis, C.G. & Kiosseoglou, V.D. (2005). Rheological properties and stability of model salad dressing emulsions prepared with a dry-heated soybean protein isolate-dextran mixture. *Food Hydrocolloids*, **19(6)**, 1025-1031.
- Doublier, J.L., Garnier, C., Renard, D. & Sanchez, C. (2000). Protein-polysaccharide interactions. *Current Opinion in Colloid & Interface Science*, **5**, 202-214.
- Elleuch, M., Bedigian, D., Roiseux, O., Besbes, S. & Blecker, C. (2011). Dietary fibre and fibre-rich by-products of food processing; Characterisation technological functionality and commercial applications: A review. *Food Chemistry*, **124**, 411-421.
- Eltayeb, A. R. S. M., Ali O. Ali., Abou-Arab, A.A. & Abu-Salem, F.M. (2011). Paper Chemical composition and functional properties of flour and protein isolate extracted from Bambara groundnut (*Vigna subterranean*). *African Journal of Food Science*, **5(2)**, 82-90
- Enyidi, C. & Onyenakazi, G. (2019). Effects of Substitution of Fishmeal with Bambaranut Meal on Growth and Intestinal Microbiota of African Catfish (*Clarias gariepinus*). *Aquaculture Studies*, **19(1)**, 9-23.
- Evans, M., Ratcliffe, I. & Williams, P.A. (2013). Emulsion stabilisation using polysaccharide-protein complexes. *Current Opinion in Colloid & Interface Science*, **18**, 272-282.
- Fang, Y., Li, L., Inoue, C., Lundin, L. & Appelqvist, I. (2006). Associative and segregative phase separations of gelatin - carrageenan aqueous mixtures. *Langmuir*, **22(23)**, 9532-9537.
- Fasinu, E.G., Ikhu-Omoregbe, D.I.O. & Jideani, V.A. (2015). Influence of selected physicochemical factors on the stability of emulsions stabilized by Bambara groundnut flour and starch. *Journal of Food Science and Technology*, **52(11)**, 7048-7058.
- Flanagan, J. & Singh, H. (2006). Recent Advances in the Delivery of Food-Derived Bioactives and Drugs Using Microemulsions. In: *Nanocarrier Technologies. Frontiers of Nanotherapy*. 95-111. Springer.
- Feys, D., Verhoeven, R. & De Schutter, G. (2007). Evaluation of time independent rheological models applicable to fresh self-compacting concrete. *Applied Rheology*, **17(5)**, 1-10.
- Fischer, P. & Windhab, E.J. (2011). Rheology of food materials. *Current Opinion in Colloid and Interface Science*, **16(1)**, 36-40.
- Fitzsimons, S.M., Mulvihill, D.M. & Morris, E.R. (2008). Segregative interactions between gelatin and polymerised whey protein. *Food Hydrocolloids*, **22(3)**, 485-491.
- Kelly, D. (2019). Non-Newtonian fluids. Fluid Flow. <https://fluidflowinfo.com/non-newtonian-fluids/> Accessed: 20 April 2020.
- Foodstuffs, Cosmetics and Disinfectants Act. (1972). Regulations Governing The Labelling and Advertising of Foodstuffs, Regulation No. R146. In: Foodstuffs, Cosmetics and

- Disinfectants Act and Regulations, 54/1972. Updated 1 March 2010. Cape Town, Johannesburg: LexNexis Butterworths.
- Gabriel, E.G., Jideani, V.A., & Ikhu-Omoregbe, D.I.O. (2013). Investigation of the emulsifying properties of Bambara groundnut flour and starch. *International Journal of Biological, Veterinary, Agricultural and Food Engineering*, **7(11)**, 724-732.
- Gallegos, C., Franco, J.M. & Partal, P. (2004). Rheology of food dispersions. *The British Society of Rheology*, 19-65.
- Gammans, M., Merel, P. & Ortiz-Bobea, A. Negative impacts of climate change on cereal yields: statistical evidence from France. *Environmental Research Letters*, **12(5)**, 054007.
- Gao, Z., Fang, Y., Cao, Y., Liao, H., Nishinari, K. & Phillips, G.O. (2017). Hydrocolloid food component interactions. *Food Hydrocolloids*, **68**, 149-156.
- Gharibzahedi, S.M.T., Mousavi, S.M., Hamed, M. & Ghasemlou, M. (2012). Response surface modeling for optimization of formulation variables and physical stability assessment of walnut oil-in-water beverage emulsions. *Food Hydrocolloids*, **26**, 293-301.
- Ghosh, S. & Rousseau, D. (2012). Fat crystals and water-in-oil emulsion stability. *Current Opinion in Colloid and Interface Science*, **16(5)**, 421-431.
- Gill, P., Moghadam, T.T. & Ranjbar, B. (2010). Differential scanning calorimetry techniques: Applications in biology and nanoscience. *Journal of Biomolecular Techniques*, **21(4)**, 167-193.
- Given, P.S. (2009). Encapsulation of flavors in emulsions for beverages. *Current Opinion in Colloid and Interface Science*, **14(1)**, 43-47.
- Groenewoud, W.M. (2001). Thermogravimetry. In: *Characterisation of Polymers by Thermal Analysis*. Pg 61-76. Netherlands: Elsevier Science.
- Gulu, N.B. (2018). Functional and rheological properties of Bambara groundnut starch-catechin complex obtained by chemical grafting. Master of Food Science and Technology. Cape Peninsula University of Technology, Cape Town, South Africa.
- Gulu, N.B., Jideani, V.A. & Jacobs, A. (2019). Functional characteristics of Bambara groundnut starch-catechin complex formed using cyclodextrins as initiators. *Heliyon*, **5**, 2-25.
- Guzey, D. & McClements, D.J. (2006). Formation, stability and properties of multilayer emulsions for application in the food industry. *Advances in Colloid and Interface Science*, **128130**, 227-248.
- Hanazawa, T. & Murray, B.S. (2014). The influence of oil droplets on the phase separation of proteinopolysaccharide mixtures. *Food Hydrocolloids*, **34**, 128-137.
- He, H.J., Yu, R.P., Zhu, T., Gu, Z.B. & Xu, H. (2006). Study of fluorescence spectra of starch suspension. *Guang Pu Xue Yu Guang Pu Fen Xi*, **26(9)**, 1636-1639.

- Hoover, R., Hughes, T., Chung, H.J. & Liu, Q. (2010). Composition, molecular structure, properties, and modification of pulse starches: A review. *Food Research International*, **43**, 399-413.
- Ikhu-Omoregbe, D. and Bushi, G.M. (2008). Rheological characteristics of South African commercial sauces. *International Journal of Food Science and Technology*, **43**, 2230-2236.
- Izidorio, D.R., Scheer, A. & Sierakowski, M. (2009). Rheological properties of emulsions stabilized by green Banana (*Musa cavendishii*) pulp fitted by Power Law model. *Brazilian Archives of Biology and Technology*, **52**, 1541-1553.
- Jha, P.K., Desai, P.S., Li, J. & Larson, R.G. (2014). pH and salt effects on the associative phase separation of oppositely charged polyelectrolytes. *Polymer*, **6(5)**, 1414-1436.
- Jia, W., Cui, B., Ye, T., Lin, L., Zheng, H. & Yan, X. (2014). Phase behavior of ovalbumin and carboxymethylcellulose composite system. *Carbohydrate Polymers*, **109**, 64-70.
- Jiao, J. & Burgess, D.J. (2003). Ostwald ripening of water-in-hydrocarbon emulsions. *Journal of Colloid and Interface Science*, **264(2)**, 509-516.
- Jimenez-Castano, L., Villamiel, M. & López-Fandiño, R. (2007). Glycosylation of individual whey proteins by Maillard reaction using dextran of different molecular mass. *Food Hydrocolloids*, **21(3)**, 433-443.
- Jideani, V.A. & Mpotokwane, S.M. (2009). Modelling of water absorption of Botswana Bambara varieties using Peleg's equation. *Journal of Food Engineering*, **92(2)**, 182-188.
- Kaptso, K.G., Njintang, Y.N., Nguemtchouin, M.M.G., Scher, J., Hounhouigan, J. & Mbofung, C.M. (2014). Physicochemical and micro-structural properties of flours, starch and proteins from two varieties of legumes: bambara groundnut (*Vigna subterranea*). *Journal of Food Science and Technology*, **52**, 4915-4924.
- Kasran, M. (2013). Development of protein polysaccharide complex for stabilization of oil-in-water emulsions. PhD Thesis. University of Guelph.
- Kerkhofs, S., Lipkens, H., Velghe, F., Verlooy, P., Martens, J.A. (2011). Mayonnaise production in batch and continuous process exploiting magnetohydrodynamic force. *Journal of Food Engineering*, **106(1)**, 35-39.
- Kim, R.J., Kim, Y., Choi, N. & Lee, I. (2015). Polymerization shrinkage, modulus, and shrinkage stress related to tooth-restoration interfacial debonding in bulk-fill composites. *Journal of Dentistry*, **43(4)**, 430-439.
- Khalil, M. & Jan, B.M. (2012). Herschel-Bulkley rheological parameters of a novel environmentally friendly lightweight biopolymer drilling fluid from xanthan gum and starch. *Journal of Applied Polymer Science*, **124(1)**, 595-606.

- Koocheki, A., Ghandi, A., Razavi, S.M.A., Mortazavi, S.A. & Vasiljevic, T. (2009). The rheological properties of ketchup as a function of different hydrocolloids and temperature. *International Journal of Food Science and Technology*, **44**(3), 596-602.
- Lawal, O.S. & Adebawale, K.O. (2005). Physicochemical characteristics and thermal properties of chemically modified jackbean (*Canavalia ensiformis*) starch. *Carbohydrate Polymers*, **60**, 331-341.
- Lim, S.S., Baik, M.Y., Decker, E.A., Henson, L., Popplewell, M.L., McClements, D.J. & Choi, S.J. (2011). Stabilization of orange oil-in-water emulsions: A new role for ester gum as an Ostwald ripening inhibitor. *Food Chemistry*, **128**(4), 1023-1028.
- Liu, Y., Chen, W., Chen, C. & Zhang, J. (2015). Physicochemical Property of Starch-Soluble Dietary Fiber Conjugates and Their Resistance to Enzymatic Hydrolysis. *International Journal of Food Properties*, **18**, 2457-2471.
- Lorenzo, G., Zaritzky, N. & Califano, A. (2008). Modeling Rheological Properties of Low-in-fat O/W emulsions stabilized with Xanthan/guar mixtures. *Food Research International*. **41**, 452-494.
- Mackie, A. (2009). Structure of adsorbed layers of mixtures of proteins and surfactants. *Current Opinion in Colloid and Interface Science*, **9**, 357-361.
- Maphosa, Y. (2016). Characterisation of Bambara groundnut (*Vigna Subterranea* (L) Verdc.) non-starch polysaccharides from wet milling as prebiotics. Master of Technology Thesis, Cape Peninsula University of Technology.
- Maphosa, Y. & Jideani, V.A. (2016). Physicochemical characteristics of Bambara groundnut dietary fibres extracted using wet milling. *South African Journal of Science*, **112**(1/2), 1-8.
- Maphosa, Y, Jideani VA. & Adeyi O. (2017). Effect of soluble dietary fibres from Bambara groundnut varieties on the stability of orange oil beverage emulsion. *African Journal of Science, Technology, Innovation and Development*, **9**(1), 69-76.
- Maphosa, Y. & Jideani, V.A. (2017). The Role of Legumes in Human Nutrition. In: *Functional Food - Improve Health through Adequate Food*. Edited by Maria Chavarri Hueda.
- Maphosa, Y. & Jideani, V. A. (2018). Factors Affecting the Stability of Emulsions Stabilised by Biopolymers, Chapter 5 in *Science and Technology Behind Nanoemulsions*. (Editor: Selcan Karakuş).
- Martin-Pelaez, S., Gibson, G.R., Martin-Orue, S.M., Klinder, A., Rastall, R.A., La Ragione, R.M., Woodward, M.J. & Costabile, A. (2008). *In vitro* fermentation of carbohydrates by porcine faecal inocula and their influence on *Salmonella* Typhimurium growth in batch culture systems. *Federation of European Microbiological Societies Microbial Ecology*, **66**, 608-619.
- Mao, L. & Miao, S. (2015). Structuring food emulsions to improve nutrient delivery during digestion. *Food Engineering Reviews*, **7**, 439-451.

- Mayes, S., Ho, W.K., Chai, H.H., Gao, X., Kundy, A.C., Mateva, K.I., Zahrulakmal, M., Hahiree, M.K.I.M., Kendabie, P., Licea, L.C.S., Massawe, F., Mabhaudhi, T., Modi, A.T., Berchie, J.N., Amoah, S., Faloye, B., Abberton, M., Olaniyi, O. & Azam-Ali, S.N. (2019). Bambara groundnut: an exemplar underutilised legume for resilience under climate change. *Planta*, **250**, 803-820.
- McClements, D.J. (2005). Food Emulsions. In: *Principles, Practices and Techniques*. 2nd ed. Boca Raton: Taylor & Francis: CRC Press
- McClements, D.J., Decker, E.A. & Weiss, J. (2007). Emulsion-based delivery systems for lipophilic bioactive components. *Journal of Food Science*, **72(8)**, 109-124.
- Mession, J.L., Assifaoui, A., Lafarge, C., Saurel, R. & Cayot, P. (2012). Protein aggregation induced by phase separation in a pea proteins-sodium alginate-water ternary system. *Food Hydrocolloids*, **28(2)**, 333-343.
- Mohan, S., Oluwafemi, O.S., Kalarikkal, N., Thomas, S. & Songca, S.P. (2016). Biopolymers-application in nanoscience and nanotechnology. In: Perveen FK, editor. *Recent Advances in Biopolymers*. pp. 47-72. Croatia: InTech.
- Mubaiwa, J., Fogliano, V., Chidewe, C. & Linnemann, A.R. (2018). Bambara groundnut (*Vigna subterranea* (L.) Verdc.) flour: A functional ingredient to favour the use of an unexploited sustainable protein source. *Plos One*, **13(10)**, e0205776.
- Mukhopadhyay, S., RanjanDe, P., Bhattacharyya, K. & Layek, G.C. (2013). Casson fluid flow over an unsteady stretching surface, **4(4)**, 933-938.
- Muntz, L.J. (2017). Rheometer Market Analysis. Dissertation: Degree of Bachelor of Science. Worcester Polytechnic Institute.
- Murevanhema, Y.Y. & Jideani, V.A. (2015). Potential of Bambara groundnut (*Vigna subterranea* (L.) Verdc) milk as a probiotic beverage: A review. *Critical Reviews in Food Science and Nutrition*, **53(9)**, 954-967.
- Nawaz, H., Waheed, R., Nawaz, M. & Shahwar, D. (2020). Physical and Chemical Modifications in Starch Structure and Reactivity. In: Chemical Properties of Starch. Edited by Martins Emeje. InTech. Pp 170.
- Neelam, K., Vijay, S. & Lalit, S. (2012). Various techniques for the modification of starch and the applications of its derivatives. *International Research Journal of Pharmacy*, **3**, 25-31.
- Olayinka, F.S., Olayinka, O.O., Olu-Owolabi, B.I. & Adebawale, K.O. (2015). Effect of chemical modifications on thermal, rheological and morphological properties of yellow sorghum starch. *Journal of Food Science and Technology*, **52(12)**, :8364-8370.
- Oliver, C.M., Melton, L.D. & Stanley, R.A. (2006). Creating proteins with novel functionality via the maillard reaction: A review. *Critical Reviews in Food Science and Nutrition*, **46(4)**, 337-350.

- Onsaard, E., Vittayanont, M., Srigam, S. & McClements, D.J. (2006). Comparison of properties of oil-in-water emulsions stabilized by coconut cream proteins with those stabilized by whey protein isolate. *Food Research International*, **39(1)**, 78-86.
- Oyeyinka, S.A., Singha, S., Adebola, P. & Amonsou, E. (2015). Physicochemical properties of starches with variable amylose contents extracted from Bambara groundnut genotypes. *Carbohydrate polymer*, **133**, 171-178.
- Oyenyika, S.A., Singh, S., Ma, Y. & Amonsou, E.O (2016). Effect of high-pressure homogenization on structural, thermal and rheological properties of bambara starch complexed with different fatty acids. *Royal Society of Chemistry*, **6**, 80174-80180.
- Oyeyinka, S.A. & Oyeyinka, A.T. (2017). A review on isolation, composition, physicochemical properties and modification of Bambara groundnut starch. *Food Hydrocolloid*, **75**, 62-71.
- Partal, P. & Ma Franco, J. (2006). Non-Newtonian Fluids. *Encyclopedia of Life Support Systems. Rheology*, **1**.
- Payet, L. & Terentjev, E.M. (2008). Emulsification and stabilization mechanisms of O/W emulsions in the presence of chitosan. *Langmuir*, **24(21)**, 12247-12252.
- Piorkowski, D.T. & McClements, D.J. (2014). Beverage emulsions: Recent developments in formulation, production, and applications. *Food Hydrocolloids*, **42**, 5-41.
- Rajisha, K.R., Deepa, B., Pothan, L.A. & Thomas, S. (2011). Thermomechanical and spectroscopic characterization of natural fibre composites. In: *Interface Engineering of Natural Fibre Composites for Maximum Performance* - Woodhead Publishing Limited. Pp 241-274.
- Rao, M.A. & Cooley, H.J. (1983). Applicability of flow models with yield for tomatoes concentrates. *Journal of Food process Engineering*, **6**, 159-173.
- Roberts, G.P., Banes, H.A. & Carew, P. (2001). Modeling the flow behaviour of very shear-thinning liquids. *Chemical Engineering Science*, **56**, 5617-5623.
- Robins, M.M., Watson, A.D. & Wilde, P.J. (2002). Emulsions – Creaming and rheology. *Current Opinion in Colloid and Interface Science*, **7**, 419-425.
- Rodriguez Patino, J.M. & Pilosof, A.M.R. (2011). Protein-polysaccharide interactions at fluid interfaces. *Food Hydrocolloids*. **25(8)**, 1925-1937.
- Ron, E.Z. & Rosenberg, E. (2002). Biosurfactants and oil bioremediation. *Current Opinion in Biotechnology*, **13**, 249-252.
- Roselli M., Finamore A., Garaguso I., Britti M. S. & Mengheri E. (2003). Zinc oxide protects cultured enterocytes from the damage induced by *Escherichia coli*. *Journal of Nutrition*, **133**, 4077-4082.
- Russ, B., Glauddell, A., Urban, J., Chabiny, M.L. & Segalman, R.A. (2016). Organic thermoelectric materials for energy harvesting and temperature control. *Nature Reviews Materials*, **1**, 16050.

- Saberi, B., Vuong, Q.V., Chockchaisawasdee, S., Golding, J.B., Scarlett, C.J. & Stathopoulos, C.E. (2016). Mechanical and Physical Properties of Pea Starch Edible Films in the Presence of Glycerol. *Journal of Food Processing and Preservation*, **40(6)**, 1600227
- Saha, D. & Bhattacharya, S. (2010). Hydrocolloids as thickening and gelling agents in food: A critical review. *Journal of Food Science and Technology*, **47(6)**, 587-597.
- Sahin, S. & Sumnu, S.G. (2006). Rheological properties of foods. In: *Physical properties of Foods*. Pp. 39-105. Turkey: Springer.
- Sanchez, C.C. & Patino, J.M.R. (2005). Interfacial, foaming and emulsifying characteristics of sodium caseinate as influenced by protein concentration in solution. *Food Hydrocolloids*, **19(3)**, 407-416.
- Sandhu, K.S. & Lim, S.T. (2008). Digestibility of legume starches as influenced by their physical and structural properties. *Carbohydrate Polymers*, **71**, 245-252.
- Shachman, M. (2004). Emulsions. In: *The soft drinks companion. A technical handbook for the beverage industry*. Pp. 41-53. New York: CRC Press.
- Schmitt, C., Sanchez, C., Desobry-Banon S. & Hardy, J. (1998). *Structure and Technofunctional Properties of Protein-Polysaccharide Complexes: A Review*, **38(8)**, 689-753.
- Skoog, D.A., Crouch, S.R. & Holler, F.J. (2006). *Principles of Instrumental Analysis*. 6th edition.
- Siddiqui, A.M., Farooq, A.A. & Rana. M.A. (2015). A Mathematical Model for the Flow of a Casson Fluid due to Metachronal Beating of Cilia in a Tube. *Scientific World Journal*, **2015**, 487819.
- Singh, V.K. & Kumar, D. (2014). Effect of fibres on properties of concrete. *International Journal of Computer and Mathematical Sciences*, **3(6)**, 111-119.
- Singh, T., Shukla, S., Kumar, P. & Wahla, V. (2017). Application of Nanotechnology in Food Science: Perception and Overview. *Frontiers in Microbiology*, **8(1501)**, 1-7.
- Sirivongpaisal, P. (2008). Structure and functional properties of starch and flour from bambarra groundnut. *Songklanakarin Journal of Science and Technology*, **30**, 51-56.
- Sjoblom, J. (2006). Emulsion and emulsion stability. In: *Surfactant Science Series*. 2nd Edition Pp. 185-223.
- Slavin, J. (2013). Fiber and Prebiotics: Mechanisms and Health Benefits. *Nutrients*, **5(4)**, 1417-1435.
- Song, W.L., Wang, P., Cao, L., Anderson, A., Meziani, M.J. & Farr, A.J. (2011). Polymer/boron nitride nanocomposite materials for superior thermal transport performance. *Angewandte Chemie, International Edition*, **51(26)**, 6498-6501.

- Spizzirri, U.G., Parisi, O.I., Iemma, F., Cirillo, G., Puoci, F. & Curcio, M. (2010). Antioxidant polysaccharide conjugates for food application by eco-friendly grafting procedure. *Carbohydrate Polymers*, **79(2)**, 333-340.
- Stern, P., Velentova, H. & Pokorny, J. (2001). Rheological properties and sensory texture of mayonnaise. *European Journal of Lipid Science and Technology*, **103(1)**, 23-28.
- Tabilo-Munizaga, G. & Barbosa-Canovas, G.V. (2005). Rheology for the food industry. *Journal of Food Engineering*, **67**, 147-156.
- Tadros, T. (2013). Creaming of emulsions. In: *Encyclopedia of Colloid and Interface Science*. (Edited by T. Tadros). Berlin Heidelberg: Springer.
- Tarasov, A. (2012). Thermal Analysis: methods, principles and application. http://www.fhi-berlin.mpg.de/acnew/departement/pages/teaching/pages/teaching_wintersemester_2012_2013/andrey_tarasov_thermal_analysis_121026.pdf Accessed: 30/06/2020
- Tolstoguzov, V.B. (2003). Some thermodynamic considerations in food formulation. *Food Hydrocolloids*, **17(1)**, 1-23.
- Tolstoguzov, V.B. (2006). Phase behavior in mixed polysaccharide systems. In: *Food Polysaccharides and Their Applications*. 2nd edition. Edited by A.M. Stephen., G.O. Philips. & P.A. Williams. Pp. 589-627. London: Taylor & Francis, CRC Press.
- Tosh, S.M. & Yada, S. (2010). Dietary fibres in pulse seeds and fractions: Characterisation, functional attributes and applications. *Food Research International*, **43(2)**, 450-460.
- Vazquez, J.A., Rodriguez-Amado, I., Montemayor, M.I., Fraguas, J., Gonzalez, M.D.P. & Murado, M.A. (2013). Chondroitin Sulfate, Hyaluronic Acid and Chitin/Chitosan Production Using Marine Waste Sources: Characteristics, Applications and Eco-Friendly Processes: A Review. *Marine Drugs*, **11(3)**, 747-774.
- Verma, A.K. & Banerjee, R. (2010). Dietary fibre as functional ingredient in meat products: a novel approach for healthy living - A review. *Journal of Food Science and Technology*, **47(3)**, 247-257.
- Wang, S., Wang, J., Zhang, W., Li, C., Yu, J. & Wang, S. (2015). Molecular order and functional properties of starches from three waxy wheat varieties grown in China. *Food Chemistry*, 181, 43-50.
- Weiss, J. (2005). Emulsion stability determination. In: Wrolstad RE, editor. *Handbook of Food Analytical Chemistry*. New Jersey: John Wiley & Sons Inc. 2005. pp. 591-607.
- Williams, PA. (2001). Food emulsions: Principles, practice, and techniques. *International Journal of Food Science and Technology*, **36(2)**, 223-224.
- Winarti, C., Sunarti, T., Mangunwidjaja, D. & Richana, N. (2014). Preparation of arrowroot starch nanoparticles by butanol-complex precipitation, and its as bioactive encapsulation matrix. *International Food Research Journal*, **21(6)**, 2207-2213.
- Yadav, M.P., Johnston, D.B., Hotchkiss, A.T. & Hicks, K.B. (2007). Corn fibre gum: A potential gum arabic replacer for beverage flavor emulsification. *Food Hydrocolloids*,

21(7), 1022-1030.

- Yang, S.C. & Lai, L.S. (2003). Dressings and mayonnaise: Chemistry of the Products. In: *Encyclopedia of Food Sciences and Nutrition*. 2nd edition. China: Elsevier.
- Yang, H., Yan, R., Chen, H. & Lee, D.H. (2007). Characteristics of hemicellulose, cellulose and lignin pyrolysis. *Fuel*, **86**, 1781-1788.
- Yang, N., Liu, Y., Ashton, J., Gorczyca, E. & Kasapis, S. (2013). Phase behaviour and *in vitro* hydrolysis of wheat starch in mixture with whey protein. *Food Chemistry*, **137(1-4)**, 76-82.
- Yang, G., Gong, H., Liu, T., Sun, X., Cheng, L. & Liu, Z. (2015). Two-dimensional magnetic WS₂@Fe₃O₄ nanocomposite with mesoporous silica coating for drug delivery and imaging-guided therapy of cancer. *Biomaterials*, **60**, 62-71.
- Yao, D.N., Kouassi, K.N., Erda, D., Scazzina, F., Pellegrini, N. & Casiraghi, M.C. (2015). Nutritive Evaluation of the Bambara Groundnut Ci12 Landrace [*Vigna subterranea* (L.) Verdc. (Fabaceae)] Produced in Côte d'Ivoire. *International Journal of Molecular Sciences*, **(16)**, 21428-21441.
- Ye, A. (2008). Complexation between milk proteins and polysaccharides via electrostatic interaction: Principles and applications: A review. *International Journal of Food Science and Technology*, **43**, 406-415.
- Yin, B., Zhang, R. & Yao, P. (2015). Influence of Pea Protein Aggregates on the Structure and Stability of Pea Protein/Soybean Polysaccharide Complex Emulsions. *Molecules*, **20**, 5165-5183.
- Yu, Y., Huang, X. & Yu, W. (2014). High Performance of Bamboo-Based Fiber Composites from Long Bamboo Fiber Bundles and Phenolic Resins. *Journal of Applied Polymer Science*, **131(12)**, 1-8.
- Zengeni, B.T. (2016). Bingham yield stress and Bingham plastic viscosity of homogeneous non-Newtonian slurries. Master of Technology in Mechanical Engineering Dissertation. Cape Peninsula University of Technology.
- Zhang, J. (2011). Novel emulsion-based delivery systems. PhD Thesis, University of Minnesota.
- Zhang, J & Wang, Z.W. (2013). Soluble dietary fibre from *Canna edulis* Ker by-product and its physicochemical properties. *Carbohydrate Polymers*, **92**, 289-296.
- Zhang, R. & McClements, D.J. (2016). Enhancing nutraceutical bioavailability by controlling the composition and structure of gastrointestinal contents: Emulsion-based delivery and excipient systems. *Food Structure*, **10**, 21-36.
- Zhang, J., Gao, Y., Qian, S., Liu, X. & Zu, H. (2011). Physicochemical and pharmacokinetic characterization of a spray-dried malotilate emulsion. *International Journal of Pharmaceutics*, **414(1-2)**, 186-192.

Zhao, X., Liu, F., Ma, C., Yuan, F. & Gao Y. (2015) Effect of carrier oils on the physicochemical properties of orange oil beverage emulsions. *Food Research International*. **74**, 260-268.

CHAPTER THREE

PHASE BEHAVIOUR OF BAMBARA GROUNDNUT (*VIGNA SUBTERRANEA* [L.] VERDC)

STARCH-SOLUBLE DIETARY FIBRE NANOCOMPOSITE

Abstract

Bambara groundnut (BGN) (*Vigna subterranea* [L.] Verdc.) is high in soluble dietary fibre (SDF) (17%, dry mass) and starch (50%, dry mass) making this legume a great source of the two polysaccharides. Bambara groundnut starch-soluble dietary fibre nanocomposite (STASOL) was produced by grafting BGN soluble dietary fibre (BGN-SDF) onto BGN starch (BGNS) using ascorbic acid (1% w/w) and hydrogen peroxide (16.5% w/w) as a redox initiator pair. The particle sizes, functional groups, crystallinity, morphology and thermal properties of BGNS, BGN-SDF and STASOL were studied using a zetasizer, fourier transform infrared (FTIR), X-ray diffraction (XRD), scanning electron microscope (SEM) and differential scanning calorimetry (DSC), respectively. The phase behaviour of different ratios of BGNS and BGN-SDF revealed 15:1.95 g/g BGNS:BGN-SDF as the most stable combination and it was thus used in the production of STASOL. STASOL was a stable composite with an average particle size of 74.01 nm which qualified it as a nanocomposite (nano = <100 nm). The average particle sizes of STASOL and BGN-SDF were not significantly different while both were significantly ($p = 0.000$) different from the average particle size of BGNS. The conductivity of STASOL, BGN-SDF and BGNS was -57.3, -6.03 and -2.03 mV, respectively, suggesting very high stability of STASOL. Crystallinity studies using XRD revealed BGN-SDF and STASOL as amorphous. On the other hand, BGNS showed strong peaks at 15, 17 and 23° (2θ), thus classifying it as type C starch, typical of legumes. STASOL, BGN-SDF and BGNS had functional groups in the regions 3600-2900, 1641.71, 1200-900, 1300-800 cm^{-1} which were attributed to the vibrations of C-H and OH, C=O and OH, C-C and C-H-O as well as C-O and C-C bonds, respectively. Peaks shifted from wavenumbers 3281.84, 1641.71, 1076.45, 434.37 cm^{-1} in BGNS IR spectra and 3280.17, 1633.68, 1078.70, 421.69 cm^{-1} in BGN-SDF IR spectra to 3279.87, 1631.18, 1077.11 and 419.64 cm^{-1} in STASOL IR spectra. This further confirmed the successful formation of a new complex from BGNS and BGN-SDF. Morphology studies using SEM showed BGNS particles as smooth, oval structures while BGN-SDF and STASOL exhibited irregular, polygonal morphologies. STASOL was the most thermally stable biopolymer, with final disintegration at 293°C, therefore suggesting that it would find use in high-temperature food applications such as baking and extrusion. The grafting process successfully mitigated the undesirable characteristics of native BGNS and BGN-SDF while retaining the desirable characteristics of both biopolymers and gaining new improved properties.

3.1 Introduction

Composites are functionalised molecules that possess the characteristics of both the grafted molecules and the natural polymer (Spizzirri *et al.*, 2011). Various researchers have studied the application of composites and nanocomposites in food packaging materials (Avella *et al.*, 2005). However, there is very limited information on their synthesis and incorporation in food products. Polymer-polysaccharide and polysaccharide-polysaccharide composites are preferred in the food industry because of their non-toxicity, stability, nutritional benefits, biocompatibility, biodegradability and relatively low cost (Bandyopadhyay *et al.*, 2012; Yu *et al.*, 2014). Complexes that have been studied include starch-dietary fibre conjugates (Liu *et al.*, 2015), starch-lipid composites (Singh *et al.*, 2010), starch-wheat bran composites (Fama *et al.*, 2009), protein-dietary fibre complexes and starch-pectin blends (Liu, 2014).

Several methods can be employed in the formation of nanocomposites. These include complex coacervation, desolvation, reactive extrusion, crosslinking, free radical-induced grafting, acid hydrolysis and self-assembling (Bhattacharya & Misra, 2004; Spizzirri *et al.*, 2010; Song *et al.*, 2012; Yu *et al.*, 2014; Winarti *et al.*, 2019). The choice of method depends on factors such as required particle size, source of polymer, thermal stability, physicochemical stability of active agent, stability of the final product, residual toxicity and desired end use of composite (Yu *et al.*, 2014). A commonly employed method is the free radical-induced grafting method. This method is commonly coupled with a self-assembling method in mediums such as ethanol (Spizzirri *et al.*, 2010; Yu *et al.*, 2014). The free radical-induced grafting method employs an ascorbic acid-hydrogen peroxide redox pair as a biocompatible initiator system (Spizzirri *et al.*, 2010). Hydrogen peroxide oxidises ascorbic acid-forming hydroxyl and ascorbate radical intermediates (Spizzirri *et al.*, 2010). When added to polysaccharides like starch, the ascorbic acid-hydrogen peroxide combination catalyses the activation of the polysaccharide chains towards radical reaction. The initiator system produces hydroxyl radicals that abstract hydrogen atoms from the polysaccharide's OH groups, leaving the polysaccharide chain exposed thus allowing it to form self-aggregates with other compounds by forming intra- and inter-molecular associations (Liu *et al.*, 2015). In polysaccharide-polysaccharide complexing, the more robust polysaccharide forms a protective layer around the weaker polysaccharide, forming a composite of high resistance and strength (Liu *et al.*, 2015). The free radical-induced grafting method can be used in the formation of biopolymer nanocomposites (Maphosa & Jideani, 2017).

In this study, the free radical-induced grafting method was used to complex Bambara groundnut starch (BGNS) and Bambara groundnut soluble dietary fibre (BGN-SDF) to synthesise a nanocomposite (STASOL). The complexing of these two biopolymers was

expected to combine the properties of both polysaccharides thereby providing superior physicochemical and functional characteristics. As such, STASOL was expected to possess improved properties such as solubility, swelling power, thickening, viscosity, gelation and thermal stability. A nanocomposite like STASOL would be applicable in macromolecular purification, microencapsulation, food formulations and in the synthesis of biomaterials (Bandyopadhyay *et al.*, 2012). The objectives of this chapter were to produce STASOL and characterise the particle sizes, conductivity, functional groups, crystallinity, morphology and thermal properties.

3.2 Materials and Methods

3.2.1 Source of materials and equipment

Bambara groundnut (BGN) seeds purchased from Triotrade, Johannesburg, South Africa were used in this study. The seeds were manually sorted and only the Black-eye variety was used. Analytical grade chemicals were used in this study (Sigma-Aldrich). Equipment from the Departments of Food Science and Technology and Oxidative Stress Research Centre and Chemical Engineering of the Cape Peninsula University of Technology were used. The experimental design of this chapter is illustrated in Figure 3.1.

3.2.2. Extraction of Bambara groundnut soluble dietary fibre and starch

The method of Maphosa & Jideani (2016) was followed in the extraction of BGN soluble dietary fibre (SDF) and BGN starch (BGNS) as illustrated in Figure 3.2. Whole seeds were washed, dried at 50°C for 48 h (Cabinet dryer, Model: 1069616; Geiger Klotzbucher, South Africa) and milled using a hammer mill (Trapp TRF 40, Animal ration shredder Brazil) with a sieve size of 250 µm. Flour (200 g) and distilled water (500 mL) were then blended (Cuisine systeme 5200 XL automatic, Magimix®, France) for 3 min and the slurry was centrifuged (15 min, 25°C, 1500 x g) (Avanti® J-E Centrifuge, JSE111330, Beckman Coulter Inc., USA). The supernatant and residue were used for the isolation of BGN-SDF and BGNS, respectively. From the supernatant, proteins were precipitated by adjusting the pH of the soluble fraction to pH 9 using 1 N NaOH. Following precipitation, the soluble fraction was centrifuged (10 min, 25°C, 1500 x g) and the supernatant was filtered against four diafiltration volumes of Millipore water (Diedericks & Jideani, 2015) and subjected to a tangential flow filtration system (Spectrum Laboratories Inc., USA) and the recovered BGN-SDF fraction was freeze-dried. The residue was wet screened in 2 L of water through a 53 µm sieve (Endecotts Limited, London, England) and the filtrate was centrifuged (10 min, 25°C, 1500 x g). The resultant pellet was air-dried as starch. The yield of BGNS and BNG-SDF was expressed as a percentage.

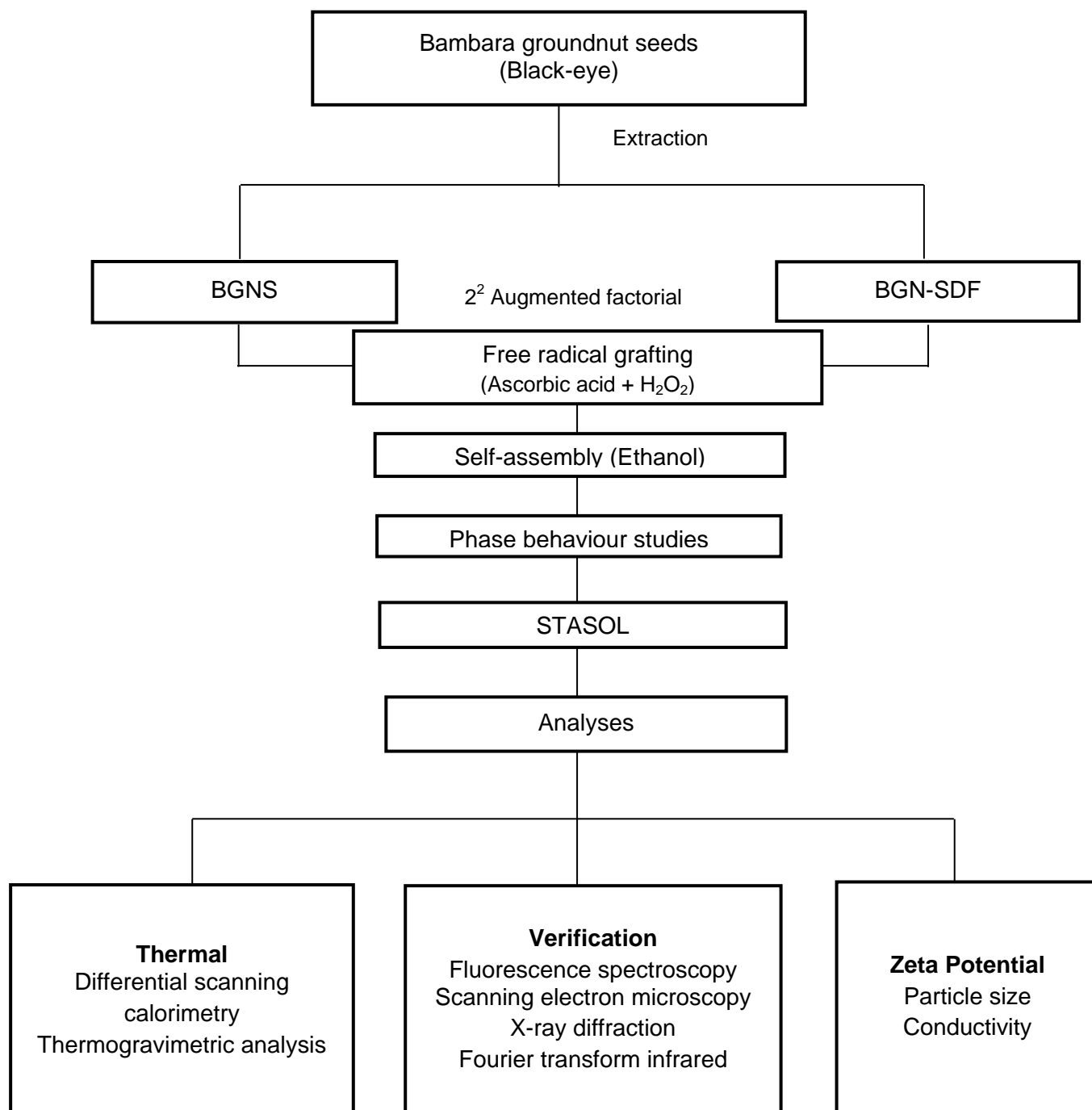


Figure 3.1 Outline of chapter 3.

BGNS: Bambara groundnut starch; BGN-SDF: Bambara groundnut soluble dietary fibre; STASOL: Bambara groundnut starch-soluble dietary fibre nanocomposite.

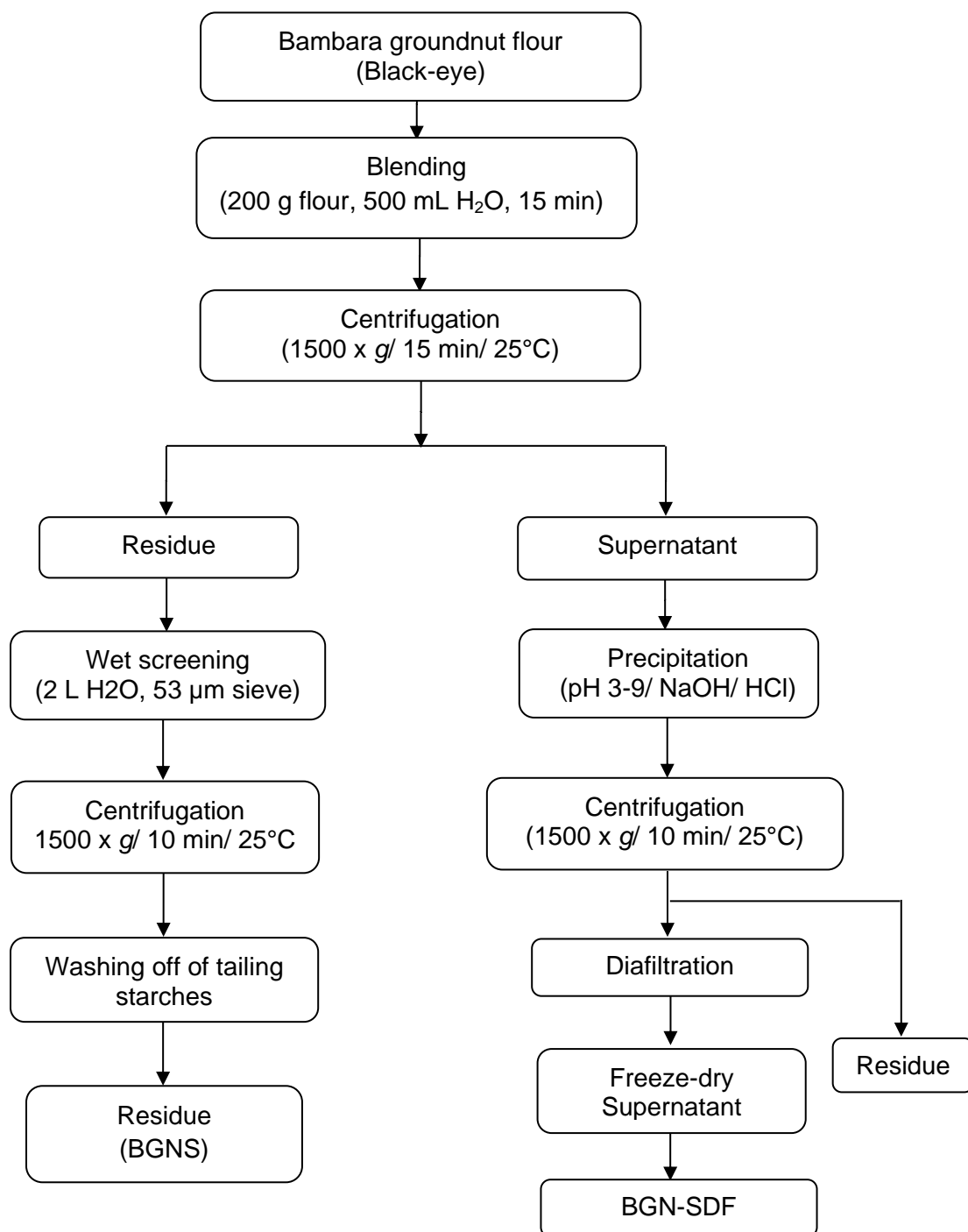


Figure 3.2 Isolation of Bambara groundnut STASOL (Dalgetty & Baik, 2003; Maphosa & Jideani, 2016).

BGNS: Bambara groundnut starch; BGN-SDF: Bambara groundnut soluble dietary fibre; STASOL: Bambara groundnut starch-soluble dietary fibre.

3.2.3 Phase behaviour study of Bambara groundnut starch and soluble dietary fibre

The phase behaviour of different concentrations of BGNS:BGN-SDF were studied using an augmented 2^2 factorial design (Table 3.1). Samples were weighed into centrifuge tubes then mixed with 0.1 M NaCl and 10 mM tris-HCl buffer at pH 7.2. The mixture was vortexed at high speed for 1 min then left to stand overnight at 20°C. Visual detection of samples was carried out and pictorial representations were obtained.

Table 3.1 Phase behaviour analysis of BGNS and BGN-SDF

	BGNS level	BGN-SDF level	BGNS (g)	BGN-SDF (g)
1	-1	-1	5	0.65
a	+1	-1	10	1.30
b	-1	+1	15	1.95
ab	+1	+1	15	0.65
	0	0	5	1.95

BGNS: Bambara groundnut starch; BGN-SDF: Bambara groundnut soluble dietary fibre.
-1: low level; 0: middle level; +1: high level.

Phase separation was also determined using the Turbiscan (Turbiscan MA 2000, Formulacion, Toulouse, France) following the method of Adeyi *et al.* (2014). Each sample (7 mL) was placed in a 65 mm long Turbiscan tube and scanned along the height of the tube at 10 min intervals for 1 h. Multiple scans were carried out and from these, phase separation of the biopolymers was observed. Each scan provided a curve and all curves were laid on a single graph. From these scans, stability or separation was observed. The curves generated during the measurements were used to provide the backscattering (BS) and transmission flux percentage relative to the instrument's internal standard as a function of the height of the sample.

3.2.4 Production of starch-soluble dietary fibre nanocomposite

A modified method of Spizzirri *et al.* (2011) was adopted in the preparation of STASOL from BGNS and BGN-SDF. An ascorbic acid/hydrogen peroxide redox pair was employed as the initiator system. In a 100 mL Schott bottle, BGNS (15 g) and deionised water (37.5 mL) were mixed. Then H_2O_2 (120 v) and ascorbic acid were added as determined by the augmented 2^2 factorial experiment (Table 3.2) and the mixture was incubated at 90°C for 45 min in a

temperature-controlled water bath (Ecobath, LaboTec). The mixture was then cooled to room temperature before precipitating with absolute ethanol (EtOH).

Table 3.2 Process variables and levels used for 2^2 augmented factorial design

Variable	Coded variable level (x_i)		
	-1	0	+1
Ascorbic acid (X_1)	0.1	0.4	0.7
Hydrogen peroxide (X_2)	8.5	12.5	16.5

-1 = Low level; 0 = middle level; +1 = High level. The transformation from the coded to the uncoded values: $X_1 = 0.3x + 0.4$; $X_2 = 4x + 12.5$

Absolute ethanol (40 mL) was added drop wise to the mixture with continuous agitation in a sonicator (Sonicator-Heat systems-Ultrasonics, Inc., Model W-225R, Krugersdorp, South Africa) for 10 min at high speed. The mixture was then centrifuged (Jouan MR1812 Thermo Electron Corporation) at 6 000 rpm for 5 min and the supernatant was discarded. To obtain the regenerated BGNS particles, the residue was rinsed three times with absolute ethanol (40 mL) by centrifugation to remove H_2O_2 and ascorbic acid. To complex BGNS and BGN-SDF to produce STASOL, 1.95 g of BGN-SDF was added to the obtained BGNS particles according to the method of Liu *et al.* (2015) and left to react for 24 h, on a magnetic stirrer (Dragon Lab, MS-H-Pro), in a dark place. The resulting solution was freeze-dried (VirTis Genesis 25EL). The controls were BGNS and BGN-SDF and were subjected to the same conditions (Gulu, 2018).

3.2.5 Verification of starch-soluble dietary fibre nanocomposite

The authenticity of STASOL was verified using a Zetasizer, FTIR, XRD, SEM and spectrofluorimeter. Each analysis was carried out in duplicate.

1. Conductivity and particle size determination of Bambara groundnut starch, soluble dietary fibre and starch-soluble dietary fibre nanocomposite

Conductivity and particle sizes of the biopolymers were analysed at a temperature of 25°C and viscosity of 10 cP using a Zetasizer (Nano ZS90, Malvern Nanoseries Instruments). Samples (0.2 g) were suspended in 5 mL methanol and a polystyrene zeta potential cell (zen1020, Malvern Instruments) was used in the analysis of particle size. A dip cell (zen1002, Malvern Instruments) with a pair of parallel Pd electrodes was used to provide an electrical trigger on

charged particles. All samples were run 11 times with each run lasting 10 s. Data were analysed using the Zetasizer Software.

2. *Functional groups of Bambara groundnut starch, soluble dietary fibre and starch-soluble dietary fibre nanocomposite*

Fourier transform infrared spectra were carried out on a Golden-gate Diamond single reflectance ATR in an FTS 7000 FT-IR spectrometer with a DGTS detector (DIGILAB, Randolph, MA) as described by Kasran (2013). Finely powdered samples were accurately weighed and mixed with dry KBr (1:100, sample:KBr) in a vibratory ball mill capsule for 5 min. The mixture was transferred to a specadie producing an 8.5 mm diameter film which was analysed in the beam of the FTIR spectrophotometer. The spectra were recorded at absorbance mode from 1200 to 800 cm^{-1} at a resolution of 4 cm^{-1} with 128 co-added scans.

3. *Crystallinity of Bambara groundnut starch, soluble dietary fibre and starch-soluble dietary fibre nanocomposite*

Powder X-ray diffraction (XRD) patterns were collected in transmission using an X-ray diffractometer (Phillips PW 3830/40 Generator) following the method of Afolabi (2012). Samples of BGNS, BGN-SDF and STASOL were measured in the 2θ angle range between 5° and 70° at a step size of 0.034, target voltage of 40 kV, target current of 100 mA, the ageing time of 5 min and radiation wavelength of 0.1542 nm.

4. *Morphology and microstructure of Bambara groundnut starch, soluble dietary fibre and starch-soluble dietary fibre nanocomposite*

To study morphology and microscopic structure of BGNS, BGN-SDF and STASOL, a scanning electron microscope (SEM, Leo^(R) 1430VP) was used. A freeze-dried thin layer of the sample was mounted on aluminium stubs with double-sided carbon tape then coated with a thin layer of gold to make it electrically conductive. Two fields per sample were studied to obtain a representative number of particles ($n = 300\text{-}800$ particles). The samples were examined at 7 kV (Rosell *et al.*, 2009).

5. *Fluorescence analysis of Bambara groundnut starch, soluble dietary fibre and starch-soluble dietary fibre nanocomposite*

Samples (10 mg) of BGNS, BGN-SDF and STASOL were dissolved in 50 mL deionised water then transferred to cuvettes (1 cm path length) and their fluorescence was measured using a spectrofluorometer (Perkin Elmer, LS 55, Fluorescence Spectrometer, Llantrisant, UK) following

the method of Singh *et al.* (2010). The settings used were: excitation and emission slit (2.5 nm), acquisition interval (1 nm), integration time for the total luminescence spectra (0.1 s) and integration time for the synchronous scan method (0.05 s). The excitation-emission matrices spectra were recorded from 250 to 500 nm at 5 nm intervals, while the emission spectra ranged between 280 to 600 nm at 5 nm intervals. Excitation and emission monochromators in the range of 250-500 nm were run concurrently to obtain a synchronous fluorescence spectrum.

3.2.6 Thermal analysis of Bambara groundnut starch, soluble dietary fibre and starch-soluble dietary fibre nanocomposite

The thermal analysis of BGNS, BGN-SDF and STASOL was carried out using differential scanning calorimetry (DSC) (Perkin Elmer, DSC 6000, United Kingdom) and thermogravimetric analysis (TGA) (Perkin Elmer, TGA 4000, United Kingdom) according to a modified method of Liu *et al.* (2015) and Maphosa & Jideani (2016).

1. Differential scanning calorimetry

Samples (2 mg) were placed in DSC pans and empty pans were used as references. Differential scanning calorimetry was conducted at a linear heating rate of 10°C/min from 25 to 400°C under nitrogen, at a flow rate of 20 mL/min. The temperature difference across the sample and the reference chromel wafers gave a measurement of heat flow. A pure indium standard was used for calibration. The thermal behaviour of samples was observed as peaks and the extrapolated peak (T_p), peak area as well as enthalpy of gelatinisation (ΔH) were recorded.

2. Thermogravimetric analysis

Samples (7 mg) were placed in aluminium pans and empty pans were used as references. Thermogravimetric analysis was conducted at a linear heating rate of 20°C/min from 25 to 700°C under nitrogen, at a flow rate of 20 mL/min. Mass loss was graphically represented and observed as peaks.

3.2.7 Data analysis

All experiments were carried out in triplicate. Data were expressed as mean \pm standard deviation. For statistical analysis, IBM Statistical Package for the Social Science (SPSS) was used. The results were subjected to multivariate analysis of variance (MANOVA) to establish differences between treatments. Duncan's multiple range test was used to separate means where a significant difference existed at $p \leq 0.05$.

3.3 Results and Discussion

The yields of Bambara groundnut starch, soluble dietary fibre and starch-soluble dietary fibre nanocomposite are discussed in the following sections.

3.3.1 Yield of Bambara groundnut starch, soluble dietary fibre and starch-soluble dietary fibre nanocomposite

The objective of isolating BGNS and BGN-SDF using the method of Maphosa (2016) was successfully achieved. Figure 3.3 shows visual representations of the extracted BGNS, BGN-SDF and STASOL. The yields of BGNS and BGN-SDF were calculated based on 100 g BGN flour.



Figure 3.3 Pictorial representation of BGNS, BGN-SDF and STASOL.

BGNS: Bambara groundnut starch; BGN-SDF: Bambara groundnut soluble dietary fibre; STASOL: Bambara groundnut starch- soluble dietary fibre nanocomposite.

1. Yield of Bambara groundnut starch

The yield of BGNS was 35% and the starch obtained was a flat and odourless white powder (Figure 3.3). The yield of BGNS obtained in this study differed from previously reported values. It was higher than the 31.4% reported by Gabriel *et al.* (2013) and 32% by Gulu *et al.* (2018) but lower than the 37.5-38.2% reported by Adebowale *et al.* (2002). The yield of BGNS ranges from 22-46% (Afolabi, 2012) and the results in this study were within this range. The varying amounts

of BGNS among studies can be attributed to the different starch extraction methods used, namely wet milling (Adebowale *et al.*, 2002), dry milling (Gabriel *et al.*, 2013; Gulu *et al.*, 2018) and alkaline extraction (Sirivongpaisal, 2008). Dry milling was used in this study. It was observed that wet milling methods gave higher starch yield than dry milling methods. In wet milling extraction of starch, seeds are soaked in water overnight before milling (Beaulieu *et al.*, 2020). This allows for the release of starch granules from cells into water, which increases the amount of extracted starch. In dry milling, flour is hydrated instead of seeds (Liaotrakoon *et al.*, 2014; Beaulieu *et al.*, 2020). The dry milling process of the seeds is suggested to be responsible for the loss of starch hence the relatively lower amount observed (Gulu, 2018). Despite the lower yield, dry milling was used in this study because of its water-energy efficiency compared to wet milling (Liaotrakoon *et al.*, 2014). Other factors that could have contributed to the different yields include differences in varieties as well as climatic, environmental and soil conditions in which the BGN seeds were grown.

2. *Yield of Bambara groundnut soluble dietary fibre and Bambara groundnut starch-fibre nanocomposite*

The wet milling method was successfully applied in the extraction of SDF from BGN flour yielding an average of 15.2% BGN-SDF. The dietary fibre obtained was a flat, odourless, fluffy and off-white powder (Figure 3.3). The BGN-SDF yield in this study was comparable to the 15.4% previously reported by Maphosa & Jideani (2016) and higher than the 1.3-3.5% reported by Diedericks (2014). The lower yields reported by Diedericks (2014) can be attributed to the enzymatic-gravimetric method that was applied in the extraction of BGN-SDF from BGN flour. The enzymatic-gravimetric method exposes the flour to a succession of enzymes, buffers and chemicals, namely, α -amylase, pancreatin, pepsin, amyloglucosidase, sodium acetate, phosphate buffer, trizma maleate, sodium hydroxide, hydrochloric acid and ethanol. The repeated processing of the flour results in the loss of soluble dietary fibre at each step. Furthermore, the chemicals employed solubilise SDF resulting in a low recovery of dietary fibre (Maphosa, 2016).

The SDF content of legumes such as peas and soybeans have been reported to range from 3.3 to 13.8% (Guillon & Champ, 2002). The yield of SDF in this study was higher and could indicate that BGN is a superior source of SDF compared to other legumes, and would therefore have a market advantage. The sugar composition of legumes also affects their SDF percentage. Arabinose was reported to be absent in pea and lentil SDF (Dalgetty & Baik, 2003) while 9.4-19.6% were reported in BGN-SDF (Maphosa, 2016). From the yield obtained, BGN was concluded to be high in SDF as the South African Foodstuffs, Cosmetics and Disinfectants

Act, 1972 (Revised on 1 March 2010) defines 'High in Fibre' as more than 6 g per 100 g dry solids. STASOL was composed of BGNS and BGN-SDF at a ratio of 15:1.95 dry weight. The resultant nanocomposite (Figure 3.3) was a tasteless, odourless and fine white powder.

3.3.2 Predicted formation mechanism for STASOL

The preparation and study of starch-dietary fibre conjugates are very important, considering the different physical, chemical, functional and physiological properties of starch and SDF. The complexing of BGNS and BGN-SDF took into consideration the type and nature of bonds present in both polysaccharides, the gelatinisation temperatures of starch, the reaction between starch and chemical initiators as well as the self-assembling abilities of the polysaccharides in ethanol. An ascorbic acid-hydrogen peroxide redox pair was used as the chemical initiator for the production of STASOL. The free radical-induced grafting method (Spizzirri *et al.*, 2010) was coupled with a self-assembling method (Kim *et al.*, 2015; Yu *et al.*, 2014) to covalently bind BGN-SDF onto BGNS. An ascorbic acid-hydrogen peroxide redox pair was employed as a water-soluble, biocompatible initiator system (Gulu *et al.*, 2018). The radical scavenging activity involved the oxidation of ascorbic acid by H_2O_2 at ambient temperature forming ascorbate and hydroxyl radical intermediates (Nimse & Pal, 2015; Gulu, 2018). These intermediates then initiated the reaction (Spizzirri *et al.*, 2010). The reaction mechanism occurred in three steps as illustrated in Figure 3.4.

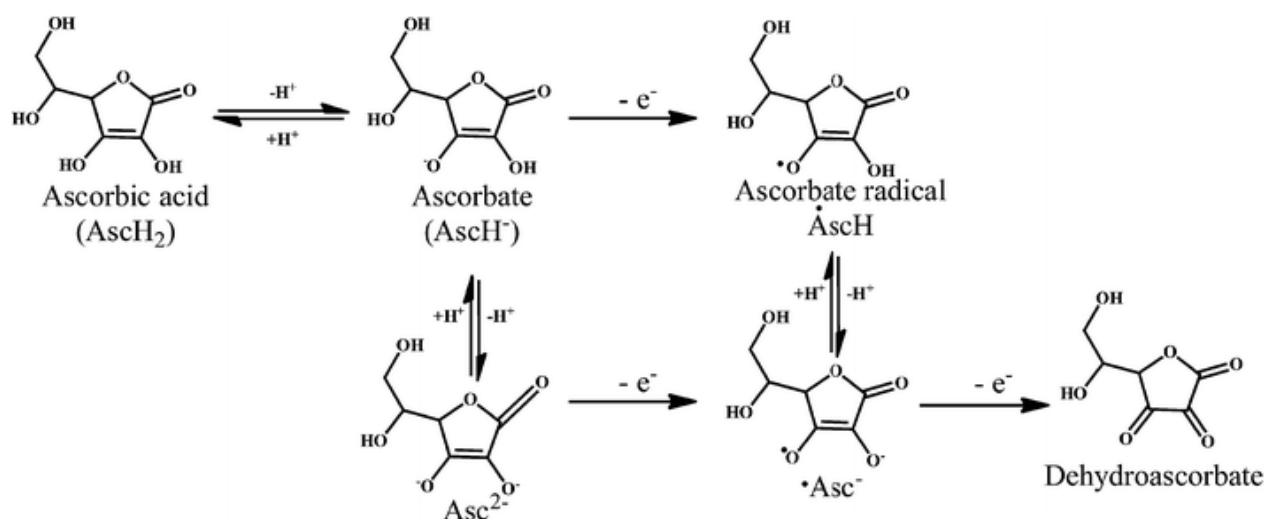


Figure 3.4 Mechanism of radical scavenging activity of ascorbic acid (Nimse & Pal, 2015).

The first step involved the activation of the BGNS chain towards radical reaction as well as the formation of hydroxyl radicals. The second step involved the abstraction of hydrogen atoms from the hydroxyl groups generated in step one. This left the BGNS chain exposed, thus allowing it to form self-aggregates with other compounds by forming intra- and inter-molecular associations (Liu *et al.*, 2015). The third step involved the employment of ethanol as an initiator of self-assembly. At the self-assembling stage, the BGNS had been modified and was therefore soluble in the aqueous medium. As such, dispersing the modified BGNS and BGN-SDF in ethanol, with continuous agitation, resulted in the attachment of BGN-SDF onto the outer layer of BGNS granules, forming linkages with 2, 3 and/or 6 OH of glucose molecules in the amorphous region of BGNS blocks derived from the destructive modification method (Liu *et al.*, 2015). In polysaccharide-polysaccharide complexing, the more robust polysaccharide commonly forms a protective layer around the weaker polysaccharide, thereby forming a composite of high resistance and strength (Liu *et al.*, 2015). As such, it is predicted that BGN-SDF formed a protective layer around modified BGNS molecules.






3.3.3 Phase behaviour of various Bambara groundnut starch and soluble dietary fibre concentrations in solution

Five combinations of BGNS and BGN-SDF were successfully studied and the visual, pictorial and initial backscattering of BGNS-BGN-SDF combinations are presented in Table 3.3. According to the Turbiscan analysis (Table 3.4), the least (BS = 77.1%) and most stable (BS = 86.9%) combinations were 15:0.65 and 15:1.95 (BGNS:BGN-SDF), respectively. However, the least stable combination according to visual evaluation was 5:0.65 (BGNS:BGN-SDF) as syneresis and a visible separation of polymer phases were observed.

Figure 3.5 shows possible modes of interaction between BGNS and BGN-SDF. Different polysaccharides are not compatible when there is no attraction between them or when the entropy difference exceeds the enthalpy of mixing (Jha *et al.*, 2014). Complexing macromolecules involves a low entropy change, hence, the weak intermolecular interactions become adequate to stabilise the complex. Such interactions are characteristic of unfolded chains able to form inter-chain contacts (Tolstoguzov, 2006). As biopolymer concentration increases, the interaction between unfolded biopolymer chains also increases thus increasing the stability of biopolymer-biopolymer in the resultant complex (Jha *et al.*, 2014).

Stability was also observed as the extent of separation between the Turbiscan backscattering scans. The Turbiscan profiles of all combinations followed the same path as the initial scan. However, with the increase in time, a decrease in backscattering flux percentage was observed resulting in scans that were not perfectly overlaid.

Table 3.3 Visual representation of phase separation between BGNS and BGN-SDF

BGNS:BGN-SDF	Visual observation	Initial BS (%)	Pictorial representation
5:0.65	Visible separation of polymer phases. Syneresis	78.4	
10:1.3	A thin layer of SDF observed on the top No syneresis observed Two layers of polymers observed	79.8	
15:1.95	No separation observed	82.9	
15:0.65	No separation observed	77.1	
5:1.95	A thin layer of SDF observed on the top No syneresis observed Two layers of polymers observed	80.9	

BGNS: Bambara groundnut starch; BGN-SDF: Bambara groundnut soluble dietary fibre.

Table 3.4 Backscattering of BGNS and BGN-SDF combinations

BGNS:BGN-SDF	Initial BS (%)
5:0.65	78.4
10:1.3	79.8
15:1.95	82.9
15:0.65	77.1
5:1.95	80.9

BGNS: Bambara groundnut starch; BGN-SDF: Bambara groundnut soluble dietary fibre;
BS: Backscattering

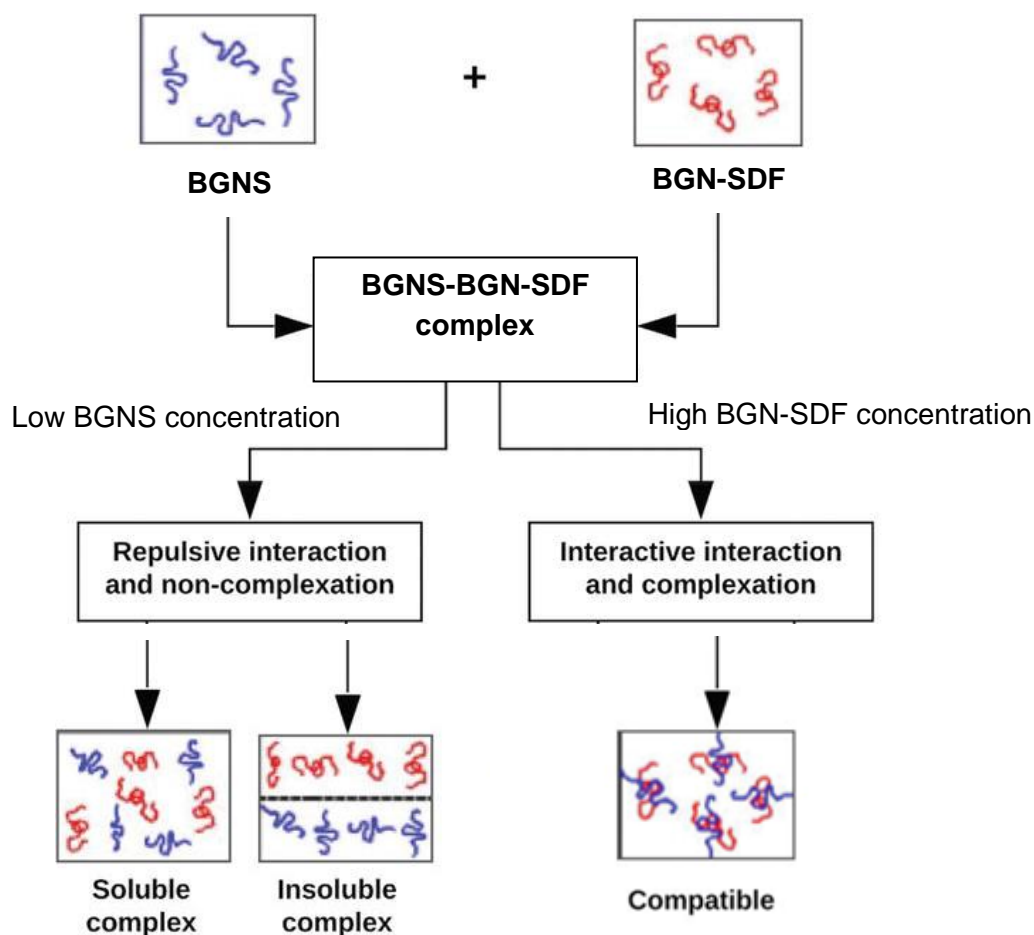
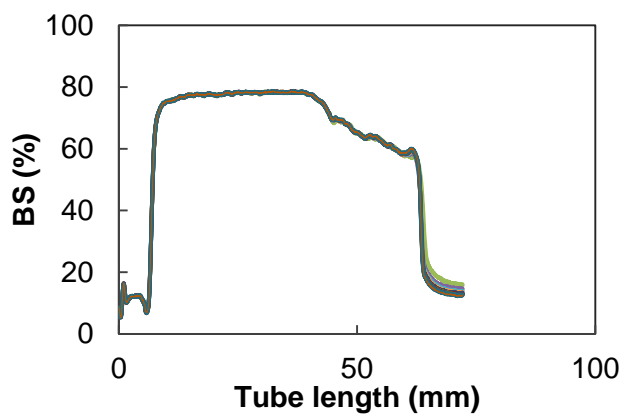


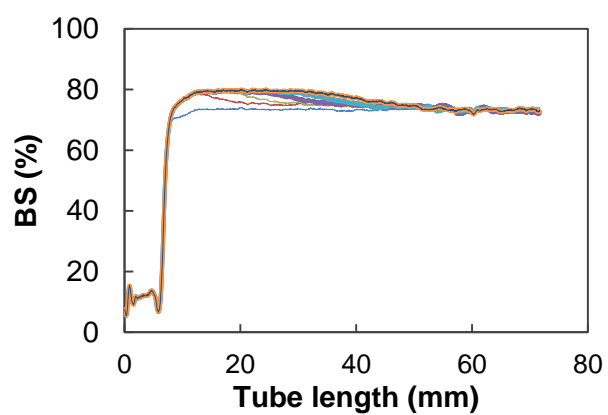
Figure 3.5 Possible modes of interaction between BGNS and BGN-SDF.
BGNS: Bambara groundnut starch; BGN-SDF: Bambara groundnut soluble dietary fibre.

The most stable combination exhibited the least separated backscattering scans (Diedericks & Jideani, 2014; Maphosa, 2016). The phenomenon responsible for instability and separation of BGNS and BGN-SDF fractions was proposed to be segregative phase separation. This form of separation occurs between biopolymers with a similar charge, two neutral biopolymers or between a neutral biopolymer and a charged biopolymer (Maphosa & Jideani, 2017). At low concentrations, segregative phase separation leads to electrostatic repulsion or steric exclusion, resulting in the biopolymers separating into two phases (Jha *et al.*, 2014; Gao *et al.*, 2017).

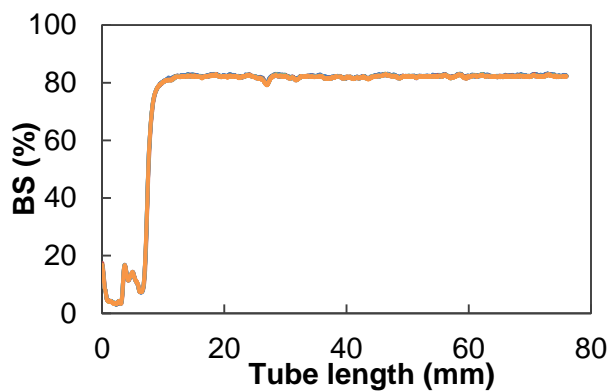
The Turbiscan profiles of the different BGNS and BGN-SDF combinations were detailed in Figure 3.6. The x-axis denotes the height of the tube and the y-axis denotes the backscattering flux percentage (Adeyi, 2014).



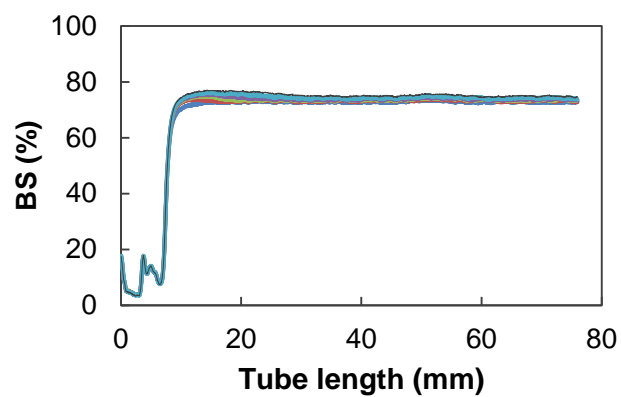
a



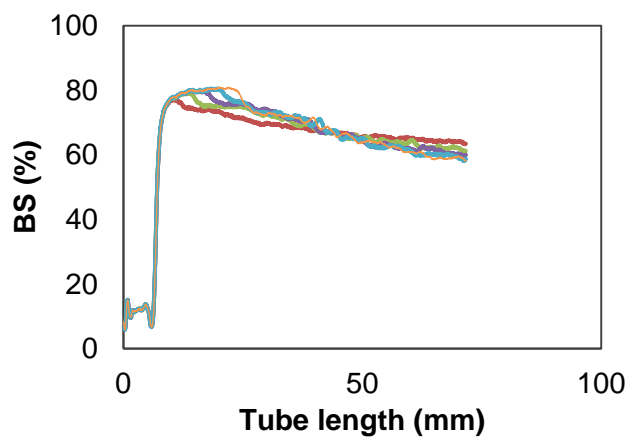
b



c



d



e

Figure 3.6 Changes in the backscattering (BS) profile (%) as a function of sample height with varying BGNS:BGN-SDF ratios at a) 5:0.65 b) 10:1.3 c) 15:1.95 d) 15:0.65 e) 5:1.95.

The initial backscattering flux percentage ranged from 78.4% (5 g BGNS:0.65 g BGN-SDF) to 82.9% (15 g BGNS:1.95 g BGN-SDF). The most stable combination was composed of 15:1.95 (BGNS:BGN-SDF) as the backscattering scans were the least separated (Figure 3.6). The path taken by the scans suggested particle aggregation, which could be attributed to either flocculation or coalescence, as the main phenomenon of destabilisation in the emulsions. This was in agreement with Diedericks (2014) and Maphosa (2016) who reported flocculation as the main phenomenon responsible for destabilisation of BGN-SDF stabilised emulsions.

3.3.4 Particle sizes and conductivity of Bambara groundnut starch, soluble dietary fibre and starch-soluble dietary fibre nanocomposite

The particle sizes and conductivity of BGNS, BGN-SDF and STASOL were determined using a zetasizer.

1. Particle sizes of Bambara groundnut starch, soluble dietary fibre and starch-soluble dietary fibre nanocomposite

The particle sizes (diameters) of BGNS, BGN-SDF and STASOL were 237.9, 118.3 and 74.01 nm, respectively (Figure 3.7).

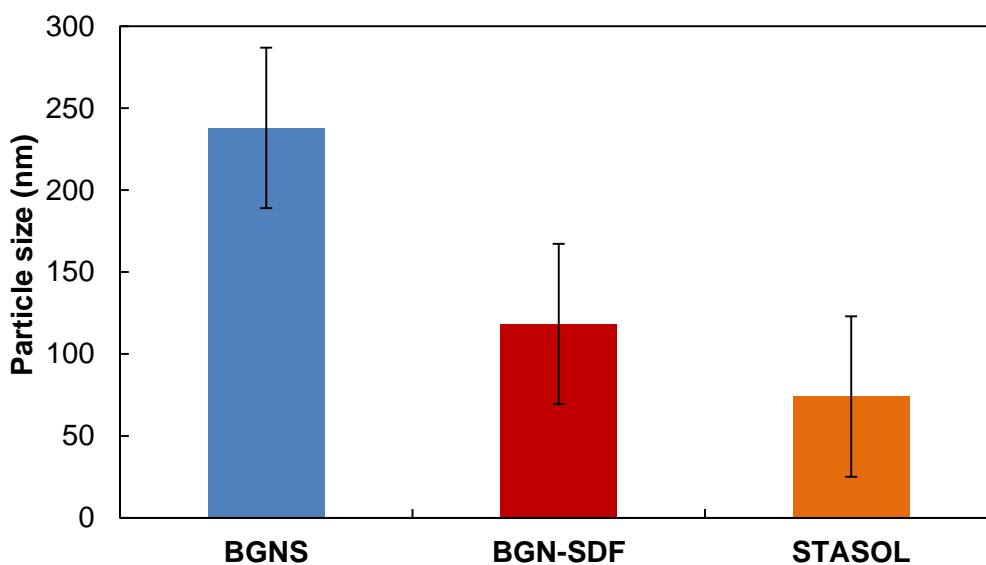


Figure 3.7 Particle sizes of BGNS, BGN-SDF and STASOL.

BGNS: Bambara groundnut starch; BGN-SDF: Bambara groundnut soluble dietary fibre; STASOL: Bambara groundnut starch-soluble dietary fibre nanocomposite.

Particle size analysis gives information on the size and distribution of particles, therefore, allowing for the prediction of their behaviour when exposed to certain conditions. A smaller particle size translates to an increased surface area thereby improving dissolution and reaction rates (Elder *et al.*, 2018). The average particle sizes of STASOL and BGN-SDF were not significantly different while both were significantly ($p = 0.000$) different from that of BGNS. For composites to be considered nanocomposites, at least one dimension should be within the nano level (<100 nm) (Rauscher *et al.*, 2017). As such, STASOL was confirmed to be a nanocomposite (Figure 3.7). Although BGNS and BGN-SDF were nanosized, they could not be considered nanocomposites because their sizes were above 100 nm. Based on particle size, STASOL would be expected to have the highest solubility index and dissolution rate which would make it a desirable ingredient in water-based food systems.

2. Conductivity of Bambara groundnut starch, soluble dietary fibre and starch-soluble dietary fibre nanocomposite

The zeta potential or conductivity of BGNS, BGN-SDF and STASOL was -57.3, -6.03 and -2.03 mV, respectively (Figure 3.8).

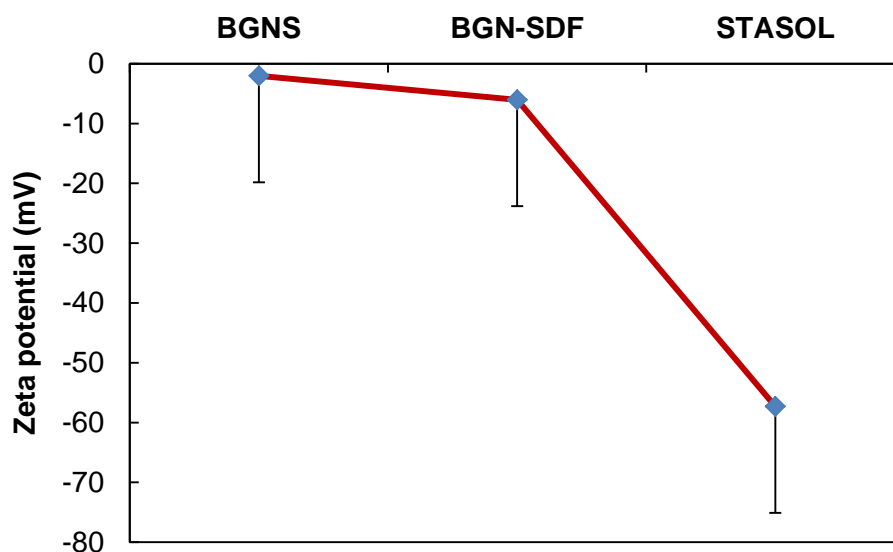


Figure 3.8 Zeta potential of BGNS, BGN-SDF and STASOL.
 BGNS: Bambara groundnut starch; BGN-SDF: Bambara groundnut soluble dietary fibre; STASOL: Bambara groundnut starch-soluble dietary fibre nanocomposite.

Zeta potential is the electric potential due to surface charge on a particle (Bassioni & Taqvi, 2019), and is dependent on the functional groups of the particles under study. As such, zeta potential is the difference in potential between the interfacial double layer of a solid particle submerged in a conducting liquid and the liquid (Bassioni & Taqvi, 2019). The conductivity of BGNS and BGN-SDF were not significantly different while both were significantly ($p = 0.000$) different from that of STASOL. A negative zeta potential indicates the stability of a compound, with a higher negative value indicating higher stability. Emulsions with positive conductivity are less stable and tend to coagulate or flocculate. Zeta potential is affected by pH, temperature, mass concentration, the molecular structure of medium as well as ionic strength (Losso *et al.*, 2005). In this study, STASOL had the highest zeta potential (-57.3 mV) which was suggestive of very high stability. This was in agreement with Lu & Gao (2010) who reported high stability of emulsions with zeta potential values of -41 to -50 mV. The more negative charge represents stronger repulsive forces and consequently lower chances of aggregation of particles. Aggregation results in particles clumping together resulting in larger particle sizes. As such, the more negative the zeta potential, the larger the surface area available on particles. This was in agreement with particle size results reported in section 3.3.4 (1) where STASOL had the smallest particle size (74.01 nm) and the most stable solution according to conductivity studies.

Stability prediction between emulsions is only possible if the values are at least 10 mV apart (Roland *et al.*, 2003). Therefore, the stability between STASOL and BGN-SDF as well as between STASOL and BGNS could be compared using zeta potential values. Lu & Gao (2010) stated that emulsions with zeta potential values ranging from -11 to -20 mV were close to the threshold of agglomeration. The zeta potentials of BGNS and BGN-SDF were very low suggesting a tendency to agglomerate and form larger particles. This could be the reason for the larger particle sizes of the biopolymers reported in section 3.3.4 (1). STASOL was manufactured for use as a stabiliser in orange oil beverage emulsions. Its stability and small particle size would be expected to make it a good stabiliser. The surface charge of most emulsions is associated with their half-life stability (Losso *et al.*, 2005). As such, zeta potential can be used in the prediction of the stability and shelf life of emulsions.

3.3.5 Functional groups of Bambara groundnut starch, soluble dietary fibre and starch-soluble dietary fibre nanocomposite

Fourier transform infrared was carried out to assess the functional groups present in BGNS, BGN-SDF and STASOL. All three carbohydrate polymers have a similar composition, which explained the resemblance in their IR spectra.

1. *Native Bambara groundnut starch*

Fourier transform infrared spectra of BGNS showed a band in the region of 2800-3000 cm^{-1} with a peak at 2924.32 cm^{-1} (Figure 3.9), which could be attributed to the stretching of C-H bonds. The presence of amylose and amylopectin, the building blocks of starch, influence the absorbance of starch in this region (Kizil *et al.*, 2002; Oyeyinka & Oyeyinka, 2018). Broadband in the region 3600-3000 cm^{-1} could be attributed to the vibrational stretching of the hydrogen-bonded OH groups (Kaptso *et al.*, 2015). These are associated with the inter-and intra-molecular bound OH groups having a polymeric association, which makes up the gross structure of starch (Zhang & Han, 2006; Afolabi, 2011; Oyeyinka *et al.*, 2016; Gulu, 2018).

The peaks in the region 3380-1400 cm^{-1} are characteristic of stretching vibrations and deformation of the OH bond of water. The peak at 1641.71 cm^{-1} is characteristic of C=O of carboxyl groups as well as the vibration of OH of water molecules in the non-crystalline region of starch (Kizil *et al.*, 2002). Zhang & Han (2006) and Oyeyinka *et al.* (2016) reported similar results for pea and BGNS, respectively. The absorbance of BGNS at 995.22, 1076.45 and 1149.90 cm^{-1} fall in the region 1200-900 cm^{-1} characteristic of polysaccharides and is indicative of the vibration of C-O, C-C and C-H-O bonds (Warren *et al.*, 2015; Gulu, 2018). Absorbance at 861-400 cm^{-1} is indicative of the presence of sugars which is expected because starch is composed of long chains of glucose molecules. Peaks at lower wavenumbers are characteristic of the vibration of the glucose pyranose ring (Zeng *et al.*, 2011). This further confirmed the presence of C, H and O atoms which make up the skeleton of starch molecules. The bands between 1300 and 800 cm^{-1} represent the vibration of C-O and C-C bonds. The peaks at 860.59, 571.59 and 522.93 cm^{-1} were only detected in BGNS. The FTIR spectra of the biopolymers are presented in Table 3.5. The peaks observed in this study were comparable to peaks of BGNS reported in the literature (Zeng *et al.*, 2011).

2. *Bambara groundnut soluble dietary fibre*

The IR spectra for BGN-SDF (Figure 3.10) had similar peaks to BGNS spectra at 3280.17 (OH stretch), 2924.24 (C-H stretch) and 1633.68 cm^{-1} (C=O and OH vibrations) (Table 3.5). The observed behaviour was typical of polysaccharides. The bands at 1633.68 and 1537.56 cm^{-1} could be attributed to the deformation of groups of primary amide NH suggesting the presence of protein (Warren *et al.*, 2015). The sharp peak at 2853.99 cm^{-1} which could be attributed to the C-H stretch of sugars was more pronounced in BGN-SDF than in BGNS. This could be because starch is only composed of glucose molecules while BGN-SDF has glucose, arabinose, galactose, fucose, fructose, mannose and xylose (Maphosa, 2016). The peaks at 1743.34, 1537.56, 1452.68 and 1237.96 cm^{-1} were present in BGN-SDF but absent in BGNS.

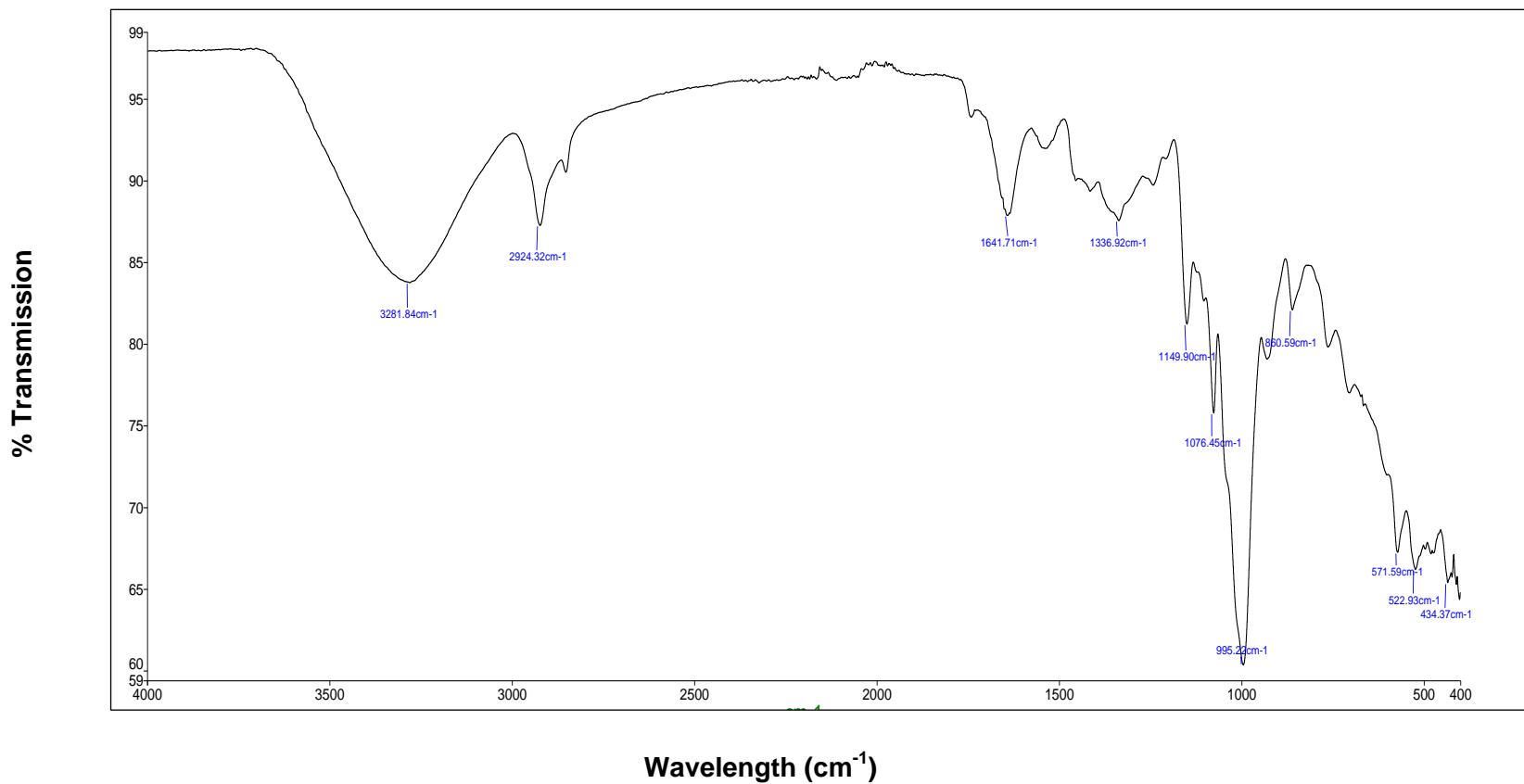


Figure 3.9 Fourier transform infrared (FTIR) spectra of native Bambara groundnut starch (BGNS).

Table 3.5 FTIR spectra of BGNS, BGN-SDF and STASOL

Polysaccharide	Initiator	Wavelength cm^{-1}
BGNS	Native	3281.84, 2924.32, 1641.71, 1336.92, 1149.90, 1076.45, 995.22, 860.59, 571.59, 522.93, 434.37
BGN-SDF	Native	3280.17, 2924.24, 2853.99, 1743.34, 1633.68, 1537.56, 1452.68, 1393.61, 1237.96, 1159.48, 1078.70, 512.26, 421.69, 408.71
STASOL	AA + H_2O_2	3279.87, 2923.77, 1631.18, 1531.55, 1368.24, 1149.26, 1077.11, 996.68, 419.64

BGNS: Bambara groundnut starch; BGN-SDF: Bambara groundnut soluble dietary fibre; STASOL: Bambara groundnut starch-fibre nanocomposite; FTIR: Fourier transform infrared.

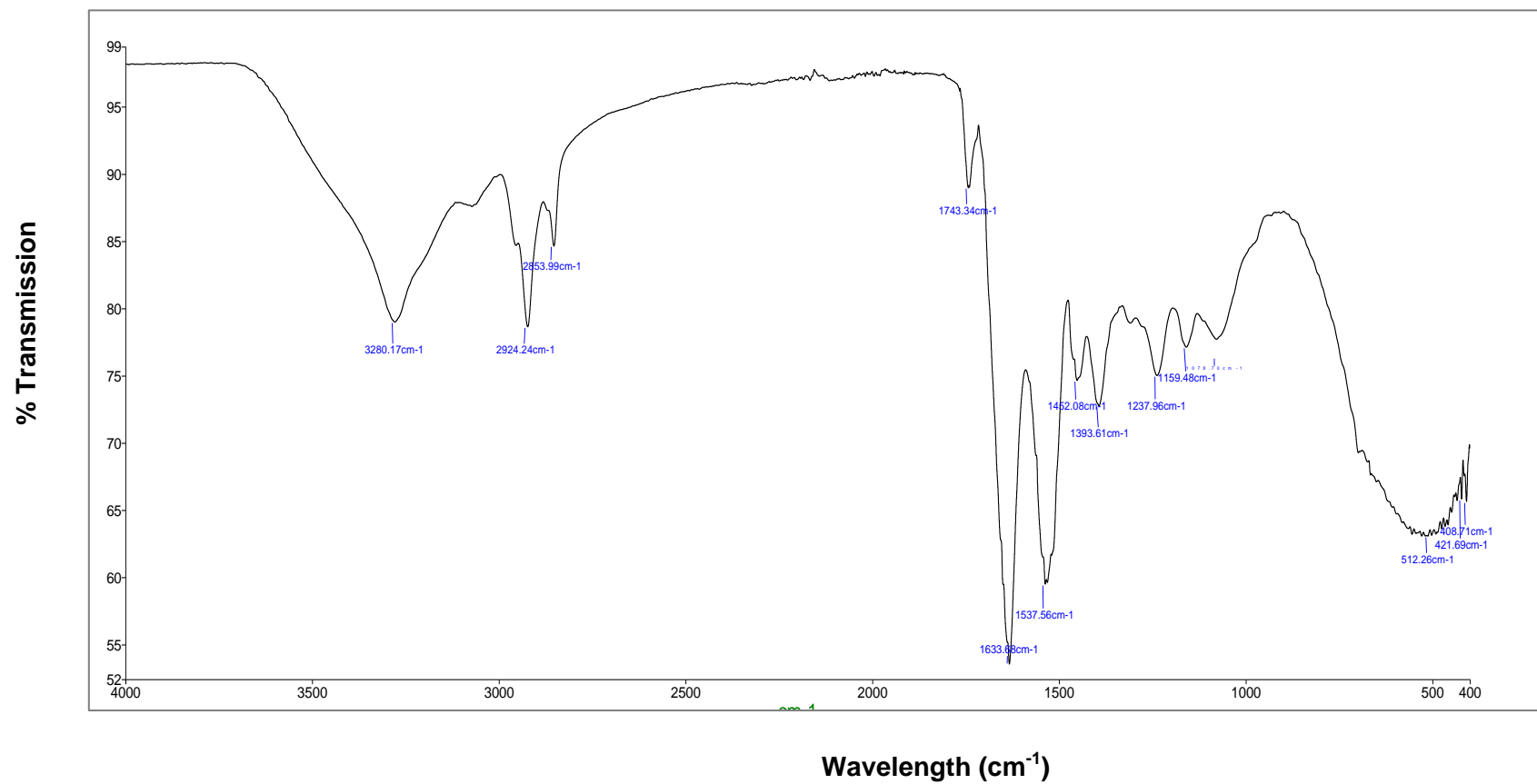


Figure 3.10 Fourier transform infrared (FTIR) spectra of Bambara groundnut soluble dietary fibre (BGN-SDF).

These are characteristic of the deformation of the OH of water, the vibration of CH₃ anti-symmetry deformation, bending of CH₂ and CH₃ as well as the C-O-C vibration of esters typical of acetates, respectively (Afolabi, 2012). At 1237.96 cm⁻¹, the peak could be representative of the C-O stretch of CH₂OH. A pronounced peak at 1393.61 cm⁻¹ was observed and is characteristic of CH₃ vibration. This peak was absent in both BGNS and STASOL. The suggestive presence of amides and esters in BGN-SDF confirmed the complex nature of the dietary fibre.

3. *Bambara groundnut starch-soluble dietary fibre nanocomposite*

STASOL is a biopolymer nanocomposite made from starch (88.5%) and soluble dietary fibre (11.5%). As predicted, the IR spectra resembled those of BGNS and BGN-SDF (Table 3.5). FTIR spectra of STASOL showed a polysaccharide typical band with a peak at 2923.77 cm⁻¹ which is characteristic of the stretching of C-H bonds (Figure 3.11). This peak was observed in both BGNS and BGN-SDF (Figure 3.12). Peaks at wavenumbers/wavelengths 3279.87 and 1631.18 cm⁻¹ were observed and can be attributed to the stretching vibrations and deformation of the OH bond of water. Both these peaks were similar to peaks observed in both BGNS and BGN-SDF. The peak at 1641.71 cm⁻¹ is also an indication of the presence of C=O of carboxyl groups (Kizil *et al.*, 2002; Zhang & Han, 2006; Oyeyinka *et al.*, 2015).

The peak at 419.64 cm⁻¹ can be attributed to the vibration of the C, H and O atoms making up the glucose pyranose ring and are indicative of the presence of sugars (Zeng *et al.*, 2011). The peak at 1368.24 cm⁻¹ could be attributed to the twisting of CH₂ bonds. The absorbance at 996.68, 1077.11 and 1149.26 cm⁻¹ falls in the region 1200-900 cm⁻¹ characteristic of polysaccharides and is indicative of the vibration of C-O, C-C and C-H-O bonds (Warren *et al.*, 2016; Gulu, 2018). The wavenumber 1077.11 cm⁻¹ showed sharp peaks in BGNS (1076.45 cm⁻¹) and BGN-SDF (1078.70 cm⁻¹) but was not sharp in STASOL signifying a change in the structure of the new compound.

BGNS and BGN-SDF had peaks in the region 512-523 cm⁻¹ while no peaks were detected in STASOL. The disappearance of these spectral bands in STASOL showed that BGNS and BGN-SDF were successfully conjugated resulting in the disruption of C-H bonds as new bonds were formed. Of particular interest was the peak at wave number 1531.55 cm⁻¹ which was also observed on the IR spectrum of BGN-SDF (1537.56 cm⁻¹) but was absent in BGNS. The peak is due to the deformation of the NH of the primary amide group. The absence in BGNS could be attributed to the absence or very low protein in the BGNS. A peak was observed in STASOL at wave number 996.68 cm⁻¹ which corresponded with the peak in the BGNS spectrum (995.22 cm⁻¹) but was absent in BGN-SDF. The peak fell in the range 1300 and 800 cm⁻¹ which is representative of the vibration of C-O and C-C bonds (Warren *et al.*, 2015; Gulu *et al.*, 2018).

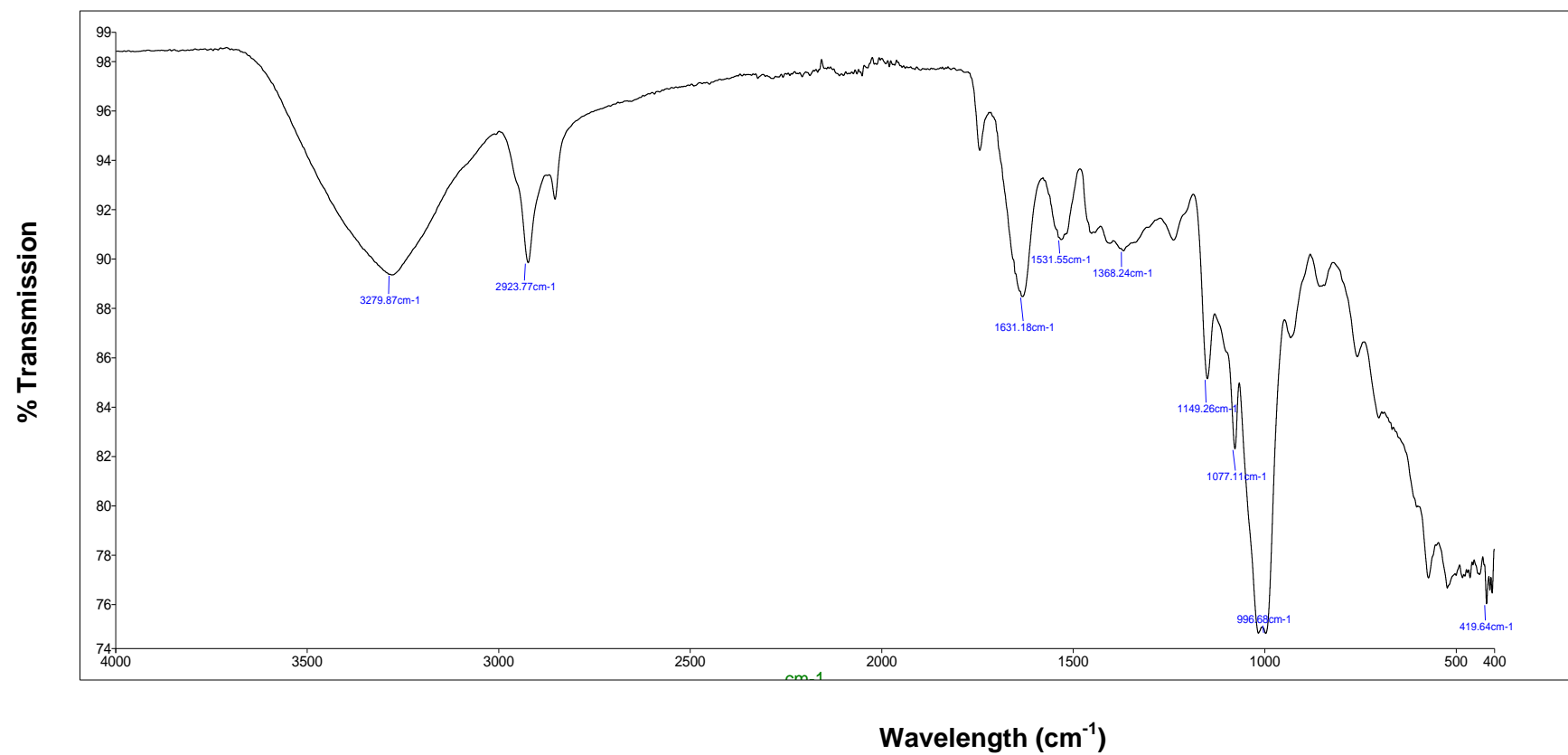


Figure 3.11 Fourier transform infrared (FTIR) spectra of Bambara groundnut starch-soluble dietary fibre nanocomposite (STASOL).

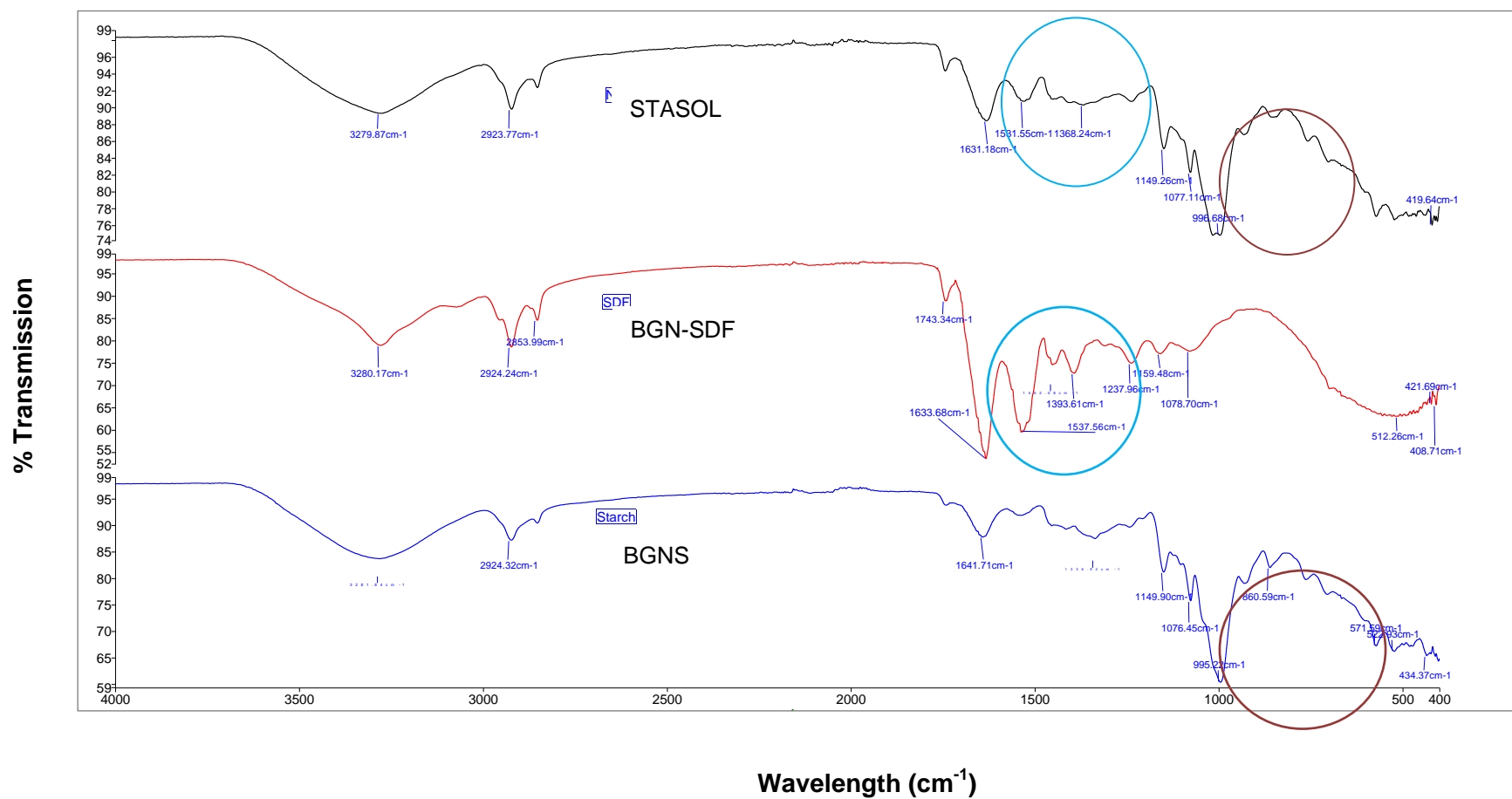


Figure 3.12 Fourier transform infrared (FTIR) spectra of BGNS, BGN-SDF and STASOL.

BGNS: Bambara groundnut starch; BGN-SDF: Bambara groundnut soluble dietary fibre; STASOL: Bambara groundnut starch-soluble dietary fibre nanocomposite.

The peak in the STASOL spectrum was not as pronounced as the corresponding one observed in the BGNS spectrum owing to the lower starch in STASOL than in BGNS. These observations indicated that STASOL possessed characteristics of both BGNS and BGN-SDF. A shift in peaks was observed in the STASOL (Figure 3.12). The wavenumbers 3281.84, 1641.71, 1076.45, 434.37 cm^{-1} in BGNS IR spectra and 3280.17, 1633.68, 1078.70, 421.69 cm^{-1} in BGN-SDF IR spectra shifted to 3279.87, 1631.18, 1077.11 and 419.64 cm^{-1} in STASOL. This further confirmed the successful formation of a new complex.

3.3.6 Crystallinity of Bambara groundnut starch, soluble dietary fibre and starch-soluble dietary fibre nanocomposite

The crystalline patterns of BGNS, BGN-SDF and STASOL are shown in Figure 3.13. X-ray diffraction is used to reveal the characteristics of the crystalline structure of starch granules (Kaptso *et al.*, 2015).

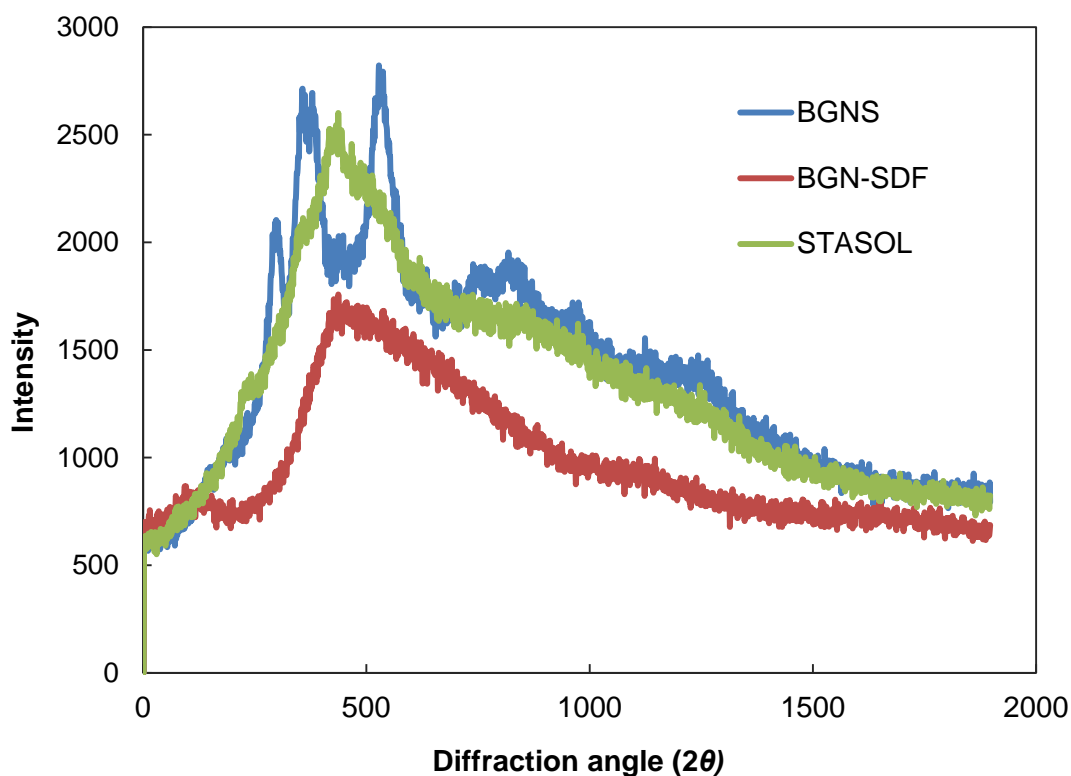


Figure 3.13 Powder X-ray diffraction patterns of BGNS, BGN-SDF and STASOL. BGNS: Bambara groundnut starch; BGN-SDF: Bambara groundnut soluble dietary fibre; STASOL: Bambara groundnut starch-soluble dietary fibre nanocomposite.

1. *X-ray diffraction patterns of BGNS*

The crystallinity of starch can be described as Type A, B or C (Wang *et al.*, 2018). BGNS exhibited strong peaks at 15, 17 and 23° (2 θ) which is typical of a C-type diffraction pattern (Gulu, 2018, Oyeyinka & Oyeyinka, 2018). Type C consists of a mixture of type A and B polymorphs, and the ratio, as well as the arrangement of the polymorphs within the granule, affects XRD reflection (Sandhu & Lim, 2018). Type C starch can be further classified as C_A-type (closer to A-type), C_B-type (closer to B-type) and C_C-type (typical C-type) according to the proportion of A- and B-type allomorphs. The XRD patterns of C_A- and C_B-type starches are similar to that of C_C-type, but exhibit a shoulder peak at about 18° 2 θ . A strong singlet peak is exhibited at 23° 2 θ for C_A-type starch while two shoulder peaks at about 22° and 24° 2 θ for C_B-type starch are common (Cai *et al.*, 2014). An extra peak was observed at 18° therefore BGNS was classified as C_A-type. Sandhu & Lim (2008) also reported the presence of a peak at 18° for type C Blackgram, mung bean and pigeon pea starches. Type C crystallinity has been reported for leguminous starch from cowpea, pea and BGN (Afolabi, 2012; Sandhu & Lim, 2018). Type C starch is characterised by lower digestibility compared to type A starches, typical of cereals. This in turn suggests a low glycemic index (GI) thereby making BGN starch suitable for diabetics and desirable for weight-conscious consumers (Gulu, 2018).

Several studies on BGN starches reported type A patterns (Sirivongpaisal, 2008; Kaptso *et al.*, 2014, Oyeyinka *et al.*, 2016) and type C patterns (Afolabi, 2012, Oyeyinka *et al.*, 2016; Oyeyinka & Oyeyinka, 2018). Differences in crystallinity of starches can be attributed to the botanical origin, arrangement of the crystalline lamellae of amylopectin, growth location, climate, soil composition as well as inherited genetic patterns (Ashogbon, 2014).

2. *X-ray diffraction patterns of BGN-SDF and STASOL*

The biopolymers BGN-SDF and STASOL did not exhibit any crystallinity. Crystallinity is lost when starch is exposed to heat and water, causing the swelling of granules until they rupture. The rupturing action results in the disruption and breakage of bonds, exposing functional groups and making them more available to reactions with water. The loss of crystallinity of legume starch following chemical treatment has been widely reported (Afolabi, 2012; Gulu, 2017). Loss of crystallinity makes starch amorphous thus increasing its water solubility. As such, STASOL would be expected to have high solubility. This prediction was in agreement with the particle size result where the average particle size of STASOL was 74.01 nm, indicating a large surface area (Figure 3.7). Therefore, STASOL could find use as a stabiliser and as an ingredient in other food systems that require dispersion in water.

3.3.7 Microstructure and morphology of Bambara groundnut starch, soluble dietary fibre and starch-soluble dietary fibre nanocomposite

Scanning electron micrographs (SEM) of BGNS, BGN-SDF and STASOL at a resolution of 20-200 μm are shown in Figure 3.14. Scanning electron microscopy gives the morphology and microstructure of a material and is useful in studying the physicochemical properties of biopolymers (Diedericks, 2014). All studied biopolymers consisted of particles of different shapes and sizes. BGNS granules exhibited a spherical structure with a smooth, unfractured surface typical of BGN starches (Kaptso *et al.*, 2015; Oyeyinka *et al.*, 2016). Bambara groundnut starch surfaces have been reported to be smooth with no fractures, suggesting a significant purity of the extracted starches (Sirivongpaisal, 2008; Oyeyinka *et al.*, 2015; Gulu, 2018). Oval and irregularly shaped BGNS granules were reported by (Oyeyinka *et al.*, 2015; Oyeyinka & Oyeyinka, 2017; Enyidi, & Onyenakazi, 2019). Polygonal and spherical shaped granules have been reported for starch extracted from white and black BGN varieties, respectively (Kaptso *et al.*, 2014). Variances in the shape and size of BGNS granules could be attributed to different cultivars, growth stage at harvest, environmental factors as well as milling, extraction and purification methods (Sirivongpaisal, 2008; Kaptso *et al.*, 2014; Oyeyinka *et al.*, 2015; Oyeyinka *et al.*, 2016).

BGN-SDF exhibited irregular and polygonal forms. The results obtained in this study were in agreement with the findings of Diedericks (2014) and Maphosa & Jideani (2016) who reported irregular forms of SDF from several BGN varieties. Similar microstructures of leguminous dietary fibres have been reported for pea (Dalgetty & Baik, 2003). Dietary fibres extracted from peas have been shown to possess comparable physicochemical properties to BGN dietary fibres (Elleuch *et al.*, 2011).

STASOL exhibited irregular and polygonal morphologies as illustrated in Figure 3.14. STASOL is produced from BGNS and BGN-SDF through a chemical grafting process that employs an ascorbic acid-hydrogen peroxide redox pair as an initiator. The process resulted in the disruption of existing bonds as well as the formation of new bonds as outlined in FTIR studies in section 3.3.5. Therefore, although BGNS comprises the higher proportion of STASOL, the modification process resulted in the loss of crystallinity of the BGNS component resulting in the loss of its typically round, oval structure. This corresponds with XRD patterns in Figure 3.13 (Section 3.3.6). The microstructure of STASOL suggested the successful formation of a new compound from BGNS and BGN-SDF.

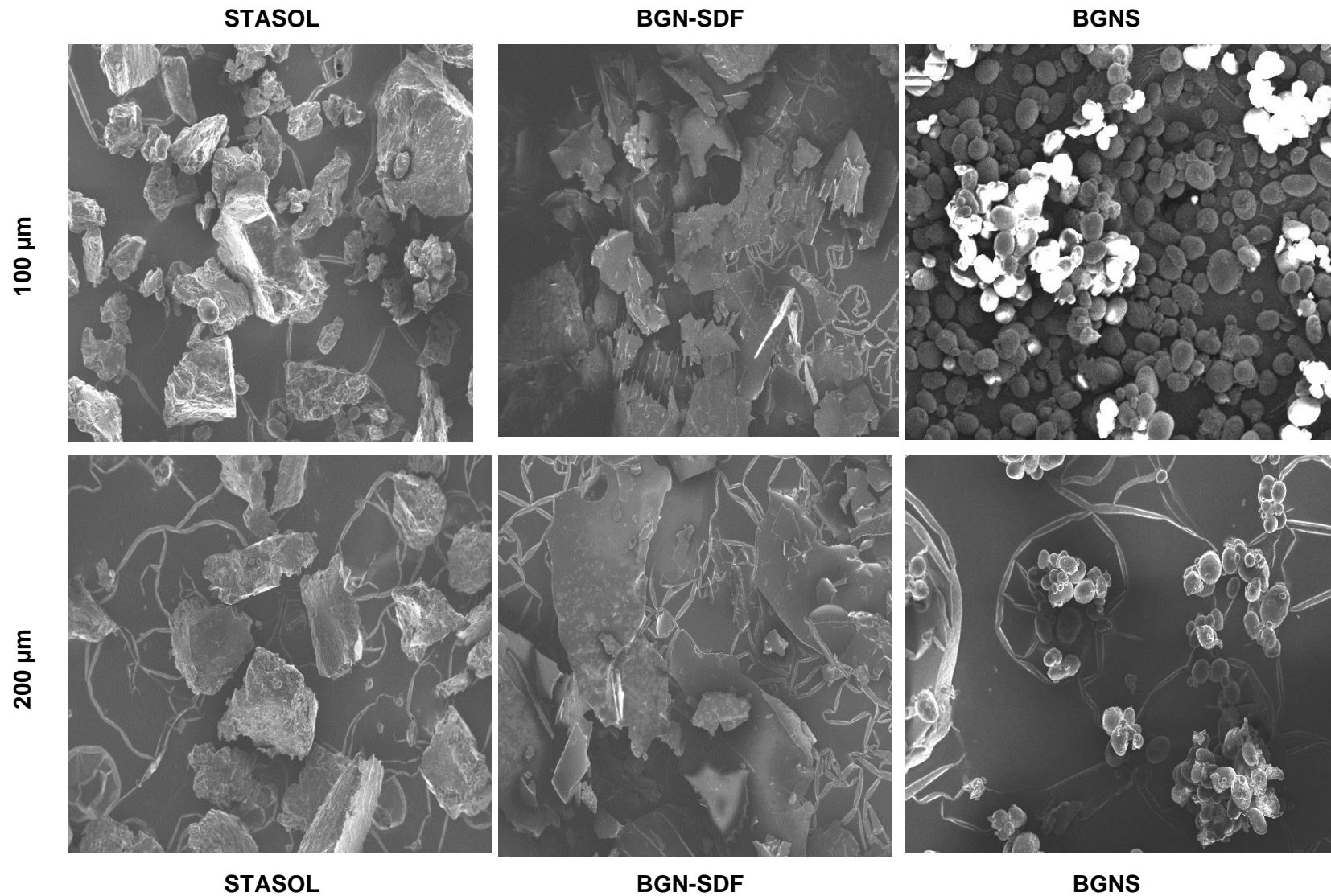


Figure 3.14 Microstructure of BGNS, BGN-SDF and STASOL.

BGNS: Bambara groundnut starch; BGN-SDF: Bambara groundnut soluble dietary fibre; STASOL: Bambara groundnut starch-soluble dietary fibre nanocomposite.

3.3.8 Fluorescence spectra of Bambara groundnut starch, soluble dietary fibre and starch-soluble dietary fibre nanocomposite

Fluorescence spectroscopy involves the excitation (absorption) and emission (fluorescence) of wavelengths and the subsequent collection of two spectra. It can be used as a non-destructive analytical technique to provide information on the presence of fluorescent molecules (Skoog et al., 2006). The intrinsic emission fluorescence spectroscopy technique reveals the conformational changes in modified starches (He et al., 2006). The fluorescence spectra of BGNS, BGN-SDF and STASOL are shown in Figure 3.15.

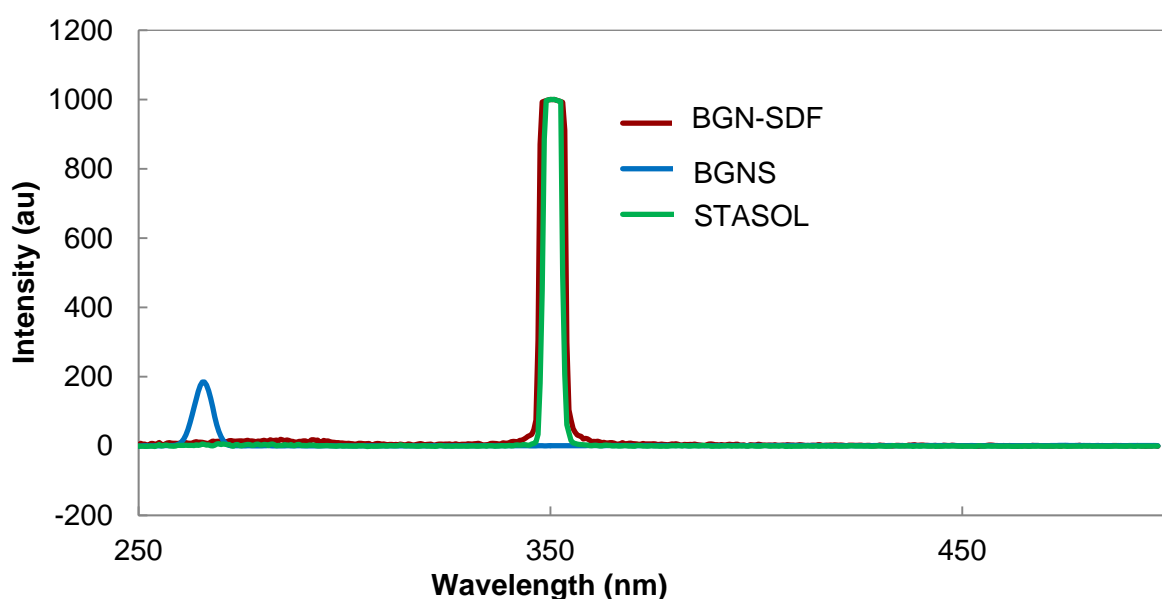


Figure 3.15 Fluorescence spectra of BGNS, BGN-SDF and STASOL.

BGNS: Bambara groundnut starch; BGN-SDF: Bambara groundnut soluble dietary fibre; STASOL: Bambara groundnut starch-soluble dietary fibre nanocomposite.

BGNS had a significantly ($p = 0.000$) lower emission spectrum at 255 nm while BGN-SDF and STASOL had higher emission spectra at 350 nm. STASOL consists of BGNS (88.5%) and BGN-SDF (11.5%) therefore it would be expected to have an emission spectrum close to that of starch. However, a significant shift in the emission spectrum was observed with STASOL emitting at 350 nm. Gulu (2018) reported the fluorescence spectrum of native BGNS as 270 nm

and that of modified BGNS as 350 nm, which was in agreement with the findings of this study. The chemical grafting of BGN-SDF onto BGNS involved the modification of BGNS using an ascorbic acid-hydrogen peroxide redox pair. The process caused a change in the intra- and intermolecular bonds of BGNS and BGN-SDF was grafted onto the exposed functional groups forming a new complex (Section 3.3.3). This explained the shift in the emission wavelength of BGNS from 255 nm to 350 nm (STASOL). The higher spectrum of STASOL than of BGNS indicated that the nanocomposite was successfully formed. The shift in the emission peaks suggests the formation of new functional groups as seen in the FTIR analyses [Section 3.3.5 (3)]. The total phenolic content of black-eye BGN-SDF is 20 mg GAE/g (Maphosa, 2016) and STASOL having BGN-SDF as one of its components would be expected to possess phenolic compounds. The phenolic compounds present in BGN-SDF and STASOL could be largely responsible for the fluorescence emission at 350 nm.

Parri *et al.* (2020) reported the emission of phenolic acids and flavonoids in honey samples in wavelengths between 340-350 nm. This was further supported by reports in the Perkin Elmer fluorescence spectroscopy handbook where phenols were reported to exhibit emission spectra from 330 nm upwards (Anon., 2000). This suggested that BGN-SDF and STASOL would be important as antioxidant containing ingredients in food products like fatty foods. Antioxidants are important protectors against radicals and lipid peroxidation in food products (Elleuch *et al.*, 2011).

3.3.9 Thermal properties of Bambara groundnut starch, soluble dietary fibre and starch-soluble dietary fibre nanocomposite

The thermal properties of BGNS, BGN-SDF and STASOL were determined using DSC and TGA. The study of the thermal behaviour of materials is important in establishing a relationship between temperature and specific physical properties (Gill *et al.*, 2010). The data collected gives insight into the behaviour of a particular material when exposed to varying temperatures.

1. *Thermal properties of BGNS, BGN-SDF and STASOL using differential scanning calorimetry*

Three major peaks were observed on the BGNS thermographs while two major peaks were observed on BGN-SDF and STASOL thermographs (Table 3.6). The initial peak thermal transition of the three biopolymers ranged from 65.50 to 77.19°C and could be attributed to the loss of moisture and volatile compounds, which is a typical endothermic process (Zhang & Wang, 2013). The first peak of BGNS at 77.19°C represents the gelatinisation of starch (Liu, 2006).

Table 3.6 Thermal properties of BGNS, BGN-SDF and STASOL using differential scanning calorimetry

	Peak 1			Peak 2			Peak 3		
	Peak (°C)	Area (mJ)	ΔH (J/g)	Peak (°C)	Area (mJ)	ΔH (J/g)	Peak (°C)	Area (mJ)	ΔH (J/g)
BGNS	77.19 ± 0.4 ^a	1420.91 ± 49 ^a	458.36 ± 16 ^a	279.52 ± 0.3 ^a	18.10 ± 6 ^a	5.84 ± 1.9 ^a	322.86 ± 0.9	-183 ± 14	-59.03 ± 4
BGN-SDF	68.84 ± 2.3 ^{ab}	397.79 ± 127 ^b	297.54 ± 110 ^b	230.30 ± 0.2 ^a	18.70 ± 2 ^a	13.9 ± 1.8 ^{ab}			
STASOL	65.50 ± 1.4 ^b	875.01 ± 33 ^b	261.36 ± 15 ^b	293.14 ± 12 ^a	83.98 ± 6 ^b	25.09 ± 2.3 ^b			

Values are mean ± standard deviation. Means within a column followed by different superscripts are significantly [$p \leq 0.05$] different. BGNS: Bambara groundnut starch; BGN-SDF: Bambara groundnut soluble dietary fibre; STASOL: Bambara groundnut starch-soluble dietary fibre nanocomposite.

Maphosa (2016) also reported minor undulations in the thermographs of BGN-SDFs at temperatures below 100°C and attributed it to the loss of moisture which could have been absorbed by the hygroscopic powders. Higher results of the peak degradation of starch due to gelatinisation were reported for BGNS (81.66°C) and BGN flour (81°C) by Kaptso *et al.* (2015) and Mubaiwa *et al.* (2018), respectively. Lower gelatinisation temperatures of BGNS were reported as 75.33°C (Sirivongpaisal, 2008) and 76.4°C (Oyeyinka *et al.*, 2016).

The peak gelatinisation of cowpea starches was reported in the range of 67-78°C (Kaptso *et al.*, 2015). The peak gelatinisation temperature (77.19°C) of BGNS in this study was within this range thereby suggesting that BGNS and cowpea would have similar pasting characteristics and could be used interchangeably in food systems. The areas of the first peaks of the biopolymers were 1420.91, 397.79 and 875.01 mJ for BGNS, BGN-SDF and STASOL, respectively. The enthalpy changes (ΔH) of BGN-SDF (297.54 J/g) and STASOL (261.36 J/g) were not significantly different while both differed significantly ($p = 0.000$) from that of BGNS (458.36 J/g). The loss of humidity from the lowest to the highest temperature was from STASOL < BGN-SDF < BGNS. This corresponded with the particle sizes of the biopolymers reported in section 3.3.3 where STASOL and BGNS had the smallest and highest average particle sizes of 74.0 and 237.9 nm, respectively. Therefore, STASOL had the largest surface area, meaning its particles were more exposed. This meant that more heat was absorbed by the water molecules in STASOL leading to increased kinetic energy and the subsequent faster rate of evaporation (Maleque, 2013). BGN-SDF, with a smaller particle size (118.3 nm) than BGNS (237.9 nm) (Figure 3.7), lost moisture at a temperature lower than BGNS because of the relatively larger surface area.

The endothermic enthalpy changes of reaction of the first peaks of the three biopolymers were positive indicating heat absorption by the particles (Maleque, 2013). The enthalpy changes (ΔH) of the BGNS, BGN-SDF and STASOL were 458.36, 297.54 and 261.36 J/g. As observed, less energy was required in dispelling moisture from STASOL as it had the minimum reported moisture content. The surface area could have contributed to the amounts of energy absorbed by each biopolymer.

All three biopolymers did not differ significantly in the peak temperatures of their second peaks. The areas of the second peaks were not significantly different for BGNS (18.10 mJ) and BGN-SDF (18.70 mJ) while both differed significantly ($p = 0.000$) from that of STASOL (83.98 mJ). The enthalpy change of reaction of the second peaks was not significantly different for BGNS (5.84 J/g) and BGN-SDF (13.90 J/g) as well as for BGN-SDF and STASOL (25.09 J/g). The maximum degradation of the biopolymers occurred at 230.30, 279.52 and 293.14°C for BGN-SDF, BGNS and STASOL, respectively. STASOL had the highest enthalpy change of

reaction (25.09 J/g) while BGNS had the lowest (5.84 J/g). This was an indication that STASOL had higher thermal stability than both BGNS and BGN-SDF. This was suggestive of the introduction of strong intra- and intermolecular bonds during the production of STASOL from BGNS and BGN-SDF. BGNS required the least amount of energy for the disintegration of bonds because it is relatively simple in structure. It is composed of repeating glucose units, meaning only glycosidic bonds had to be disrupted for the molecule to disintegrate. BGN-SDF on the other hand consists of chemically complex polysaccharides. STASOL was produced from the conjugation of BGNS and BGN-SDF, introducing new functional groups during the chemical grafting process, as confirmed by FTIR results reported in section 3.3.5. The bonds in BGN-SDF and STASOL included hydrogen, covalent and hydroxyl bonds (Yang *et al.*, 2007; Maphosa, 2016). The presence of proteins in BGN-SDF and STASOL could have added to the stability of these biopolymers. This was suggested by the presence of the NH group of the primary amide group in FTIR studies (Section 3.3.5). The deformation of the NH bond could have added to the amount of energy required for the disintegration of the biopolymers hence the higher ΔH compared to BGNS. The degradation of STASOL peaked at 239°C. This was indicative of its ability to withstand high thermal processing such as baking, at which temperatures can vary between 176°C and 250°C (Therdthai *et al.*, 2002; Mondal & Datta, 2008).

The DSC thermographs of BGNS, BGN-SDF and STASOL are shown in Figure 3.16. A pronounced peak at 322.86°C was observed on the BGNS thermograph representing the final decomposition of starches. The exothermic behaviour suggested that the starch was charred instead of volatilised at the final degradation stage meaning the BGNS molecules released energy as they combusted (Yang *et al.*, 2007). The peak is representative of the complete breakdown of glucose chains and rings. Starches are carbonised at temperatures exceeding 260°C (Wahyuningtiyas *et al.*, 2017), and this was confirmed by examining the DSC pans post-analysis revealing charred samples. Endothermic DSC peaks were emitted earlier than the exothermic peaks for BGNS indicating that the energetic effect is tested earlier than weight loss (Zhang & Wang, 2013). This is due to conformational transformation before the degradation of weight loss, which requires more energy. The change in conformation might be the transformation from the stable 4C_1 chair conformation of the glucose ring via a ${}^{1,4}B$ conformation to the inverse 1C_4 chair conformation that has higher Gibbs free energy (Zhang & Wang, 2013).

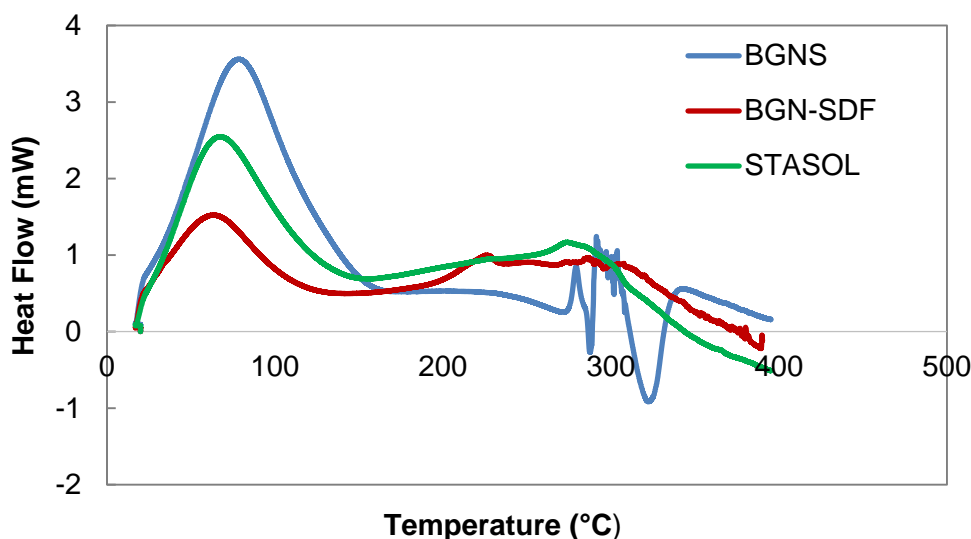


Figure 3.16 Thermal properties of BGNS, BGN-SDF and STASOL using differential scanning calorimetry (DSC). BGNS: Bambara groundnut starch; BGN-SDF: Bambara groundnut soluble dietary fibre; STASOL: Bambara groundnut starch-soluble dietary fibre nanocomposite.

2. *Thermal properties of Bambara groundnut starch, soluble dietary fibre and starch-soluble dietary fibre nanocomposite using thermogravimetric analysis*

Table 3.7 shows the thermogravimetric analysis (TGA) parameters of BGNS, BGN-SDF and STASOL. Thermogravimetric analysis measures the loss of mass in a sample as a function of temperature (Groenewoud, 2001). The initial weight loss of BGNS, BGN-SDF and STASOL was 11.84, 11.30 and 11.25% and did not differ significantly for all three biopolymers. The initial weight loss from 30-320°C occurred due to the evaporation of water and loss of volatile compounds (Davies, 2020). The initial weight loss temperature was 319.82°C (BGNS), 295.37°C (BGN-SDF) and 311.66°C (STASOL) and all differed significantly ($p = 0.000$). BGNS showed higher resilience and started degrading at 319°C, a temperature higher than that of the degradation of BGN-SDF and STASOL. The degradation at this stage was attributed to the decomposition of carbohydrates.

Figure 3.17 shows the TGA decomposition curves of BGNS, BGN-SDF and STASOL. All curves followed a similar course. The final weight and final weight loss temperature for BGNS, BGN-SDF and STASOL were 20.09% at 359.85°C, 24.78% at 440.01°C and 25.64% at 373.90°C, respectively.

Table 3.7 Thermal properties of BGNS, BGN-SDF and STASOL using thermogravimetric analysis

	Initial Weight (%)	Initial weight loss temperature (°C)	Final weight (%)	Final weight loss temperature (°C)
BGNS	88.16 ± 1.88 ^a	319.82 ± 0.07 ^a	20.09 ± 2.63 ^a	359.85 ± 3.65 ^a
BGN-SDF	88.70 ± 1.89 ^a	295.37 ± 9.79 ^b	24.78 ± 2.37 ^b	440.01 ± 5.05 ^b
STASOL	88.75 ± 0.05 ^a	311.66 ± 3.70 ^c	25.64 ± 0.60 ^b	373.90 ± 2.85 ^a

Values are mean ± standard deviation. Means within a column followed by different superscripts are significantly [$p \leq 0.05$] different; BGNS: Bambara groundnut starch; BGN-SDF: Bambara groundnut soluble dietary fibre; STASOL: Bambara groundnut starch-fibre nanocomposite; TGA: Thermogravimetric analysis.

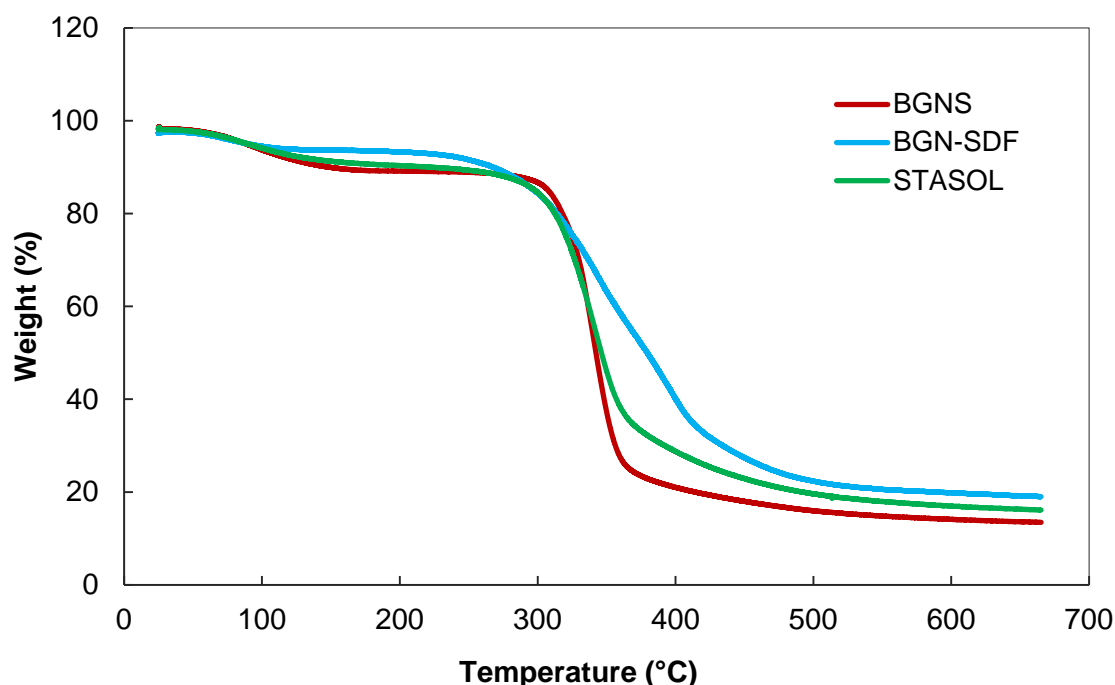


Figure 3.17 Thermal properties of BGNS, BGN-SDF and STASOL using TGA.
 BGNS: Bambara groundnut starch; BGN-SDF: Bambara groundnut soluble dietary fibre; STASOL: Bambara groundnut starch-fibre nanocomposite; TGA: Thermogravimetric analysis.

There was no significant difference in the final weight of BGN-SDF and STASOL while both differed significantly ($p = 0.000$) from the final weight of BGNS. The final weight loss temperature of BGNS and BGN-SDF as well as BGN-SDF and STASOL differed significantly ($p = 0.000$). The remaining mass at the end of TGA is ash (Wahyuningtiyas *et al.*, 2017). The final degradation temperature of BGNS was 359.85°C which was similar to the 322.83°C reported as the final degradation of BGNS in DSC studies (Table 3.6). The main thermal decomposition occurred at the final stage with the highest level of material lost.

Total weight lost from BGNS, BGN-SDF and STASOL was 79.91, 75.22 and 74.36%, respectively. The largest amount of weight was lost from BGNS and that could be attributed to the relative simplicity of starch compared to the complex BGN-SDF and STASOL. The decomposition at the final stage was independent of moisture lost at the dehydration stage at temperatures below 100°C (Liu *et al.*, 2015). The degradation of carbohydrates occurs in a series of simultaneous and successive reactions. Intermediate products, such as levoglucosan, are usually undetected and final products, such as C, CO, CO₂, H₂O and combustible volatiles can be analysed.

3.3.10 Choice of chemicals for a greener method

Several chemical methods have been applied in the modification of BGN starches and their effects on starch are outlined in Table 3.8.

Table 3.8 Effects of modification methods on the functional properties of starch

Method	Effect on functional property	Reference
Hypochlorite oxidation	Reduced swelling ability	Adebowale <i>et al.</i> (2002)
Acetylation	Increased swelling power	Adebowale <i>et al.</i> (2002)
Carboxymethylation	Increased swelling power	Afolabi (2012)
	Loss of crystallinity	
	Increase in the hydrophilic amorphous region	
Acetylation	Setback viscosity reduced by 17%	Adebowale <i>et al.</i> (2002)
	Reduced retrogradation tendencies	
Oxidation	Setback viscosity reduced by 40%	Adebowale <i>et al.</i> (2002)
	Reduced retrogradation tendencies	
Redox pair (Ascorbic acid, Hydrogen peroxide)	Improved thermal stability	Gulu <i>et al.</i> (2018)
	Improved solubility	
	Loss of crystallinity	
Stearic acid	Improved thermal stability	Oyeyinka <i>et al.</i> (2016)
	Improved water vapour permeability	
	Acceptable tensile strength	

These include acetylation, carboxymethylation and oxidation (Adebowale *et al.*, 2002; Afolabi, 2012; Gulu *et al.*, 2018). The choice of modification method is dependent on several factors such as end-use, desired functional properties, toxicity levels as well as permitted chemical residues in the final modified starch. The application of harsh chemicals is largely discouraged in starch modification processes as chemical residues may end up in food products (Boye & Arcand, 2013). As such, this study looked into the employment of ‘greener’ chemicals, namely, ascorbic acid, hydrogen peroxide and ethanol, in the modification of BGNS as well as the complexing of BGNS and BGN-SDF to form STASOL. For a method applied in food processing to be considered ‘green’, it should be sustainable, harmless to the environment and natural.

Such chemical processes can be used in the conversion of raw products into value-added foods and ingredients (Beaulieu *et al.*, 2020). The 'greenness' of chemicals used in this study is discussed in the following sections.

1. *Hydrogen peroxide*

Hydrogen peroxide (H_2O_2) is a chemical compound with two hydrogen atoms and two oxygen atoms joined by a single covalent bond. It is the simplest member of the peroxide group (Varvara *et al.*, 2016). Hydrogen peroxide does not leave toxic residues hence its 'green' status. It is rapidly decomposed into H_2O and O_2 at elevated temperatures such as those applied in the drying stage of this study (USCFR 2003; JETRO 2011). Hydrogen peroxide is commonly consumed in small quantities and any residues that remain in food products are easily decomposed in the mouth by peroxidases excreted in the saliva (Varvara *et al.*, 2016). Also, H_2O_2 is environmentally compatible as it easily degrades to water and oxygen and is compatible with the most common processing techniques. When properly handled, H_2O_2 is safe and easy-to-use. It does not have reported genotoxicity to humans as an additive when ingested in normal use because of its rapid metabolism and decomposition. The Food Safety Commission of Japan (FSCJ) concluded that H_2O_2 does not pose any carcinogenic concern in humans with normal catalase activity (JETRO, 2011). The no-observed-adverse-effect-level (NOAEL) of H_2O_2 is 30 mg/kg/day (Varvara *et al.*, 2016). In July of 1986, the U.S. Food and Drug Administration (FDA) (Borderias *et al.*, 2005) affirmed the generally recognised as safe (GRAS) status of H_2O_2 as a direct component of food. As such, according to the Food Standards of Australia and New Zealand and the FDA, the use of H_2O_2 as a processing aid for food products is acceptable and does not raise any public health and safety issues for consumers (Varvara *et al.*, 2016).

2. *Ascorbic acid*

Ascorbic acid is a reducing agent therefore it is strongly oxidised in the presence of oxygen (Silva & Lidon, 2016). Ascorbic acid and its derivatives are approved in South Africa, Europe, USA, Australia and New Zealand (Varvara *et al.*, 2016). Additives based on ascorbic acid are used in the production and transformation phases of several foods and are approved for use even in products for infants and children's feeding (Reg. EC 1129/2011; European Commission, 2011). Ascorbic acid is used as an acidity regulator, antioxidant and a flour treatment agent in various food products following good manufacturing practices (GMP) (Codex, 1995; South African Foodstuffs, Cosmetics and Disinfectants Act, 1972, revised 1 March 2010).

3. Ethanol

Ethanol is a natural by-product of plant fermentation. It can also be produced through the hydration of ethylene. Pure ethanol is non-toxic and it quickly degrades into harmless substances (Gorgus *et al.*, 2016). Ethanol is a natural constituent in food and non-food applications where it is used as a preservative, an extraction solvent or a diluent in pharmaceutical products (CHMP, 2014). There is no tolerable ADI currently assigned for ethanol and it is generally recognised as safe (GRAS) by the FDA. The reasons why ethanol is regarded as 'green' include the following: (1) It is a natural constituent of the human diet (2) It occurs in very small amounts in human blood, even if controlled studies guarantee that no alcoholic beverages have been consumed and (3) Regular consumption of small amounts may be beneficial for health and increase life expectancy (Gorgus *et al.*, 2016).

3.4 Conclusions

The nanocomposite, STASOL, was successfully synthesised from BGNS and BGN-SDF using an ascorbic acid-hydrogen peroxide redox reaction. The grafting process successfully mitigated the undesirable characteristics of native BGNS and BGN-SDF while retaining the desirable characteristics of both biopolymers and gaining new improved properties. The amorphosity of STASOL suggested that it would have a relatively lower digestibility [low glycemic index (GI)] and would therefore play a role against diseases of lifestyle such as diabetes, obesity and cardiovascular conditions. The high thermal resistance of STASOL indicated that it would be useful in food applications that require high-temperature processing such as extruded and baked products. STASOL is a natural, biocompatible, biodegradable, non-toxic and economic ingredient. Additionally, STASOL possesses therapeutic properties because it possesses antioxidant components as suggested by fluorescence studies as well as a low rate of digestibility hence a low GI because of its type C crystallinity. These properties make STASOL very desirable for health-conscious consumers.

References

- Adebowale, K.O., Adeniyi Afolabi, T. & Lawal, O.S. (2002). Isolation, chemical modification and physicochemical characterisation of Bambara groundnut (*Voandzeia subterranea*) starch and flour. *Food Chemistry*, **78**, 305-311.
- Adeyi, O., Ikhu-Omoregbe, D. & Jideani, V. (2014). Emulsion stability and steady shear characteristics of concentrated oil-in-water emulsion stabilized by gelatinized bambara groundnut flour. *Asian Journal of Chemistry*, **26**, 4995-5002.
- Adeyi, O. (2014). Effect of Bambara groundnut flour on the stability and rheological properties of

- oil-in-water emulsion. PhD Thesis, Cape Peninsula University of Technology.
- Afolabi, T.A. (2012). Synthesis and physicochemical properties of carboxymethylated bambara groundnut (*Voandzeia subterranea*) starch. *International Journal of Food Science and Technology*, **47**, 445-451.
- Anonymous. (2000). Thermogravimetric Analysis (TGA). Perkin Elmer. https://www.perkinelmer.com/lab-solutions/resources/docs/faq_beginners-guide-to-thermogravimetric-analysis_009380c_01.pdf. Accessed: 10 May 2020.
- Ashogbon, A.O. & Akintayo, E.T. Morphological and functional properties of starches from cereal and legume: A comparative study. *International Journal of Biotechnology and Food Science*, **1**(4), 72-83.
- Avella, M., Cosco, S., Volpe, G. Della & Errico, M.E. (2005). Crystallization behavior and properties of exfoliated isotactic polypropylene/organoclay nanocomposites. *Advances in Polymer Technology*, **24**, 132-144.
- Bandyopadhyay, P., Ghosh, A.K. & Ghosh, C. (2012). Recent developments on polyphenol–protein interactions: Effects on tea and coffee taste, antioxidant properties and the digestive system. *Food & Function*, **3**(6), 592-605.
- Bassioni, G. & Taqvi, S.T. Wettability studies using zeta potential measurements. *Journal of Chemistry*, 2015(743179), 1-6.
- Beaulieu, J.C., Reed, S.S., Obando-Ulloa, J.M. & McClung, A.M. (2020). Green processing protocol for germinating and wet milling brown rice for beverage formulations: Sprouting, milling and gelatinization effects. *Food Science and Nutrition*, **00**, 1-13.
- Bhattacharya, A. & Misra, B.N. (2004). Grafting: A versatile means to modify polymers: Techniques, factors and applications. *Progress in Polymer Science (Oxford)*, **29**, 767-814.
- Borderias, A.J., Sanchez-Alonso, I. & Perez-Mateos, M. (2005). New applications of fibres in foods: addition to fishery products. *Trends in Food Science and Technology*, **16**, 458-465.
- Boye, J.I. & Arcand, Y. (2013). Current Trends in Green Technologies in Food Production and Processing. *Food Engineering Reviews*, **5**, 1-17.
- Cai, J., Cai, C., Man, J., Zhou, W., & Wei, C. (2014). Structural and functional properties of C-type starches. *Carbohydrate polymers*, **101**, 289-300.
- CHMP. (2014) Questions and Answers on Ethanol in the context of the revision of the guideline on ‘Excipients in the label and package leaflet of medicinal products for human use’. EMA/CHMP/507988/2013.
- Codex. (1995). Ascorbic acid. Codex general standard for food additives. Codex stan 192-1995.
- Dalgetty, D.D. & Baik, B. (2003). Isolation and characterisation of cotyledon fibres from Peas, Lentils, and Chickpeas. *American Association of Cereal Chemists*, **80**(3), 310-315.
- Davies, P. (2020). Thermogravimetric Analysis. Advanced techniques for better materials

- characterisation. *TA Instruments UK*. https://www.tainstruments.com/wp-content/uploads/8-Philip_Davies.pdf. Accessed: 03 August 2020.
- Diedericks, C.F. (2014). Functional properties of Bambara groundnut (*Vigna Subterranea* (L.) Verdc.) non-starch polysaccharides in model and food systems. Master of Technology: Food Technology Thesis, Cape Peninsula University of Technology.
- Diedericks, C.F. & Jideani, V.A. (2014). Nutritional, Therapeutic and Prophylactic Properties of *Vigna subterranea* and *Moringa oleifera*. *The Journal of Food Science and Technology*, **52(7)**, 4078-4089.
- Diedericks, C. & Jideani, V. (2015). Physicochemical and Functional Properties of Insoluble Dietary Fiber Isolated from Bambara Groundnut (*Vigna subterranea* [L.] Verdc.). *Journal of Food Science*, **80(9)**, 1933-1944.
- Elder, D., Pacowski, G., Nelson, P. & Tindal, S. (2018). The importance of particle size analysis. *European Pharmaceutical Review*, **22(6)**, 58-61.
- Elleuch, M., Bedigian, D., Roiseux, O., Besbes, S. & Blecker, C. (2011). Dietary fibre and fibre-rich by-products of food processing; Characterisation technological functionality and commercial applications: A review. *Food Chemistry*, **124**, 411-421.
- Enyidi, C. & Onyenakazi, G. (2019). Effects of Substitution of Fishmeal with Bambara nut Meal on Growth and Intestinal Microbiota of African Catfish (*Clarias gariepinus*). *Aquaculture Studies*, **19(1)**, 9-23.
- European Commission. (2011). Regulation EC 1333/2008 of the European Parliament and of the Council of 2011.
- Fama, L., Gerschenson, L. & Goyanes, S. (2009). Starch-vegetable fibre composites to protect food products. *Carbohydrate Polymers*, **75(2)**, 230-235.
- Foodstuffs, Cosmetics and Disinfectants Act. (1972). Regulations Governing The Labelling and Advertising of Foodstuffs, Regulation No. R146. In: Foodstuffs, Cosmetics and Disinfectants Act and Regulations, 54/1972. Updated 1 March 2010. Cape Town, Johannesburg: LexNexis Butterworths.
- Gabriel, E.G., Jideani, V.A. & Ikhu-omoregbe, D.I.O. (2013). Investigation of the Emulsifying Properties of Bambara Groundnut Flour and Starch. *International Journal of Food Science and Engineering*, **7**, 539-547.
- Gao, Z, Fang, Y, Cao, Y, Liao, H, Nishinari, K. & Phillips, G.O. (2017). Hydrocolloid-food component interactions. *Food Hydrocolloids*. **68**, 149-156.
- Gill, P., Moghadam, T.T. & Ranjbar, B. (2010). Differential scanning calorimetry techniques: Applications in biology and nanoscience. *Journal of Biomolecular Techniques*, **21(4)**, 167-193.
- Gorgus, E., Hittinger, M. & Schrenk, D. (2016). Estimates of Ethanol Exposure in Children from

- Food not Labeled as Alcohol-Containing. *Journal of Analytical Toxicology*, **40**(7), 537-542.
- Groenewoud, W.M. (2001). Thermogravimetry. In: *Characterisation of Polymers by Thermal Analysis*. Pg 61-76. Netherlands: Elsevier Science.
- Guillon, F. & Champ, M.M. (2002). Structural and physical properties of dietary fibres, and consequences of processing on human physiology. *Food Research International*, **33**, 233-245.
- Gulu, N.B. (2018). Functional and rheological properties of Bambara groundnut starch-catechin complex obtained by chemical grafting. Master of Food Science and Technology. Cape Peninsula University of Technology, Cape Town, South Africa.
- Gulu, N.B., Jideani, V.A. & Jacobs, A. (2018). Functional characteristics of Bambara groundnut starch-catechin complex formed using cyclodextrins as initiators. *Heliyon*, **5**, 2-25. e01562.
- He, H.J., Yu, R.P., Zhu, T., Gu, Z.B. & Xu, H. (2006). Study of fluorescence spectra of starch suspension. *Guang Pu Xue Yu Guang Pu Fen Xi*, **26**(9), 1636-1639.
- IBM Corp. (2013). IBM Statistical Package for the Social Science (SPSS), Statistics for Windows, Version 22.0. Armonk, NY: IBM Corp.
- JETRO. (2011). Hydrogen Peroxide as a Processing Aid. Risk and Technical Assessment Report – Application A1068. Australia New Zealand Food Standards Code.
- Jha, P.K., Desai, P.S., Li, J. & Larson, R.G. (2014). pH and salt effects on the associative phase separation of oppositely charged polyelectrolytes. *Polymer*, **6**(5):1414-1436.
- Kaptso, K.G., Njintang, Y.N., Nguemtchouin, M.M.G., Scher, J., Hounhouigan, J. & Mbofung, C.M. (2015). Physicochemical and micro-structural properties of flours, starch and proteins from two varieties of legumes: bambara groundnut (*Vigna subterranea*). *Journal of Food Science and Technology*, **52**, 4915-4924.
- Kasran, M. (2013). Development of protein polysaccharide complex for stabilization of oil-in-water emulsions. PhD Thesis. University of Guelph.
- Kim, R.J., Kim, Y., Choi, N. & Lee, I. (2015). Polymerization shrinkage, modulus, and shrinkage stress related to tooth-restoration interfacial debonding in bulk-fill composites. *Journal of Dentistry*, **43**(4), 430-439.
- Kizil, R., Irudayaraj, J. & Seetharaman, K. (2002). Characterization of irradiated starches by using FT-Raman and FTIR spectroscopy. *Journal of Agricultural and Food Chemistry*, **50**(14), 3912-3918.
- Liaotrakoon, W., Liaotrakoon, V., Wongsangtham, W. & Rodsiri, S. (2014). Influence of dry- and wet-milling processes on physicochemical properties, syneresis, pasting profile and microbial count of job's tear flour. *International Food Research Journal*, **21**(5), 1745-1749.
- Liu, Y. & Shi, Y. (2006). Phase and State Transitions in Granular Starches Studied by Dynamic Differential Scanning Calorimetry. *Starch - Stärke*, **58**(9), 433-442.

- Liu, Y., Chen, W., Chen, C. & Zhang, J. (2015). Physicochemical Property of Starch-Soluble Dietary Fiber Conjugates and Their Resistance to Enzymatic Hydrolysis. *International Journal of Food Properties*, **18**, 2457-2471.
- Losso, J.N., Khachatryan, A., Ogawa, M. & Godber, J.S. (2013). Random centroid optimization of phosphatidylglycerol stabilized lutein-enriched oil-in-water emulsions at acidic pH. *Food Chemistry*, **92(4)**, 737-744.
- Lu, G.W. & Gao, P. (2010). Emulsions and Microemulsions for Topical and Transdermal Drug Delivery. *Handbook of Non-Invasive Drug Delivery Systems*, **2015**, 59-94.
- Maleque, K.A. (2013). Effects of Exothermic/Endothermic Chemical Reactions with Arrhenius Activation Energy on MHD Free Convection and Mass Transfer Flow in Presence of Thermal Radiation. *Journal of Thermodynamics*, **2013**, 1-11.
- Maphosa, Y. (2016). Characterisation of Bambara groundnut (*Vigna subterranea* (L.) Verdc.) non-starch polysaccharides from wet milling as prebiotics. Master of Technology Thesis, Cape Peninsula University of Technology.
- Maphosa, Y. & Jideani, V.A. (2016). Physicochemical characteristics of Bambara groundnut dietary fibres extracted using wet milling. *South African Journal of Science*, **112(1/2)**, 1-8.
- Maphosa, Y. & Jideani, V.A. (2017). The Role of Legumes in Human Nutrition. In: *Functional Food - Improve Health through Adequate Food*. Edited by Maria Chavarri Hueda.
- Mondal, A. & Datta, (2008). A.K. Bread making – A review. *Journal of Food Engineering*, **86**, 465-474.
- Mubaiwa, J., Fogliano, V., Chidewe, C. & Linnemann, A.R. (2018). Bambara groundnut (*Vigna subterranea* (L.) Verdc.) flour: A functional ingredient to favour the use of an unexploited sustainable protein source. *Plos One*, **13(10)**, e0205776.
- Nimse, S.B. & Pal, D. (2015). Free radicals, natural antioxidants, and their reaction mechanisms. *Royal Society of Chemistry Advances*, **5**, 27986-28006.
- Oyeyinka, S.A., Singha, S., Adebola, P. & Amonsou, E. (2016). Physicochemical properties of starches with variable amylose contents extracted from bambara groundnut genotypes. *Carbohydrate polymer*, **133**, 171-178.
- Oyeyinka, S.A. & Oyeyinka, A.T. (2018). A review on isolation, composition, physicochemical properties and modification of Bambara groundnut starch. *Food Hydrocolloid*, **75**, 62-71.
- Parri, E., Santinami, G. & Domenici, V. (2020). Front-Face Fluorescence of Honey of Different Botanic Origin: A Case Study from Tuscany (Italy). *Applied Sciences*, **10(5)**, 1-25.
- Rauscher, H., Rasmussen, K. & Sokull-Klüttgen, B. (2017). Regulatory Aspects of Nanomaterials in the EU. *Chemie Ingenieur Technik*, **89(3)**, 224 - 231.
- Roland, I., Piel, G., Delattre, L., & Evrard, B. (2003). Systematic characterization of oil-in-water emulsions for formulation design. *International journal of pharmaceutics*, **263(1-2)**, 85-94.

- Rosell, C.M., Santos, E. & Collar, C. (2009). Physico-chemical properties of commercial fibres from different sources: A comparative approach. *Food Research International*, **42**, 176-184.
- Sandhu, K.S. & Lim, S.T. (2008). Digestibility of legume starches as influenced by their physical and structural properties. *Carbohydrate Polymers*, **71**, 245-252.
- Silva, M. & Lidon, F.C. (2016). Food preservatives - An overview on applications and side effects. *Emirates Journal of Food and Agriculture*, **28(6)**,1.
- Singh, S., D'Sa, E. & Swenson, E. (2010). Seasonal variability in CDOM absorption and fluorescence properties in the Barataria Basin, Louisiana, USA. *Journal of Environmental Sciences*, **22**, 1481-1490.
- Sirivongpaisal, P. (2008). Structure and functional properties of starch and flour from bambarra groundnut. *Songklanakarin Journal of Science and Technology*, **30**, 51-56.
- Skoog, D.A., Crouch, S.R. & Holler, F.J. (2006). *Principles of Instrumental Analysis*. 6th edition.
- Song, W.L., Wang, P., Cao, L., Anderson, A., Meziani, M.J., Farr, A.J. & Sun, Y.P. (2012). Polymer/boron nitride nanocomposite materials for superior thermal transport performance. *Angewandte Chemie - International Edition*, **51**, 6498-6501.
- Spizzirri, U.G., Altimari, I., Puoci, F., Parisi, O.I., Iemma, F. & Picci, N. (2011). Innovative antioxidant thermo-responsive hydrogels by radical grafting of catechin on inulin chain. *Carbohydrate Polymers*, **84**, 517-523.
- Spizzirri, U.G., Parisi, O.I., Iemma, F., Cirillo, G., Puoci, F. & Curcio, M. (2010). Antioxidant polysaccharide conjugates for food application by eco-friendly grafting procedure. *Carbohydrate Polymers*, **79(2)**, 333-340.
- Therdthai, N., Zhou, W. & Adamczak, T. (2002). Optimisation of the temperature profile in bread baking. *Journal of Food Engineering*, **55**, 41-48.
- Tolstoguzov, V. (2006). Food Polysaccharides and Their Applications. In: Food Science and Technology. 2nd Edition. edited by Alistair M. Stephen Glyn O. Phillips Peter A. Williams. New York: Taylor & Francis. CRC Press. Pp 589.
- USCFR. (2003) USA Code of Federal Regulations. 21 CFR Ch. I (4-1-03 Edition). 184.1366. p. 514.
- Varvara, M., Bozzo, G., Celano, G., Disanto, C., Pagliarone, C. N., & Celano, G. V. (2016). The Use of Ascorbic Acid as a Food Additive: Technical-Legal Issues. *Italian journal of food safety*, **5(1)**, 4313.
- Wahyuningtiyas (2017). Analysis of Biodegradation of Bioplastics Made of Cassava Starch, *Journal of Mechanical Engineering Science and Technology*, **1(1)**, 41-54.
- Wang, S., Wu, T., Cui, W., Liu, M., Wu, Y., Zhao, C., Zheng, M., Xu, X. & Liu, J. (2020). Structure and in vitro digestibility on complex of corn starch with soy isoflavone. *Food Science & Nutrition*, **8(11)**, 6061-6068.

- Warren, F. J., Gidley, M. J. & Flanagan, B. (2015). Infrared spectroscopy as a tool to characterise starch ordered structure- a joint FTIR-ATR, NMR, XRD and DSC study. *Carbohydrate Polymers*, **139**, 35-42.
- Winarti, C., Sunarti, T., Mangunwidjaja, D. & Richana, N. (2014). Preparation of arrowroot starch nanoparticles by butanol-complex precipitation, and its as bioactive encapsulation matrix. *International Food Research Journal*, **21(6)**, 2207-2213.
- Yang, N., Li, N., Wang, L. & Li, B. Thermal rectification and negative differential thermal resistance in lattices with mass gradient. *Physical Review B*, **76(2)**, 020301.
- Yu, Y., Huang, X. & Yu, W. (2014). High Performance of Bamboo-Based Fiber Composites from Long Bamboo Fiber Bundles and Phenolic Resins. *Journal of Applied Polymer Science*, **131(12)**, 1-8.
- Zeng, J., Li, G., Gao, H. Ru, Z. (2011). Comparison of A and B Starch Granules from Three Wheat Varieties. *Molecules*, **16(12)**, 10570-10591.
- Zhang, Y. & Han, J.H. (2006). Plasticization of Pea Starch Films with Monosaccharides and Polyols. *Journal of Food Science*, **71(6)**, E253-E261.
- Zhang, J & Wang, Z.W. (2013). Soluble dietary fibre from *Canna edulis* Ker by-product and its physicochemical properties. *Carbohydrate Polymers*, **92**, 289-296.

CHAPTER FOUR

FUNCTIONAL AND ANTIOXIDANT PROPERTIES OF *VIGNA SUBTERRANEA* STARCH-SOLUBLE DIETARY FIBRE NANOCOMPOSITE

Abstract

Bambara groundnut soluble dietary fibre (SDF) is rich in bioactive compounds, namely, uronic acids (11.8%) and hydrolysable polyphenols (20 mg/g Gallic acid equivalent), with crucial physiological and functional benefits. The pasting properties by rapid visco analysis, chemical composition following AOAC procedures, hydration properties (solubility and water holding capacities), oil binding capacity (OBC), emulsion activity index (EAI), emulsion stability index (ESI) and antioxidant properties of BGNS, BGN-SDF and STASOL were studied. Unlike BGNS, BGN-SDF and STASOL did not exhibit typical pasting properties. Bambara groundnut starch was high in carbohydrates (86.79%), low in fat (0.56%), ash (0.07%) and proteins (1.74%) while STASOL was high in carbohydrates (78.69%) and proteins (6.96%), low in fat (0.84) and had a considerable amount of ash (4.88%). The three biopolymers were high in energy, with the least and highest being 1443.47 kJ (BGN-SDF) and 1525.78 kJ (BGNS), respectively, and showed significant ($p = 0.000$) differences in solubility index (SI). Bambara groundnut starch was insoluble in water (SI = 0.9%). The EAI of BGNS, BGN-SDF and STASOL were 23.25, 85.71 and 90.65%, respectively, and the ESI of BGNS, BGN-SDF and STASOL were 23.33, 87.13 and 87.49%, respectively. The significantly ($p = 0.000$) lower EAI and ESI of BGNS compared to those of BGN-SDF and STASOL could be attributed to the insolubility and low hydration properties of native starch while the high ESI (90.65%) and EAI (87.49%) of STASOL suggested that the nanocomposite would be a suitable stabiliser in emulsion systems. The OBCs of BGNS, BGN-SDF and STASOL differed significantly ($p = 0.000$) and were 1.13, 3.78 and 1.61 g/g, respectively. The lightness (L^*), redness/greenness (a^*), yellowness/blueness (b^*), chroma and hue angles were 87.94, 1.33, 12.43, 12.50 and 83.87° (BGNS), 76.12, 2.21, 18.86, 18.96 and 83.32° (BGN-SDF) as well as 89.16, 0.4, 14.61, 14.62 and 88.42° (STASOL), respectively. The three biopolymers differed significantly ($p = 0.000$) in all colour characteristics. The polyphenolic content of BGNS, BGN-SDF and STASOL was 0.10, 6.59 and 0.46 mg GAE/g, respectively, and their ferric reducing antioxidant power (FRAP) values were 1.16, 4.77 and 1.45 $\mu\text{mol AAE/g}$, respectively. The phenolic compounds chlorogenic acid (18 mg/g), monocrotaline (20 mg/g), luteolin 7-O-(6"-malonylglucoside) (4 mg/g) and casuarine 6- α -D-glucoside (27 mg/g) were present in BGN-SDF and absent in BGNS and STASOL while blumealactone C (7 mg/g) was present in BGNS and absent in BGN-SDF and STASOL. It was concluded that STASOL possesses desirable physicochemical and therapeutic properties thus making it desirable for

health-conscious consumers and food manufacturers. Furthermore, the antioxidant capacity of STASOL confirmed its capability in delivering active compounds in food systems.

4.1 Introduction

The demand for innovative food products formulated with natural components has driven the constant search for new biopolymer complexes with improved properties. The increasing demand for such complexes, both by consumers and the food industry, has led to the utilisation of biopolymers from underutilised and orphan crops, such as Bambara groundnut (BGN) (Bamshaiye *et al.*, 2011). Starch and dietary fibres from different sources have been studied and applied in the production of various food products (Adebowale & Lawal, 2003). Starch and starch-based composites immensely contribute to the functional properties of food products (Singh & Kaur, 2004). The major functional properties of starches and dietary fibres include thickening, swelling, gelation, water absorption, water binding, foaming, emulsification and bulk density (Maphosa, 2016; Ogundele, 2016). Bambara groundnut starch and soluble dietary fibres have been reported to possess good functional properties (Oyeyinka *et al.*, 2016; Gulu, 2018) and their complexes have improved pasting, thickening, viscoelastic and thermal properties than individual starches (Wu *et al.*, 2015).

Previous studies have reported the effect of complexing starch with other biopolymers on the functionality, antioxidant composition and overall behaviour of the complexes. Such studies reported on composites made from potato starch and waxy maize starch (Park *et al.*, 2009), waxy rice starch and non-waxy starch (Lin *et al.*, 2013), lima bean starch and cassava starch (Novelo-Cen & Betancur-Ancona, 2005), potato starch and maize starch (Zhang *et al.*, 2011), pigeon pea starch and rice starch (Baljeet *et al.*, 2011) and starch and soluble dietary fibre (Liu *et al.*, 2015). It is important to study the functional and physicochemical properties of food components as they affect sensory characteristics as well as the physical behaviour of food during formulation, processing, storage and distribution (Adebowale & Lawal, 2003; Gulu, 2018). Knowledge of the functional and antioxidant properties of biopolymer composites enables their maximal utilisation and application in food systems for human nutrition and health (Oyeyinka *et al.*, 2016).

The nanocomposite used in this study was STASOL, produced from the chemical complexing of 1.95 g BGN-SDF and 15 g BGNS (Chapter 3). STASOL was verified and characterised for particle size, functional groups, crystallinity, morphology and thermal properties using a zetasizer, fourier transform infrared (FTIR), X-ray diffraction (XRD), scanning electron microscope (SEM) and differential scanning calorimetry (DSC), respectively (Chapter 3). STASOL was reported to have an average particle size of 74.01 nm which qualified it as a nanocomposite (nano = <100 nm). The employment of STASOL in a food system would

produce a relatively "green" product as all components used were natural. The objective of this study was to characterise the antioxidant, functional and physicochemical properties of STASOL.

4.2 Materials and Methods

4.2.1 Source of materials and equipment

STASOL is a nanocomposite made from the chemical complexing of BGN-SDF (1.95 g) and BGNS (15 g). The STASOL used in this study was obtained according to the method described in chapter 3 [Section 3.2.4]. Analytical grade chemicals were used in this study (Sigma-Aldrich). Equipment from the Departments of Food Science and Technology, Oxidative Stress and Chemical Engineering of the Cape Peninsula University of Technology as well as the Central Analytical Facilities (CAF) of Stellenbosch University, Cape Town were used. The outline of chapter 4 is illustrated in Figure 4.1.

4.2.2 Pasting properties of Bambara groundnut starch, soluble dietary fibre and starch-soluble dietary fibre nanocomposite

The pasting properties of BGNS, BGN-SDF and STASOL were carried out using a Rapid Visco Analyser (RVA 4500 Perten Instruments, Australia) following the method of Gulu (2018). A suspension of 3 g sample (14% moisture) in 25 g deionised water was subjected to a heating and cooling cycle while continuously under shear. The samples were held at 50°C for 1 min then heated at a ramp of 6°C/min from 50 to 95°C. Thereafter, the temperature was decreased to 50°C at a ramp of 6°C/min and held for 5 min. The pasting time, peak viscosity, pasting temperature, breakdown viscosity, cold paste viscosity and setback viscosity were obtained from the RVA curves and viscosities were expressed as centipoise units (Cp).

4.2.3 Colour characteristics of Bambara groundnut starch, soluble dietary fibre and starch-soluble dietary fibre nanocomposite

Colour characteristics of BGNS, BGN-SDF and STASOL were determined using spectrophotometry (Spectrophotometer, model CM-5, Konica Minolta Sensing inc, Japan) set at standard observer 10° and D65 following a method of Murevhanema & Jideani (2013). The spectrophotometer was calibrated with a black tile ($L^* = 5.49$, $a^* = 7.08$, $b^* = 4.66$) and a white tile ($L^* = 93.41$, $a^* = 1.18$, $b^* = 0.75$) followed by zero calibration (Maphosa, 2015). Enough samples to completely cover the bottom of the glass sample holders (diameter 30 mm) were used.

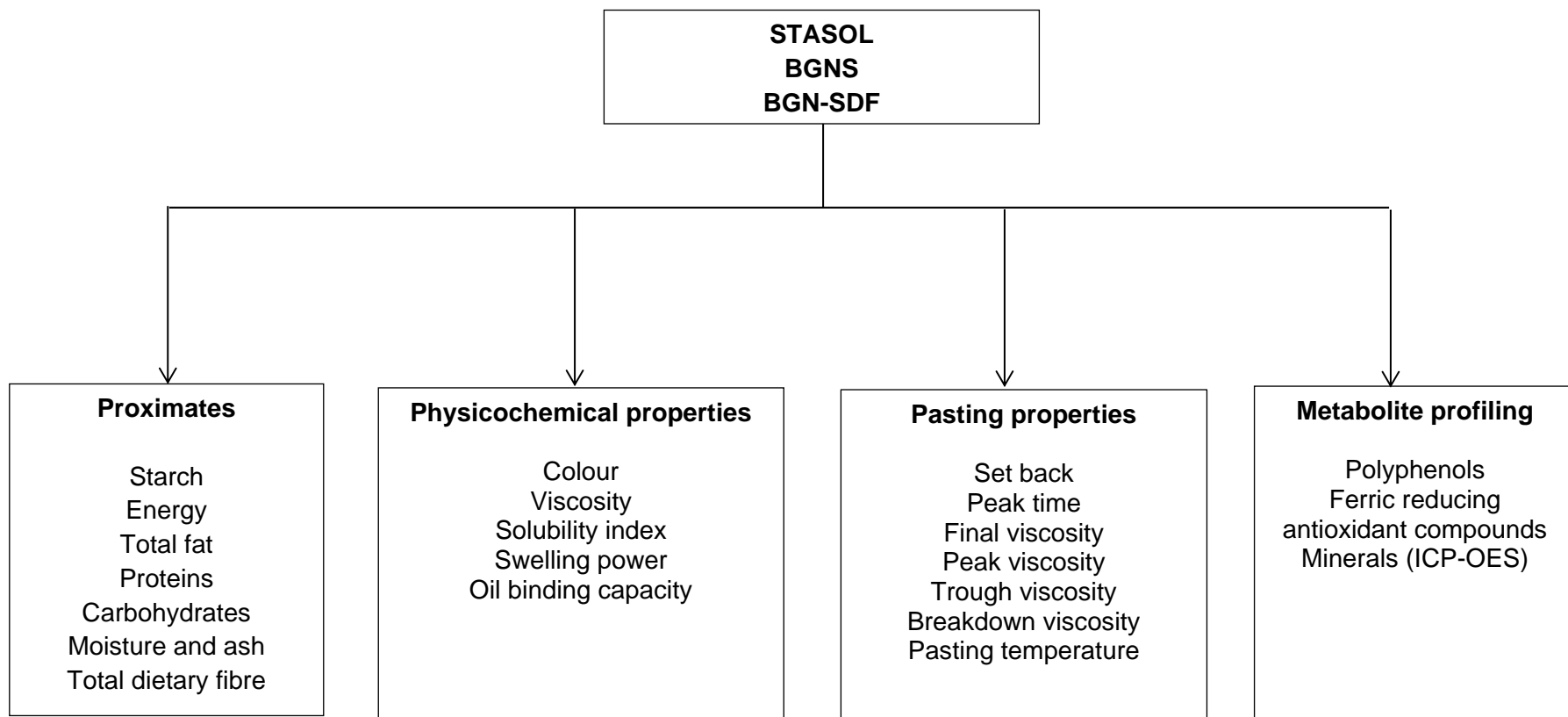


Figure 4.1 Outline of Chapter 4.

STASOL: Bambara groundnut starch-soluble dietary fibre nanocomposite; ICP-OES: Inductively coupled plasma-optical emission spectrometry. BGNS: Bambara groundnut starch; BGN-SDF: Bambara groundnut soluble dietary fibre.

Lightness (L^*), redness/greenness (a^*), yellowness/blueness (b^*), hue and chroma were assessed using $L^*C^*h^*$ and CIE- $L^*a^*b^*$ colour space systems. Measurements were carried out in triplicate. Colour differences (ΔE) were calculated using equation 4.1 (Sharma, 2005).

$$\Delta E = \sqrt{(\Delta L^{*2} + \Delta a^{*2} + \Delta b^{*2})} \quad \text{Equation 4.1}$$

Where: L^* : lightness; a^* : redness/greenness; b^* : yellowness/blueness

4.2.4 Chemical analysis of Bambara groundnut starch, soluble dietary fibre and starch-soluble dietary fibre nanocomposite

The chemical profiles of BGNS, BGN-SDF and STASOL were determined according to AOAC procedures (2011). Fatty acids and total fat content (Gas Chromatography), protein (Leco, TruSpec® N), moisture (Moisture analyser, Denver Instrument 1R-30), ash (muffle furnace) and carbohydrates (calculated by difference) were determined. Energy (kJ) was calculated using the corresponding values of fat (37 kJ/g), protein (17 kJ/g) and carbohydrates (17 kJ/g) (FAO, 2003).

4.2.5 Determination of elemental content of Bambara groundnut starch, soluble dietary fibre and starch-soluble dietary fibre nanocomposite by inductively coupled plasma-optical emission spectrometry (ICP-OES)

The AOAC (2011) inductively coupled plasma-optical emission spectrometry (ICP-OES) method was followed in the determination of the mineral composition of BGNS, BGN-SDF and STASOL. A commercially prepared stock standard solution, SEP-4, was used in the preparation of calibration standards. Samples (0.5 g) and HNO_3 (6 mL) were accurately measured into 55 mL CEM Mars Xpress Teflon digestion vessel liners and left to stand for 10 min at ambient temperature in a fume cupboard. Teflon plugs were then carefully placed on the liner and capped until the correct torque was reached using the CEM Mars Xpress capping station. The vessels were inserted into the carousel, starting with the outer ring and filling up towards the inner ring. The carousel was placed into the CEM Mars Xpress microwave at 170°C for 45 min. After digestion and the subsequent cooling to room temperature, the contents were quantitatively transferred to 50 mL volumetric flasks and made up to volume with deionised water. The contents of the volumetric flasks were transferred to polyethylene sample tubes and submitted to ICP-OES for analysis.

4.2.6 Hydration properties of Bambara groundnut starch, soluble dietary fibre and starch-soluble dietary fibre nanocomposite

The water absorption capacity (WAC) and solubility index (SI) of BGNS, BGN-SDF and STASOL were determined according to the methods of Lai *et al.* (2012). All measurements were performed in triplicate.

1. Water absorption capacity

Samples (0.2 g, dry basis) were weighed into a centrifuge tube and mixed with 9.8 g of deionised water. The suspensions were heated at 70°C for 10 min in a shaking temperature-controlled water bath (Ecobath, LaboTec) then transferred to a boiling water bath (Ecobath, LaboTec) for another 10 min. The suspensions were cooled in cold water for 5 min before centrifuging at 40 000 x *g* at 5°C for 30 min (Centrifuge, Model MR 812, Jonan, Thermo Electron Corporation). Water absorption capacity was then determined as the ratio of the weight of swollen samples after centrifugation (g) to their dry mass (g).

2. Solubility index

To determine the SI of BGNS, BGN-SDF and STASOL, the supernatant from WAC analysis was decanted into tared evaporating crucible dishes and dried overnight at 110°C. Solubility index was then calculated as the ratio of the weight of solids after drying (g) to the initial weight of the dry sample (g).

4.2.7 Oil binding capacity of Bambara groundnut starch, soluble dietary fibre and starch-soluble dietary fibre nanocomposite

The method described by Maphosa & Jideani (2016) was applied in the determination of the oil binding capacities (OBC) of BGNS, BGN-SDF and STASOL. A sample (1 g) was mixed with canola oil (5 g) in a 50 mL centrifuge tube. The mixture was vortexed for 30 s at 5 min intervals for 30 min then centrifuged (Centrifuge, Model MR 812, Jonan, Thermo Electron Corporation) at 1600 x *g* for 25 min at 23°C. Thereafter, the free oil was decanted and accurately measured. The difference between the original weight of oil (5 g) and the weight of the decanted oil was considered as retained oil. Oil binding capacity was calculated using equation 4.2.

$$\text{Oil binding capacity (g/g)} = \frac{\text{Weight of oil retained (g)}}{\text{Weight of sample (g)}} \quad \text{Equation 4.2}$$

4.2.8 Emulsion activity and stability of Bambara groundnut starch, soluble dietary fibre and starch-soluble dietary fibre nanocomposite

The emulsion activity indexes (EAI) of BGNS, BGN-SDF and STASOL were determined following the method of Chove *et al.* (2001). A sample (1 g) was dissolved in 10 mL deionised water and homogenised (Ultra Turrax T-25 Homogeniser, IKA, Germany) at 4500 x *g* for 2 min. Orange oil (10 mL) was added and the solution was homogenised at 6000 x *g* for 1 min then centrifuged again at 1200 x *g* for 5 min. The emulsion volume was then measured as the volume of the emulsified layer per entire layer in the centrifuge tube and EAI was expressed as a percentage (%).

Emulsion stability index (ESI) was determined following the method of Mora *et al.* (2013). A sample (1 g) was dissolved in 10 mL deionised water, and the mixture was homogenised at 4500 x *g* for 2 min. Orange oil (10 mL) was added and the solution was further homogenised at 6000 x *g* for 1 min and then centrifuged at 1200 x *g* for 5 min. The emulsion was then heated at 80°C for 30 min. After cooling at ambient temperature, the emulsion was centrifuged at 1200 x *g* for 5 min. Emulsion stability was calculated as the height of the emulsified layer after heating divided by the height of total content before heating and expressed as a percentage (%).

4.2.9 Antioxidant properties of Bambara groundnut starch, soluble dietary fibre and starch-soluble dietary fibre nanocomposite

Total phenolic compounds (TPC) and ferric reducing antioxidant power (FRAP) were determined in BGNS, BGN-SDF and STASOL.

1. Determination of total phenolic compounds

The method of Maphosa & Jideani (2016) was adopted in the assessment of TPC. Samples (250 mg) were mixed with 10 mL of distilled water and 1 mL of H₂SO₄ in 14 mL centrifuge tubes. The samples were incubated for 20 h at 80°C then centrifuged at 4000 x *g* for 5 min at 21°C. The supernatant was diluted tenfold and analysed in a 96 well plate using the Folin-Ciocalteu assay by mixing 25 µL of a sample with 125 µL of 0.2 M Folin-Ciocalteu and 100 µL of 7.5% (w/v) Na₂CO₃ solution. The mixtures were left to stand for 2 h in the dark then absorbance was measured using a spectrophotometer (Multiskan Spektrum) at a wavelength of 765 nm using a gallic acid standard calibration curve. The results were expressed as mg/g gallic acid equivalents (GAE) of dry extract.

2. Determination of ferric reducing antioxidant power

Ferric reducing antioxidant power (FRAP) assay was conducted following a modified method of Gullon *et al.* (2017) with Vitamin C as a standard. Samples (250 mg) were diluted tenfold then

mixed with 0.3 mL of FRAP reagent (30 mL acetate buffer, 3 mL FeCl₃, 3 mL TPTZ and 6 mL of H₂O). The mixture was poured into a 96 well plate, left to stand for 30 min and then read in a spectrophotometer (Multiskan spectrum) at a wavelength of 593 nm.

4.2.10 Determination of glucose in Bambara groundnut starch, soluble dietary fibre and starch-soluble dietary fibre nanocomposite

Sample (0.1 g) and 5 mL 2 M trifluoroacetic acid were accurately measured into a 10 mL headspace tube and hydrolysed at 110°C for 12 h. The mixture was then diluted with water:acetonitrile water (0.2% triethylamine and 0.2% NH₄OH in water) and acetonitrile (0.2% triethylamine and 0.1% 2-propanol and 0.2% NH₄OH in acetonitrile). The diluted samples were transferred into glass vials and analysed by UPLC-ELSD with a Waters Acquity BEH Amide 2.1 x 100 mm, 1.7 µm column. An injection volume of 5 µL was used with a column temperature of 50°C, seal wash of 5 min, run time of 10 min and a pressure gradient of 0-15000 psi/m.

4.2.11 Phenolic profiling of Bambara groundnut starch, soluble dietary fibre and starch-soluble dietary fibre nanocomposite

Sample (2 g) and 15 mL of 50% methanol/1% formic acid were accurately measured into a 50 mL centrifuge tube with a screw-cap then vortexed for 1 min, followed by extraction in an ultrasonic bath for 1 h. A sample (2 mL) was then centrifuged at 14000 rpm for 5 min and the supernatant was transferred into 1.5 mL glass vials using Liquid Chromatography-Mass Spectrometry (LCMS) analysis. A Waters Synapt G2 Quadrupole time-of-flight (QTOF) mass spectrometer (MS) connected to a Waters Acquity ultra-performance liquid chromatography (UPLC) (Waters, Milford, MA, USA) was used for high-resolution UPLC-MS analysis. The column eluate first passed through a Photodiode Array (PDA) detector prior to flowing through the mass spectrometer, allowing concurrent collection of UV and MS spectra. Electrospray ionisation was used in negative mode with a cone voltage of 15 V, desolvation temperature of 275°C, desolvation gas at 650 L/h, and the rest of the MS settings optimised for best resolution and sensitivity. Data were acquired by scanning from 150 to 1500 m/z in resolution mode as well as in MSE mode. In MSE mode two channels of MS data were acquired; one at low collision energy (4 V) and the second using a collision energy ramp (40-100 V) to obtain fragmentation data as well. Leucine enkephalin was used as a reference mass and the instrument was calibrated with sodium formate. Separation was achieved on a Waters HSS T3, 2.1 × 100 mm, 1.7 µm column and the mobile phase was made up of 0.1% formic acid (solvent A) and acetonitrile containing 0.1% formic acid (solvent B). The parameters used were, injection volume (2 µL), flow rate (0.3 mL/min) and column temperature (55°C).

The gradient began at 100% solvent A for 1 min, then went to 28% solvent B over 22 min, then changed to 40% solvent B over 50 s and a wash step of 1.5 min at 100% solvent B, and finally re-equilibrated to initial conditions for 4 min. A range of catechin standards were injected from 0.5 to 100 mg/L and used to establish a calibration curve against which compounds were quantified. Data were processed using MSDIAL and MSFINDER (RIKEN Center for Sustainable Resource Science: Metabolome Informatics Research Team, Kanagawa, Japan) (Anon., 2015; Anon., 2018).

4.2.12 Data analysis

For statistical analysis, IBM Statistical Package for the Social Science (SPSS) version 25 was used. All experiments were carried out in triplicate. Data were expressed as mean \pm standard deviation. The results were subjected to multivariate analysis of variance (MANOVA) to establish differences between treatments. Duncan's multiple range test was used to separate means where a significant ($p \leq 0.05$) difference existed.

4.3 Results and Discussion

4.3.1 Pasting properties of Bambara groundnut starch, soluble dietary fibre and starch-soluble dietary fibre nanocomposite by rapid visco analyser

Pasting is a term used to describe the changes in the structure of starch molecules post gelatinisation (Sirivongpaisal, 2008). It describes the changes in starch such as further swelling, leaching of molecular components and disruption of granules. Several studies have reported the pasting properties of BGNS (Adebowale *et al.*, 2002; Sirivongpaisal, 2008; Oyeyinka *et al.*, 2016, Gulu, 2018). Pasting properties measured peak viscosity, trough viscosity, breakdown viscosity, final viscosity, set back, pasting temperature and peak time. The pasting characteristics of BGNS, BGN-SDF and STASOL are given in Table 4.1. The shapes of the pasting curves were different for each polymer as shown in Figure 4.2.

1. Peak viscosity

Peak viscosity refers to the highest viscosity of starch obtained during gelatinisation (Mensah, 2011). It is indicative of the strength of starch pastes and their water holding capacities (Ragaei & Abdel-Aal, 2006; Amoo *et al.*, 2014). The peak viscosities of BGNS, BGN-SDF and STASOL were 4875, 150 and 435 cP and all three differed significantly ($p = 0.000$).

Table 4.1 Pasting properties of BGNS, BGN-SDF and STASOL

	Peak Viscosity (cP)	Trough viscosity (cP)	Breakdown viscosity (cP)	Final viscosity (cP)	Set back viscosity (cP)	Peak time (min)	Pasting temperature (°C)
BGNS	4875 ± 219.01 ^a	1984 ± 944.31 ^a	2890 ± 1143.22 ^a	4621 ± 500.00 ^a	2637 ± 577.29 ^a	4.78 ± 0.48 ^a	77.9 ± 1.75 ^a
BGN-SDF	150 ± 10.00 ^b	143 ± 0.58 ^b	7 ± 0.58 ^b	271 ± 9.29 ^b	128 ± 0.00 ^b	6.87 ± 0.06 ^b	87.4 ± 0.49 ^b
STASOL	435 ± 15.59 ^c	412 ± 19.63 ^b	24 ± 4.04 ^b	537 ± 8.66 ^b	122 ± 8.66 ^b	7.00 ± 0.12 ^c	96.7 ± 2.89 ^c

Values are mean ± standard deviation. Means within a column followed by different superscripts are significantly [p ≤ 0.05] different. BGNS: Bambara groundnut starch; BGN-SDF: Bambara groundnut soluble dietary fibre; STASOL: Bambara groundnut starch-soluble dietary fibre nanocomposite.

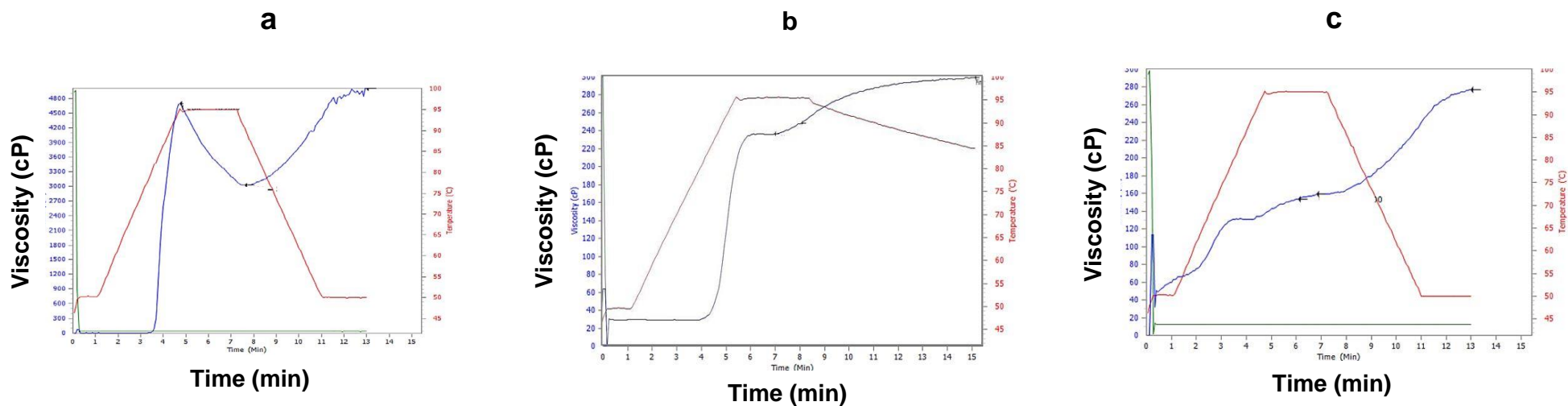


Figure 4.2 Pasting properties of (a) Bambara groundnut starch; (b) Bambara groundnut soluble dietary fibre; (c) Bambara groundnut starch-soluble dietary fibre nanocomposite (STASOL).

Peak viscosity is an indication of structural damage due to factors such as temperature and shear, with high values indicating more extensive damage (Adebowale *et al.*, 2002; Falade *et al.*, 2014). STASOL had a significantly ($p = 0.000$) lower peak viscosity and would therefore be expected to maintain its structure at relatively high temperatures. This was confirmed by thermal characteristics of the biopolymers [Section 3.3.9, Tables 3.6 and 3.7] where their structural degradation occurred at 77.19°C (BGNS) and 293.14°C (STASOL). The structural damage of BGNS at a lower temperature was due to its ability to gelatinize (Afolabi, 2012).

Starch is composed of repeating glucose units, soluble dietary fibre is a mixture of chemically complex non-starch polysaccharides and STASOL is a complex compound made from BGNS and BGN-SDF, suggesting that new functional groups were introduced during the chemical grafting process as confirmed in Chapter 3 FTIR studies [Section 3.3.5]. The significantly ($p = 0.000$) reduced peak viscosity of STASOL could be attributed to factors such as the disruption of starch granules during the chemical grafting process resulting in loss of gelatinisation ability as well as the simplicity of the starch molecule compared to the other two compounds, hence allowing it to swell unrestrictedly (Adebowale *et al.*, 2002). Furthermore, the difference in the microstructure and morphology of BGNS and STASOL were discussed in Chapter 3 [Section 3.3.7] and shown in Figure 3.14 where BGNS granules were spherical with smooth surfaces while STASOL granules were irregular and polygonal. These differences were attributed to the disruption of BGNS bonds during chemical grafting as well as the formation of new bonds when BGN-SDF was added in the formation of STASOL. Since peak viscosity is also an indication of water-binding capabilities (Falade *et al.*, 2014); the higher peak viscosity of BGNS means that in comparison to BGN-SDF and STASOL, BGNS granules would swell more easily when heated and form a thicker paste.

Gulu (2018) reported a similar trend in the peak viscosity of native and chemically modified starches reporting a reduction in their peak viscosities from 4876 to 435 cP, respectively. Oyeyinka & Oyeyinka (2016) reported a lower peak viscosity of 3293 cP for BGNS. The difference in the reported peak viscosity could be due to the fact that starches from different BGN varieties were studied. Starch from the black-eye variety was used in this study while the cream BGN variety was used by Oyeyinka & Oyeyinka (2016). Lower starch peak viscosities were reported as 1335, 2152 and 4145 cP for wheat (Ragae & Abdel-Aal, 2006), barley (Gujral *et al.*, 2011) and potato (Kaur *et al.*, 2007), respectively. Differences in peak viscosities of starches can be attributed to the source of starch, differences in amylose and amylopectin contents, strength of amylose-amylose and amylose-amylopectin chain interactions as well as the molecular structures of amylose and amylopectin (Ragae & Abdel-Aal, 2006).

2. *Trough viscosity*

Trough viscosity is also known as hot paste viscosity and it describes the rate of breakdown in viscosity at equilibrium (Ragaei & Abdel-Aal, 2006). A low trough viscosity indicates higher stability. The trough viscosity of BGNS (1984 cP) was significantly ($p = 0.012$) higher than that of BGN-SDF (143 cP) and STASOL (412 cP). Gulu (2018) reported a similar observation, where chemical modification of BGNS using hydrogen peroxide and ascorbic acid resulted in a decrease in trough viscosity. Gulu (2018) reported a trough viscosity of 88 cP for chemically modified BGNS while a trough viscosity of 143 cP was reported in this study. The difference in results suggests that grafting catechin onto BGNS as was done by Gulu (2018) resulted in the formation of a more robust complex compared to grafting BGN-SDF onto BGNS to form STASOL. Trough viscosity is dependent on temperature, degree of shear stress applied to a mixture as well as the nature of the material of interest (Kaur *et al.*, 2007). A higher trough viscosity (3013 cP) for native BGNS was reported by Gulu (2018). The difference in the results could be due to that starch from a mixture of different varieties of BGN seeds was studied by Gulu (2018) while starch from the black-eye variety was evaluated in the present study.

Trough viscosities of 560 cP for wheat starch (Ragaei & Abdel-Aal, 2006), 1423 cP for barley starch (Gujral *et al.*, 2011), 2351 cP for potato starch (Kaur *et al.*, 2007) and 5280 cP for barley starch (Fan *et al.*, 2019) were reported. These are starches commonly used in the food industry. Their trough viscosities were very high indicating that they would breakdown when exposed to elevated temperatures and form unstable pastes. As such, more stable composites such as STASOL with low trough viscosities (412 cP) would be desirable replacements. The relatively low trough viscosity of STASOL suggests that the nanocomposite would find use in high-temperature food systems such as baking and high shear processes such as those involved in the production of emulsions and dough.

3. *Final viscosity*

The final viscosities of BGNS, BGN-SDF and STASOL were 4621, 271 and 537 cP, respectively. There was no difference in the final viscosity of BGN-SDF and STASOL while both were significantly ($p = 0.000$) lower than that of BGNS. Final viscosity indicates a starch's ability to form a gel or viscous paste after cooking and cooling (Araujo-Farro *et al.*, 2005; Jan *et al.*, 2013). It is also used to determine the quality and stability of a cooked starch paste in food products. According to Falade *et al.* (2014), final viscosity plays a vital role in the rigidity and stability of the swollen granule structure. Higher final viscosities of 4867, 4876, 4989 and 5591 cP were reported for rice starch (Araujo-Farro *et al.*, 2005), BGNS (Gulu, 2018), quinoa starch (Araujo-Farro *et al.*, 2005) and barley starch (Fan *et al.*, 2019). The lower final viscosity of STASOL was due to the loss of crystallinity during the grafting process. This was confirmed by

crystallinity studies using powder XRD [Section 3.3.6, Figure 3.13] where native BGNS was described as crystalline while STASOL was amorphous. The transformation from crystalline to amorphous nature of legume starch as a result of chemical treatment has been widely reported (Afolabi, 2012). The lower final viscosities of BGN-SDF and STASOL would result in the formation of more stable food systems, therefore these two biopolymers would make suitable alternatives to modified starches.

4. Breakdown viscosity

The breakdown viscosities of BGNS, BGN-SDF and STASOL were 2890, 7 and 24 cP. Both BGN-SDF and STASOL had a significantly ($p = 0.003$) lower breakdown viscosity than BGNS. Breakdown viscosity is an indication of the starch organisational structure and measures the susceptibility of starch granules to disintegration (Jan *et al.*, 2013). A higher breakdown viscosity means the material has low heat and shear resistance (Falade *et al.*, 2014). Bambara groundnut starch had the highest breakdown viscosity, therefore, would have low thermal stability in comparison to BGN-SDF and STASOL (Amoo *et al.*, 2014). This was in agreement with thermal studies reported in Chapter 3 [Section 3.3.9, Tables 3.6 and 3.7]. Bambara groundnut starch had a higher breakdown viscosity than potato starch (2195 cP), wheat starch (775 cP) and barley starch (1938 cP) (Ragaei & Abdel-Aal, 2006; Kaur *et al.*, 2007; Fan *et al.*, 2019). As such, the modification of native BGNS was necessary to improve its robustness. The low breakdown viscosity of STASOL would render the nanocomposite stable at high processing temperatures due to their high thermal stabilities, making it a suitable ingredient for food products that are cooked at elevated temperatures and undergo extensive mixing in the preparation stage.

5. Setback viscosity

The setback viscosities of BGNS, BGN-SDF and STASOL were 2637, 128 and 122 cP, respectively (Table 4.1). Both BGN-SDF and STASOL had a significantly lower ($p = 0.000$) setback viscosity than BGNS. Setback viscosity refers to the tendency of starch to retrograde and undergoes syneresis (Gulu, 2018). After gelatinisation, amylopectin recrystallises and transforms from an amorphous state to a more crystalline state causing the starch pastes to thicken and form stiff gels (Cornejo-Ramírez *et al.*, 2018). Setback viscosity is an indication of gel stability (Mensah, 2011). When starch pastes cool down there is re-association between amylose and amylopectin molecules, which results in the formation of a gel structure and consequently, increased viscosity (Jan *et al.*, 2013; Falade *et al.*, 2014). A high setback viscosity, as exhibited by BGNS, indicates a high tendency towards retrogradation and syneresis (Amoo *et al.*, 2014). Bambara groundnut SDF and STASOL are complex polymers with

hydrogen and covalent bonds which inhibit the re-association of bonds following heating. The lower setback viscosity of STASOL compared to BGNS could be attributed to the introduction of BGN-SDF during the manufacturing process resulting in the formation of new functional groups as shown by FTIR studies [Chapter 3, section 3.3.5]. These functional groups indicate the formation of new bonds which restrict the re-association of starch molecules after cooling. This further proved that BGN-SDF was successfully grafted onto BGNS, reinforced the matrix and improved its characteristics. The decrease in setback viscosity of BGNS decreases with starch modification and this was confirmed by Sirivongpaisal (2008) and Afolabi (2012). Gulu (2018) reported the setback viscosity of BGNS as 1957 cP and established that inclusion complexes stabilise BGN starches. The differences in setback viscosities among studies could be attributed to starch extraction methods, machines used as well as plant variety.

6. *Pasting temperature*

When starch granules are exposed to elevated temperatures in the presence of water, they absorb water, swell and eventually rupture. The temperature at which they begin swelling is known as the pasting temperature. Pasting temperature indicates the minimum temperature required to initiate starch gelatinisation (Jan *et al.*, 2013). The pasting temperatures of BGNS (77.9°C), BGN-SDF (96.7°C) and STASOL (87.4°C) were significantly ($p = 0.000$) different. The results of the thermal properties of BGNS [Chapter 3, Table 3.6] were in fair agreement with the pasting properties of BGNS where initial peak thermal degradation due to gelatinisation of native BGNS was reported as 77.19°C. Higher pasting temperatures of 84 and 83.2°C were reported by Adebowale *et al.* (2002) and Afolabi (2012), respectively, for BGNS. Pasting temperatures higher than those of BGNS but lower than those of STASOL and BGN-SDF were reported for Mucuna bean starch (82°C) (Adebowale & Lawal, 2003) and barley starch (82.2°C) (Gujral *et al.*, 2011). The pasting temperature of starch observed in this study is similar to those of Sirivongpaisal (2008) and Gulu (2018) who reported the pasting temperature of BGNS as 77.7 and 79.90°C, respectively. Pasting temperatures of BGNS range between 78 and 84°C depending on the source and variety of seeds (Sirivongpaisal, 2008; Oyeyinka *et al.*, 2016). These are higher than those of potato starch (66.2-68.6°C) and comparable to those of corn starch (77-88°C) (Joshi *et al.*, 2013). The relatively high pasting temperature of pulses such as BGN could be accredited to their high amylose contents (Hoover *et al.*, 2010). The pasting temperature of BGNS in this study was within this range but those of STASOL and BGN-SDF were out of this range. A higher pasting temperature is an indication of thermal stability as more energy is required to rupture the granules. The higher pasting temperature of STASOL was a confirmation of the presence of stronger bonds in STASOL which required more energy to disrupt. The introduction of new functional groups as well as the disappearance and shifting of

functional groups in STASOL in FTIR studies confirmed the formation of a new, stronger complex [Section 3.3.5].

7. *Peak time*

Peak time is the time when peak viscosity is reached (Griess *et al.*, 2011) and is a function of shear rate, shear stress and temperature. The peak times of BGNS, BGN-SDF and STASOL were 4.78, 6.87 and 6.97 min, respectively (Table 4.1). The peak times of all three biopolymers were significantly ($p = 0.000$) different. A similar peak time of 4.70 min for BGNS was reported by Gulu (2018). Complexing increases the time required to reach peak viscosity (Gulu, 2018) because more time is needed to break down the structure of the material under study. Hence, STASOL (a biopolymer nanocomposite) and BGN-SDF (a complex polysaccharide) exhibited higher peak times than BGNS (a simple polysaccharide). A comparable peak time of 4.33 min for potato starch was reported by Kaur *et al.* (2007). Potato starch is commonly used as a thickener in soups, sauces, custards and puddings (Jane *et al.*, 1999) hence suggesting that BGNS could be employed for similar use in these systems. Pasting studies showed that the pasting properties of BGNS would render it unsuitable for use as an ingredient in many food systems as it would breakdown at temperatures below 100°C, gelatinise, retrograde and be prone to syneresis. As such, the modification of BGNS by grafting it with BGN-SDF to form STASOL was justified. STASOL has improved properties and would be useful as an ingredient in various food systems as it withstands high shear rates and temperatures. STASOL exhibited similar behaviour to modified starches commonly used in the food industry suggesting that it would behave in a similar desirable manner.

4.3.2 **Colour characteristics of Bambara groundnut starch, soluble dietary fibre and starch-soluble dietary fibre nanocomposite**

The colour attributes of BGNS, BGN-SDF and STASOL are presented in Table 4.2. Lightness describes the luminous intensity of colour and is measured on a scale of 0 to 100, with 0 indicating black and 100 indicating white. Chroma is how vivid or saturated a colour is (Maphosa, 2016) and hue describes how a colour is perceived (Murevhanema & Jideani, 2013). The redness and greenness of a colour are described by a positive a^* and a negative a^* , respectively. The yellowness and blueness of a colour are described by a positive b^* and a negative b^* , respectively. For both a^* and b^* , 0 is neutral.

Table 4.2 Colour attributes of BGNS, BGN-SDF and STASOL

	L*	a*	b*	C*	h°
BGNS	87.94 ± 0.0058 ^a	1.33 ± 0.0058 ^a	12.43 ± 0.0000 ^a	12.50 ± 0.0058 ^a	83.87 ± 0.0058 ^a
BGN-SDF	76.12 ± 0.0058 ^b	2.21 ± 0.0058 ^b	18.86 ± 0.0265 ^b	18.96 ± 0.0058 ^b	83.32 ± 0.0058 ^b
STASOL	89.16 ± 0.0058 ^c	0.40 ± 0.0000 ^c	14.61 ± 0.0000 ^c	14.62 ± 0.0058 ^c	88.42 ± 0.0000 ^c

Values are mean ± standard deviation. Means within a column followed by different superscripts are significantly [$p \leq 0.05$] different; L*: lightness; a*: red/ green; b*: yellow/blue; C*: chroma; h°: hue; SDF: soluble dietary fibre; STASOL: Bambara groundnut starch-soluble dietary fibre nanocomposite.

The lightness (L^*), redness/greenness (a^*), yellowness/blueness (b^*), chroma and hue angles were 87.94, 1.33, 12.43, 12.50 and 83.87° (BGNS), 76.12, 2.21, 18.86, 18.96 and 83.32° (BGN-SDF) as well as 89.16, 0.4, 14.61, 14.62 and 88.42° (STASOL), respectively. The three biopolymers differed significantly ($p = 0.000$) in all colour characteristics. The relatively higher degree of lightness observed in STASOL can be attributed to the bleaching properties of H_2O_2 used in the formulation of the nanocomposite. All the polymers had positive a^* and b^* values indicating that they were more associated with redness and yellowness, respectively. The redness and yellowness of BGN-SDFs relate to phenolics and other antioxidant-possessing chemicals such as anthocyanins, cyanidins as well as a wide range of isoflavones and phenolic acids (Murevhanema & Jideani, 2013; Maphosa, 2016).

The lightness of biopolymers destined for food use is of importance in the final products as it determines how much the original colour of the food system will be affected (Rosell *et al.*, 2009; Tosh & Yada, 2010; Maphosa, 2016; Agyepong & Barimah, 2018). As such, STASOL can be used as an ingredient in food systems without negatively impacting their colour. It was observed that lightness increased with increasing hue and this was in agreement with Maphosa (2016). Maphosa (2016) studied BGN-SDF from the black-eye variety and reported the colour attributes as L^* (73.0), a^* (1.7), b^* (13.8), chroma (13.9) and hue angle (83.1°). These were comparable with the colour attributes reported in this study, L^* (76.1), a^* (2.2), b^* (18.9), chroma (19.0) and hue (83.9°).

1. Colour differences

A colour difference (ΔE) of 1 is known as a just-noticeable difference (JND) and is the threshold at which trained observers notice the difference between two colours (Sharma, 2005). The difference between two colours can be noticeable but still considered acceptable. A ΔE between 4 and 8 is acceptable. Above 8, the colour difference is deemed unacceptable and likely to be rejected by consumers (Sharma, 2005). Table 4.3 gives the colour differences among BGNS, BGN-SDF and STASOL.

Table 4.3 Colour difference among BGNS, BGN-SDF and STASOL

	ΔE
BGNS-STASOL	6.60
BGNS-SDF	13.48
BGN-SDF-STASOL	14.22

BGNS: Bambara groundnut starch; BGN-SDF: Bambara groundnut soluble dietary fibre; STASOL: Bambara groundnut starch-soluble dietary fibre nanocomposite.

The colour differences between BGNS and STASOL, BGNS and BGN-SDF, and BGN-SDF and STASOL were 6.60, 13.48 and 14.22, respectively. There was a noticeable difference in colour among the three biopolymers. The difference between BGNS and STASOL ($\Delta E = 6.60$) was considered acceptable as it falls in the region 4-8 (Maphosa, 2016). BGNS-BGN-SDF and BGN-SDF-STASOL had ΔE above 8 meaning their colour differences would be very apparent if they were used interchangeably.

4.3.3 Chemical composition of Bambara groundnut starch, soluble dietary fibre and starch-soluble dietary fibre nanocomposite

The chemical composition of BGNS, BGN-SDF and STASOL is given in Table 4.4. Bambara groundnut starch had a low amount of proteins (1.7%), BGN-SDF was relatively high in proteins (15.5%) and STASOL had a considerable amount of proteins (7.0%). Bambara groundnut starch and BGN-SDF did not differ significantly in their moisture ($p = 0.620$) and fat ($p = 0.116$) content and both had a significantly ($p = 0.000$) higher moisture content and a significantly ($p = 0.000$) lower fat content than STASOL. All three biopolymers differed significantly ($p = 0.000$) in energy, protein and carbohydrate composition. Bambara groundnut SDF and STASOL were not significantly ($p = 0.217$) different in their ash content and both had a significantly ($p = 0.000$) higher ash content than BGNS. Ash is an indication of the mineral content of samples and the high values obtained in BGN-SDF and STASOL suggested that they may contribute micro and macro elements to food systems (Sirivongpaisal, 2008; Eltayeb *et al.*, 2011). Lower protein values of 0.3 and 0.61% for BGNS have been reported by Oyeyinka (2017) and Sirivongpaisal (2008), respectively, while comparable protein values in BGNS (1.77%) were reported by Afolabi (2012). Generally, it was established that BGN starches have very low protein content indicating high purity.

The moisture content of the biopolymers, BGNS (10.84%), BGN-SDF (10.82%) and STASOL (8.63%), was in fair agreement with differential scanning calorimetry studies (Table 3.6) where less energy was required in dispelling moisture from STASOL as it had the minimum reported moisture content. These results were further confirmed by thermogravimetric analysis [Chapter 3, section 3.3.9] where the highest and lowest mass loss due to moisture was observed in BGNS and STASOL, respectively. The moisture content of all three biopolymers in this study was similar to that of cassava starches (8.21-12.39%) (Agyepong & Barimah, 2018), lower than that of BGNS (14.11%) (Afolabi, 2012) and higher than that of BGNS (6.5-8.9%) (Oyeyinka & Oyeyinka, 2016; Sirivongpaisal, 2008).

Table 4.4 Chemical composition of BGNS, BGN-SDF and STASOL

	Moisture (%)	Ash (%)	Protein (%)	Fat (%)	Carbohydrates (%)	Energy (kJ)
BGNS	10.84 ± 0.0436 ^a	0.07 ± 0.0100 ^a	1.74 ± 0.3487 ^a	0.56 ± 0.0222 ^a	86.79 ± 0.3134 ^a	1525.78 ± 0.6897 ^a
BGN-SDF	10.82 ± 0.0839 ^a	4.90 ± 0.0900 ^b	15.54 ± 0.3029 ^b	0.54 ± 0.0162 ^a	68.20 ± 0.1811 ^b	1443.47 ± 2.2137 ^b
STASOL	8.63 ± 0.2500 ^b	4.88 ± 0.0666 ^b	6.96 ± 0.6749 ^c	0.84 ± 0.0100 ^b	78.69 ± 0.5500 ^c	1487.08 ± 5.5500 ^c

Values are mean ± standard deviation. Means within a column followed by different superscripts are significantly [$p \leq 0.05$] different; BGNS: Bambara groundnut starch; BGN-SDF: Bambara groundnut soluble dietary fibre; STASOL: Bambara groundnut starch-soluble dietary fibre nanocomposite.

The amount of ash remaining when studied using TGA (Table 3.7) was STASOL > BGN-SDF > BGNS and this was in agreement with the trend of ash studied using the muffle furnace (Table 4.4): STASOL (4.90%) > BGN-SDF (4.88%) > BGNS (0.07%). The ash content of all studied biopolymers was higher in TGA studies than in muffle furnace studies and this could be attributed to the longer heating time in the muffle-furnace which could be indicative of incompleteness of the thermogravimetric process. Higher ash values for BGNS reported in literature include 0.2% (Oyeyinka & Oyeyinka, 2016), 0.21% (Afolabi, 2012) and 0.47% (Sirivongpaisal, 2008).

Lower ash values (0.38-0.98%) were reported for cassava modified starches (Agyepong & Barimah, 2018). These were considerably lower than those of STASOL and this could be because the modification of BGNS in the formation of STASOL involved the introduction of a new biopolymer (BGN-SDF) which had relatively higher ash content (4.90%). Other starches are commonly modified using methods that involve the use of enzymes, heat and chemicals without the introduction of a second nutritional compound hence, the ash content is solely an indication of the minerals present in the starch. As such STASOL would make a better fortifier of minerals in food products.

4.3.4 Determination of Bambara groundnut starch, soluble dietary fibre and starch-soluble dietary fibre nanocomposite minerals using elemental content by inductively coupled plasma-optical emission spectrometry (ICP-OES)

The mineral composition of BGNS, BGN-SDF and STASOL determined using ICP-OES is presented in Figure 4.3. Minerals are of importance in the physiological functioning of the human body. BGNS contained the highest amount of potassium (15.69 mg/L) and zinc (0.72 mg/L) but the lowest amount of sodium (1.42 mg/L) and magnesium (4.39 mg/L). BGN-SDF had the highest amount of zinc (0.34 mg/L) and the highest amount of sodium (1.67 mg/L), magnesium (14.66 mg/L) and iron (1.41 mg/L). STASOL had the lowest amount of iron (0.98 mg/L) but a high amount of potassium (11.64 mg/L) and magnesium (10.47 mg/L).

Yao *et al.* (2015) reported lower values of magnesium (3.02 mg/L), comparable values of zinc (0.5 mg/L) and higher values of iron (33.58 mg/L) for BGN seeds. The total mineral content of the biopolymers determined using ICP-OES agreed with the total ash studies (Section 4.3.3), with BGN-SDF having the highest ash content and BGNS the least (Table 4.4). Bambara groundnut SDF had the highest amount of ash (4.90 g) and the highest total mineral composition (31.55 mg/L) while BGNS had the lowest amount of ash (0.07 g) and the lowest total mineral composition (23.25 mg/L). This was because the minerals in STASOL were from the BGNS and BGN-SDF used in the production.

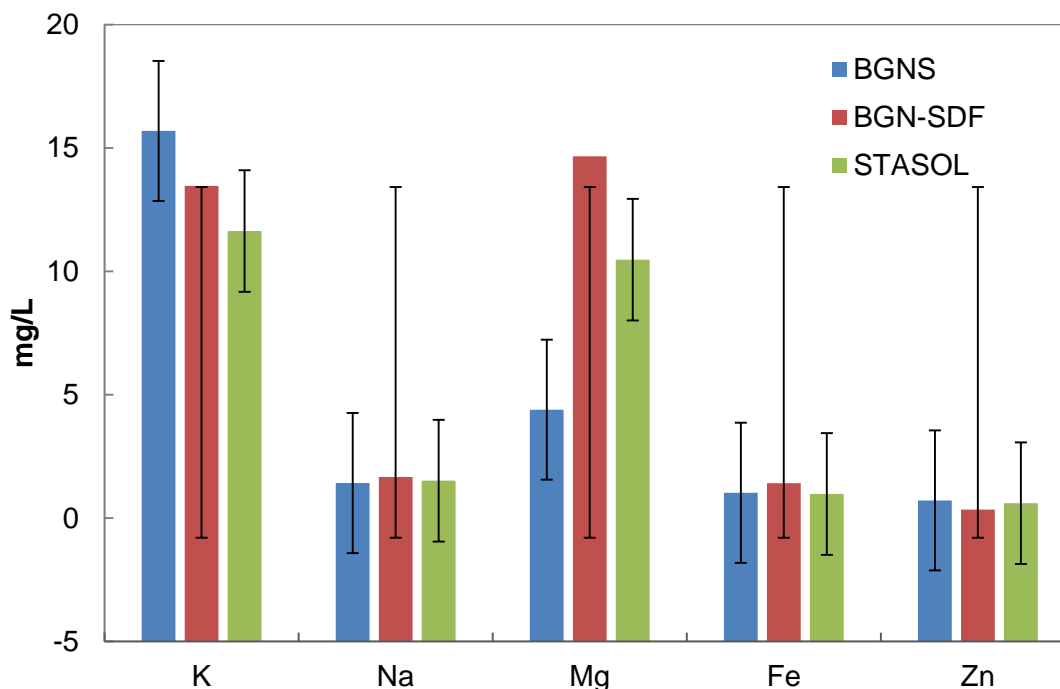


Figure 4.3

Mineral composition of BGNS, BGN-SDF and STASOL.

BGNS: Bambara groundnut starch; BGN-SDF: Bambara groundnut soluble dietary fibre; STASOL: Bambara groundnut starch-soluble dietary fibre nanocomposite.

Bambara groundnut seeds contain minerals such as zinc (Zn), iron (Fe), calcium (Ca), sodium (Na) and potassium (K) but are poor in magnesium (Mg) (Afolabi, 2012; Gabriel *et al.*, 2013; Murevanhema & Jideani, 2013; Mubaiwa *et al.*, 2017). Several studies have reported the mineral composition of BGN seeds as potassium (5.1-18.7 mg/L), sodium (2.1-2.4 mg/L), magnesium (2.1-6.4 mg/L), iron (0.2-0.6 mg/L) and zinc (0.5-2.6 mg/L) (Adebowale *et al.*, 2002; Aremu *et al.*, 2006; Olaleye *et al.*, 2013; Ndidi *et al.*, 2014). Generally, the values for most of the minerals in this present study are less than those reported for BGN seeds. This was expected as only parts of BGN seeds (BGNS and BGN-SDF) were analysed in this study while whole seeds were used by other researchers.

Minerals are of importance in the physiological functioning of the human body. Magnesium maintains the electrical potential in nerves and is a component of several enzymes (Aremu *et al.*, 2006). Sodium and potassium are necessary for maintaining osmotic balance and pH of body fluids, regulation of muscle and nerve irritability, controlling glucose

absorption as well as enhancing normal retention of protein during growth (Olaleye *et al.*, 2013). Iron facilitates the oxidation of carbohydrates, proteins and fats as well as plays a major role in the functioning of the central nervous system (Adeyeye & Fagbohun, 2005). Zinc is present in all tissues of the body and is a component of numerous enzymes (Aremu *et al.*, 2006). As such, STASOL would play an important physiological role by contributing minerals to the body and as a fortifier in food systems.

4.3.5 Hydration properties of Bambara groundnut starch, soluble dietary fibre and starch-soluble dietary fibre nanocomposite

The solubility index (SI) and water absorption capacity (WAC) of BGNS, BGN-SDF and STASOL are given in Table 4.5 and discussed in the following sections.

1. Solubility index

Solubility is defined by the IUPAC (2006) as the analytical composition of a saturated solution expressed as a proportion of a designated solute in a designated solvent. A high SI positively affects the functional properties of food both in food systems and in the gastrointestinal canal (Rosell *et al.*, 2009; Daou & Zhang, 2012). It largely affects the efficiency of processing, flow behaviour, texture, viscosities as well as physiological roles such as nutrient absorption (Rosell *et al.*, 2009; Dhingra *et al.*, 2012; Wang *et al.*, 2020). The SI of BGNS, BGN-SDF and STASOL was 0.9, 95.26 and 93.22%, respectively. All biopolymers showed significant ($p = 0.000$) differences in SI, with native BGNS being practically insoluble in water (0.9%).

Native starch is insoluble in cold water because amylose and amylopectin chains are arranged in a tight interlocking structure that becomes the hydrophobic crystalline-like starch granule (Gulu, 2018). This was in agreement with the results of Agyepong & Barimah (2018) who reported very low solubility of native cassava starch (1.29-7.38%) and an increase in solubility of starch after modification. This observation was also made for STASOL in this study. STASOL had high solubility despite having BGNS as the highest constituent. This was a piece of evidence that the modification of BGNS by complexing with BGN-SDF was successful. The smaller average particle size (74.01 nm) of STASOL [Chapter 3, section 3.3.4 (1)] translated to a larger surface area, hence increasing its interaction with water molecules and consequently increasing their solubility. The high solubility of STASOL and the insolubility of BGNS were in agreement with crystallinity studies (Chapter 3, section 3.3.6) where BGNS was crystalline and STASOL was amorphous.

Table 4.5 Physicochemical properties of BGNS, BGN-SDF and STASOL

	Water absorption capacity (g/g)	Solubility index (%)	Oil binding capacity (g/g)	Emulsion activity (%)	Emulsion stability (%)
BGNS	1.62 ± 0.1852 ^a	0.90 ± 0.2196 ^a	1.13 ± 0.0451 ^a	23.25 ± 31.9612 ^a	23.33 ± 18.2050 ^a
BGN-SDF	5.53 ± 0.2987 ^b	95.26 ± 0.0400 ^b	3.78 ± 0.1069 ^b	85.71 ± 6.0017 ^b	87.13 ± 6.5124 ^b
STASOL	4.66 ± 0.2650 ^c	93.27 ± 0.0500 ^c	1.52 ± 0.0692 ^c	90.65 ± 1.8900 ^c	87.49 ± 3.3000 ^c

Values are mean ± standard deviation. Means within a column followed by different superscripts are significantly [$p \leq 0.05$] different; BGNS: Bambara groundnut starch; BGN-SDF: Bambara groundnut soluble dietary fibre; STASOL: Bambara groundnut starch-soluble dietary fibre nanocomposite.

Starch granules rupture and lose crystallinity when exposed to heat and water resulting in the disruption of bonds thereby exposing functional groups and making them more available to chemical reactions with water (Afolabi, 2012; Gulu, 2017). Amorphosity increases the solubility of compounds in water thus explaining the high solubility of STASOL. The high SI of STASOL would make it a useful ingredient in various food preparations such as beverages (Adeleke *et al.*, 2017). Furthermore, the high SI of STASOL would make its delivery of active compounds in food systems easier.

2. *Water absorption capacity*

Water absorption capacity is a useful indicator of whether molecules can be incorporated into aqueous food formulations or not (Adebowale *et al.*, 2011). The WAC of BGNS was 1.62 g/g and that of BGN-SDF and STASOL could not be determined as they were significantly ($p = 0.000$) soluble in water (Table 4.5). This was a desirable observation as it further proved that STASOL was a new compound and its improved solubility was a result of the successful modification of BGNS. The WAC of BGNS is dependent on the swelling power of its granules. The swelling of starch is predominantly determined by the amylose content (Singh *et al.*, 2003) with lower amylose contents resulting in higher swelling capacities (Oyeyinka *et al.*, 2016). Other factors that affect the amount of water that starch granules can absorb include botanical origin, variety, growth conditions, granule shape and size as well as the magnitude of interactions between amorphous and crystalline regions of amylose and amylopectin.

Leguminous starch such as BGNS has been reported to exhibit single-stage restricted swelling accompanied by minimal leaching of amylose when compared to cereal starches such as that from potatoes (Hoover *et al.*, 2010). This was speculated to be a result of the closely packed amylose chains within the amorphous region of pulse-starch granules (Hoover *et al.*, 2010). Hence, although the major compounds that enhance the WAC of a compound are carbohydrates, the morphology and crystalline nature of starch render it highly hydrophobic restricting its water absorption.

The WAC of BGNS in this study was 1.62 g/g. A similar WAC (1.67 g/g) of BGNS was reported by Sirivongpaisal (2008) although an alkaline extraction method was applied. This indicated that the two extraction methods did not impact the WAC. Gulu (2018) reported a lower water absorption capacity (1.17 g/g) for BGNS, which could be attributed to different varieties used. Gulu (2018) used mixed BGN seeds while only the black-eye variety was used in the production of STASOL. The black-eye variety was reported by Maphosa & Jideani (2016) to have a superior WAC than the other varieties, which could explain the higher values reported in this study. Adebowale *et al.* (2002) reported a higher WAC (2.0 g/g) for BGNS and this could be attributed to the different extraction methods used. Adebowale *et al.* (2002) employed a wet

milling method while a dry milling method was used in this study. Several studies have reported differing WAC for BGNS (Adebowale *et al.*, 2002; Sirivongpaisal, 2008; Afolabi, 2012). The relatively lower water absorptivity reported in this study suggests that BGNS may find use in food applications where swelling is not required (Eltayeb *et al.*, 2011).

4.3.6 Oil binding properties of Bambara groundnut starch, soluble dietary fibre and starch-soluble dietary fibre nanocomposite

The oil binding capacities (OBC) of BGNS, BGN-SDF and STASOL differed significantly ($p = 0.000$) and were 1.13, 3.78 and 1.61 g/g, respectively. Oil binding capacity is the ability of lipids to form interactions with non-polar side chains of molecules (Eltayeb *et al.*, 2011). Oil binding is affected by factors such as particle size, surface area, charge and hydrophobicity (Adebowale *et al.*, 2011). Oil binding capacity works on the principle of physically entrapping oil through capillary attraction. It indicates the ability and extent to which biopolymers can stabilise high-fat food products and emulsions as well as act as fat binders and replacers in products such as meat (Elleuch *et al.*, 2011).

The OBC of native BGNS in this study (1.13 g/g) was lower than the WAC (1.62 g/g) reported in Table 4.5, which indicated a higher level of hydrophilicity compared to hydrophobicity. The OBC of BGNS reported in this study was higher than the 1.01 g/g reported by Sirivongpaisal (2008). The differences could be attributed to the use of dehulled, mixed variety of BGN seeds milled using the wet-milling method used by Sirivongpaisal (2008) compared to whole, black-eye BGN seeds milled using the dry method used in this study. The OBC of BGNS agreed with the observations reported by Adebowale *et al.* (2002), Sirivongpaisal (2008) and Gulu (2018) for native BGNS. The OBC of BGNS was 1.01, 1.06 and 1.76 g/g as reported by Gulu (2018), Sirivongpaisal, (2008) and Adebowale *et al.* (2002), respectively, which was similar to the 1.13 g/g reported for BGNS in this study. The low OBC of BGNS compared to STASOL and BGN-SDF could be attributed to the low levels of proteins in BGNS. The proteins present in STASOL and BGN-SDF (Table 4.4) may be hydrophobic hence would display superior lipid-binding characteristics (Adeleke, 2017).

Modified BGNS complexed with cyclodextrins and catechin had OBCs in the range 1.02-1.07 g/g (Gulu, 2018) which was lower than the 1.61 g/g reported for STASOL. This suggested that the modification of BGNS by complexing with BGN-SDF yielded better properties than complexing with cyclodextrins and catechin. The positive effects of complexing BGNS with BGN-SDF on the OBC of STASOL can be ascribed to the emergence of new binding sites that result from the dissociation and formation of bonds during the chemical modification process (Mubaiwa *et al.*, 2018).

This study showed that BGN-SDF would be the most suitable biopolymer to render the desirable properties compared to BGNS and STASOL. This was confirmed by Maphosa (2016) who reported relatively higher OBC for SDF from four BGN varieties. The ability of biopolymers to bind oil can be harnessed by the food industry in reducing fat losses during cooking as well as in emulsion stabilisation (Elleuch *et al.*, 2011; Slavin, 2013). Also, OBC plays a major role in foodstuffs such as meat, emulsions and baked goods by improving palatability, flavour retention and shelf life extension (Adebowale & Lawal, 2003; Aremu *et al.*, 2007; Gulu, 2018). Physiologically, the OBC of biopolymers would allow them to play a significant role in bile acid absorption and consequently cholesterol reduction (Tosh & Yada, 2010). A higher OBC indicates a greater ability to fulfil these functions.

4.3.7 Emulsion activity and stability indexes of Bambara groundnut starch, soluble dietary fibre and starch-soluble dietary fibre nanocomposite

The emulsion activity index (EAI) of BGNS, BGN-SDF and STASOL was 23.25, 85.71 and 90.65%, respectively. Emulsification is an important process in the manufacturing of several formulated foods. The study of emulsifying properties is useful in the prediction of the behaviour of emulsions during large scale production, distribution, storage and utilisation stage (Guzey *et al.*, 2004; Fasinu *et al.*, 2015). Emulsions normally dissociate due to creaming, flocculation, coalescence, Ostwald ripening and phase inversion (Guzey *et al.*, 2004). The stability of emulsions is affected by factors such as pH, nature of stabiliser, pressure, temperature, particle size as well as environmental stresses like agitation and light.

Emulsion activity is the ability of a compound to participate in the formation and stabilisation of a newly created emulsion (Zayas, 1997; Mora *et al.*, 2013). The emulsion stability index (ESI) of BGNS, BGN-SDF and STASOL was 23.33, 87.13 and 87.49%, respectively. Emulsion stability measures the ability of an emulsion to resist changes to its structure and maintain its physicochemical properties (Eltayeb *et al.*, 2011; Fasinu *et al.*, 2015; Mubaiwa *et al.*, 2018). The significantly ($p = 0.000$) lower emulsion activity and stabilising properties of BGNS can be attributed to its insolubility and low WAC (Table 4.5). Emulsions consist of an aqueous phase and a lipid phase, and the role of the stabiliser is to keep the two phases together. Most polysaccharides stabilise emulsions by increasing the viscosity of the system thereby retarding oil droplet migration (Dickinson, 1994). To successfully increase the viscosity of a system, the polysaccharide needs to have adequate solubility in the aqueous phase. The low hydration properties of BGNS hindered it from being an emulsion stabiliser. As emulsions have a lipid component, a suitable stabiliser needs a suitable degree of hydrophobicity. BGNS had a low OBC (Table 4.5) and that played a role in making it an unsuitable stabiliser. BGN-SDF and STASOL both exhibited significantly ($p = 0.000$) high

hydration and OBC (Table 4.5). As such, they could enhance emulsion stability by increasing the viscosity of the system (Chanamai & McClements, 2000; Yadav *et al.*, 2007; Saha & Bhattacharya, 2010; Kerkhofs *et al.*, 2011; Acton, 2012; Gharibzahedi *et al.*, 2012; Cheong *et al.*, 2014; Adeyi, 2014).

4.3.8 Glucose composition of Bambara groundnut starch, soluble dietary fibre and starch-soluble dietary fibre nanocomposite

Table 4.6 shows the glucose composition of BGNS (87.9%), BGN-SDF and STASOL (63.4%).

Table 4.6 Glucose composition of BGNS, BGN-SDF and STASOL

	Glucose (%)
BGNS	87.9
BGN-SDF	ND
STASOL	63.4

ND: Not detected; BGNS: Bambara groundnut starch; BGN-SDF: Bambara groundnut soluble dietary fibre; STASOL: Bambara groundnut starch-soluble dietary fibre nanocomposite.

In Table 4.4, the carbohydrates composition of BGNS was 86.8%. This was in fair agreement with the results of this section. Starch is made up of repeating units of glucose (Tayade *et al.*, 2019) hence its hydrolysis yielded 87.9% glucose similar to its carbohydrate content. STASOL had a higher carbohydrate content (78.7%) as reported in Table 4.4 compared to its glucose content (63.4%). Proportionately, the glucose composition of STASOL should have been higher, however some may have been lost during production. STASOL is a nanocomposite made from BGNS:BGN-SDF (15:1.95) hence the quantified glucose would be from the hydrolysis of BGNS and the difference would have been carbohydrates from BGN-SDF that were not made up of glucose units. No glucose was detected in BGN-SDF. This was in agreement with Maphosa (2016) who reported an insignificant amount of glucose (<1%) in BGN-SDFs.

4.3.9 Polyphenolic compounds in Bambara groundnut starch, soluble dietary fibre and starch-soluble dietary fibre nanocomposite

Table 4.7 shows the phenolic composition of BGNS, BGN-SDF and STASOL. All three biopolymers showed appreciable amounts of phenolics. The phenolic compounds chlorogenic

acid (18 mg/g), monocrotaline (20 mg/g), luteolin 7-O-(6''-malonylglucoside) (4 mg/g) and casuarine 6- α -D-glucoside (27 mg/g) were present in BGN-SDF and absent in BGNS and STASOL while blumealactone C (7 mg/g) was present in BGNS and absent in BGN-SDF and STASOL. Of the three biopolymers, BGN-SDF had the highest quantity of phenolics compared to BGNS and STASOL, with high levels of (+)-sesamin (12 mg/g), 12,13-TriHOME (8602 mg/g), dronabinol (3389 mg/g), 9(S)-HPODE (50 mg/g), α -dimorphecolic acid (273 mg/g), dimethyltryptamine (7281 mg/g) and [1R-(1 α ,4 β ,6 α ,8 α)]-1,2,4a,5,6,8a-Hexahydro-6-hydroxy-4,7-dimethyl-a-methylene-1-naphthaleneacetic acid methyl ester (7594 mg/g).

The polyphenolic compounds in this section were in agreement with the TPC and FRAP results (Table 4.8) where BGN-SDF had the highest amount of total polyphenols as well as the strongest ferric acid-reducing power. BGNS is generally low in antioxidant activity (Maphosa, 2016) and this was demonstrated by its relatively lower phenolic composition (Table 4.7). The presence of phenolic compounds in STASOL demonstrated that active compounds were successfully delivered from BGN-SDF to BGNS, therefore it was concluded that STASOL possessed appreciable amounts of antioxidant compounds. However, the phenolic compounds furcadin, dimethyltryptamine, isatidine, casuarine and 6- α -D-glucoside [1R-(1 α ,4 β ,6 α ,8 α)]-1,2,4a,5,6,8a-Hexahydro-6-hydroxy-4,7-dimethyl-a-methylene-1-naphthaleneacetic acid methyl ester, luteolin 7-O-(6''-malonylglucoside) were present in high quantities in BGNS and BGN-SDF but were either not delivered at all to STASOL or were delivered in very low quantities. This was attributed to the low amount of BGN-SDF used in the formulation of STASOL. As such, future studies should look into using a higher amount of BGN-SDF to increase the antioxidant capacity of STASOL.

The findings of this study highlight the potential of BGN as an economic source of natural antioxidants for human consumption and could therefore open horizons to its industrial use in the development of functional food. The antioxidant activity of BGN seeds and constituents has been reported by several researchers (Murevhanema & Jideani, 2013; Harris *et al.*, 2014; Nyau *et al.*, 2015; Oyeyinka *et al.*, 2016). The antioxidant behaviour of phenolics arises from the ability of their hydroxyl groups to donate hydrogen, react with oxygen and react with nitrogen species, producing radical species in a termination reaction (Valentao *et al.*, 2002). Phenolic compounds such as those identified in BGNS, BGN-SDF and STASOL have been reported to possess many desirable characteristics such as anti-inflammatory, anti-microbial, anti-fungal, anti-allergic, anti-oxidant, anti-apoptotic, anti-tumour and estrogenic activity (Sanzani *et al.*, 2014; Salawu, 2016; Gagliardini *et al.*, 2017; Harris *et al.*, 2018).

Table 4.7 Phenolic composition of BGNS, BGN-SDF and STASOL

Phenolics	Phenolic group	Elution time (min)	BGNS (mg/g)	BGN-SDF (mg/g)	STASOL (mg/g)
Scoparone	Flavonoid phytoalexin	7.19	0	11	28
Chlorogenic acid	Phenol esters	7.60	0	18	0
Blumealactone C	Terpene lactone	7.71	7	0	0
(+)-Sesamin	Polyphenol	8.12	4	12	11
4-hydroxymethyl-2-methoxyphenyl-1-O-beta-D-apiofuranosyl-(1->6)-O-beta-D-glucopyranoside	Flavonone	8.40	0	10	6
Furcatin	Phenylpropene	8.72	4	6	0
Monocrotaline	Pyrrolizidine alkaloid	9.30	0	20	0
[1R-(1alpha,4abeta,6alpha,8aalpha)]-1,2,4a,5,6,8a-Hexahydro-6-hydroxy-4,7-dimethyl-a-methylene-1-naphthaleneacetic acid methyl ester	Sesquiterpenoid	9.99	237	7594	8
Luteolin 7-O-(6"-malonylglucoside)	Flavonoid	10.23	0	4	0
Dimethyltryptamine	Phenol amide	10.48	1446	7281	13
Isatidine	Pyrrolizidine alkaloid	10.63	8	27	0
Casuarine 6-alpha-D-glucoside	Pyrrolizidine alkaloid	10.95	0	27	0
9,12,13-TriHOME	Linoleic acid derivative	12.92	396	8602	3009
Dronabinol	Tetrahydrocannabinol	13.94	103	3389	643
9(S)-HPODE	Linoleic acid derivative	14.12	26	50	63
Alpha-dimorphecolic acid	Linoleic acid derivative	14.35	49	273	161

BGNS: Bambara groundnut starch; BGN-SDF: Bambara groundnut soluble dietary fibre; STASOL: Bambara groundnut starch-soluble dietary fibre.

Table 4.8 Antioxidant properties of BGNS, BGN-SDF and STASOL

	Polyphenols (mg GAE/g)	FRAP (μmol AAE/g)
BGNS	0.10 ± 0.011 ^a	1.16 ± 0.3958 ^a
BGN-SDF	6.59 ± 0.1766 ^b	4.77 ± 0.7770 ^b
STASOL	0.46 ± 0.0481 ^c	1.45 ± 0.2359 ^c

Values are mean ± standard deviation. Means within a column followed by different superscripts are significantly [$p \leq 0.05$] different; BGNS: Bambara groundnut starch; BGN-SDF: Bambara groundnut soluble dietary fibre; STASOL: Bambara groundnut starch-soluble dietary fibre nanocomposite. FRAP: Ferric reducing antioxidant power.

The consumption of phenolic-rich food has been associated with the prevention of chronic diseases such as some cancers, diabetes and osteoporosis (Zhu, 2015b). They accomplish this by chelating metal ions involved in the production of free radicals (Yang *et al.*, 2001) and by inhibiting enzymes involved in radical generation such as lipoxygenases and cyclooxygenase, (Parr & Bolwell, 2002).

4.3.10 Antioxidant properties of Bambara groundnut starch, soluble dietary fibre and starch-soluble dietary fibre nanocomposite

The total polyphenolic compounds (TPC) and ferric reducing antioxidant power (FRAP) in biopolymers is suggestive of the presence of antioxidant properties. The TPC of BGNS, STASOL and BGN-SDF were 0.10, 0.46 and 6.59 mg GAE/g, respectively. All three differed significantly ($p = 0.000$) in their TPC. STASOL is a nanocomposite made from BGN-SDF grafted onto BGNS at a ratio of 15:1.95 (BGNS:BGN-SDF). BGN-SDF is rich in antioxidant compounds while starches are generally low in active compounds (Maphosa, 2016). This validated the results obtained in this study, with BGN-SDF having the highest amount of TPC and FRAP while BGNS had significantly ($p = 0.000$) low antioxidant capabilities (Table 4.8). This proved that antioxidant compounds were successfully delivered from BGN-SDF to BGNS. However, since a low percentage (11.5%) of BGN-SDF was incorporated into STASOL, the total antioxidant activity of STASOL was lower than that of BGN-SDF.

Jayawardena *et al.* (2015) reported the total phenolic composition of 22 fruit juices in the range 0.24-0.39 mg GAE/g. These could be a result of the presence of common antioxidants such as Vitamin C, especially in citrus juices. These results were lower than those reported for STASOL (0.46 mg GAE/g). Fruit juices are a reliable source of antioxidants, therefore STASOL having superior antioxidant properties compared to the mentioned citrus juices is a positive characteristic. The significantly ($p = 0.000$) higher phenolic content of STASOL compared to BGNS could also be attributed to the chemical modification process used in the production of STASOL. To expose the reactive functional

groups in BGNS, ascorbic acid was oxidised by hydrogen peroxide resulting in the formation of hydroxyl and ascorbate radical intermediates (Spizzirri *et al.*, 2010). These intermediates may have interfered with the hydrogen atom transfer mechanism of oxygen radical absorbance capacity (ORAC) assay thereby influencing the antioxidant mechanism (Gulu, 2018) leading to the higher antioxidant capacity of STASOL.

The FRAP of BGNS, STASOL and BGN-SDF was 1.16, 1.45 and 4.77 $\mu\text{mol AAE/g}$, respectively (Table 4.8). All three biopolymers differed significantly ($p = 0.000$) in their ferric reducing capabilities. The FRAP assay is based on the reduction of ferric ions to ferrous ions and is commonly used to measure the antioxidant capacity of foods and beverages containing polyphenols (Marc *et al.*, 2019). The ability of natural antioxidants to donate electrons or hydrogen atoms can be evaluated using the FRAP assay (Pownall *et al.*, 2010). The polyphenolic composition of STASOL suggested that it could be exploited as a novel antioxidant and would be of importance in protecting against superoxide radicals, hydroxyl free radicals and lipid peroxidation. The nanocomposite would therefore find use in fatty food products as a fortifier to improve oxidative stability, thereby extending shelf life (Elleuch *et al.*, 2011). As a natural antioxidant containing compound, STASOL would be a suitable alternative source to artificial antioxidants. Artificial antioxidants have been reported to be carcinogenic and teratogenic hence their use in food products is discouraged (Betancur-Ancona *et al.*, 2004).

Apart from food functions, antioxidants have essential physiological functions. Highly reactive oxygen species and free radicals oxidise nucleic acids, proteins and lipids, initiating numerous degenerative conditions such as cellular injury, aging, cancer as well as hepatic, neurodegenerative, cardiovascular and renal disorders (Tomas *et al.*, 2004; Tsimikas, 2006). Antioxidants react with free radicals forming stable or non-reactive radicals thereby retarding or completely preventing the oxidation of molecules (Betancur-Ancona *et al.*, 2004; Valadez-Vega *et al.*, 2013). Plant-based foods have been reported to be rich in redox-active antioxidant containing properties such as polyphenols, carotenoids, and ascorbic acid (Liu *et al.*, 2015). STASOL would play an important physiological role as an antioxidant containing compound as well as be applied as a valuable ingredient for delivering active compounds in food systems.

4.4 Conclusions

The nanocomposite, STASOL, was successfully synthesised from BGNS and BGN-SDF and its antioxidant and functional properties were successfully characterised. STASOL displayed desirable physicochemical, antioxidant and functional properties as evidenced by their good hydration properties, oil binding capabilities, improved solubility, high emulsion stabilising properties, chemical composition, as well as possession of antioxidant properties. The grafting of BGN-SDF onto BGNS successfully mitigated the undesirable characteristics of

native BGNS and native BGN-SDF while retaining the desirable characteristics of both biopolymers and gaining new improved properties. STASOL is a natural, biocompatible, biodegradable and economic ingredient and could be concluded to possess therapeutic and low glycemic index (GI) properties, making it desirable for health-conscious consumers. Native starches, modified starches and hydrocolloids are available in the food industry. However, unlike STASOL, their use is limited to altering functional properties in food systems and does not extend to delivering active compounds to the food systems. Modified starches that exhibit similar characteristics to STASOL are widely employed in food systems for baked products, confectionery, gravies, soups, sauces, mayonnaise, salad dressing, ice cream, spreads, pasta, puddings, custards and beverages. STASOL is also expected to find use in these systems as a stabiliser and for delivering active compounds such as phenolics.

References

- Acton, A. (2012) Beverage emulsions as functions of main emulsion components. In: *Issues in Food production, Processing and Preparation*. Atlanta: Scholarly Editions.
- Adebowale, K.O. & Lawal, O.S. (2003). Functional properties and retrogradation behaviour of native and chemically modified starch of Mucuna Bean (*Mucuna pruriens*). *Journal of the Science of Food and Agriculture*, **83**, 1541-1546.
- Adebowale, K.O., Afolabi, T.A. & Lawal, O.S. (2002). Isolation, chemical modification and physicochemical characterisation of Bambarra groundnut (*Voandzeia subterranea*) starch and flour. *Food Chemistry*, **78**, 305-311.
- Adebowale Y.A., Schwarzenbolz, U. & Henle, T. (2011). Protein Isolates from Bambara Groundnut (*Voandzeia subterranean* L.): Chemical Characterization and Functional Properties, *International Journal of Food Properties*, **14(4)**, 758-775.
- Adeleke, O.R., Adiamo, O. Q. & Fawale, O.S. (2017). Nutritional, physicochemical, and functional properties of protein concentrate and isolate of newly-developed Bambara groundnut (*Vigna subterreneae* L.) cultivars. *Food Science and Nutrition*, **24;6(1)**, 229-242.
- Adeyeye, E.I. & Fagbohun, E.D. (2005). Proximate, mineral and phytate profiles of some selected spices found in Nigeria. *Pakistan Journal of Scientific and Industrial Research*, **4(1)**, 14-22.
- Adeyi, O. (2014). Effect of Bambara groundnut flour on the stability and rheological properties of oil-in-water emulsion. PhD Thesis, Cape Peninsula University of Technology.
- Afolabi, T.A. (2012). Synthesis and physicochemical properties of carboxymethylated bambara groundnut (*Voandzeia subterranea*) starch. *International Journal of Food Science and Technology*, **47**, 445-451.

- Agyepong, J.K. & Barimah, J. (2018). Physicochemical properties of starches extracted from local cassava varieties with the aid of crude pectolytic enzymes from *Saccharomyces cerevisiae* (ATCC 52712). *African Journal of Food Science*, **12(7)**, 151-164.
- Amoo, A.R.N., Wireko-Manu, F.D. & Oduro, I. (2014) Physicochemical and pasting properties of starch extracted from four yam varieties. *Journal of Food and Nutrition Sciences*, **2(6)**, 262-269.
- Anonymous. (2015). SWATH-MS/MS and DIA-MS: MS-DIAL: data independent MS/MS deconvolution for comprehensive metabolome analysis. *Nature Methods*, **12**, 523-526.
- Anonymous. (2018). Identifying metabolites by integrating metabolome databases with mass spectrometry cheminformatics. *Nature Methods*, **15**, 53-56.
- AOAC. (1997). Association of Official Analytical Chemists International Official Methods of Analysis. 16th Edition, AOAC, Arlington.
- Araujo-Farro, P.C., Amaral, J.P. & Menegalli, F.C. (2005). Comparison of starch pasting and retrogradation properties of Quinoa (*chenopodium quinoa wild*), rice, potato, cassava, wheat and corn starches, 1-7.
- Aremu, M.O., Olafe, O. & Akintayo, E.T. (2006). Chemical Composition and Physicochemical Characteristics of Two Varieties of Bambara Groundnut (*Vigna subterreneae*) Flours. *Journal of Applied Sciences*, **6(9)**, 1900-1903.
- Baljeet, Y. (2011). Effect of frying, baking and storage conditions on resistant starch content of foods. *British Food Journal*, **113(6)**, 710-719.
- Bamshaiye, O.M., Adegbola, J.A. & Bamishaiye, E.I. (2011). Bambara groundnut: An underutilized nut in Africa. *Advances in Agricultural Biotechnology*, **1**, 60-72.
- Betancur-Ancona, D., Perza-Mercado, G., Moguel-Ordonez, Y. & Fuertes-Blanco, S. (2004). Physicochemical characterisation of lima beans (*Phaseolus lunatus*) and jack bean (*Canavalia ensiformis*) fibrous residues. *Food Chemistry*, **84**, 287-295.
- Chanamai, R. & McClements, D.J. (2000). Impact of weighting agents and sucrose on gravitational separation of beverage emulsions. *Journal of Agricultural and Food Chemistry*, **48**, 5561.
- Cheong, K.W., Tan, C.P., Mirhosseini, H., Joanne-Kam, W.Y., Hamid, N.S.A. & Basri, M. (2014). The effect of prime emulsion components as a function of headspace concentration of soursop flavor compounds. *Chemistry Central Journal*, **8(23)**, 1-11.
- Chove, B., Grandison, A. & Lewis, M. (2001). Emulsifying properties of soy protein isolates obtained by isoelectric precipitation. *Journal of the Science of Food and Agriculture*, **81**, 759-763.
- Cornejo-Ramírez, Y.I., Martínez-Cruz, O., Del Toro-Sánchez, C.L., Wong-Corral, F.J., Borboa-Flores, J. & Cinco-Moroyoqui, F.J. (2018). The structural characteristics of starches and their functional properties. *CyTA - Journal of Food*, **16(1)**, 1003-1017.
- Daou, C. & Zhang, H. (2011). Physico-chemical properties and antioxidant activities of

- Dietary Fibre derived from defatted rice bran. *Advance Journal of Food Science and Technology*, **3(5)**, 339-347.
- Dhingra, D., Michael, M., Rajput, H. & Patil, R.T. (2012). Dietary fibre in foods: a review. *Journal of Food Science and Technology*, **49(3)**, 255-266.
- Dickinson, E. (1994). Protein-stabilized emulsions. *Journal of Food Engineering*, **22(1-4)**, 59-74.
- Elleuch, M., Bedigian, D., Roiseux, O., Besbes, S. & Blecker, C. (2011). Dietary fibre and fibre-rich by-products of food processing; Characterisation technological functionality and commercial applications: A review. *Food Chemistry*, **124**, 411-421.
- Eltayeb, A. R. S. M., Ali O. Ali., Abou-Arab, A.A. & Abu-Salem, F.M. (2011). Paper Chemical composition and functional properties of flour and protein isolate extracted from Bambara groundnut (*Vigna subterranean*). *African Journal of Food Science*, **5(2)**, 82-90
- Falade, K.O., Semon, M., Fadairo, O.S., Oladunjoye, A.O. & Orou, K.K. (2014). Functional and physico-chemical properties of flours and starches of African rice cultivars. *Food Hydrocolloids*, **39**, 41-50.
- Fan, X., Zhu, J., Dong, W., Sun, Y., Lv, C. & Guo, B. (2019). Comparison of pasting properties measured from the whole grain flour and extracted starch in barley (*Hordeum vulgare* L.). *PLoS ONE*, **14(5)**, e0216978.
- FAO (2003). Food energy - methods of analysis and conversion factors. *Report of a Technical Workshop*. Food and Agriculture Organization of the United Nations. Rome, 3-6 December 2002.
- Fasinu, E.G., Ikhu-Omoregbe, D.I.O. & Jideani, V.A. (2015). Influence of selected physicochemical factors on the stability of emulsions stabilized by Bambara groundnut flour and starch. *Journal of Food Science and Technology*, **52(11)**, 7048-7058.
- Gabriel, E.G., Jideani, V.A. & Ikhu-omoregbe, D.I.O. (2013). Investigation of the Emulsifying Properties of Bambara Groundnut Flour and Starch. *International Journal of Food Science and Engineering*, **7**, 539-547.
- Gagliardini, E., Benigni, A. & Perico, N. (2017). Pharmacological Induction of Kidney Regeneration. In: *Kidney Transplantation, Bioengineering and Regeneration. Kidney Transplantation in the Regenerative Medicine Era*, 1025-1037.
- Gharibzahedi, S.M.T., Mousavi, S.M., Hamed, M. & Ghasemlou, M. (2012). Response surface modeling for optimization of formulation variables and physical stability assessment of walnut oil-in-water beverage emulsions. *Food Hydrocolloids*, **26**, 293-301.
- Griess, J.K., Mason, S.C., Jackson, D.S., Galusha, T.D., Pedersen, J.F. & Yaseen, M. (2011). Environment and Hybrid Influences on Rapid-Visco-Analysis Flour Properties of Food-Grade Grain Sorghum. *Crop Science*, **51**, 1758-1766.
- Gujral, H.S., Sharma, P., Kaur, H. & Singh, J. (2011). Physiochemical, Pasting, and

- Thermal Properties of Starch Isolated from Different Barley Cultivars, *International Journal of Food Properties*, **16(7)**, 1494-1506.
- Gullon, B., Gullon, P., Lu-Chau, T.A., Moreira, M.T., Lema, J.M. & Eibes, G. (2017). Optimization of solvent extraction of antioxidants from *Eucalyptus globulus* leaves by response surface methodology: Characterization and assessment of their bioactive properties. *Industrial Crops and Products*, **108**, 649-659.
- Gulu, N.B. (2018). Functional and rheological properties of Bambara groundnut starch-catechin complex obtained by chemical grafting. Master of Food Science and Technology. Cape Peninsula University of Technology, Cape Town, South Africa.
- Guzey, D., Kim, H.J. & McClements, D.J. (2004). Factors influencing the production of O/W emulsions stabilized by beta-lactoglobulin-pectin membranes. *Food Hydrocolloids*, **18(6)**, 967-975
- Harris, T., Jideani, V.A. & Le Roes-Hill, M. (2014). Flavonoids and tannin composition of Bambara groundnut (*Vigna subterranean*) of Mpumalanga, South Africa. *Heliyon*, **4**, e00833.
- Hoover, R., Hughes, T., Chung, H.J. & Liu, Q. (2010). Composition, molecular structure, properties, and modification of pulse starches: A review. *Food Research International*, **43**, 399-413.
- IBM Corp. (2013). IBM Statistical Package for the Social Science (SPSS), Statistics for Windows, Version 22.0. Armonk, NY: IBM Corp.
- IUPAC. (2006). *Compendium of Chemical Terminology*. In: Gold Book. 2nd ed. IBM Corp. (2013). IBM Statistical Package for the Social Science (SPSS), Statistics for Windows, Version 22.0. Armonk, NY: IBM Corp.
- Jan, R., Sharma, S. & Saxena, D.C. (2013). Pasting and thermal properties of starch extracted from chenopodium album grain. *International Journal of Agriculture and Food Science Technology*, **4(10)**, 981-988.
- Jane, J., Chen, Y. Y., Lee, L. F., McPherson, A. E., Wong, K. S., Radosavljevic, M. & Kasemsuwan, T. (1999). Effects of Amylopectin Branch Chain Length and Amylose Content on the Gelatinization and Pasting Properties of Starch. *Journal of Cereal Chemistry*, **76(5)**, 629-637.
- Jayawardena, N., Watawana, M.I. & Waisundara, V.Y. (2015). The total antioxidant capacity, total phenolics content and starch hydrolase inhibitory activity of fruit juices following pepsin (gastric) and pancreatin (duodenal) digestion. *Journal für Verbraucherschutz und Lebensmittelsicherheit*, **10**, 349-357.
- Joshi, M., Aldred, P., Mcknight, S. & Panozzo, J. (2013). Physicochemical and functional characteristics of lentil starch. *Carbohydrate Polymers*, **92(2)**, 1484-1496.
- Kaur, A., Singh, N., Ezekiel, R. & Guraya, H.S. (2007). Physicochemical, thermal and pasting properties of starches separated from different potato cultivars grown at different

- locations. *Food Chemistry*, **101**, 643-651.
- Kerkhofs, S., Lipkens, H., Velghe, F., Verlooy, P., Martens, J.A. (2011). Mayonnaise production in batch and continuous process exploiting magnetohydrodynamic force. *Journal of Food Engineering*, **106(1)**, 35-39.
- Lai, P., Shiau, C.J. & Wang, C.C. (2012). Effects of oligosaccharides on phase transition temperatures and rheological characteristics of waxy rice starch dispersion. *Journal of Science and Food Agriculture*, **92(7)**, 1389-1394.
- Lin, J.H., Kao, W.T., Tsai, Y.C. & Chang, Y.H. (2013). Effect of granular characteristics on pasting properties of starch blends. *Carbohydrate Polymer*, **98(2)**, 1553-1560.
- Liu, Y., Chen, W., Chen, C. & Zhang, J. (2015). Physicochemical Property of Starch-Soluble Dietary Fiber Conjugates and Their Resistance to Enzymatic Hydrolysis. *International Journal of Food Properties*, **18**, 2457-2471.
- Maphosa, Y. (2016). Characterisation of Bambara groundnut (*Vigna Subterranea* (L) Verdc.) non-starch polysaccharides from wet milling as prebiotics. Master of Technology Thesis, Cape Peninsula University of Technology.
- Maphosa, Y. & Jideani, V.A. (2016). Physicochemical characteristics of Bambara groundnut dietary fibres extracted using wet milling. *South African Journal of Science*, **112**, 1-8.
- Marc, G., Stana, A., Oniga, S.D., Pîrnău, A., Vlase, L. & Oniga, O. (2019). New Phenolic Derivatives of Thiazolidine-2,4-dione with Antioxidant and Antiradical Properties: Synthesis, Characterization, In Vitro Evaluation, and Quantum Studies. *Molecules*, **24** (2060), 1-19.
- Mensah, N.G. (2011). Modification of Bambara groundnuts starch, composited with defatted Bambara groundnut flour for noodle formulation. Kwame Nkrumah University of Science and Technology, Kumasi College of Science. Msc: Food Science and Technology.
- Mora, Y.N., Contreras, J.C., Aguilar, C.N., Meléndez, P., De la Garza, I. & Rodriguez, R. (2013). Chemical composition and functional properties from different sources of dietary fiber. *American Journal of Food and Nutrition*, **1(3)**, 27-33
- Mubaiwa, J., Fogliano, V., Chidewe, C. & Linnemann, A.R. (2018). Bambara groundnut (*Vigna subterranea* (L.) Verdc.) flour: A functional ingredient to favour the use of an unexploited sustainable protein source. *Plos One*, **13(10)**, e0205776.
- Murevanhema, Y.Y. & Jideani, V.A. (2013). Potential of Bambara groundnut (*Vigna subterranea* (L.) Verdc) milk as a probiotic beverage: A review. *Critical Reviews in Food Science and Nutrition*, **53(9)**, 954-967.
- Ndidi, U.S., Ndidi, C.U., Aimola, I.A., Bassa, O.Y., Mankilik, M. & Adamu, Z. (2014). Effects of Processing (Boiling and Roasting) on the Nutritional and Antinutritional Properties of Bambara Groundnuts (*Vigna subterranea* [L.] Verdc.) from Southern Kaduna, Nigeria. *Journal of Food Processing*, **Article ID 472129**, 1-9.
- Novelo-Cen, L. & Betancur-Ancona, D. (2005). Chemical and functional properties of

- Phaseolus lunatus* and *Manihot esculenta* starch blends. *Starch*, **57**, 431-441.
- Ogundele, O.M. (2016). Nutritional and functional properties of soaked and micronized Bambara groundnut seeds and their flours. PhD Thesis. University of Pretoria, South Africa.
- Olayele, A.A., Adeyeye, E.I. & Adesina, A. J. (2013). Chemical composition of bambara groundnut (*V. subterranea* L. Verdc) seed parts. *Bangladesh Journal of Scientific and Industrial Research*, **48(3)**, 167-178.
- Oyeyinka, S.A., Singha, S., Adebola, P. & Amonsou, E. (2016). Physicochemical properties of starches with variable amylose contents extracted from bambara groundnut genotypes. *Carbohydrate polymer*, **133**, 171-178.
- Oyeyinka, S.A. & Oyeyinka, A.T. (2016). A review on isolation, composition, physicochemical properties and modification of Bambara groundnut starch. *Food Hydrocolloid*, **75**, 62-71.
- Park, E.Y., Kim, H.N., Kim, J.Y. & Lim, S.T. (2009). Pasting Properties of Potato Starch and Waxy Maize Starch Mixtures. *Starch*, **61(6)**, 352-357.
- Parr, A.J. & Bolwell, J.P. Phenols in the plant and in man. The potential for possible nutritional enhancement of the diet by modifying the phenols content or profile. *Journal of Science, Food and Agriculture*, **80**, 985-1012.
- Pownall, T.L., Udenigwe, C.C. & Aluko, R.E. (2010). Amino acid composition and antioxidant properties of pea seed (*Pisum sativum* L.) enzymatic protein hydrolysate fractions. *Journal of Agricultural and Food Chemistry*, **58**, 4712-4718.
- Ragaeaa, S. & Abdel-Aal, E.M. (2006). Pasting properties of starch and protein in selected cereals and quality of their food products. *Food Chemistry*, **95(1)**, 9-18.
- Rosell, C.M., Santos, E. & Collar, C. (2009). Physico-chemical properties of commercial fibres from different sources: A comparative approach. *Food Research International*, **42**, 176-184.
- Saha, D. & Bhattacharya, S. (2010). Hydrocolloids as thickening and gelling agents in food: A critical review. *Journal of Food Science and Technology*, **47(6)**, 587-597.
- Salawu, S.O. (2016). Comparative study of the antioxidant activities of methanolic extract and simulated gastrointestinal enzyme digest of Bambara nut (*Vigna subterranea*) FUTA Journal of Research in Sciences, **1**, 107-120.
- Sanzani, S.M., Schena, L. & Ippolito, A. (2014). Effectiveness of phenolic compounds against citrus green mould. *Molecules*, **19(8)**, 12500-12508.
- Singh, N. & Kaur, L. (2004). Morphological, thermal, rheological and retrogradation properties of potato starch fractions varying in granule size. *Journal of the Science of Food and Agriculture*, **84**, 1241-1252.
- Sirivongpaisal, P. (2008). Structure and functional properties of starch and flour from bambara groundnut. *Songklanakarin Journal of Science and Technology*, **30**, 51-56.
- Sharma, A. (2005). Understanding Color Management. In: *Color Management: IPA Bulletin*.

- Pp. 16-21. USA: Thomson Delmar Learning.
- Slavin, J. (2013). Fibre and Prebiotics: Mechanisms and Health Benefits. *Nutrients*, **5**(4), 1417-1435.
- Spizzirri, U.G., Parisi, O.I., Iemma, F., Cirillo, G., Puoci, F., Curcio, M. & Picci, N. (2010). Antioxidant-polysaccharide conjugates for food application by eco-friendly grafting. *Carbohydrate Polymers*, **79**(2), 333-340.
- Tayade, R., Kulkarni, K. P., Jo, H., Song, J. T., & Lee, J. D. (2019). Insight Into the Prospects for the Improvement of Seed Starch in Legume-A Review. *Frontiers in plant science*, **10**, 1213.
- Tomas, M., Latorre, G., Senti, M. & Marrugat, J. (2004). The antioxidant function of high density lipoproteins: A new paradigm in atherosclerosis. *Revista Espanola de Cardiologia*, **57**(6), 557-569.
- Tosh, S.M. & Yada, S. (2010). Dietary fibres in pulse seeds and fractions: Characterisation, functional attributes and applications. *Food Research International*, **43**(2), 450-460.
- Tsimikas, S. (2006). Lipoproteins and oxidation. In: *Antioxidants and Cardiovascular Disease*. 2nd ed. (Edited by M.G. Bourassa & J.C. Tardif). Pp 17. Montreal: Springer.
- Valadez-Vega, C., Delgado-Olivares, L., Morales González, J.A., García, E.A., Ibarra, J.R.V., Moreno, E.R., Gutiérrez, M.S., Martínez, M.T.S., Clara, Z.P. & Ramos, Z.C. (2013). The Role of Natural Antioxidants in Cancer Disease. In: *Oxidative Stress and Chronic Degenerative Diseases - A Role for Antioxidants*. Edited by Jose Antonio Morales-Gonzalez.
- Valentao, P., Fernandes, E. Carvalho, F., Andrade, P.B., Seabra, R.M. & Bastos, M.L. (2002). Studies on the antioxidant activity of *Hypericum androsaemum* infusion: scavenging activity against superoxide radical, hydroxyl radical and hypochlorous acid. *Biological and Pharmaceutical Bulletin*, **25**, 1324-1327.
- Wang, N. & Toews, R. (2011). Certain physicochemical and functional properties of fibre fractions from pulses. *Food Research International*, **44**(8), 2515-2523.
- Wu, Y., Xu, H., Lin, Q., Wu, W. & Liu, Y. (2015). Pasting, Thermal and Rheological Properties of Rice Starch in Aqueous Solutions with Different Catechins. *Journal of Food Processing and Preservation*, **39** (6), 2074-2080.
- Yadav, M.P., Johnston, D.B., Hotchkiss, A.T. & Hicks, K.B. (2007). Corn fibre gum: A potential gum arabic replacer for beverage flavor emulsification. *Food Hydrocolloids*, **21**(7), 1022-1030.
- Yao, D.N., Kouassi, K.N., Erda, D., Scazzina, F., Pellegrini, N. & Casiraghi, M.C. (2015). Nutritive Evaluation of the Bambara Groundnut Ci12 Landrace [*Vigna subterranea* (L.) Verdc. (Fabaceae)] Produced in Côte d'Ivoire. *International Journal of Molecular Sciences*, **(16)**, 21428-21441.
- Zayas J.F. (1997) Emulsifying properties of Proteins. In: *Functionality of Proteins in Food*.

Springer, Berlin, Heidelberg.

- Zhang, J., Gao, Y., Qian, S., Liu, X. & Zu, H. (2011). Physicochemical and pharmacokinetic characterization of a spray-dried malotilate emulsion. *International Journal of Pharmaceutics*, **414**(1-2), 186-192.
- Zhu, F. (2015). Interactions between starch and phenolic compound. *Trends in Food Science and Technology*, **43**(2), 129-143.

CHAPTER FIVE

RHEOLOGICAL AND STABILITY PROPERTIES OF BAMBARA GROUNDNUT STARCH-SOLUBLE DIETARY FIBRE NANOCOMPOSITE STABILISED EMULSIONS

Abstract

Emulsions are expected to be stable for reasonable periods under varying stresses. As such, stabilisers such as biopolymers and hydrocolloids are often included in emulsion formulations. The effect of Bambara groundnut starch-soluble dietary fibre nanocomposite (STASOL), orange oil and water on the rheological and stability properties of orange-oil beverage emulsion systems was assessed. A randomised D-optimal exchange mixture design was used to determine the ratio of STASOL, orange oil and water required in the formulation of a stable emulsion. The time-dependent and independent rheological properties of STASOL stabilised emulsions were evaluated using a hybrid rheometer and described using rheological models. Emulsion stability was measured using the Turbiscan stability index (TSI) as well as the optical characterisation method which gives information on initial stability after homogenisation. The mean initial backscattering (BS_{AVO}) along the length of the Turbiscan tube obtained from backscattering profiles of STASOL stabilised emulsions ranged from 50.73 for Formulation 8 (14:30:56 STASOL:oil:water) to 70.47% for Formulation 11 (20:30:50 STASOL:oil:water). The TSI of the emulsions ranged from 0.0005 to 0.1000 for formulation 11 (20:30:50 STASOL:oil:water) and formulation 5 (8:42:50 STASOL:oil:water), respectively. High TSI values indicate a high probability of phase separation. Orange oil and water showed synergy, with an increase in both resulting in an increase in TSI. The hysteresis loop area (HLA) of STASOL stabilised emulsions ranged from 2.04 Pas^{-1} [Formulation 10 (12:34:54 STASOL:oil:water)] to 43.09 Pas^{-1} [Formulation 2 (20:30:50 STASOL:oil:water)]. Orange oil and water showed synergy, with an increase in both resulting in an increase in the HLA of STASOL stabilised emulsions, while both orange oil and water were antagonistic to STASOL. The time-dependent rheological experimental data was fitted to Weltman and first-order stress decay with a zero equilibrium stress value. The first-order stress decay with a zero equilibrium stress value and Herschel-Bulkley models were the best predictors of time-dependent and time-independent rheological flow behaviour. The most stable emulsion system was characterised by the highest STASOL (20%), lowest orange oil (30%) and lowest water (50%) concentrations. It was characterised by the highest BS_{AVO} percentage (70.47%) and lowest TSI (0.0005) indicating high initial stability after homogenisation and a low probability of phase separation, respectively. All emulsions were non-Newtonian, time-dependent, thixotropic, shear-thinning and possessed yield stress. It was concluded that an increase in STASOL concentration coupled with a decrease in oil concentration results in a stable emulsion.

5.1 Introduction

Emulsions are metastable colloidal systems, consisting of at least two immiscible liquids, one of which is dispersed in another, stabilised by an emulsifying agent (Given, 2009; Trujillo-Cayado *et al.*, 2016; Maphosa *et al.*, 2017). Emulsions are made up of aqueous and oil phases, with the former consisting of water and hydrocolloids and the latter consisting of substances such as citrus oil, weighting agent, brominated vegetable oil, sucrose acetate iso-butyrate and bees-wax (McClements *et al.*, 2012; Ushikubo & Cunha, 2014). Emulsions meant for human consumption must be safe, relatively stable as well as have acceptable consistency and mouth feel (Sun *et al.*, 2011; Kakran & Antipina, 2014; Galus & Kadzińska, 2015). To meet these requirements, the formulator needs to consider factors such as droplet size and droplet distribution as well as choice of stabilisers or emulsifiers (Tadros, 2004; María *et al.*, 2015).

An emulsion is expected to be stable for reasonable periods of time (up to 6 months for beverage emulsions) under varying stresses (Buffo *et al.*, 2001; Mirhosseini *et al.*, 2008b; Piorkowski & McClements, 2013; Rezvani *et al.*, 2014). It should be stable against temperature and pH fluctuations, exposure to light, oxygen, microorganisms and mechanical forces (stirring, pumping, filling), ingredient interactions as well as vibrations due to transport, handling and distribution (Tadros, 2004; McClements *et al.*, 2007; Adeyi *et al.*, 2014). The stability of food emulsions is very important as destabilisation affects the product's appearance, which hugely affects consumer acceptance.

Emulsions are thermodynamically unstable due to the increase in interfacial area following emulsification (Rezvani *et al.*, 2012; Maphosa *et al.*, 2017). They destabilise due to various physicochemical phenomena such as (1) gravitational separation [creaming or sedimentation], (2) flocculation, (3) droplet growth [Ostwald ripening], (4) coalescence, (5) phase inversion and (6) lipid oxidation (Lorenzo *et al.*, 2008; Taherian *et al.*, 2008; Given, 2009; Trujillo-Cayado *et al.*, 2016). The kinetic stability of emulsions can be obtained by increasing their activation energy. This can be achieved by incorporating stabilisers such as thickeners, weighting agents, ripening inhibitors, texture modifiers and emulsifiers, in the formulation (Chanamai & McClements, 2000; Prestidge & Simovic, 2006; Hasenhuettl, 2008; Dickinson, 2009; Cottrell & Van Peij, 2014; Chen, 2015; Gruner *et al.*, 2015; Ritzoulis & Karayannakidis, 2015).

Apart from stability; rheology, physicochemical, functional and sensory characteristics are integral properties of emulsions (Dickinson, 2001; Lee, 2006; Tadros, 2013; Alam *et al.*, 2014). Rheology plays a major role in technical production processes such as mixing, extrusion, pumping and filling and in long term emulsion stabilisation (Maphosa *et al.*, 2017). It is influenced by particle-particle interaction, nature of particles, particle size and distribution, nature of stabiliser and nature of continuous phase (Lorenzo *et al.*, 2008). Rheological characteristics such as steady shear, stress, strain and oscillatory studies

provide insight into the consistency and physical stability of an emulsion and allow for the prediction of its behaviour over varying deformations and external conditions (Aggarwal & Sarkar, 2008; Oliveira & Cunha, 2015).

Recent trends have seen polymers being increasingly used as stabilisers (Trujillo-Cayado *et al.*, 2016). Polysaccharides are preferred for their biocompatibility, biodegradability, non-toxicity, nutritional properties, edibility and low cost (Liu *et al.*, 2015; Yin *et al.*, 2015). They increase creaming stability (Fernandez *et al.*, 2004; Chern, 2006) by increasing the viscosity of the aqueous phase in the low stress range and imparting elastic properties to the entire system (McClements, 1999). Furthermore, amphiphilic polysaccharides, such as some modified starches, adsorb to oil droplets during the homogenisation process and thereby stabilise droplets against aggregation. The non-polar side of amylopectin binds to the oil phase while the polar chains bind to the surrounding aqueous phase, protecting the droplets against flocculation and coalescence (McClements, 2005; Mirhosseini *et al.*, 2008a; Lim *et al.*, 2011; Yin *et al.*, 2015). The effectiveness of a polysaccharide as an emulsion stabiliser is dependent on its concentration in the system, structural features of the polysaccharide-aqueous phase system, as well as the shape and size of molecules (Trujillo-Cayado *et al.*, 2016).

With the increase in demand for healthy and natural foods by consumers, research has shifted towards the application of natural nanocomposites as ingredients in various food systems. Nanocomposites are important in food processing as anticaking agents, nutritional additives, texture improvers and nanocarriers to protect aroma and flavour (Singh *et al.*, 2017). Nanocomposites have improved solubility, high stability at high temperature and pressures, extended shelf life and can deliver food components to food systems (Singh *et al.*, 2017). In emulsions, they would be expected to stabilise systems at lower concentrations than polysaccharides. STASOL studied in this chapter was formed and characterised in chapters 3 and 4. However, nothing is known about its performance in beverage emulsions. As such, the objective of this chapter was to assess the effect of STASOL on the rheological and stability properties of orange-oil beverage emulsion systems composed of different concentrations of STASOL, orange oil and water, with a view to identify the best combination for a stable emulsion.

5.2 Materials and Methods

The outline of chapter 5 is illustrated in Figure 5.1. The STASOL used in this study was obtained according to the method described in chapter 3 [Section 3.2.4]. Cold-pressed orange oil (Puris Natural Aroma Chemicals, South Africa), commercial grade citric acid, potassium sorbate and sodium benzoate (Sigma-Aldrich, Johannesburg, South Africa) were used in emulsion preparation.

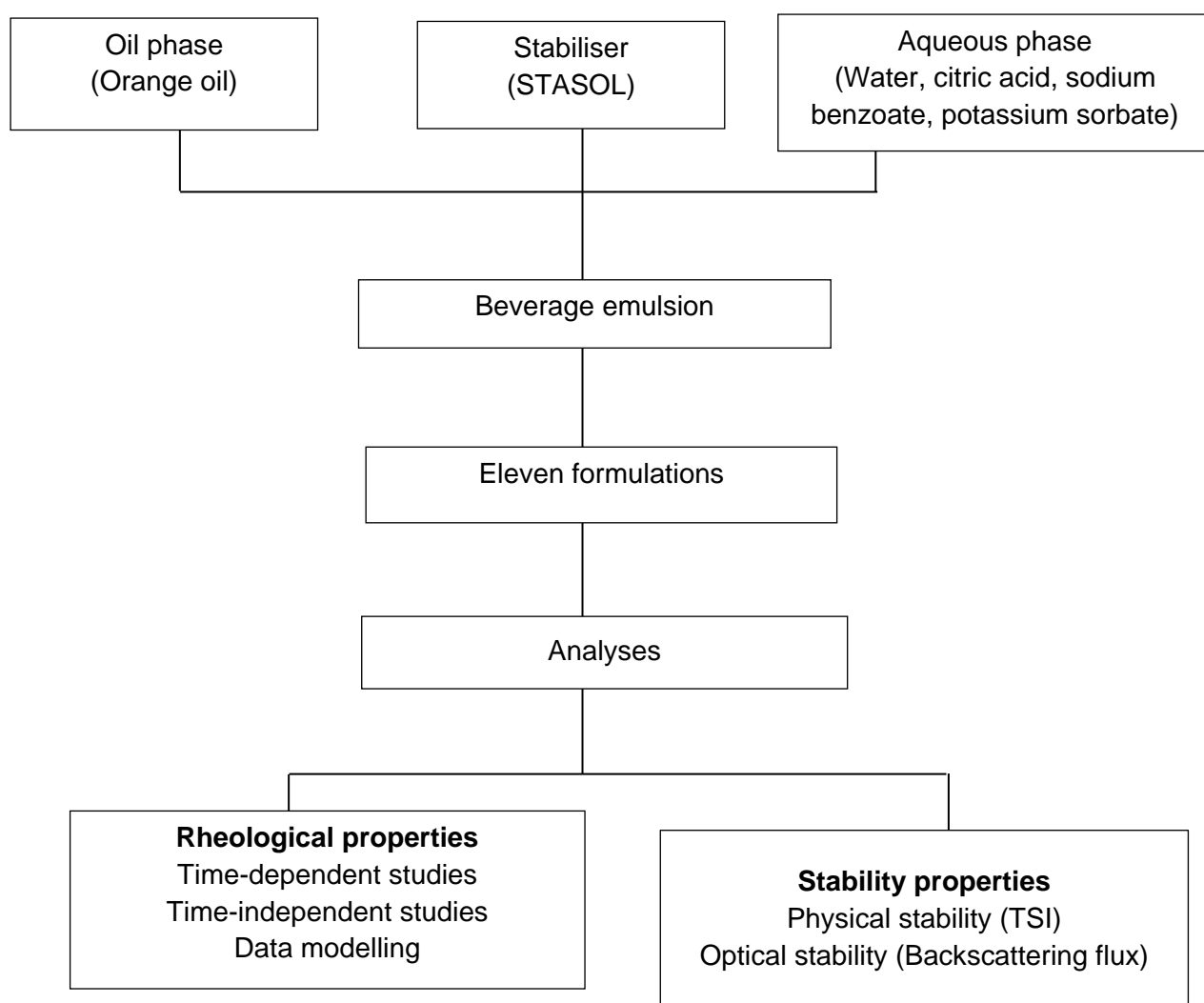


Figure 5.1 Outline of Chapter 5.

STASOL: Bambara groundnut starch-soluble dietary fibre nanocomposite;

TSI: Turbiscan index stability.

Equipment from the Departments of Food Science and Technology and Chemical Engineering of the Cape Peninsula University of Technology were used.

5.2.1 Effects of emulsion components and concentrations on emulsion stability

A randomised D-optimal point exchange mixture design was used to determine the amount of the independent variables; STASOL, orange oil and water, required in the formulation of a stable emulsion. The design consists of six models, three lack of fit and two replicate points. The design space consists of four vertex, four centre edge, two axial CB and one centre. Eleven emulsion formulations were prepared, and the experimental design is presented in Table 5.1.

Table 5.1 Randomised D-optimal point exchange mixture design for STASOL* stabilised emulsion

Formulation	STASOL (%)	Orange oil (%)	Water (%)
1	8	42	50
2	20	30	50
3	8	36	56
4	10	38	62
5	8	42	50
6	8	30	62
7	10	32	58
8	14	30	56
9	14	36	50
10	12	34	54
11	20	30	50

*STASOL: Bambara groundnut starch-soluble dietary fibre nanocomposite.

Empirical models were developed as a function of emulsion components and used in estimating the optimal STASOL, orange oil and water combination for a stable emulsion using Design-Expert 9 version 9. The empirical models used were the quadratic mixture model for describing the effect of emulsion components on the hysteresis loop area and apparent viscosity of STASOL stabilised emulsions. The reduced special quartic mixture model was used to explain the effect on backscattering and the linear mixture model was used to describe the effect on turbiscan stability index. Data was described in real, actual and L pseudo components.

5.2.2 Preparation of beverage emulsions

The method of Maphosa *et al.* (2017) was adopted in the preparation of beverage emulsions. Emulsion components: 0.4% citric acid, 0.1% sodium benzoate and 0.1% potassium sorbate were combined with the appropriate amounts of STASOL, orange oil and water as indicated in Table 5.1. Citric acid, sodium benzoate, potassium sorbate and deionised water were blended for 2 min at low speed (Waring blender) then STASOL was slowly added to the mixture to avoid lumping and blended for another 2 min at high speed. Orange oil was added to the mixture and further blended at high speed for 2 min. The resultant mixture was homogenised at 12000 rpm (Ultra Turrax homogeniser, IKA T25 digital, Janke and Kunkel, Staufen, Germany) for 5 min. The stability and rheological properties of emulsions were analysed immediately after homogenisation.

5.2.3 Emulsion stability evaluation

Emulsion stability was measured using the optical characterisation method which measures backscattering flux using the Turbiscan (Roland *et al.*, 2003) as well as the physical stability method of Perez-Mosqueda *et al.* (2015) which measures TSI. The Turbiscan analysis (Turbiscan MA 2000, Formulaction, Toulouse, France) was carried out to measure the stability of emulsions according to the method of Adeyi *et al.* (2014). Each emulsion (7 mL) was transferred into a Turbiscan tube (65 mm length) and scanned along its height for 60 min at 10 min intervals. The curves generated were used to provide the backscattering (BS) and transmission flux percentages relative to the instrument's internal standard as a function of sample height. Each scan provided a curve and all curves were laid on a single graph. The stability or instability of the emulsions was determined by carrying out multiple scans.

The physical stability of emulsions was described using the TSI calculated from Turbiscan analysis data. The TSI is a relative number calculated from the differences in the rate of backscattering or transmission intensity of the sample compared to the original (Luo *et al.*, 2017). It is negatively related to emulsion stability, therefore high values indicate unstable systems (Liu *et al.*, 2015). The TSI was used to quantify destabilisation processes in the emulsions and was calculated according to equation 5.1.

$$TSI = \sqrt{\frac{\sum_{i=1}^n (x_i - x_{BS})^2}{n - 1}} \quad \text{Equation 5.1}$$

Where: TSI = Turbiscan stability index; \sum = sum of all the scan differences from the bottom to the top of the Turbiscan tube; x_i = average value of the scattered light intensity at each time; x_{BS} = average of x_i ; n = number of scans.

5.2.4 Rheological measurements of emulsions

The rheological properties of the emulsions were evaluated using an MCR 300 Paar physical rheometer (Discovery HR-1) at 20°C. The methods of Adeyi *et al.* (2014) were adopted and applied in the evaluation of the time-dependent and time-independent properties of the emulsions.

1. Time-dependent rheological measurements

Time-dependent rheological experiments of the emulsions were conducted without previous shearing. Emulsions (25 mL) were carefully transferred into the rheometer cup and left to stand for 5 min. The emulsions were then subjected to increasing shear rates from 0.01 to 1000 s⁻¹ followed by a decreasing shear rate from 1000 to 0.01 s⁻¹, thus giving information on the change in viscosity as a function of time. The experimental data (shear stress-shear rate) of forward and backward curves were fitted to the time-dependent flow behaviour models; first-order stress decay with a zero equilibrium stress value (Equation 5.2) and Weltman model (Equation 5.3). The two models were compared using their root mean squared error (RMSE), standard error (SE) and coefficient of determination (R²) to determine the most suitable model for describing the time-dependent rheological data of the emulsions.

$$\tau = \tau_o e^{-kt} \quad \text{Equation 5.2}$$

$$\tau = A + B \ln(t) \quad \text{Equation 5.3}$$

Where: τ = shear stress; t = shearing time; τ_o = initial shear stress value; k = breakdown rate constant. A and B = constants representing the initial shear stress and the time coefficient of thixotropic breakdown, respectively. A negative B value indicates the rate at which shear stress decreases from the initial value to the final equilibrium (Koocheki *et al.*, 2009; Adeyi, 2014).

The hysteresis loop area experiment was carried out in two-fold. The first part involved calculating the hysteresis loop area (Equation 5.4) as the area between the upstream and downstream data (Koocheki *et al.*, 2009). The second part involved shearing STASOL stabilised emulsions for 20 min, at 20°C and constant shear rates of 50, 100 and 150 s⁻¹. Thereafter, the viscosity of the emulsions was measured as a function of shearing time.

$$\int_{\gamma_1}^{\gamma_2} K \gamma^n - \int_{\gamma_1}^{\gamma_2} K' \gamma^{n'} \quad \text{Equation 5.4}$$

Where: K and K' = consistency coefficients and n and n' = flow behaviour indices for upward and downward measurements, respectively.

2. Time-independent rheological measurements

The viscosity of STASOL stabilised emulsions against changes in shear rate was evaluated following the method of Sahin & Sumnu (2006). Emulsions (25 mL) were transferred into the rheometer cup and left to stand for 5 min. Steady-state shear experiments were then conducted by measuring emulsion viscosity over a shear rate range of 0.01-500 s⁻¹ for 300 s. Experimental flow data were fitted to the Power law rheological model (Maphosa *et al.*, 2017) (Equation 5.5), Herschel-Bulkley model (Khalil & Mohamed, 2012) (Equation 5.6), Bingham plastic model (Zengeni, 2016) (Equation 5.7) and Casson model (Siddiqui *et al.*, 2015) (Equation 5.8).

$$\tau = K \gamma^n \quad \text{Equation 5.5}$$

$$\tau = \tau_o + K \dot{\gamma}^n \quad \text{Equation 5.6}$$

$$\tau = \tau_{y\beta} + K_\beta \gamma \quad \text{Equation 5.7}$$

$$\tau^{1/2} = \tau_o^{1/2} + (K \gamma)^{1/2} \quad \text{Equation 5.8}$$

Where: n = flow behaviour index which indicates the tendency of a fluid to shear-thinning; K = consistency coefficient; γ = shear rate; τ = shear stress; τ_o = yield stress; $\tau_{y\beta}$ = Bingham yield stress; K_β = Bingham plastic viscosity; μ = the viscosity coefficient.

5.2.5 Modelling the effect of STASOL, orange oil and water on emulsion stability and rheology

Stability and rheological data obtained from the randomised D-optimal point exchange mixture design (Table 5.1) was used to establish the relationship between emulsion properties (rheological and stability characteristics) and main emulsion components (STASOL, orange oil and water). The variance for each parameter was represented using a quadratic mixture model equation (Equation 5.9). The statistical significance of each parameter was determined using analysis of variance (ANOVA).

$$Y = \beta_1 X_1 + \beta_2 X_2 + \beta_3 X_3 + \beta_{12} X_1 X_2 + \beta_{13} X_1 X_3 + \beta_{23} X_2 X_3 \quad \text{Equation 5.9}$$

Where: Y = estimated parameters response; β = equation coefficients; X_1 , X_2 and X_3 = emulsion components (STASOL, orange oil and water, respectively). X_1X_2 = interaction between STASOL and orange oil, X_1X_3 = interaction between STASOL and water and X_2X_3 = interaction between orange oil and water.

The goodness-of-fit of the models was assessed using the coefficient of determination (R^2) (Equation 5.10), root mean squared error (RMSE) (Equation 5.11) and standard error (SE) (Equation 5.12). Other mixture response surface parameters described were adjusted R^2 (adj R^2), coefficient of variation (CV) and degrees of freedom (DF).

$$R^2 = 1 - \frac{SSE}{SST} \quad \text{Equation 5.10}$$

$$RMSE = \left[\frac{\sum (Y_m - Y_c)^2}{n} \right]^{1/2} \quad \text{Equation 5.11}$$

$$SE = \left[\frac{\sum (Y_m - Y_c)^2}{n-1} \right]^{1/2} \quad \text{Equation 5.12}$$

Where: SSE = sum of squares; SST = total corrected sum of squares; Y_m = measured value; Y_c = calculated value for each data point; n = number of observations.

The coefficient of determination (R^2) is a relative measure of goodness of fit between experimental data and predicted model data. It ranges from 0 to 1, with 0 indicating poor prediction and 1 indicating perfect prediction. High R^2 and adequate precision are an indication that the model can be accurately employed for predicting the intrinsic rheological emulsion properties as a function of water, orange oil and STASOL (Gomez-Romero *et al.*, 2014). The root mean squared error (RMSE) is the square root of the variance of the residuals. It suggests goodness of fit or how well the model predicts actual values of a model to data. Lower values of RMSE, closer to zero, indicate better fit. The sum of squared errors (SSE) is a measure of the amount of variance in a data set that is not explained by a regression model. It provides information on how far from each point the best-fitting regression line is. Lower SSE values, closer to zero, indicate a tight fit of the model to the data.

5.2.6 Data analysis

All experiments were carried out in duplicate. Data was expressed as mean \pm standard deviation. The results were subjected to multivariate analysis of variance (MANOVA) to determine mean differences between treatments. Duncan's multiple range tests were conducted to separate means where significant differences existed (IBM SPSS version 23,

2016). Rheological models were used to describe rheological data to predict the behaviour of STASOL stabilised emulsions, using the MatLab (2017) software.

5.3 Results and Discussion

5.3.1 Effect of Bambara groundnut starch-soluble dietary fibre nanocomposite, orange oil and water on initial backscattering of STASOL stabilised emulsions

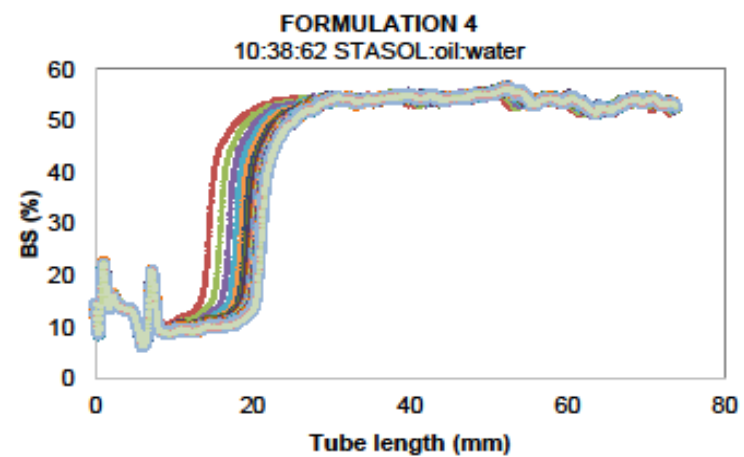
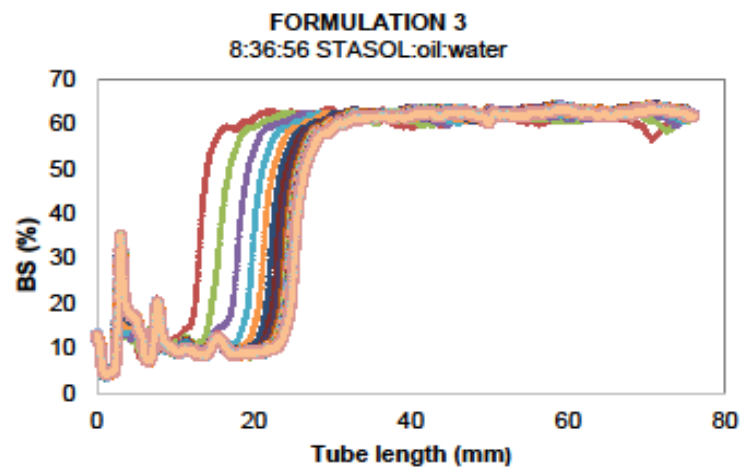
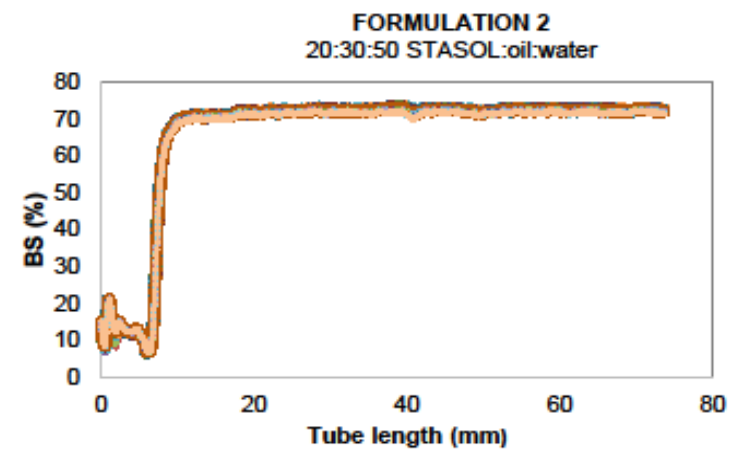
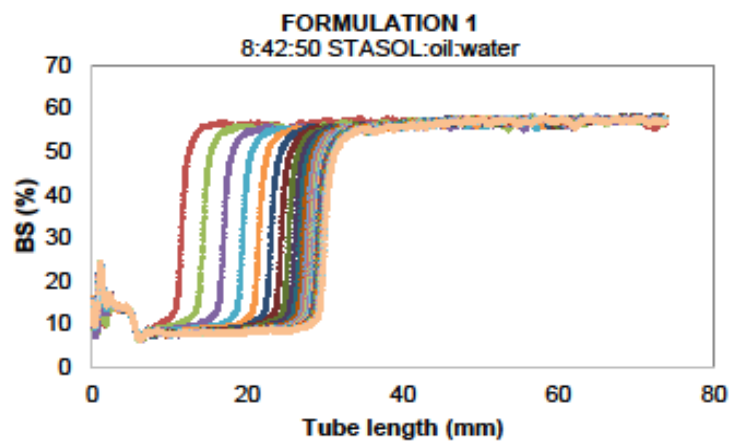
Emulsion stability refers to the ability of an emulsion to maintain its properties over some time (Eltayeb *et al.*, 2011; Mubaiwa *et al.*, 2018). The initial backscattering (BS_{AVO}) and transmission curves generated during scanning provided data on the BS_{AVO} and transmission flux relative to the Turbiscan's internal standard as a function of the height of the sample in the tube. The mean emulsion BS_{AVO} values along the length of the Turbiscan tube obtained from backscattering profiles were in the range 50.73% [14:30:56 (STASOL:oil:water)] to 70.47% [20:30:50 (STASOL:oil:water)] (Table 5.2).

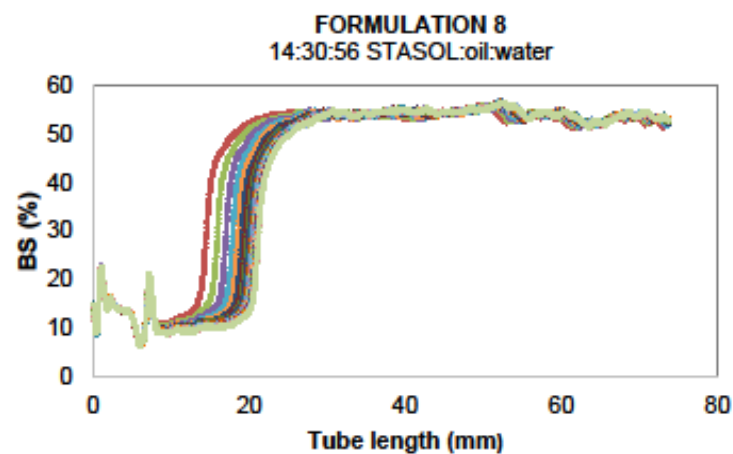
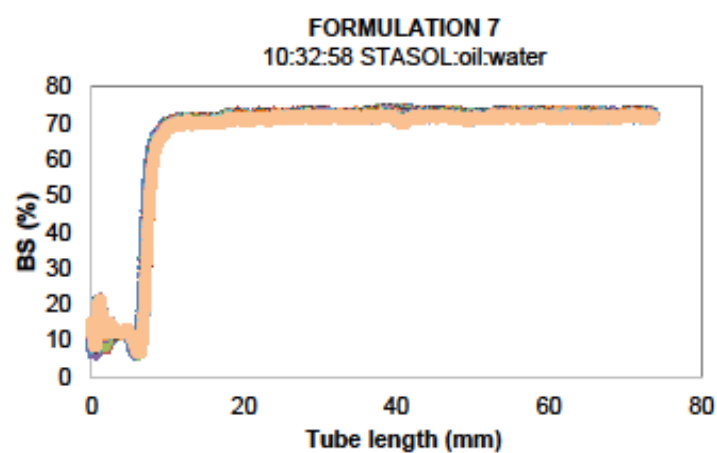
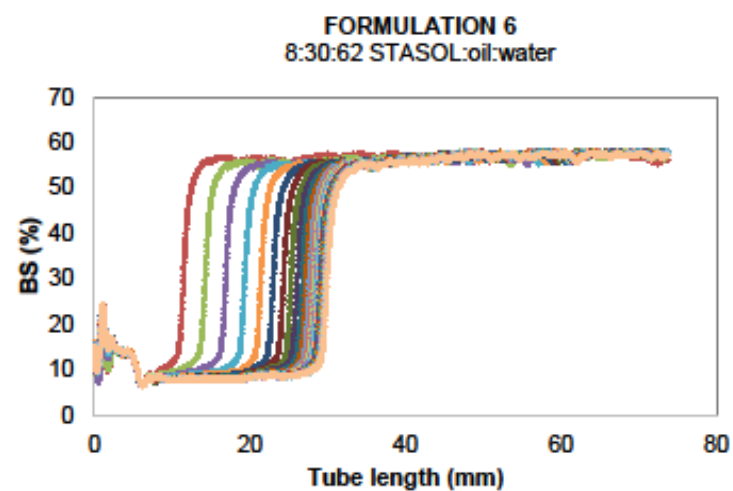
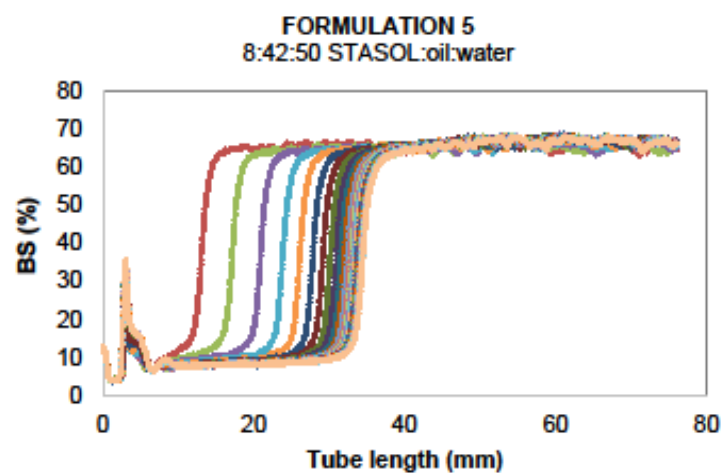
Table 5.2 Effect of STASOL, orange oil and water fractions on initial backscattering of STASOL stabilised emulsions*

Formulation	STASOL (%)	Orange oil (%)	Water (%)	Initial backscattering [BS_{AVO}] (%)
1	8	42	50	66.39 ± 1.51^{ab}
2	20	30	50	70.17 ± 4.18^a
3	8	36	56	59.12 ± 3.25^c
4	10	38	62	51.31 ± 5.35^d
5	8	42	50	63.57 ± 2.23^{bc}
6	8	30	62	55.62 ± 3.21^d
7	10	32	58	69.11 ± 1.29^a
8	14	30	56	50.73 ± 1.36^d
9	14	36	50	68.90 ± 1.42^{ac}
10	12	34	54	58.36 ± 0.49^c
11	20	30	50	70.47 ± 1.27^a

*STASOL: Bambara groundnut starch-soluble dietary fibre nanocomposite; BS_{AVO} : Initial backscattering. Values are mean \pm standard deviation. Means within a column followed by different superscripts are significantly ($p \leq 0.05$) different.

Figure 5.2 shows the backscattering profiles of STASOL stabilised emulsions. The Y-axis represents the intensity of scattered light (%) and the X-axis represents the height of the sample in the tube (Adeyi, 2014). Initial backscattering describes the stability of an emulsion immediately after homogenisation (Adeyi, 2014). Hence the retardation of droplet movement within the emulsion system and the resultant high stability of emulsions formulated with high STASOL and low water concentrations was justified.





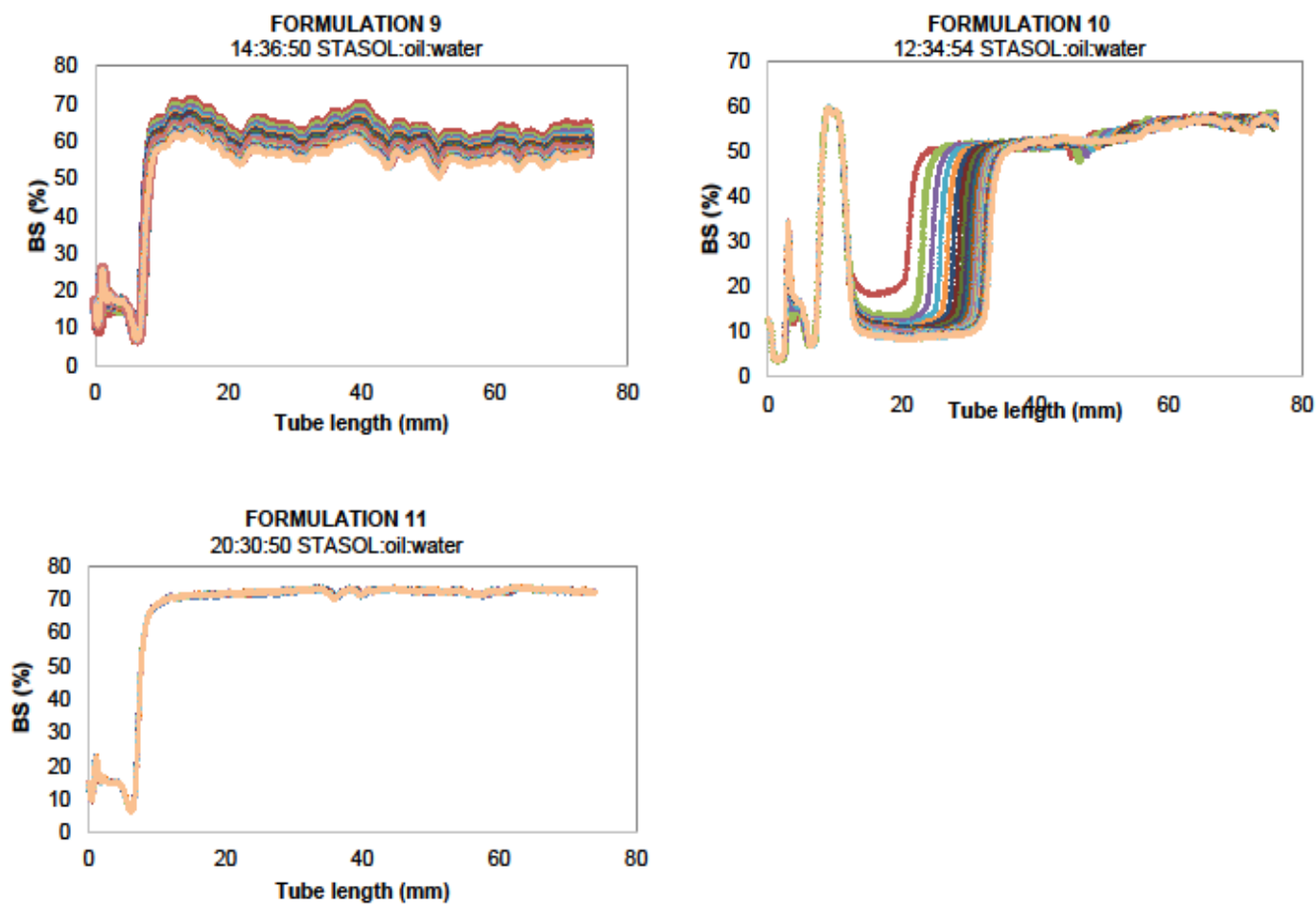


Figure 5.2 Backscattering profiles of STASOL stabilised emulsions.

STASOL: Bambara groundnut starch-soluble dietary fibre nanocomposite.

The formulation with the highest BS_{AVO} value was composed of 20:30:50 STASOL:oil:water, suggesting higher stability of the emulsion immediately after production. The BS_{AVO} values represented the initial scan of an emulsion immediately after production (Palazolo, 2006). Turbiscan analysis gives insight into the destabilisation behaviour of an emulsion and aids in the prediction of its shelf life (Blijdenstein *et al.*, 2004). As observed in Figure 5.2, the Turbiscan profiles of all emulsions followed a similar path as the curve of the initial scan. However, the scans did not overlay perfectly showing a decrease in backscattering flux along the length of the tube with increasing time. This behaviour was observed in all emulsions and it was suggestive of particle aggregation, due to either flocculation or coalescence (Adeyi, 2014). This was in fair agreement with Maphosa (2016) who reported flocculation as the main destabilisation phenomenon in STASOL stabilised orange oil emulsions.

The emulsion formulated with the highest amount of STASOL (20%) and the lowest amount of orange oil (30%) had the highest BS_{AVO}. This could be attributed to the formation of a droplet network and the retardation of droplet movement by STASOL molecules (Nikovska, 2010). Therefore, it is deduced that the availability of more STASOL molecules in the emulsion resulted in the formation of a more viscous system which impeded the movement and subsequent coalescing and/or aggregation of oil droplets. Coalescence is the process where droplets come into contact, merge and create larger droplets, consequently reducing the stability of the emulsion (Adeyi, 2014). The ANOVA developed for backscattering as a function of STASOL, water and orange oil for the reduced special quartic mixture model is presented in Table 5.3.

The employed model was significant ($p < 0.0001$) with a high R^2 (0.8969), low coefficient of variation (4.4%), adequate precision (12.224) and an insignificant (0.0894) lack of fit. A reduced special quartic mixture model was used because there were many insignificant model terms hence reduction was necessary to improve the model. The F-value of the lack of fit (3.42) showed an 8.94% chance of the model not being a suitable fit. Adequate precision measures the signal to noise ratio and a ratio greater than 4 is desirable. The adequate precision (12.22) indicated an adequate signal, therefore accepting the applied model in navigating the design space. The linear coefficients in terms of components for backscattering were expressed as:

$$\text{Backscattering} = 71.51X_1 + 64.62X_2 + 55.86X_3 - 0.50X_1X_2 - 8.30X_2X_3 - 1673.87X_1^2X_2X_3 + 1704.63X_1X_2X_3^2$$

Where: X_1 , X_2 and X_3 = STASOL, orange oil and water, respectively.

Table 5.3 ANOVA for reduced special quartic mixture model for backscattering*

Source	DF	Sum of square	Mean square	F value	p-value
Model	7	858.40	122.63	16.16	< 0.0001
Linear mixture	2	311.23	155.61	20.50	< 0.0001
AB	1	0.026	0.026	0.0034	0.9545
AC	1	237.70	237.70	31.32	< 0.0001
BC	1	6.62	6.62	0.87	0.3674
A ² BC	1	217.10	217.10	28.61	0.0001
ABC ²	1	372.09	372.09	49.03	< 0.0001
Residual	13	98.66	7.59		
Pure error	12	76.80	6.40		
Lack of fit	1	21.86	21.86	3.42	0.0894
Total	20	957.06			
R ²	0.8969				
Adj R ²	0.8414				
CV (%)	4.40				
Adequate	12.224				
Precision					

*ANOVA: Analysis of variance; A: STASOL; B: Orange oil; C: Water; R²: coefficient of determination; Adjusted R²: Adjusted coefficient of determination; CV: Coefficient of variation; DF: Degrees of freedom; STASOL: Bambara groundnut starch-soluble dietary fibre nanocomposite.

The mixture response surface and the corresponding trace graph (piepel) for the individual and simultaneous increase of STASOL, orange oil and water on the backscattering behaviour of STASOL stabilised emulsions are shown in Figure 5.3. An increase in orange oil concentration resulted in an increase in backscattering. Water and STASOL had an antagonistic effect on each other as shown by the opposing parabolic curves in Figure 5.3.

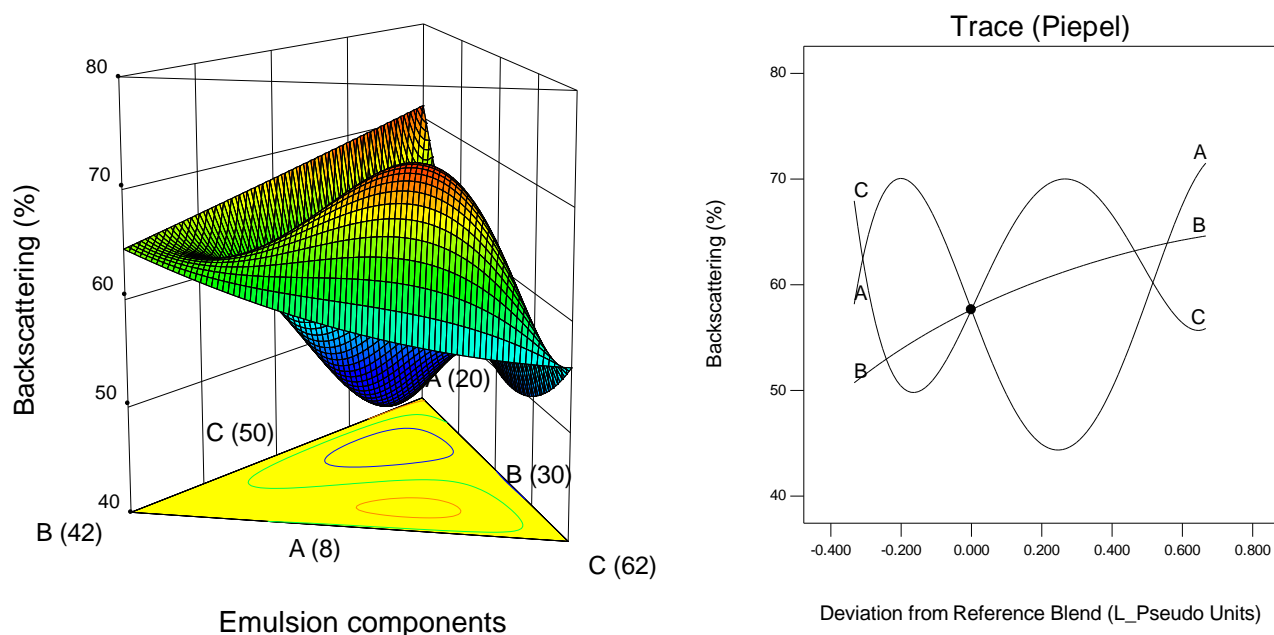


Figure 5.3 Mixture response surface (left) and Piepel graph (right) for the effect of (A) Bambara groundnut starch-soluble dietary fibre nanocomposite (STASOL), (B) orange oil and (C) water concentrations on the backscattering of STASOL stabilised emulsions.

5.3.2 Effect of emulsion components on Turbiscan stability index

The TSI is the sum of all destabilisation processes within a dispersion in the Turbiscan tube (Perez-Mosqueda *et al.*, 2015). Lower TSI values indicate the presence of smaller particle-sized droplets, thus indicating a low probability of phase separation (Perez-Mosqueda *et al.*, 2015). Table 5.4 shows the effect of varying STASOL, orange oil and water concentrations on the TSI of STASOL stabilised emulsions. The TSI ranged from 0.0005 [Formulation 11 (20:30:50 STASOL:oil:water)] to 0.1 for [Formulation 5 (8:42:50 STASOL:oil:water)]. The TSI of emulsions formulated with the highest STASOL and lowest orange oil concentrations were relatively low indicating high emulsion stability.

Table 5.4 Effect of STASOL*, water and orange oil fractions on Turbiscan stability index of STASOL stabilised emulsions

Formulation	STASOL (%)	Orange oil (%)	Water (%)	TSI
1	8	42	50	0.0943
2	20	30	50	0.0030
3	8	36	56	0.0243
4	10	38	62	0.0136
5	8	42	50	0.1000
6	8	30	62	0.0402
7	10	32	58	0.0030
8	14	30	56	0.0136
9	14	36	50	0.0207
10	12	34	54	0.0245
11	20	30	50	0.0005

*STASOL: Bambara groundnut starch-soluble dietary fibre nanocomposite. TSI: Turbiscan stability index.

This was in agreement with Zalewska *et al.* (2019) who reported a significant decrease in TSI when emulsifier concentration was increased from 5 to 15% in a plant-based dispersion. As such, it was deduced that an increase in emulsifier or stabiliser concentration in an emulsion decreases the TSI, thereby increasing stability. Higher TSI of <0.5 were reported for succinylated monoglyceride stabilised casein-maltodextrin-soybean oil compound emulsions (Liu *et al.*, 2015).

The linear coefficients in terms of actual components for TSI were expressed as natural logarithm (Ln) as:

$$\text{Ln TSI} = -0.33730 X_1 + 0.0423 X_2 - 0.0245 X_3$$

Where: X_1 , X_2 and X_3 = STASOL, orange oil and water, respectively.

The linear mixture model for TSI is presented in Table 5.5. The model was significant ($p < 0.025$) with a low R^2 value (0.6022), high coefficient of variation (38.09%), desirable adequate precision (5.878) and an insignificant lack of fit ($F = 1.21$). The low R^2 (0.5028) indicated a high lack of fit of the model to the data. Furthermore, the predicted R^2 value (0.0246) and the adjusted R^2 value (0.5028) had a difference greater than 0.2 indicating the presence of a large block effect, demonstrating that a reduction of the model would have given better results.

Table 5.5 ANOVA* for linear mixture model for Turbiscan stability index

Source	DF	Sum of square	Mean square	F value	p-value
Model	2	26.66	13.33	6.06	0.0250
Linear mixture	2	26.66	13.33	6.06	0.0250
Residual	8	17.61	2.20		
Lack of itf	6	14.42	2.40	1.51	0.4513
Pure error	2	3.19	1.60		
Total	10	44.28			
R^2	0.6022				
Adj R^2	0.5028				
Predicted R^2	0.0246				
CV (%)	38.09				
Adequate Precision	5.878				

*ANOVA: Analysis of variance. A: STASOL. B: Orange oil. C: Water. R^2 : Coefficient of determination. Adj R^2 : Adjusted coefficient of determination. CV: Coefficient of variation. DF: Degrees of freedom. STASOL: Bambara groundnut starch-soluble dietary fibre nanocomposite.

The mixture response surface and the corresponding trace graph (piepel) for the individual and simultaneous increase of STASOL, orange oil and water concentrations on the TSI of STASOL stabilised emulsions are presented in Figure 5.4.

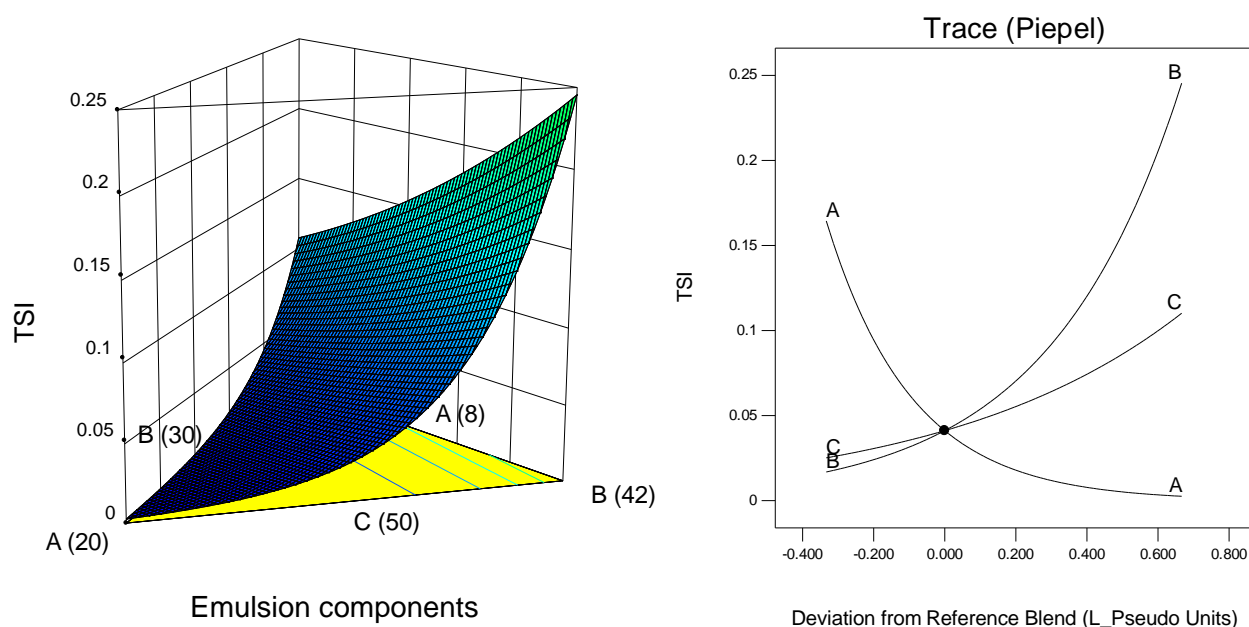


Figure 5.4 Mixture response surface (left) and Piepel graph (right) for the effect of (A) Bambara groundnut starch-soluble dietary fibre nanocomposite (STASOL), (B) orange oil and (C) water concentrations on the Turbiscan stability index (TSI) of STASOL stabilised emulsions.

Orange oil and water showed synergy, with an increase in both resulting in an increase in TSI. High TSI values indicate a high probability of instability in emulsions. Both orange oil and water showed antagonism to STASOL meaning a decrease in STASOL concentration coupled with an increase in both water and orange oil concentrations would result in an unstable emulsion, in terms of TSI. This indicated decreasing stability with decreasing stabiliser concentration as well as with increasing oil and water concentrations. High water and low STASOL concentrations result in a more dilute aqueous phase which allows for unimpeded movement of oil droplets within the emulsion system. Droplet migration results in coalescence and flocculation as well as related destabilisation phenomena.

The TSI measures the destabilisation phenomena within an emulsion system, hence it was concluded that the formulation composed of 20:30:50 (STASOL:oil:water) produced

the most stable emulsion. This observation was in agreement with BS_{AVO} (Table 5.2) and backscattering results (Figure 5.2).

5.3.3 Time-dependent rheological properties of STASOL stabilised emulsions

1. Hysteresis loop area

The hysteresis loop area (HLA) is the region between the upward and downward curves of time-dependent rheological studies (Adeyi, 2014). It is an index of the energy required to destroy the structure responsible for removing the influence of time in flow behaviour (Koocheki & Razavi, 2009). It shows the degree of breakdown within a substance as shear increases (Ghica *et al.*, 2016). The values of the HLA of STASOL stabilised emulsion systems are presented in Table 5.6 and the forward and backward sweeps are presented in Figure 5.5. The HLA of STASOL stabilised emulsions ranged from 0.37 for formulation 10 (12:34:54 STASOL:oil:water) to 5.69 Pas^{-1} for formulation 2 (20:30:50 STASOL:oil:water).

The presence of areas between the backward and forward sweeps indicated that all emulsions were time-dependent and thixotropic (Maphosa, 2016; Bergecliff, 2016). A large HLA indicates more extensive damage (Tarrega *et al.*, 2004; Junqueira *et al.*, 2018) therefore it was deduced that the structures of emulsions with relatively low HLA values maintained their initial integrity more with increasing shear than those with higher HLA values (Figure 5.5). There was an appreciable increase in structural damage with increasing STASOL concentration. This was in agreement with the oil-in-water emulsion studies of Adeyi (2014) who reported more viscous systems suffering more disintegration than less viscous systems.

STASOL is a biopolymer composite and therefore stabilised the beverage emulsions by thickening the system thus retarding droplet movement. Therefore, a higher concentration would result in more apparent destruction observed as a larger space between backward and forward curves. Higher viscosity in emulsions has been associated with higher stability due to the decreased migration rate of oil droplets (Koocheki & Razavi, 2009). A large area between the forward and backward sweeps also indicates a higher thixotropic effect (Tarrega *et al.*, 2004) as was observed in time-dependent studies of infant purees (Alvarez, 2013) and dairy desserts (Tarrega *et al.*, 2004).

The linear coefficients in terms of actual components for hysteresis loop area were expressed as:

$$\text{Hysteresis loop area} = 6.8947X_1 + 5.7293X_2 + 3.3981X_3 - 0.0940X_1X_2 - 0.1668X_1X_3 - 0.1692X_2X_3$$

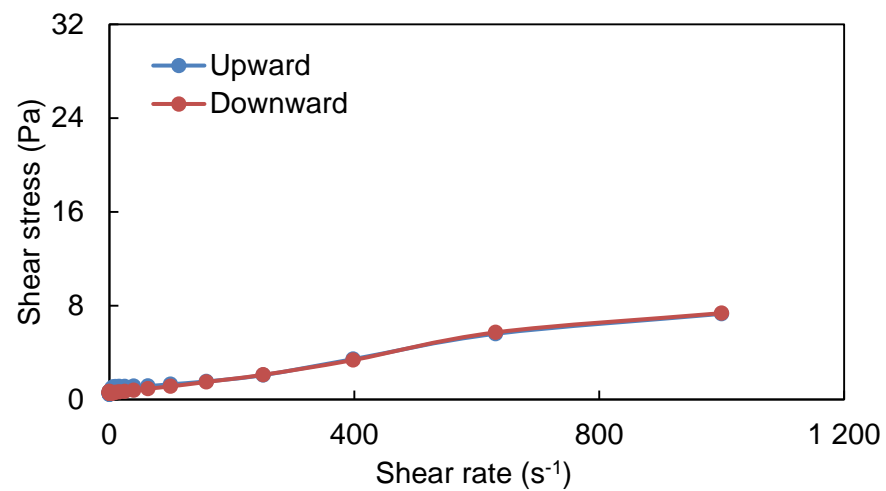
Where: X_1 , X_2 and X_3 = STASOL, orange oil and water, respectively.

Table 5.6 Effect of STASOL, orange oil and water fractions on the hysteresis loop area of STASOL stabilised emulsions*

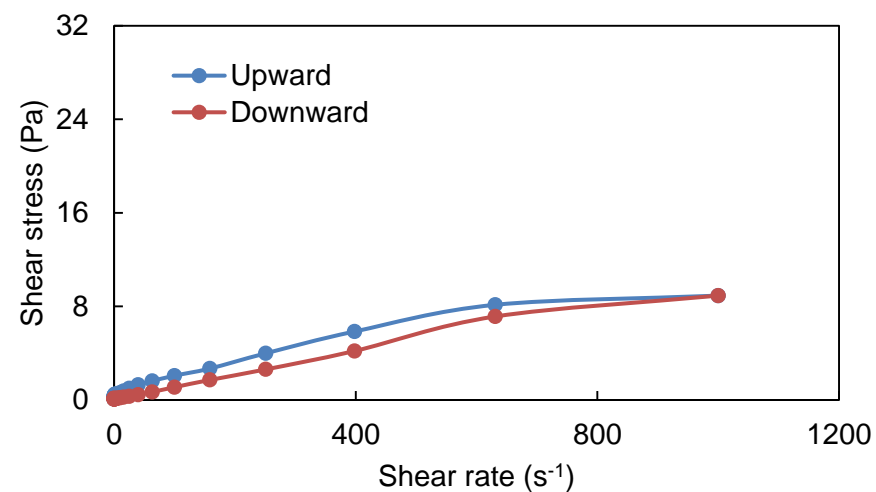
Formulation	STASOL (%)	Orange oil (%)	Water (%)	Integrating curve for upward curve	Integrating curve for downward curve	Hysteresis loop area (Pas ⁻¹)
1	8	42	50	68.22 ± 0.01	64.11 ± 0.00	4.11 ± 0.00 ^{bc}
2	20	30	50	26.92 ± 6.56	21.23 ± 8.50	5.69 ± 2.36 ^{bc}
3	8	36	56	95.61 ± 5.13	100.81 ± 55.81	5.20 ± 0.53 ^{bc}
4	10	38	62	26.87 ± 5.26	21.23 ± 5.65	5.64 ± 1.39 ^{bc}
5	8	42	50	67.43 ± 0.09	64.11 ± 0.05	3.32 ± 0.03 ^d
6	8	30	62	36.55 ± 10.56	32.67 ± 3.98	3.88 ± 0.38 ^{bc}
7	10	32	58	39.37 ± 10.56	39.74 ± 1.99	0.37 ± 0.01 ^{bc}
8	14	30	56	79.20 ± 29.01	78.80 ± 4.16	0.40 ± 0.12 ^a
9	14	36	50	73.08 ± 17.72	74.58 ± 37.14	1.50 ± 0.57 ^a
10	12	34	54	62.32 ± 2.52	64.36 ± 2.36	2.04 ± 0.17 ^{ac}
11	20	30	50	36.81 ± 4.52	35.83 ± 2.38	0.98 ± 0.04 ^b

*STASOL: Bambara groundnut starch-soluble dietary fibre nanocomposite. Values are mean ± standard deviation. Means within a column followed by different superscripts are significantly [$p \leq 0.05$] different.

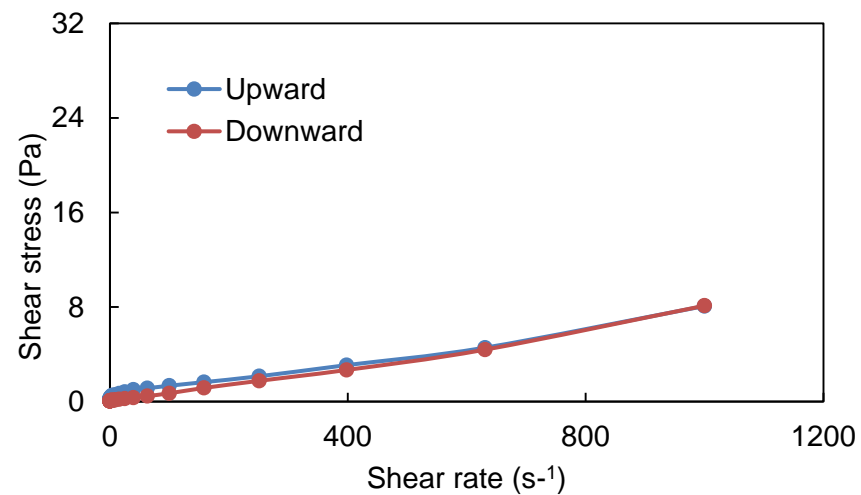
Formulation 1: 8:42:50 STASOL:oil:water



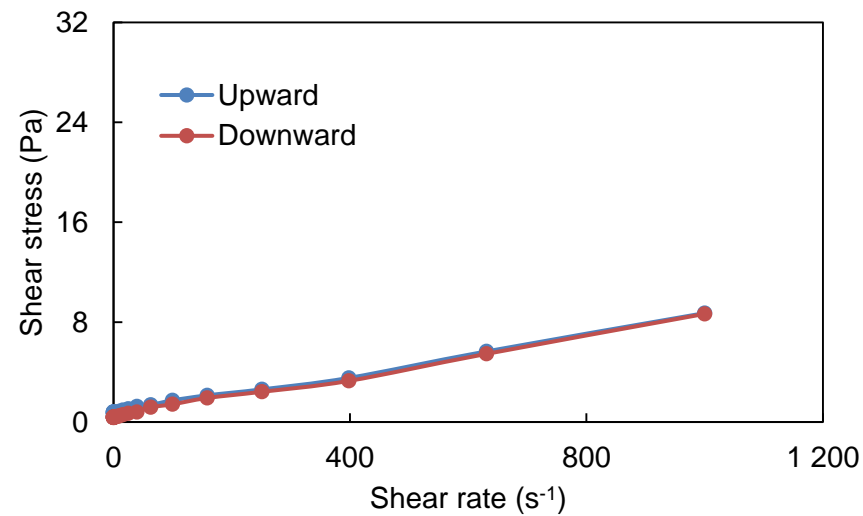
Formulation 2: 20:30:50 STASOL:oil:water



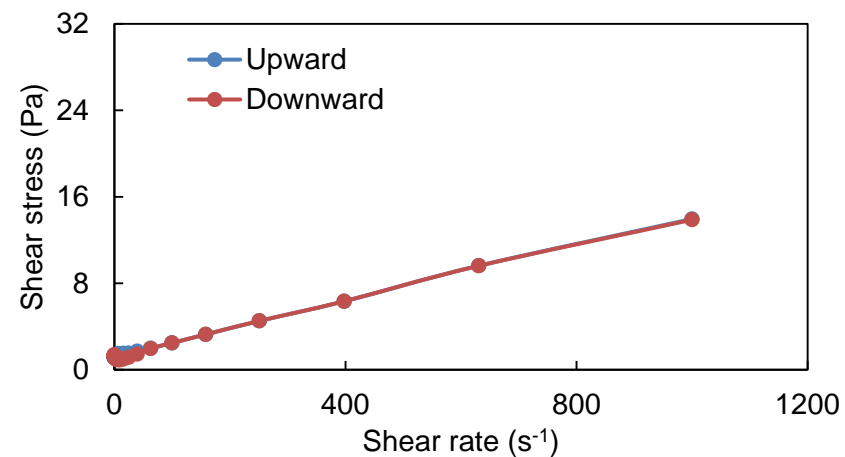
Formulation 3: 8:36:56 STASOL:oil:water



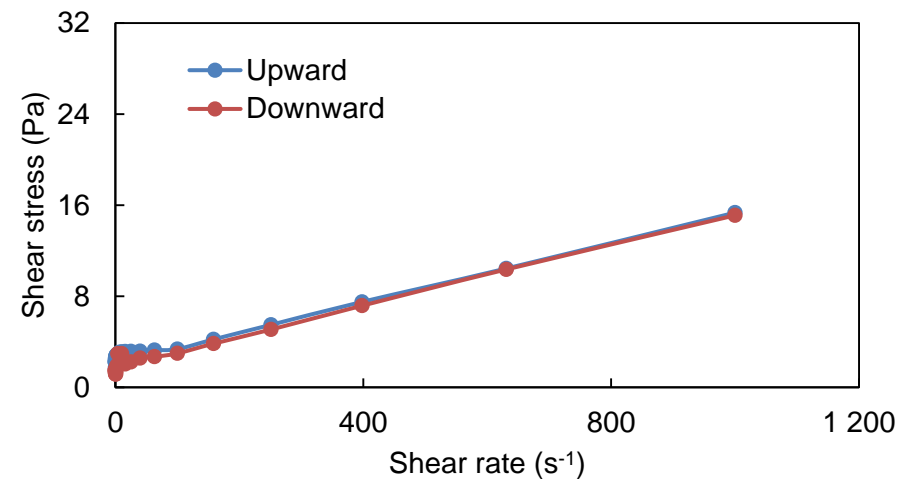
Formulation 4: 10:38:62 STASOL:oil:water



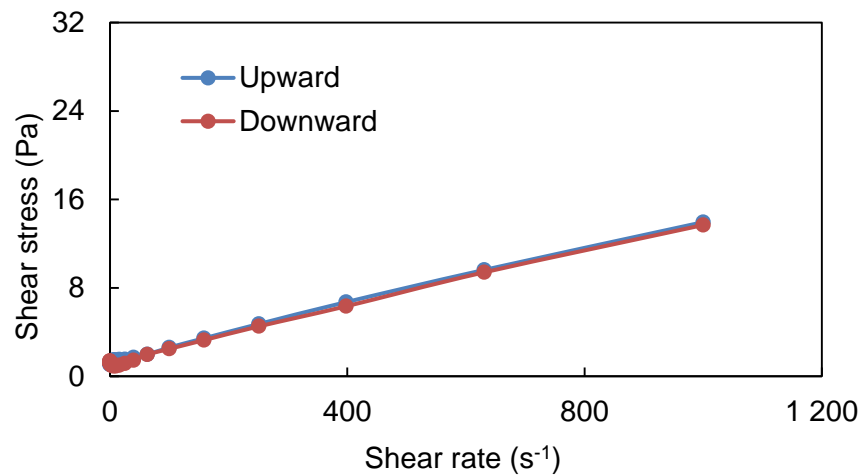
Formulation 5: 8:42:50 STASOL:oil:water



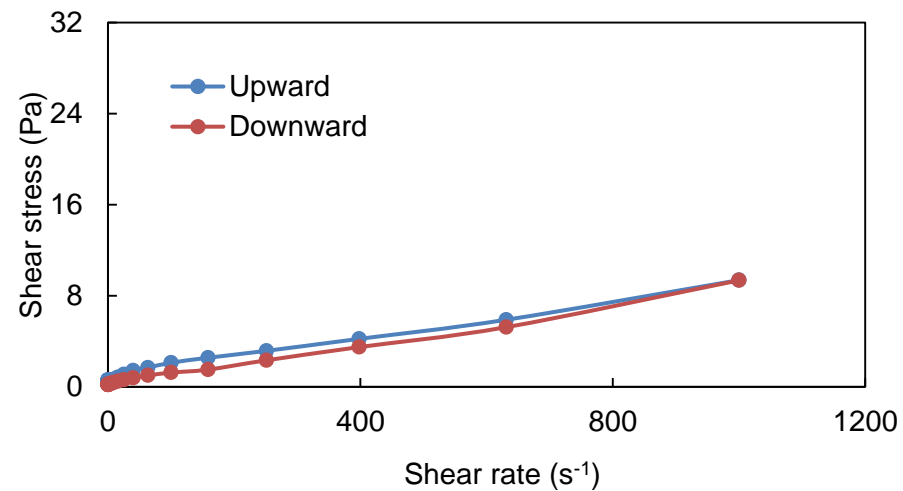
Formulation 6: 8:30:62 STASOL:oil:water



Formulation 7: 10:32:58 STASOL:oil:water



Formulation 8: 14:30:56 STASOL:oil:water



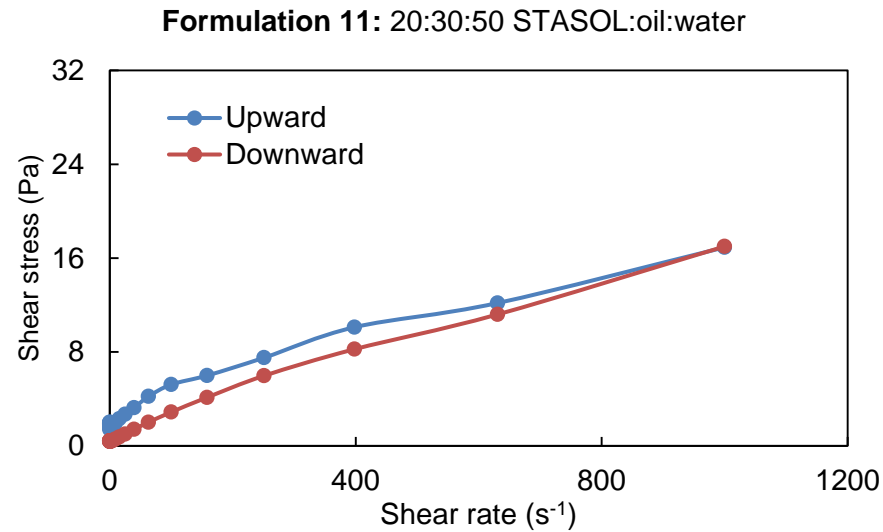
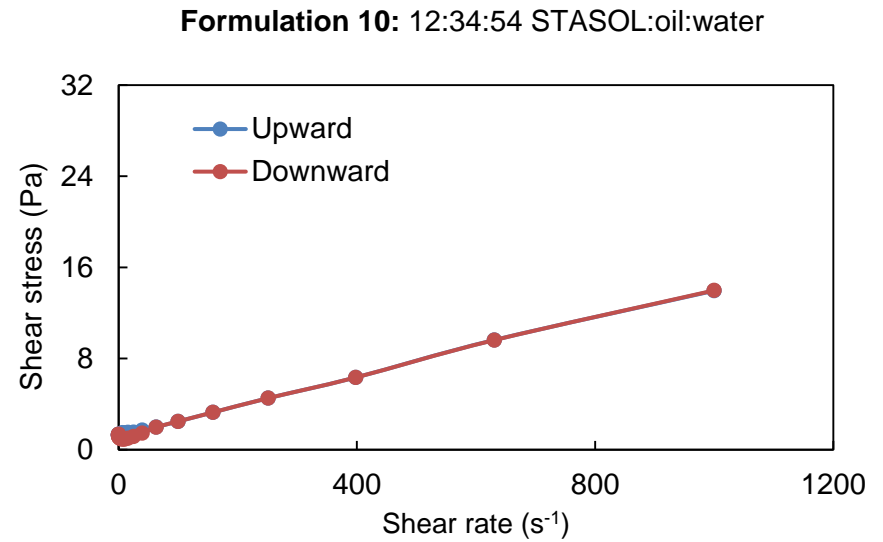
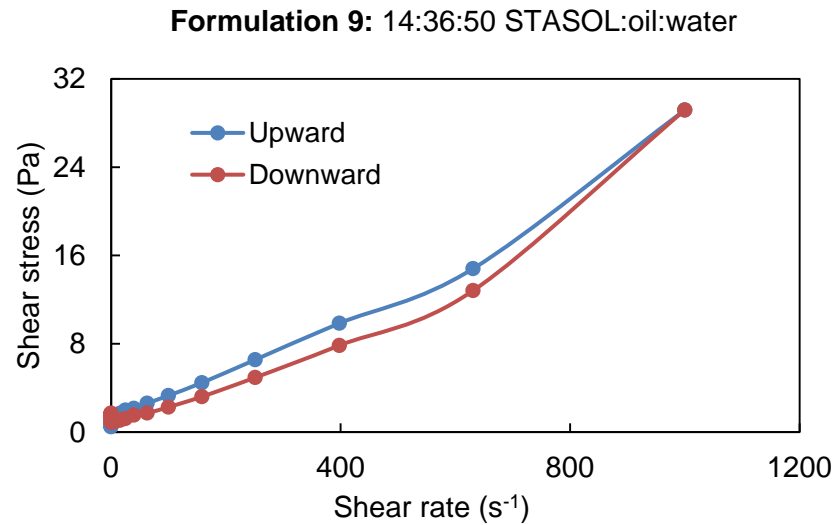


Figure 5.5 Hysteresis loop areas obtained for Bambara groundnut starch-soluble dietary fibre nanocomposite (STASOL) stabilised emulsions.

The ANOVA for the quadratic mixture model of the HLA is presented in Table 5.7. The model was significant ($p < 0.0001$) with a high R^2 value (0.9534), high coefficient of variation (17.05%), desirable adequate precision (21.634) and an insignificant lack of fit ($F = 0.86$). The high R^2 (0.9534) indicated a good fit of the model to the data. Furthermore, the predicted R^2 value (0.9082) and the adjusted R^2 value (0.9367) were in reasonable agreement, with a difference of less than 0.2, further confirming the goodness of fit of the model.

Table 5.7 ANOVA* for quadratic mixture model of hysteresis loop area

Source	DF	Sum of square	Mean square	F value	p-value
Model	5	459.12	91.82	57.24	< 0.0001
Linear mixture	2	314.09	157.05	97.89	< 0.0001
AB	1	19.11	19.11	11.91	0.0039
AC	1	54.47	54.47	33.95	< 0.0001
BC	1	23.15	23.15	14.43	0.0020
Residual	14	22.46	1.60		
Lack of fit	2	2.82	1.41	0.86	0.4468
Pure error	12	19.64	1.64		
Total	19	481.58			
R^2	0.9534				
Adj R^2	0.9367				
Predicted R^2	0.9082				
CV (%)	17.05				
Adequate Precision	21.634				

*ANOVA: Analysis of variance. A: STASOL. B: Orange oil. C: Water. R^2 : Coefficient of determination. Adj R^2 : Adjusted coefficient of determination. CV: Coefficient of variation. DF: Degrees of freedom. STASOL: Bambara groundnut starch-soluble dietary fibre nanocomposite.

The mixture response surface and the corresponding trace graph (piepel) for the individual and simultaneous increase of STASOL, orange oil and water on the HLA of STASOL stabilised emulsions are shown in Figure 5.6. High HLA values indicate more extensive damage in the structure of an emulsion. Orange oil and water showed synergy, with an increase in both resulting in an increase in the HLA of STASOL stabilised emulsions. Both

orange oil and water showed antagonism to STASOL. It was suggested that the formulation composed of 20:30:50 (STASOL:oil:water) produced the most stable emulsion.

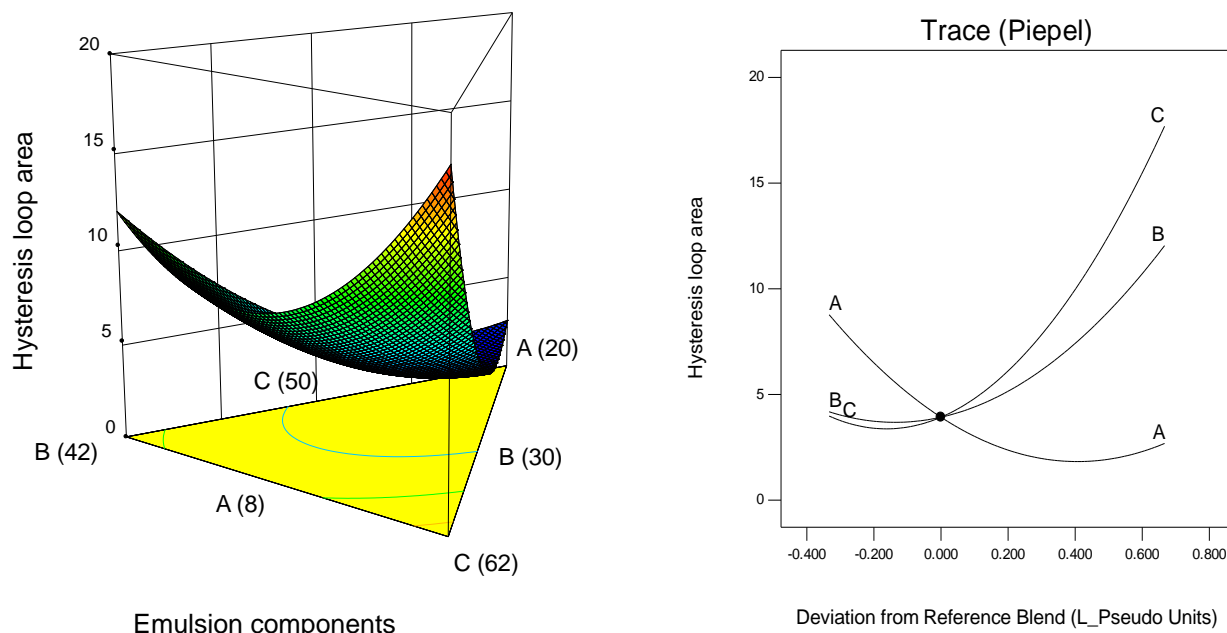


Figure 5.6 Mixture response surface (left) and Piepel graph (right) for the effect of (A) Bambara groundnut starch-soluble dietary fibre nanocomposite (STASOL), (B) orange oil and (C) water concentrations on the hysteresis loop areas of STASOL stabilised emulsions.

This was in agreement with BS_{AVO} results (Table 5.2), separation of scans observed on the backscattering profiles (Figure 5.2) and TSI results (Table 5.4).

2. Effect of constant shear decay on apparent viscosity of STASOL stabilised emulsions

Figure 5.7 shows the effect of shearing time on the apparent viscosity of STASOL stabilised emulsions. From the rheograms, all emulsions exhibited time-dependent behaviour when a constant shear rate was applied. The apparent viscosities of all emulsions decreased with increasing shearing time. When shear is applied over time, the structures of oil droplets are destroyed and coalescence is promoted thereby reducing the resistance of the system to flow (Adeyi, 2014). An increase in coalescence leads to a more unstable emulsion and consequently a decrease in viscosity of the system (Saha & Bhattacharya, 2010). Furthermore, increasing shear rate leads to an increase in the rate of breakdown of

stabilisers thereby decreasing the viscosity of the system, consequently promoting droplet movement.

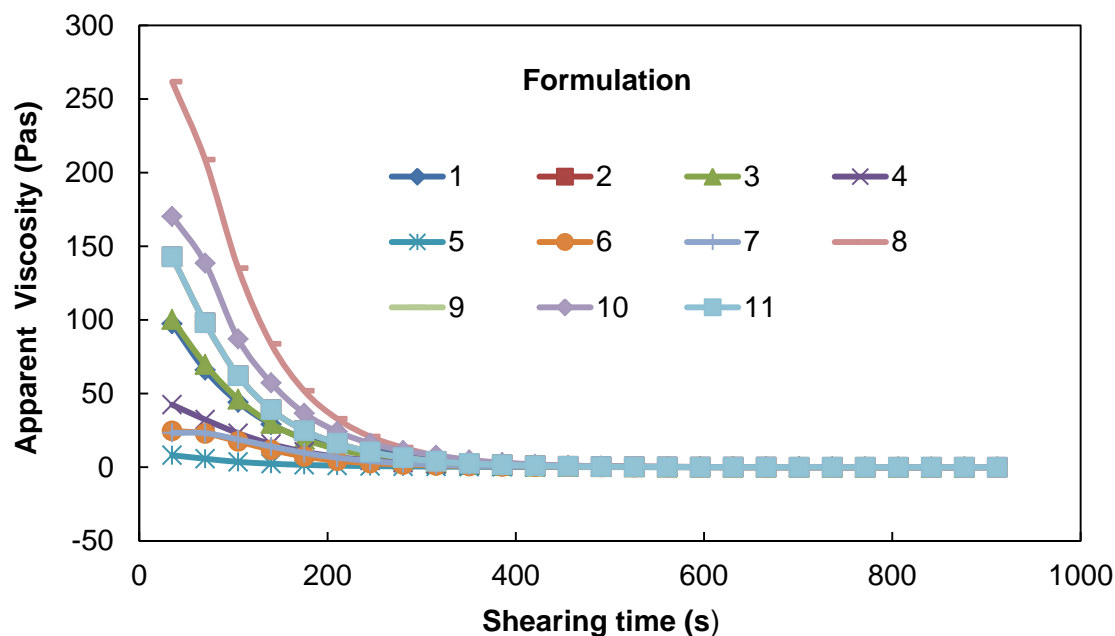


Figure 5.7 Apparent viscosity vs shearing time of Bambara groundnut starch-soluble dietary fibre nanocomposite (STASOL).

- 1 = 8:42:50 STASOL:oil:water
- 2 = 20:30:50 STASOL:oil:water
- 3 = 8:36:56 STASOL:oil:water
- 4 = 10:38:62 STASOL:oil:water
- 5 = 8:42:50 STASOL:oil:water
- 6 = 8:30:62 STASOL:oil:water
- 7 = 10:32:58 STASOL:oil:water
- 8 = 14:30:56 STASOL:oil:water
- 9 = 14:36:50 STASOL:oil:water
- 10 = 12:34:54 STASOL:oil:water
- 11 = 20:30:50 STASOL:oil:water

This behavioural pattern was also reported by Junqueira *et al.* (2018) who described a decrease in viscosity of hydrocolloid stabilised emulsion systems with increasing shearing time. All emulsions were concluded to be thixotropic. Thixotropic systems exhibit a decrease in viscosity with time when shear is applied to a system previously at rest (Ghica *et al.*, 2016). This is common in systems stabilised with hydrocolloids such as guar gum, galactomannans and xanthan gum (Bergeclif, 2016).

5.3.4 Time-dependent rheological models

The data of the time-dependent behaviour of STASOL stabilised emulsions were described using the first-order stress decay with a zero equilibrium stress value model (Equation 5.2) and the Weltman model (Equation 5.3).

1. *First-order stress decay with a zero equilibrium stress value*

The parameters of the first-order stress decay with a zero equilibrium stress model using a least-square technique are presented in Table 5.8. The coefficient of determination (R^2) of the emulsion systems was in the range 0.7011-0.9989, with 63.64% of the systems exhibiting $R^2 > 0.9000$. The RMSE and SSE were in the range 0.0542-1.6680 and 0.0705-66.7600, respectively. The relatively high R^2 , low RMSE and low SSE indicated that the model could be effectively used to describe the time-dependent data of the STASOL stabilised emulsions.

The initial stress (τ_o) of STASOL stabilised emulsions ranged from 6.63 [Formulation 6 (8:30:62 STASOL:oil:water)] to 22.51 Pa [Formulation 4 (10:38:62 STASOL:oil:water)]. The lowest and highest values of τ_o were recorded for emulsions stabilised with the least and the most concentration of STASOL, respectively. This indicated that higher stress was required to initiate flow in more viscous emulsions. The rate of breakdown of the emulsions (k) ranged from 0.0035 [Formulation 10 (12:34:54 STASOL:oil:water)] to 0.0199 s^{-1} [Formulation 2 (20:30:50 STASOL:oil:water)]. This deviated from the reports of Razavi *et al.* (2008) who reported an increase in the rate of breakdown (k) of sesame paste with increasing shear rate and stabiliser concentration. Higher values of the model parameters of the first-order stress decay with a zero equilibrium stress ($\tau_o = 9.22$ -193.99 Pa and $k = 1.39$ -3.90 s^{-1}) were reported for oil-in-water BGN flour stabilised emulsions by Adeyi (2014). Higher values of initial stress (τ_o) and comparable values of the rate of breakdown of the emulsions (k) were reported for emulsions stabilised with Balangu seed-derived hydrocolloid (Razavi & Karazhiyan, 2009). This suggested that a higher stress would be required to initiate flow in these systems than in STASOL stabilised emulsions. The application of higher stress in food production translates to more energy required for the process, which in turn translates to more money. This then makes the production and processing of STASOL stabilised emulsions more economic.

The presence of initial stress in the emulsion systems as described by the first-order stress decay with a zero equilibrium stress model confirmed that all emulsions were thixotropic and time-dependent in nature.

Table 5.8 First-order stress decay with a zero equilibrium stress value for STASOL* stabilised emulsions

Formulation	STASOL (%)	Orange oil (%)	Water (%)	τ_o (Pa)	$k \times 10^{-3}$	SSE	R ²	Adj R ²	RMSE
1	8	42	50	15.07 ± 0.12	13.76 ± 1.20	1.1610	0.9897	0.9893	0.2200
2	20	30	50	15.11 ± 0.75	19.89 ± 2.78	0.0705	0.9989	0.9989	0.0542
3	8	36	56	7.74 ± 1.24	11.87 ± 0.96	0.3476	0.9901	0.9897	0.1203
4	10	38	62	22.51 ± 0.72	9.63 ± 0.52	1.8180	0.9953	0.9951	0.2753
5	8	42	50	13.56 ± 0.60	15.43 ± 1.95	2.7320	0.9626	0.9610	0.3374
6	8	30	62	6.63 ± 1.47	5.52 ± 0.39	6.4650	0.8772	0.8720	0.5190
7	10	32	58	10.39 ± 0.58	8.61 ± 0.17	9.6440	0.8790	0.8739	0.6339
8	14	30	56	20.87 ± 1.44	9.78 ± 0.56	6.6360	0.9784	0.9775	0.5258
9	14	36	50	17.22 ± 2.85	8.61 ± 0.19	21.0100	0.9029	0.8988	0.9356
10	12	34	54	12.34 ± 1.98	3.54 ± 0.08	66.7600	0.7011	0.6887	1.6680
11	20	30	50	16.72 ± 0.89	7.39 ± 1.98	35.7800	0.8416	0.8350	1.2210

*STASOL: Bambara groundnut starch-soluble dietary fibre nanocomposite. Values are ± standard deviation. τ_o : Initial stress value; k : Rate of breakdown; R²: Coefficient of determination; Adj R²: Adjusted coefficient of determination; RMSE: Root mean squared error; SSE: Sum of squares.

This was in agreement with time-dependent studies discussed in section 5.3.3 where it was established that the viscosity of STASOL stabilised emulsions decreased when shear stress was applied.

2. *Weltman model*

The Weltman model characterises the thixotropic and anti-thixotropic behaviour of foods. Thixotropy is defined as the progressive decrease in the viscosity of a system with time under constant shearing, followed by a gradual recovery when the shear stress is removed (Abu-Jdayil & Al-Omari, 2013). The model parameters were evaluated as a function of STASOL, orange oil and water (Table 5.9). The R^2 and SSE values of the Weltman model were in the range 0.6692-0.8862 and 0.4995-1.5860, respectively. The high (>0.9) coefficient of determination (R^2) values made the Weltman model appropriate for describing the time-dependent behaviour of STASOL stabilised emulsions.

The value of the A parameter ranged from 8.12 [Formulation 3 (8:36:56 STASOL:oil:water)] to 27.81 Pa [Formulation 2 (20:30:50 STASOL:oil:water)] and the value of B ranged from -4.309 [Formulation 3 (8:36:56 STASOL:oil:water)] to -1.261 Pa [Formulation 2 (20:30:50 STASOL:oil:water)]. The model parameter A represents the initial shear stress of emulsions and was observed to be low in emulsions with low STASOL concentrations indicating that flow was easier in the relatively dilute systems. Formulation 2 (20:30:50 STASOL:oil:water) had the highest A parameter value meaning that larger stress was required to initiate the flow of the relatively viscous system. This was in agreement with the first-order stress decay with a zero equilibrium stress model [Section 5.3.4(1)]. The model parameter B represents the time coefficient of thixotropic or anti-thixotropic behaviour of emulsions and gives information on the rate of breakdown of their thixotropic structure (Koocheki & Razavi, 2009). A negative B value indicates thixotropic behaviour while a positive B value represents anti-thixotropic behaviour (Abu-Jdayil *et al.*, 2004). The model parameter B was negative meaning all emulsions were thixotropic, therefore would become less viscous when subjected to an applied stress. The B parameter was closer to zero for emulsions with low STASOL concentrations and highest in formulation 2 stabilised with the highest STASOL concentration. The value of the B parameter increases with solid content as the network needs a longer time to recover post shearing (Abu-Jdayil & Al-Omari, 2013).

The Weltman model has been reported as suitable for describing time-dependent rheological behaviour of food products such as semi-solid dairy desserts (Tarrega *et al.*, 2004), mayonnaise (Singla *et al.*, 2013), pistachio butter (Razavi *et al.*, 2010) and BGN flour stabilised emulsions (Adeyi, 2014). Higher values of Weltman model parameters ($A = 376.43\text{--}2213.49$ Pa and $B = 21.62\text{--}235.20$ Pa) were reported for pistachio butter by Razavi *et al.* (2010). This indicated that a higher initial stress had to be exerted to induce the flow of pistachio butter compared to STASOL stabilised emulsions.

Table 5.9 Weltman model parameters for STASOL* stabilised emulsions

Formulation	STASOL (%)	Orange oil (%)	Water (%)	A (Pa)	-B (Pa)	SSE	R ²	Adj R ²	RMSE
1	8	42	50	14.23 ± 2.40	-2.229 ± 0.46	25.35	0.7749	0.7655	1.0280
2	20	30	50	27.81 ± 1.31	-4.309 ± 0.85	60.38	0.8438	0.8372	1.5860
3	8	36	56	8.12 ± 2.13	-1.261 ± 1.98	7.14	0.7964	0.7879	0.5454
4	10	38	62	9.99 ± 0.42	-1.989 ± 0.64	21.92	0.6692	0.6554	0.9556
5	8	42	50	11.29 ± 3.15	-1.746 ± 0.56	19.49	0.7331	0.7220	0.9011
6	8	30	62	10.98 ± 3.01	-1.630 ± 0.97	5.99	0.8862	0.8815	0.4995
7	10	32	58	12.75 ± 4.26	-1.899 ± 2.29	16.35	0.7948	0.7863	0.8253
8	14	30	56	24.63 ± 1.51	-3.772 ± 1.65	57.82	0.8121	0.8042	1.5520
9	14	36	50	20.73 ± 5.15	-3.083 ± 0.49	49.38	0.7717	0.7622	1.4340
10	12	34	54	22.77 ± 2.17	-3.201 ± 0.33	43.36	0.8059	0.7978	1.3440
11	20	30	50	21.70 ± 2.14	-3.177 ± 0.52	48.55	0.7850	0.7760	1.4220

*STASOL: Bambara groundnut starch-soluble dietary fibre nanocomposite. A and B are constants. Values are ± standard deviation. A: Initial shear stress; B: Thixotropic or anti-thixotropic behaviour; R²: Coefficient of determination; Adj R²: Adjusted coefficient of determination; RMSE: Root mean squared error; SSE: Sum of squares.

The positive B values reported suggested that the system exhibited anti-thixotropic behaviour. Singla *et al.* (2013) reported Weltman model parameters for mayonnaise as $A = 5.05\text{--}5.11$ Pa and $B = 0.0005\text{--}0.0007$ Pa. This means that less stress was required for the mayonnaise to flow than STASOL stabilised emulsions. The B parameter values close to zero indicated that the apparent viscosity of mayonnaise was independent of time, meaning the system was neither thixotropic nor anti-thixotropic (Abu-Jdayil & Al-Omari, 2013).

3. *Comparison of the rheological models used in predicting time-dependent STASOL stabilised emulsions flow behaviour*

The data obtained from the apparent viscosity vs shearing time as well as from shear stress vs shear rate studies were fitted to the first-order stress decay with a zero equilibrium stress value and Weltman models and the suitability of each emulsion to describe time-dependent rheological data was evaluated. High R^2 and low SSE and RMSE values show the suitability of a model to accurately describe rheological data. The average coefficient of determination (R^2), SSE and RMSE for the first-order stress decay with a zero equilibrium stress value and Weltman models were 0.9197 and 0.7885, 13.86 and 32.34, 0.5919 and 1.0993, respectively. Although both models were suitable for describing the time-dependent rheological properties of STASOL stabilised emulsions, the first-order stress decay with a zero equilibrium stress value model was deemed more suitable. Both the Weltman and first-order stress decay with a zero equilibrium stress value models showed the emulsion formulated with 20:30:50 STASOL:oil:water to require the largest amount of stress to initiate flow. The viscosity of emulsion systems has been related to emulsion stability, hence the emulsion formulated with 20:30:50 STASOL:oil:water was predicted to be the most stable.

5.3.5 Time-independent rheological properties of STASOL stabilised emulsions

1. Apparent viscosity of STASOL stabilised emulsions at different shear rates

Figure 5.8 shows the influence of the ratio of STASOL:oil:water on the apparent viscosity of STASOL stabilised emulsions at selected shear rates. Steady shear studies proceeded after the inherent structures responsible for time dependency had been eliminated to obtain the steady-state condition (Adeyi, 2014). This was done so that only the time independence of the emulsions would be studied. This was achieved by pre-shearing the emulsions before shearing tests. All emulsions displayed shear-thinning behaviour evidenced by the gradual decrease in apparent viscosities with increasing shear rate (Soukoulis *et al.*, 2009). Viscosity decay was more pronounced at the initial shear stages and reached a steady state at shear rates around 250 s^{-1} .

All STASOL stabilised emulsions were non-Newtonian and exhibited shear-thinning behaviour. At very low shear rates, the change in the flow of the emulsions was not very clear but as shearing speed increased, the shear-thinning behaviour became more apparent.

This could be attributed to low shear forces not causing significant structural damages on emulsions (Adeyi, 2014).

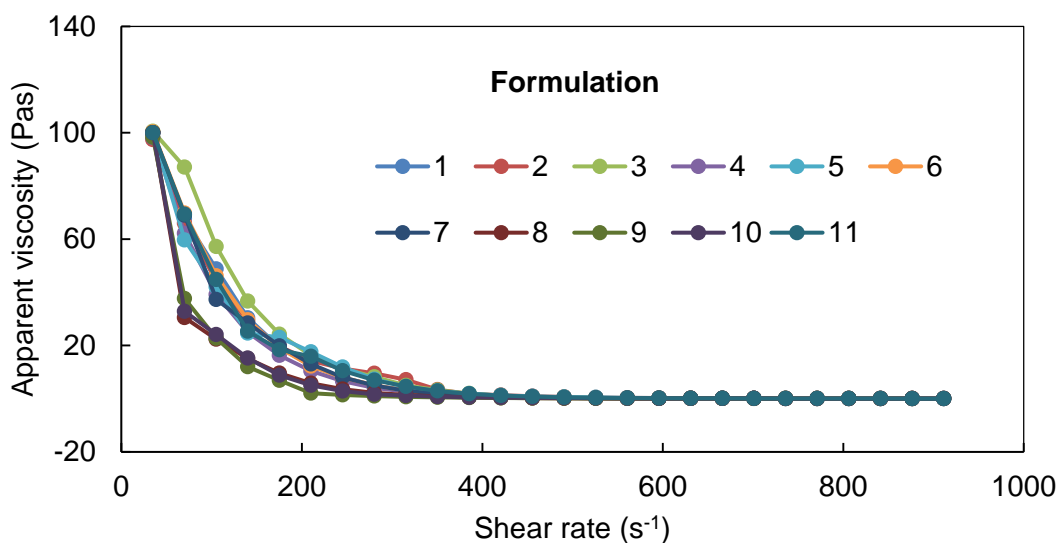


Figure 5.8 Effect of STASOL:oil:water concentrations on the apparent viscosity of beverage emulsions at different shear rates.

STASOL: Bambara groundnut starch-soluble dietary fibre nanocomposite.

1 = 8:42:50 STASOL:oil:water

2 = 20:30:50 STASOL:oil:water

3 = 8:36:56 STASOL:oil:water

4 = 10:38:62 STASOL:oil:water

5 = 8:42:50 STASOL:oil:water

6 = 8:30:62 STASOL:oil:water

7 = 10:32:58 STASOL:oil:water

8 = 14:30:56 STASOL:oil:water

9 = 14:36:50 STASOL:oil:water

10 = 12:34:54 STASOL:oil:water

11 = 20:30:50 STASOL:oil:water

The shear-thinning behaviour of the emulsions can be attributed to the gradual rearrangement of STASOL strands during the shearing process making their flow easier (Soukoulis *et al.*, 2009) hence the decrease in apparent viscosity with increasing shear rate observed in all emulsions. These results were confirmed by time-dependent experiments (Section 5.3.3) where the hysteresis loop areas proved that STASOL stabilised emulsions degraded with increasing shear.

At very high shear rates, the curves seemed to reach a constant flow. This could mean that the structures of the systems had been completely disrupted (Samavati *et al.*,

2011). The behaviour exhibited by the emulsions in this study is common in food systems (Guillon & Champ, 2000; Izidoro *et al.*, 2009) and is exhibited by many hydrocolloids and biopolymers (Mathur & Mathur, 2005). A decrease in viscosity of emulsions with increasing shear rate has been reported for systems such as walnut O/W emulsion (Nikovska, 2010), BGN flour stabilised emulsion (Adeyi, 2014), xanthan and guar gum stabilised emulsion (Lorenzo *et al.*, 2008), xanthan and guar gum stabilised salad dressing emulsion (Gallegos *et al.*, 2004) as well as gum slurries, fruit juice concentrates, tomato sauce, syrups and molasses (Phillips & Williams, 2000).

Table 5.10 summarises the effect of STASOL:oil:water concentrations on the apparent viscosities of STASOL stabilised emulsions. For comparative purposes, the apparent viscosities of the emulsions were assessed at low (35 s^{-1}), medium (245 s^{-1}) and high (560 s^{-1}) shear rates. At shear rates of 35, 245 and 560 s^{-1} the apparent viscosity ranged from 97-100, 2.82-11.85 and 0.07-0.31 Pas, respectively. The low shear rate (35 s^{-1}) represented pumping during the packaging stage of emulsions, the medium shear rate (245 s^{-1}) represented mastication in the human mouth during consumption and the high shear rate (560 s^{-1}) represented high speed mixing or stirring in the industrial production stage of emulsions (Adeyi, 2014).

5.3.6 Time-independent rheological models

The rheological properties of STASOL stabilised emulsions were modelled as a function of emulsion components (STASOL, orange oil and water), to understand the individual and combined effects of these ingredients on emulsion behaviour and stability. Rheological models are important in the designing and formulation of emulsions of predetermined properties. The Power law, Casson, Bingham plastic and Herschel-Bulkley models were used to describe the time-independent rheological behaviour of STASOL stabilised emulsions.

1. Power law model

The coefficient of determination (R^2), linear, quadratic and interaction effects for Power-law model parameters for STASOL stabilised emulsions are given in Table 5.11. Power law (Equation 5.5) describes the flow behaviour of fluids. The model consists of two parameters; the consistency coefficient (K) which describes the viscosity of a system and flow behaviour index (n) which is a measure of rigidity or reluctance of a fluid to flow and describes shear-thinning or thickening (Adeyi, 2014). In Power law, shearing behaviour is represented by a straight line with the slope of the line being the flow behaviour index (n) and log K being the intercept from which the consistency coefficient can be evaluated.

Table 5.10 Effect of STASOL*, orange oil and water fractions on the apparent viscosity of STASOL stabilised emulsions

Formulation	STASOL (%)	Orange oil (%)	Water (%)	Apparent viscosity (Pas) at:		
				35 s ⁻¹	245 s ⁻¹	560 s ⁻¹
1	8	42	50	100 ± 0.00	3.54 ± 0.03	0.07 ± 0.00
2	20	30	50	97 ± 0.00	11.34 ± 0.07	0.29 ± 0.00
3	8	36	56	98 ± 1.41	1.39 ± 0.00	0.06 ± 0.00
4	10	38	62	100 ± 0.00	8.03 ± 0.41	0.13 ± 0.00
5	8	42	50	98 ± 0.00	6.54 ± 0.16	0.12 ± 0.01
6	8	30	62	100 ± 0.00	2.82 ± 0.06	0.10 ± 0.00
7	10	32	58	100 ± 0.00	7.86 ± 0.00	0.19 ± 0.01
8	14	30	56	100 ± 0.00	10.49 ± 0.06	0.21 ± 0.06
9	14	36	50	100 ± 0.00	11.25 ± 0.04	0.16 ± 0.00
10	12	34	54	100 ± 0.00	7.95 ± 0.07	0.15 ± 0.00
11	20	30	50	100 ± 0.00	11.85 ± 0.07	0.31 ± 0.03

*STASOL: Bambara groundnut starch-soluble dietary fibre nanocomposite. Values are ± standard deviation.

Table 5.11 Power law model parameters for STASOL* stabilised emulsions

Formulation	STASOL (%)	Orange oil (%)	Water (%)	K (Pa)	n	SSE	R ²	Adj R ²	RMSE
1	8	42	50	0.03 ± 0.36	0.99 ± 0.60	14.52	0.9760	0.9750	0.78
2	20	30	50	0.15 ± 0.01	0.64 ± 0.02	24.99	0.8905	0.8860	1.02
3	8	36	56	0.07 ± 0.04	0.44 ± 0.01	18.81	0.9479	0.9457	0.89
4	10	38	62	0.05 ± 0.07	0.97 ± 0.50	7.432	0.9030	0.8990	0.56
5	8	42	50	0.02 ± 0.02	0.85 ± 0.09	2.952	0.9558	0.9540	0.35
6	8	30	62	0.07 ± 0.05	0.72 ± 0.12	2.978	0.9692	0.9679	0.35
7	10	32	58	0.16 ± 0.13	0.62 ± 0.13	4.249	0.9734	0.9723	0.42
8	14	30	56	0.13 ± 0.07	0.61 ± 0.07	7.459	0.9210	0.9177	0.56
9	14	36	50	0.12 ± 0.03	0.69 ± 0.04	22.26	0.9036	0.8996	0.96
10	12	34	54	0.09 ± 0.28	0.47 ± 0.28	46.46	0.7995	0.7912	1.39
11	20	30	50	0.17 ± 0.13	0.66 ± 0.13	23.29	0.8980	0.8937	0.99

*STASOL: Bambara groundnut starch-soluble dietary fibre nanocomposite. Values are mean ± standard deviation. K: Consistency coefficient; n: Flow behaviour index; R²: Coefficient of determination; Adj R²: Adjusted coefficient of determination; RMSE: Root mean squared error; SSE: Sum of squares.

The flow behaviour index (n) of the emulsions ranged from 0.44 [Formulation 3 (8:36:56 STASOL:oil:water)] to 0.99 [Formulation 1 (8:42:50 STASOL:oil:water)], respectively. All emulsions had flow behaviour (n) indexes less than 1, indicating shear-thinning behaviour (Maphosa *et al.*, 2017). The consistency coefficients (K) of the emulsions ranged from 0.02 [Formulation 5 (8:42:50 STASOL:oil:water)] to 0.17 [Formulation 11 (20:30:50 STASOL:oil:water)], respectively. The coefficient of determination (R^2) and adjusted R^2 of the emulsions were high, with 82% of the emulsion systems having values of ± 0.9 (Table 5.11). The R^2 values were indicative of a good level of relationship between data points, which indicated that Power law could be accurately employed for predicting the intrinsic rheological properties of the emulsions.

The consistency coefficient of all emulsions increased with increasing STASOL concentration coupled with decreasing oil concentration (Table 5.11). Higher values of the consistency coefficient (K) indicate more viscous solutions therefore the observed behaviour suggested that an increase in STASOL and a decrease in oil concentrations increased the viscosity of the system. Viscous emulsions stabilised with biopolymers have been associated with higher stability due to the decreased migration rate of oil droplets within the system (Koocheki & Razavi, 2009). This was in agreement with BS_{AVO} (Table 5.2), separation of scans observed on the backscattering profiles (Figure 5.2), TSI (Table 5.4) and hysteresis loop area results [Section 5.3.3 (1)]. Rheological studies give an idea of the mechanism of emulsion stability. In this case, it was implied that STASOL may not have exhibited interesting surface activity and only stabilised emulsions using steric hindrance (Adeyi, 2014).

2. *Herschel-Bulkley model*

The Herschel-Bulkley model (Equation 5.6) has three parameters, namely, the consistency coefficient (K), flow behaviour index (n) and yield stress (τ_o). The consistency coefficient (K) indicates the viscosity of the system with higher values representing a more viscous system. The flow behaviour index (n) serves as an indication of shear-thinning or shear-thickening by representing the reluctance of the system to flow. The yield stress (τ_o) is the minimum shear stress required to initiate the flow of a system. It is the stress applied to a sample at which irreversible plastic deformation is first observed (Ahuja *et al.*, 2020). Yield stress studies are employed in predicting factors such as product performance, processability and shelf life (Ahuja *et al.*, 2020). The Herschel-Bulkley model parameters of STASOL stabilised emulsions are presented in Table 5.12. The consistency coefficient (K) of the emulsions ranged from 0.01 (Formulations 2, 5, 9 and 11) to 0.81 Pa.s [Formulation 4 (10:38:62 STASOL:oil:water)] while the flow behaviour indexes (n) ranged from 0.44 for [Formulation 4 (10:38:62 STASOL:oil:water)] to 0.99 [Formulation 1 (8:42:50 STASOL:oil:water)].

Table 5.12 Herschel-Bulkley model parameters for STASOL* stabilised emulsions

Formulation	STASOL (%)	Orange oil (%)	Water (%)	τ_o (Pa)	K (Pa.s)	n	SSE	R ²	AdjR ²	RMSE
1	8	42	50	0.84 ± 1.19	0.08 ± 0.12	0.99 ± 0.49	1.83	0.9970	0.9967	0.28
2	20	30	50	1.28 ± 0.06	0.01 ± 0.00	0.99 ± 0.00	0.21	0.9991	0.9990	0.10
3	8	36	56	1.66 ± 0.00	0.14 ± 0.00	0.68 ± 0.00	0.73	0.9980	0.9978	0.18
4	10	38	62	0.50 ± 0.06	0.81 ± 0.21	0.44 ± 0.28	2.46	0.9679	0.9652	0.33
5	8	42	50	0.33 ± 0.05	0.01 ± 0.01	0.99 ± 0.15	1.26	0.9811	0.9795	0.23
6	8	30	62	0.28 ± 0.38	0.47 ± 0.63	0.56 ± 0.38	0.42	0.9956	0.9953	0.14
7	10	32	58	0.17 ± 0.12	0.14 ± 0.13	0.66 ± 0.17	3.80	0.9762	0.9742	0.41
8	14	30	56	0.70 ± 0.06	0.02 ± 0.02	0.90 ± 0.14	0.84	0.9911	0.9903	0.19
9	14	36	50	1.19 ± 0.14	0.01 ± 0.00	0.99 ± 0.01	0.27	0.9988	0.9987	0.11
10	12	34	54	1.86 ± 0.98	0.02 ± 0.01	0.99 ± 0.09	0.11	0.9995	0.9995	0.07
11	20	30	50	1.23 ± 0.46	0.01 ± 0.00	0.98 ± 0.02	0.25	0.9989	0.9988	0.10

*STASOL: Bambara groundnut starch-soluble dietary fibre nanocomposite. Values are mean ± standard deviation. τ_o : Yield stress; K: Consistency coefficient; n: Flow behaviour index; R²: Coefficient of determination; RMSE: Root mean squared error; SSE: Sum of squares.

All flow behaviour indexes (n) had values below 1 indicating shear-thinning behaviour (Maphosa, 2016). Quantification by the Herschel-Bulkley model revealed that STASOL stabilised emulsion systems possessed yield stress (τ_o) in the range 0.17 [Formulation 7 (10:32:58 STASOL:oil:water)] to 1.86 Pa [Formulation 10 (12:34:54 STASOL:oil:water)]. This indicated that all samples required minimum shear stress to flow (Ahuja *et al.*, 2020). The coefficient of determination (R^2) of all emulsions was considerably high (0.9679-0.9995) demonstrating a high level of relationship between data points as well as a high correlation between the experimental and predicted rheological data. The low SSE in the range 0.11 [Formulation 10 (12:34:54 STASOL:oil:water)] to 3.80 [Formulation 7 (10:32:58 STASOL:oil:water)] and the low RMSE in the range 0.77 [Formulation 10 (12:34:54 STASOL:oil:water)] to 0.41 [Formulation 7 (10:32:58 STASOL:oil:water)] showed a good fit of the Herschel-Bulkley model to the experimental data. Therefore, the coefficient of determination (R^2), SSE and RMSE values qualified the Herschel-Bulkley model suitable for describing the time-independent, shear-thinning behaviour of STASOL stabilised emulsions.

3. Bingham plastic model

The Bingham parameters of STASOL stabilised emulsions are presented in Table 5.13. The Bingham model (Equation 5.7) has two parameters, namely, the Bingham plastic viscosity (K^B) and yield stress (τ_o). The Bingham plastic viscosity (K^B) describes the viscosity of a system with higher values representing more viscous systems and yield stress (τ_o) is the minimum shear stress required before a system can flow. The yield stress (τ_o) of STASOL stabilised emulsions ranged from 0.32 [Formulation 5 (8:42:50 STASOL:oil:water)] to 1.92 Pa [Formulation 3 (8:36:53 STASOL:oil:water)]. It was evident that all STASOL stabilised emulsions needed certain shear stress applied for them to flow. The Bingham plastic viscosity (K^B) of STASOL stabilised emulsions ranged from 0.01 to 0.03 Pa.s. The coefficient of determination (R^2) was 0.99 for all but two emulsions. The R^2 of formulation 7 (10:32:58 STASOL:oil:water) and formulation 4 (10:38:62 STASOL:oil:water) were 0.94 and 0.96, respectively, which showed an adequate fitting of data to the Bingham plastic model. The RMSE of STASOL stabilised emulsions ranged from 0.0748 [Formulation 10 (12:34:54 STASOL:oil:water)] to 0.8150 [Formulation 3 (8:36:56 STASOL:oil:water)].

The SSE ranged from 0.13 [Formulation 10 (12:34:54 STASOL:oil:water)] to 15.94 [Formulation 3 (8:36:56 STASOL:oil:water)]. The high (> 0.94) coefficient of determination (R^2) showed that the Bingham plastic model could be adequately used to describe the time-independent rheological behaviour of STASOL stabilised emulsions.

4. Casson model

The Casson model parameters of STASOL stabilised emulsions are presented in Table 5.14.

Table 5.13 Bingham plastic model parameters for STASOL* stabilised emulsions

Formulation	STASOL (%)	Orange oil (%)	Water (%)	τ_o (Pa)	K^B (Pa.s)	SSE	R^2	Adj R^2	RMSE
1	8	42	50	1.06 ± 1.80	0.02 ± 0.01	3.32	0.9945	0.9943	0.3721
2	20	30	50	1.29 ± 0.06	0.01 ± 0.00	0.23	0.9990	0.9990	0.0969
3	8	36	56	1.92 ± 0.31	0.02 ± 0.00	15.94	0.9558	0.9540	0.8150
4	10	38	62	0.72 ± 0.09	0.01 ± 0.00	3.06	0.9600	0.9584	0.3573
5	8	42	50	0.32 ± 0.10	0.01 ± 0.00	1.27	0.9809	0.9801	0.2307
6	8	30	62	0.49 ± 0.23	0.01 ± 0.00	0.80	0.9917	0.9914	0.1829
7	10	32	58	0.56 ± 0.18	0.01 ± 0.00	11.06	0.9308	0.9279	0.6790
8	14	30	56	0.76 ± 0.03	0.03 ± 0.00	1.04	0.9890	0.9886	0.2078
9	14	36	50	1.20 ± 0.13	0.01 ± 0.00	0.27	0.9988	0.9988	0.1068
10	12	34	54	1.87 ± 0.91	0.01 ± 0.00	0.13	0.9994	0.9994	0.0748
11	20	30	50	1.25 ± 0.48	0.01 ± 0.00	0.26	0.9989	0.9988	0.1042

*STASOL: Bambara groundnut starch-soluble dietary fibre nanocomposite. Values are mean \pm standard deviation. τ_o : Yield stress; K^B : Bingham plastic viscosity; R^2 : Coefficient of determination; Adj R^2 : Adjusted coefficient of determination; RMSE: Root mean squared error; SSE: Sum of squares.

Table 5.14 Casson model parameters for STASOL* stabilised emulsions

Formulation	STASOL (%)	Orange oil (%)	Water (%)	τ_{oc} (Pa)	K_{oc} (Pa.s)	SSE	R^2	Adj R^2	RMSE
1	8	42	50	1.03 ± 0.28	0.13 ± 0.01	0.33	0.9864	0.9859	0.12
2	20	30	50	1.02 ± 0.03	0.08 ± 0.00	0.35	0.9696	0.9683	0.12
3	8	36	56	1.16 ± 0.15	0.09 ± 0.00	0.12	0.9925	0.9922	0.07
4	10	38	62	0.73 ± 0.02	0.06 ± 0.00	0.28	0.9616	0.9600	0.11
5	8	42	50	0.44 ± 0.07	0.07 ± 0.01	0.22	0.9738	0.9728	0.10
6	8	30	62	0.56 ± 0.15	0.07 ± 0.00	0.05	0.9944	0.9942	0.05
7	10	32	58	0.50 ± 0.02	0.09 ± 0.01	0.33	0.9779	0.9770	0.12
8	14	30	56	0.75 ± 0.02	0.07 ± 0.01	0.12	0.9848	0.9841	0.07
9	14	36	50	0.98 ± 0.06	0.08 ± 0.00	0.51	0.9569	0.9551	0.15
10	12	34	54	1.23 ± 0.35	0.07 ± 0.01	0.37	0.9634	0.9619	0.12
11	20	30	50	0.99 ± 0.22	0.08 ± 0.01	0.34	0.9706	0.9694	0.12

*STASOL: Bambara groundnut starch-soluble dietary fibre nanocomposite. Values are \pm standard deviation. τ_{oc} : Casson yield stress; K_{oc} : Consistency coefficient; n: Flow behaviour index; R^2 : Coefficient of determination; RMSE: Root mean squared error; SSE: Sum of squares.

The Casson model (Equation 5.8) has been applied to a wide range of food products (Keshani *et al.*, 2012) and has two parameters, namely the Casson yield stress (τ_{oc}) which is the minimum stress required for a system to flow and the Casson plastic viscosity (K_{oc}) which signifies the viscosity of the system (Chuah *et al.*, 2007). The Casson yield stress ranged from 0.44 [Formulation 5 (8:42:50 STASOL:oil:water)] to 1.23 Pa [Formulation 10 (12:34:54 STASOL:oil:water)]. This confirmed that STASOL stabilised emulsions were thixotropic and thus required a certain amount of stress to induce their flow, which was in agreement with Bingham model results (Table 5.13).

The Casson plastic viscosity (K_{oc}) ranged from 0.06 Pa.s [Formulation 4 (10:38:62 STASOL:oil:water)] to 0.13 Pa.s [Formulation 1 (8:42:50 STASOL:oil:water)]. The coefficient of determination (R^2) of the eleven STASOL stabilised emulsions ranged from 0.9569 [Formulation 9 (14:36:50 STASOL:oil:water)] to 0.9944 [Formulation 6 (8:30:62 STASOL:oil:water)]. The SSE of the emulsions ranged from 0.05 [Formulation 6 (8:30:62 STASOL:oil:water)] to 0.37 [Formulation 10 (12:34:54 STASOL:oil:water)] and the RMSE ranged from 0.05 [Formulation 6 (8:30:62 STASOL:oil:water)] to 0.15 [Formulation 9 (14:36:50 STASOL:oil:water)]. The high R^2 (>0.96), low SSE (<0.37) and low RMSE (<0.15) values showed a good fitting of the data to the Casson model, making it very suitable for describing the shear time-independent behaviour of STASOL stabilised emulsions.

5. *Comparison of the time-independent rheological models used predicting STASOL stabilised emulsions behaviour*

The data obtained from the shear rate vs shear stress rheological studies were fitted to four rheological models and the suitability of each model is given in Table 5.15. Higher R^2 , low SSE and low RMSE values indicate more suitability of rheological data to accurately describe emulsion stability. As such, the Herschel-Bulkley was concluded to be more suitable for describing the shear-thinning behaviour of STASOL stabilised emulsions than the Casson, Bingham and Power-law models. The Herschel-Bulkley model, also known as the yield-Power law, is more efficient in describing the behaviour of yield possessing systems than the ordinary Power-law model (Ofei, 2016).

The coefficient of determination (R^2) of the Herschel-Bulkley (0.97-0.99), Casson (0.96-0.99), Bingham (0.93-0.99) and Power law (0.80-0.98) rheological flow models were close to 1, which was an indication that they could be perfectly used to predict the flow behaviour of STASOL stabilised emulsions. The RMSE of the Herschel-Bulkley model was higher than that of the Bingham model (0.0086) while their SSE values were very similar (Table 5.15). The Power law model was considered the least suitable descriptor of the time-independent rheological data and this was attributed to the presence of yield within the emulsion systems.

Table 5.15 Comparison of the four rheological models used in predicting time-independent STASOL* stabilised emulsions behaviour

	Mean	R ²	SSE	RMSE	Adj R ²
Power law parameters					
K (Pa.s)	0.1437				
n	0.6534	0.8869	25.5200	1.0310	0.8822
Herschel-Bulkley parameters					
τ_0 (Pa)	1.2883				
K (Pa.s)	0.0133				
n	1.2154				
		0.9992	0.1754	0.0873	0.9992
Bingham model parameters					
τ_0^B (Pa)	1.2933				
K^B (Pa.s)	0.0128				
		0.9992	0.1766	0.0086	0.9992
Casson model parameters					
$\tau_{oc}^{0.5}$ (Pa)	1.0240				
K_{oc} (Pa.s)	0.0775				
		0.9640	0.4041	0.1298	0.9625

*STASOL: Bambara groundnut starch-soluble dietary fibre nanocomposite; K: consistency coefficient; n: Flow behaviour index; τ_{oc} : Yield stress; τ_0^B : Bingham yield stress; K^B : Bingham plastic viscosity; K_{oc} : Casson plastic viscosity; R²: Coefficient of determination; Adj R²: Adjusted Coefficient of determination; RMSE: Root mean squared error; SSE: Sum of squares.

5.4 Conclusions

The production of eleven emulsion formulations composed of varying concentrations of STASOL, orange oil and water was successfully carried out. The emulsion components (STASOL, orange oil and water) were found to have a profound effect on the stability and rheological properties of STASOL stabilised emulsions. Formulations 2 and 11 had the highest STASOL (20%), lowest orange oil (30%) and lowest water (50%) concentrations and were qualified as the most stable. This emulsion had the highest BS_{AVO} value (70.47%) indicating high initial stability after homogenisation and the lowest TSI (0.0005) indicating a low probability of phase separation. Furthermore, it exhibited the highest viscosity suggesting a low oil droplet movement within the emulsion matrix. The apparent viscosities of STASOL stabilised emulsions decreased with increasing shearing rate and time signifying shear-thinning behaviour. Hysteresis loop studies showed the presence of areas between the backward and forward sweeps in all emulsions as a result of structural disintegration with shear over time, hence it was concluded that STASOL stabilised emulsions are time-dependent. This was confirmed by the first-order stress decay with a zero equilibrium stress value and Weltman models which described the effect of time on the apparent viscosity and hysteresis loop areas of STASOL stabilised emulsions. These models confirmed the time dependency and thixotropic nature of STASOL stabilised emulsions. The Herschel-Bulkley, Bingham plastic, Power law and Casson models adequately described time-independent rheological behaviour of STASOL stabilised emulsions. The Herschel-Bulkley model proved to be the most suitable for describing the shear-thinning behaviour of STASOL stabilised emulsions. All emulsion systems possessed yield stress, below which the emulsions would not flow, meaning that a particular amount of stress was required to induce flow. Yield stress (T_o) as quantified by the Herschel-Bulkley model was ranged from 0.17 [Formulation 7 (10:32:58 STASOL:oil:water)] to 1.86 Pa [Formulation 10 (12:34:54 STASOL:oil:water)]. The studies revealed formulations 2 and 11 (20:30:50 STASOL:oil:water) as the most stable. The high STASOL-low oil-low water combination resulted in a viscous emulsion system which retarded the rate and extent of oil droplet migration thus delaying destabilisation. As such, it was concluded that an increase in STASOL concentration with a simultaneous decrease in oil and water concentrations results in a more stable emulsion system. Based on the results, the emulsion formulated with 20% STASOL, 30% orange oil and 50% water was selected for further studies.

References

- Abu-Jdayil, B. & Al-Omari, S.A. (2013). Rheological Behavior of Bentonite-Polyester Dispersions. *Mechanics of Composite Materials*, **49**, 277-284.
- Abu-Jdayil, B., Banat, F., Jumah, R., Al-Asheh, S. & Hammad, S. (2004). A comparative

- study of rheological characteristics of tomato paste and tomato powder solutions, *International Journal of Food Properties*, **7(3)**, 483-497.
- Adeyi, O. (2014). Effect of Bambara Groundnut flour on the stability and rheological properties of oil-in-water emulsion. PhD Thesis, Cape Peninsula University of Technology.
- Adeyi, O., Ikhu-Omoregbe, D. & Jideani, V. (2014). Emulsion stability and steady shear characteristics of concentrated oil-in-water emulsion stabilized by gelatinized bambara groundnut flour. *Asian Journal of Chemistry*, **26**, 4995-5002.
- Aggarwal, N. & Sarkar, K. (2008). Rheology of an emulsion of viscoelastic drops in steady shear. *Journal of Non-Newtonian Fluid Mechanics*, **150**, 19-31.
- Ahuja, A., Lee, R., Latshaw, A. & Foster, P. (2020). Rheology of starch dispersions at high temperatures. *Journal of Texture Studies*, **51(4)**, 575-584.
- Alam, M.M., Iemoto, S., Aramaki, K. & Oshimura, E. (2014). Self assembly and rheology of emulsions-mimicking food emulsion rheology. *Food Structure*, **1**, 137-144.
- Alvarez, D. & Barbut, S. (2013). Effect of inulin, β -Glucan and their mixtures on emulsion stability, color and textural parameters of cooked meat batters. *Meat Science*, **94(3)**, 320-327.
- Bergeclif, T. (2016). Viscosity and Acid Stability in Low-fat Mayonnaise with Varying Proportions of Xanthan Gum and Guar Gum. Bachelor Thesis, Linnaeus University.
- Blijdenstein, T.B.J. (2004). Serum separation and structure of depletion- and bridging-flocculated emulsions: a comparison. *Colloids and Surfaces. A Physicochemical and Engineering Aspects*, **245**, 1-3.
- Buffo, R., Reineccius, G.. & Oehlert, G. (2001). Factors affecting the emulsifying and rheological properties of gum acacia in beverage emulsions. *Food Hydrocolloids*, **15**, 53-66.
- Chanamai, R. & McClements, D.J. (2000). Impact of weighting agents and sucrose on gravitational separation of beverage emulsions. *Journal of Agricultural and Food Chemistry*, **48**, 5561-5565.
- Chen, L. (2015). Emulsifiers as food texture modifiers. In: *Modifying Food Texture*. Pp. 27–49.
- Chern, C.S. (2006). Emulsion polymerization mechanisms and kinetics. *Progress in Polymer Science*, **31**, 443-486.
- Chuah, T.G., Hairulnisah, H., Thomaschoong, S.Y., Chin, N.L. & Nazimah, S.A.L. (2007). Effects of temperature on viscosity of dodo I (concoction). *Journal of Food Engineering*, **80**, 423-430.
- Cottrell, T. & Van Peij, J. (2014). Introduction to Food Emulsifiers and Colloidal System. In: *Emulsifiers in Food Technology*. Edited by V. Norn. *Second Edition*. Pp. 1-20. Wiley Publishers.

- Dickinson, E. (2001). Milk protein interfacial layers and the relationship to emulsion stability and rheology. *Colloids and Surfaces B: Biointerfaces*, **20(3)**, 197-210.
- Dickinson, E. (2009). Hydrocolloids as emulsifiers and emulsion stabilizers. *Food Hydrocolloids*, **23**, 1473-1482.
- Eltayeb, A. R. S. M., Ali O. Ali., Abou-Arab, A.A. & Abu-Salem, F.M. (2011). Paper Chemical composition and functional properties of flour and protein isolate extracted from Bambara groundnut (*Vigna subterranean*). *African Journal of Food Science*, **5(2)**, 82-90
- Fernandez, P., André, V., Rieger, J. & Kühnle, A. (2004). Nano-emulsion formation by emulsion phase inversion. *Colloids and Surfaces A: Physicochemical and Engineering Aspects*, **251**, 53-58.
- Gallegos, C., Franco, J.M. & Partal, P. (2004). Rheology of food dispersions. *The British Society of Rheology*, 19-65.
- Galus, S. & Kadzińska, J. (2015). Food applications of emulsion-based edible films and coatings. *Trends in Food Science & Technology*, **45**, 273-283.
- Given, P.S. (2009). Encapsulation of Flavors in Emulsions for Beverages. *Current Opinion in Colloid and Interface Science*, **14(1)**, 43-47.
- Ghica, M.V., Hirjau, M., Lupuleasa, D. & Dinu-Pirvu, C.E. (2016). Flow and Thixotropic Parameters for Rheological Characterization of Hydrogels. *Molecules*, **21**, 786-803.
- Gruner, P., Riechers, B., Chacòn Orellana, L.A., Brosseau, Q., Maes, F., Beneyton, T., Pekin, D. & Baret, J.C. (2015). Stabilisers for water-in-fluorinated-oil dispersions: Key properties for microfluidic applications. *Current Opinion in Colloid and Interface Science*, **20(3)**, 183-191.
- Guillon, F. & Champ, M.M. (2000). Carbohydrate fractions of legumes: uses in human nutrition and potential for health. *British Journal of Nutrition*, **88(3)**, 293-306.
- Hasenhuettl, G.L. (2008). Analysis of food emulsifiers. In: *Food Emulsifiers and Their Applications: Second Edition*. Pp. 39-62.
- IBM. (2016). Statistical Package for the Social Science. IBM SPSS - IBM Analytics. IBM SPSS Software.
- Izidoro, D.R., Scheer, A. & Sierakowski, M. (2009). Rheological properties of emulsions stabilized by green Banana (*Musa cavendishii*) pulp fitted by power law model. *Brazilian Archives of Biology and Technology*, **52**, 1516-8913.
- Junqueira, L.A., Amaral, T.N., Oliveira, N.L., Prado, M.E.T. & de Resende, J.V. (2018). Rheological behavior and stability of emulsions obtained from *Pereskiaaculeata* Miller via different drying methods. *International Journal of Food Properties*, **21(1)**, 21-35.
- Kakran, M. & Antipina, M.N. (2014). Emulsion-based techniques for encapsulation in biomedicine, food and personal care. *Current Opinion in Pharmacology*, **18**, 47-55.
- Khalil, M. & Mohamed J.B. (2012). Herschel-Bulkley rheological parameters of a novel environmentally friendly lightweight biopolymer drilling fluid from xanthan gum and

- starch. *Journal of Applied Polymer Science*, **124**, 595-606.
- Koocheki, A., Ghandi, A., Razavi, S.M.A., Mortazavi, S.A. & Vasiljevic, T. (2009). The rheological properties of ketchup as a function of different hydrocolloids and temperature. *International Journal of Food Science and Technology*, **44**, 596-602.
- Lee, S.J. (2006). Emulsion rheology and properties of polymerized high internal phase emulsions. *Korea Australia Rheology Journal*, **18**, 183-189.
- Lim, S.S., Baik, M.Y., Decker, E.A., Henson, L., Michael Popplewell, L., McClements, D.J. & Choi, S.J. (2011). Stabilization of orange oil-in-water emulsions: A new role for ester gum as an Ostwald ripening inhibitor. *Food Chemistry*, **128(4)**, 1023-1028.
- Liu, Y., Chen, W., Chen, C. & Zhang, J. (2015). Physicochemical Property of Starch-Soluble Dietary Fiber Conjugates and Their Resistance to Enzymatic Hydrolysis. *International Journal of Food Properties*, **18**, 2457-2471.
- Lorenzo, G., Zaritzky, N. & Califano, A. (2008). Modeling rheological properties of low-in-fat o/w emulsions stabilized with xanthan/guar mixtures. *Food Research International*, **41(5)**, 487-494.
- Luo, M., Qi, X., Ren, T., Huang, Y., Keller, A.A. Wang, H., Wu, B., Jin, H. & Li, F. (2017). Heteroaggregation of CeO₂ and TiO₂ engineered nanoparticles in the aqueous phase: Application of turbiscan stability index and fluorescence excitation-emission matrix (EEM) spectra. *Colloids and surfaces A*, **533**, 9-19.
- Maphosa, Y. (2016). Characterisation of Bambara groundnut (*Vigna Subterranea* (L) Verdc.) non-starch polysaccharides from wet milling as prebiotics. Master of Technology Thesis, Cape Peninsula University of Technology.
- Maphosa, Y., Jideani, V.A. & Adeyi, O. (2017). Effect of soluble dietary fibres from Bambara groundnut varieties on the stability of orange oil beverage emulsion. *African Journal of Science, Technology, Innovation and Development*, **9**, 69-76.
- María, A., Zapata, O., Rodríguez-Barona, S., Inés, G., Gómez, G. & Zapata, A.M.O. (2015). Rheological characterization and stability study of an emulsion made with a dairy by-product enriched with omega-3 fatty acids. *Brazilian Journal of Food Technology Campinas*, **18**, 23-30.
- Mathur, V. & Mathur, N.K. (2005). Fenugreek and other lesser known legume galactomannans: scope for developments. *Journal of Scientific and Industrial Research*, **64**, 475-481.
- McClements, D.J. (1999). Emulsions. In: *Food Emulsions Principles, Practices, and Techniques*. LLC:CRC Press.
- McClements, D.J. (2005). Emulsions. In: *Food Emulsions Principles, Practices, and Techniques*. 2nd Ed. Boca Raton: CRC Press.
- McClements, D.J., Decker, E.A. & Weiss, J. (2007). Emulsion-based delivery systems for lipophilic bioactive components. *Journal of Food Science*, **72(8)**, 109-124.

- McClements, D.J., Henson, L., Popplewell, L.M., Decker, E.A. & Jun Choi, S. (2012). Inhibition of Ostwald ripening in model beverage emulsions by addition of poorly water soluble triglyceride oils. *Journal of Food Science*, **77**(1), 33-38.
- Mirhosseini, H., Tan, C.P., Aghlara, A., Hamid, N.S.A., Yusof, S. & Chern, B.H. (2008a). Influence of pectin and CMC on physical stability, turbidity loss rate, cloudiness and flavor release of orange beverage emulsion during storage. *Carbohydrate Polymers*, **73**, 83-91.
- Mirhosseini, H., Tan, C.P., Hamid, N.S.A. & Yusof, S. (2008b). Effect of Arabic gum, xanthan gum and orange oil contents on ζ -potential, conductivity, stability, size index and pH of orange beverage emulsion. *Colloids and Surfaces A: Physicochemical and Engineering Aspects*, **315**, 47-56.
- Mubaiwa, J., Fogliano, V., Chidewe, C. & Linnemann, A.R. (2018). Bambara groundnut (*Vigna subterranea* (L.) Verdc.) flour: A functional ingredient to favour the use of an unexploited sustainable protein source. *Plos One*, **13**(10), e0205776.
- Nikovska, K. (2010). Oxidative stability and rheological properties of oil-in-water emulsions with Walnut oil. *Advance Journal of Food Science and Technology*, **2**, 172-177.
- Ofei, T.N. (2016). Effect of yield power law fluid rheological properties on cuttings transport in eccentric horizontal narrow annulus. *Journal of fluids*, **2016**, 1-10.
- Oliveira, T.F. & Cunha, F.R. (2015). Emulsion rheology for steady and oscillatory shear flows at moderate and high viscosity ratio. *Rheologica Acta*, **54**, 951-971.
- Palazolo, G.G., Sorgentini, D.A. & Wagner, J.R. (2005). Coalescence and flocculation in o/w emulsions of native denatured whey soy proteins in comparison with soy protein isolates. *Food Hydrocolloids*, **19**, 595-604.
- Perez-Mosqueda, L., Trujillo-Cayado, L.A., Carrillo, F. & Ramirez, P. (2015). Formulation and optimization by experimental design of eco-friendly emulsions based on d-limonene. *Colloids and surfaces B: Biointerfaces*, **128**, 127-131.
- Phillips, G.O. & Williams, P.A. (2000). Hydrocolloids and emulsion stability. In: *Handbook of Hydrocolloids*. Cambridge: Woodhead Publishing Ltd.
- Piorkowski, D.T. & McClements, D.J. (2013). Beverage emulsions: Recent developments in formulation, production, and applications. *Food Hydrocolloids*, **42**(2), 5-41.
- Prestidge, C.A. & Simovic, S. (2006). Nanoparticle encapsulation of emulsion droplets. *International Journal of Pharmaceutics*, **324**, 92-100.
- Razavi, S.M.A. & Karazhiyan, H. (2009). Flow properties and thixotropy of selected hydrocolloids: experimental and modeling studies. *Food Hydrocolloids*, **23**(3), 908-912.
- Razavi, S.M.A., Habibi, N.M.B. & Alaei, Z. (2008). Rheological characterisation of low fat sesame paste blended with date syrup. *International Journal of Food Properties*, **11**, 92-101.
- Rezvani, E., Schleining, G. & Taherian, A.R. (2014). Physicochemical properties of oil-in-

- water emulsions applicable to beverages and edible films. 3rd International ISEKI-Food Conference, Athens.
- Ritzoulis, C. & Karayannakidis, P.D. (2015). Proteins as texture modifiers. In: *Modifying Food Texture*. Pp. 51-69.
- Roland, I., Piel, G., Delattre, L. & Evrard, B. (2003). Systematic characterization of oil-in-water emulsions for formulation design. *International Journal of Pharmaceutics*, **263**, 85-94.
- Saha, D. & Bhattacharya, S. (2010). Hydrocolloids as thickening and gelling agents in food: A critical review. *Journal of Food Science and Technology*, **47(6)**, 587-597.
- Sahin, S. & Sumnu, S. (2006). Rheological Properties of Foods. In: *Physical properties of food*. Pp. 39-105. Springer.
- Samavati, V., Emama-Djomeh, Z., Mohammadifar, M.A., Omid, M. & Mehdinia, A.L.I. (2011). Stability and rheology of dispersions containing polysaccharide, oleic acid and whey protein isolate. *Journal of Texture Studies*, **1**, 14.
- Siddiqui, A.M., Farooq, A.A. & Rana, M.A. (2015). A Mathematical Model for the Flow of a Casson Fluid due to Metachronal Beating of Cilia in a Tube. *Scientific World Journal*, **2015**, 487819.
- Singh, T., Shukla, S., Kumar, P. & Wahla, V. (2017). Application of Nanotechnology in Food Science: Perception and Overview. *Frontiers in Microbiology*, **8(1501)**, 1-7.
- Singla, N., Verma, P., Ghoshal, G. & Basu, S. (2013). Steady state and time dependent rheological behaviour of mayonnaise (egg and eggless). *International Food Research Journal*, **20(4)**, 191-199.
- Soukoulis, C., Lebesi, D. & Tzia, C. (2009). Enrichment of ice cream with dietary fibre: effects on rheological properties, ice crystallization and glass transition phenomena. *Food Chemistry*, **115**, 665-671.
- Sun, Y.E., Wang, W.D., Chen, H.W. & Li, C. (2011). Autoxidation of unsaturated lipids in food emulsion. *Critical Reviews in Food Science and Nutrition*, **51(5)**, 453-466.
- Tadros, T. (2004). Application of rheology for assessment and prediction of the long-term physical stability of emulsions. *Advances in Colloid and Interface Science*, **108-109**, 227-258.
- Tadros, T.F. (2013). Emulsion Formation, Stability, and Rheology. *Emulsion Formation and Stability*, 1-76. Wiley Publishers.
- Taherian, A., Britten, m., Sabik, H. & Fustier. (2010). Ability of whey protein isolate and/or fish gelatin to inhibit physical separation and lipid oxidation in fish oil-in-water beverage emulsion. *Food Hydrocolloids*, **25(5)**, 868-878.
- Tarrega, A., Duran, L. & Castell, E. (2004). Flow behavior of semi-solid dairy desserts, effect of temperature. *International Dairy Journal*, **14**, 345-353.
- Trujillo-Cayado, L.A., Alfaro, M.C., Muñoz, J., Raymundo, A. & Sousa, I. (2016).

- Development and rheological properties of ecological emulsions formulated with a biosolvent and two microbial polysaccharides. *Colloids and Surfaces B: Biointerfaces*, **141(1)**, 53-58.
- Ushikubo, F. & Cunha, R.L. (2014). Stability mechanisms of liquid water-in-oil emulsions. *Food Hydrocolloids*, **34(1)**, 145-153.
- Yin, B., Zhang, R. & Yao, P. (2015). Influence of pea protein aggregates on the structure and stability of pea protein/soybean polysaccharide complex emulsions. *Molecules*, **20**, 5165-5183.
- Zalewska, A., Kowalik, J. & Grubecki, I. (2019). Application of turbiscan lab to study the effect of emulsifier content on the stability of plant origin dispersion. *Chemical and Process Engineering*, **40(4)**, 399-409.
- Zengeni, B.T. (2016). Bingham yield stress and Bingham plastic viscosity of homogeneous non-Newtonian slurries. Master of Technology in Mechanical Engineering Dissertation. Cape Peninsula University of Technology.

CHAPTER SIX
EFFECT OF STORAGE TIME AND TEMPERATURE ON THE STABILITY AND
RHEOLOGICAL PROPERTIES OF BAMBARA GROUNDNUT STARCH-SOLUBLE
DIETARY FIBRE NANOCOMPOSITE STABILISED EMULSION

Abstract

The effect of storage time (20 days) and temperature (5, 20 and 45°C) on the rheological and stability properties of Bambara groundnut starch-soluble dietary fibre nanocomposite (STASOL) stabilised emulsions was evaluated. Orange oil (30%), water (50%) and STASOL (20%) were used in formulating the emulsions. The rheological properties and physical stability of STASOL stabilised emulsions were evaluated using a physical rheometer and a Turbiscan MA 2000, respectively. Creaming stability evaluated the rate of separation of emulsions into cream and serum while the loss of turbidity of emulsions was determined by diluting the emulsion in a 10% sugar solution to 0.25% (w/w) and storing them at 20-25°C for 20 days. The pH, microstructure and droplet sizes of the emulsions were evaluated using a Toledo Mettler pH meter, digital microscope and the Proline Android H10888M software. Destabilisation as evaluated by the Turbiscan was observed from day 3 and it progressed throughout the storage time. The backscattering profile of the emulsions stored at 5 and 45°C showed the least and most separation between scans, respectively, during the 20 day storage period. On day 20, the creaming indexes of emulsions stored at 5, 20 and 45°C were 5, 63 and 73%, respectively. At the end of the study (Day 20), the emulsions stored at 45°C had completely separated into two distinct layers. Turbidity loss studies showed a decrease in the absorbance of emulsions stored at 5, 20 and 45°C from 1.0737 (Day 1) to 0.8203, 0.6253 and 0.5009, respectively (Day 20). The pH of emulsions stored at 5, 20 and 45°C increased significantly ($p = 0.000$) from 3.47 (Day 1) to 3.68, 3.77 and 4.05, respectively on day 20. The mean droplet sizes of all studied emulsions increased significantly ($p = 0.000$) from 4.47 μm (Day 1) to 15.11 and 32.36 μm at 5 and 20°C, respectively, on day 20. At the end of the storage period, no droplets were observed in the micrograph of the emulsion stored at 45°C. The initial apparent viscosity of the emulsions stored at 5, 20 and 45°C ranged from 0.51-0.36, 0.51-0.18 and 0.51-0.12 Pas for days 1 and 20, respectively. The viscosity of emulsions stored at 5°C started significantly ($p = 0.000$) decreasing after day 9 while that of emulsions stored at 20 and 45°C significantly ($p = 0.000$) decreased after day 3. The Power Law consistency coefficient (K) and flow behaviour indexes (n) of the upward flow of all emulsions were 1.3943 $\text{Pa}\cdot\text{s}^n$ and 0.1406, respectively, on day 1 and 1.3958 $\text{Pa}\cdot\text{s}^n$ and 0.0143, 11.4460 $\text{Pa}\cdot\text{s}^n$ and 0.0269, 53.1800 $\text{Pa}\cdot\text{s}^n$ and 0.0061 for emulsions stored at 5, 20 and 45°C, respectively, on day 20. Both temperature and time largely affected the extent of destabilisation, with emulsions stored at 5 and 45°C showing the least and most destabilisation over time, respectively.

6.1 Introduction

There is a growing trend toward utilising more label-friendly ingredients in foods and beverages. As such, there has been increased interest in the utilisation of particle-based emulsion stabilisers (Dickinson, 2001, Fujisawa *et al.*, 2017). Biopolymers such as polysaccharides, gum Arabic and Guar gum are becoming widely used as stabilisers in emulsion systems as alternatives to artificial stabilisers. Emulsions are complex systems made up of two immiscible liquids, usually water and oil (Campelo *et al.*, 2017). They exhibit varying behaviours when exposed to different situations, therefore, it is necessary to study and understand their characteristics to predict their behaviour over time. The behaviour of food emulsions is defined in three parts 1) the oil within the emulsion droplet, 2) the interfacial material between the lipid and aqueous phases and 3) the aqueous phase itself (Campelo *et al.*, 2017).

Emulsions are thermodynamically unstable systems that lose their characteristics over time due to physical and chemical destabilisation phenomena such as droplet agglomeration, coalescence, creaming, phase inversion, physical instability, oxidation and hydrolysis (Zhang, 2011). Flocculation happens when droplets in an emulsion are attracted to each other and form flocs without the rupture of the stabilising layer at the interface (Adeyi, 2014). Ostwald ripening occurs when larger droplets expand at the expense of smaller ones, subsequently reducing the average droplet size (Jiao & Burgess, 2003). Coalescence occurs when droplets merge, creating larger droplets and subsequently decrease the average droplet size and the stability of the emulsion (Chanamai & McClements, 2000; Tadros, 2013). Creaming occurs as a consequence of upward gravitational separation (Mao & Miao, 2015), while sedimentation occurs due to downward gravitational separation (Payet & Terentjev, 2008). Creaming appears when droplets within an emulsion merge, form larger droplets and rise towards the surface due to oil droplets being less dense than water (Choi *et al.*, 2014; Campelo *et al.*, 2017). The extent of creaming in emulsions can be measured by visual observation or by optical imaging (Cha *et al.*, 2019) and described using the creaming index which is an indirect indicator of the extent of droplet aggregation, with a larger creaming index value indicating a larger amount of agglomerated droplets (Onsaard *et al.*, 2006; Maphosa & Jideani, 2018). These destabilisation phenomena occur due to the nature and concentration of stabiliser, pH, temperature and homogenisation parameters (McClements, 2005; Sjoblom, 2006). As such, stabilisers are introduced to increase the kinetic stability of emulsion systems, thereby increasing their stability for extended periods (Payet & Terentjev, 2008; Kerkhofs *et al.*, 2011).

The emulsions in this study were orange oil beverage emulsions. Orange oil is a complex organic compound consisting of more than 200 constituents. It is widely used as a flavouring ingredient in food and beverage products and is the main constituent of orange oil beverage emulsions (Choi *et al.*, 2011). Orange oil beverage emulsions are oil emulsion and

flavour cloud emulsion. The former consists of orange oil emulsified into water and are used as a concentrate to provide cloud and flavour to beverages. The latter has less orange oil and also contains vegetable oil to produce a cloud in the beverage (Tan, 1990). The STASOL produced in chapter 3 and the optimum STASOL:water:orange oil ratio determined in Chapter 5 were used in this study. The objective of this chapter was to assess the effect of storage time and temperature on the rheological and stability properties of three Bambara groundnut starch-soluble dietary fibre nanocomposite (STASOL) stabilised emulsions stored at 5, 20 and 45°C for 20 days.

6.2 Materials and Methods

STASOL obtained from Chapter 3 (section 3.2.4) was used to prepare orange oil beverage emulsions. Cold pressed orange oil (Puris Natural Aroma Chemicals, South Africa) was used as the oil phase and deionised water was used as the water phase. The experimental design of Chapter 6 is outlined in Figure 6.1.

6.2.1 Preparation of STASOL stabilised beverage emulsions

Emulsions were prepared according to the method described in Chapter 5, section 5.2.2. The optimum combination of emulsion components [STASOL (20%), orange oil (30%) and deionised water (50%)] determined in Chapter 5 was used in the formulation of emulsions in this study.

6.2.2 Effect of storage time and temperature on the rheological properties of STASOL stabilised emulsions

The rheological properties of the emulsions were evaluated using an MCR 300 Paar Physical Rheometer at 20°C following the procedures described in Chapter 5, section 5.2.4. Analyses were carried out after storage at 5, 20 and 45°C on days 1, 3, 9, 15 and 20. Samples of emulsions stored at 5 and 45°C were removed from the refrigerator and incubator, respectively, and allowed to stand before analysis to bring them to room temperature.

6.2.3 Effect of storage time and temperature on the stability of STASOL stabilised emulsions

Physical and intrinsic emulsion stability measured Turbiscan stability and creaming indexes of STASOL stabilised emulsions stored at 5, 20 and 45°C for 20 days.

1. *Turbiscan stability analysis*

Physical emulsion stability measurements were carried out using the Turbiscan MA 2000 following the method described in Chapter 5, section 5.2.3. Analyses were carried out after storage at 5, 20 and 45°C on days 1, 3, 9, 15 and 20.

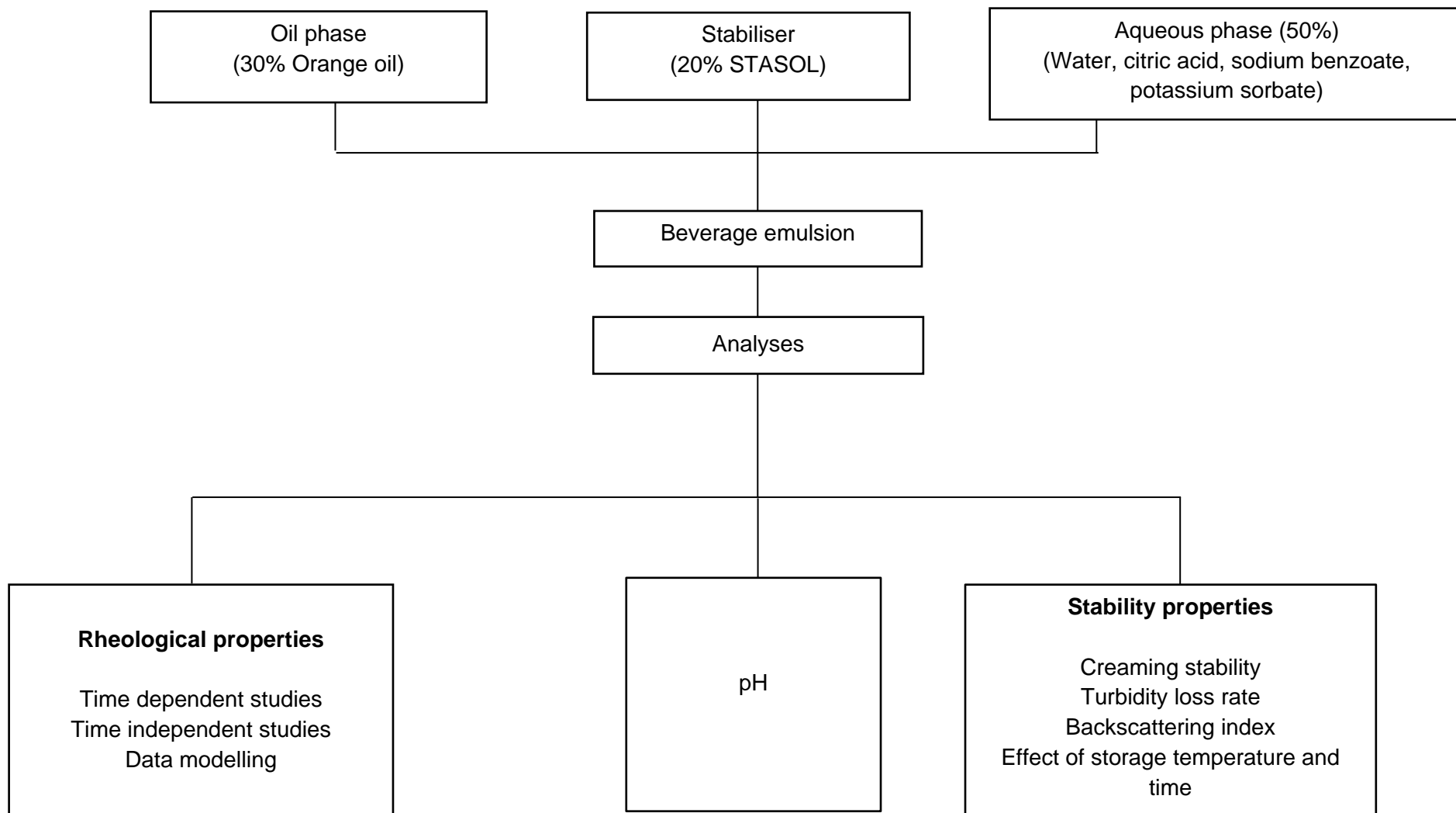


Figure 6.1 Outline of Chapter 6.
STASOL: Bambara groundnut starch-soluble dietary fibre nanocomposite.

2. Creaming stability

Emulsions were kept in test tubes at 20°C for 20 days. The separation of the emulsions into an opaque layer (cream) at the top and a turbid or transparent (serum) layer at the bottom, the total height of emulsion in the tubes (H_E) and the height of the serum layer (H_S) were measured. The extent of creaming, characterised by creaming index (CI) was calculated according to equation 6.1.

$$CI = \frac{H_S}{H_E} \quad \text{Equation 6.1}$$

6.2.4 Turbidity loss rate of STASOL stabilised emulsions

Emulsions were diluted to 0.25% (w/w) in a 10% sugar solution and stored at room temperature (20-25°C) in plastic bottles for 20 days (Gharibzahedi *et al.*, 2012). Absorbance readings were taken on emulsions stored at 5, 20 and 45°C on days 1, 3, 9, 15 and 20 using a temperature-controlled (20°C) UV-visible spectrophotometer (UV-1700 PharmsSpec, Shimadzu, Japan) at a wavelength of 500 nm. Plastic cuvettes were used (Macro PS, Lasec, 10X10X45 mm).

6.2.5 Effect of storage time and temperature on the pH of STASOL stabilised emulsions

The pH of STASOL stabilised emulsions was carried out on days 1, 3, 9, 15 and 20, on emulsions stored at 5, 20 and 45°C, by diluting 5 g of emulsion with 20 mL of deionised water. The pH of the diluted samples was measured by inserting the electrode of a Toledo Mettler pH meter directly into the sample. The equipment was calibrated with buffer solutions and pH readings were taken at 25°C.

6.2.6 Effect of storage time and temperature on the microstructure of STASOL stabilised emulsions

The microstructures of emulsions stored at 5, 20 and 45°C were assessed using a digital microscope (Olympus CX31 – U-CMAD3, Japan) mounted with a digital camera (Moticam BTW HD 1080, China) on days 1, 3, 9, 15 and 20. Each emulsion was diluted with deionised water at a ratio 1:3 (w/w), [emulsion:water] to avoid overlapping of oil droplets. A single drop of each diluted emulsion was placed on a microscope slide, covered with a coverslip and observed at 100X magnification. Images were recorded using an android tablet (Proline Android H10888M).

6.2.7 Effect of storage time and temperature on the droplet sizes of STASOL stabilised emulsions emulsions

Droplet sizes of STASOL stabilised emulsions stored at 5, 20 and 45°C were assessed on days 1, 3, 9, 15 and 20 using images obtained from the emulsions discussed in section 6.2.6. The diameters of the oil droplet were measured individually using the Proline Android H10888M software, and a mean was obtained.

6.2.8 Data analysis

All experiments were carried out in triplicate. Data were expressed as mean \pm standard deviation. For statistical analysis, IBM Statistical Package for the Social Science (IBM, 2016) was used. The results were subjected to multivariate analysis of variance (MANOVA) to determine mean differences between treatments. Duncan's multiple range tests were conducted to separate means where differences existed ($p \leq 0.05$).

6.3 Results and Discussion

6.3.1 Effect of storage time and temperature on stability of STASOL stabilised emulsions

STASOL stabilised beverage emulsions were stored at 5, 20 and 45°C and their stability was assessed over 20 days. Emulsions stored at 5, 20 and 45°C were photographed on the third day and the images are presented in Figure 6.2.

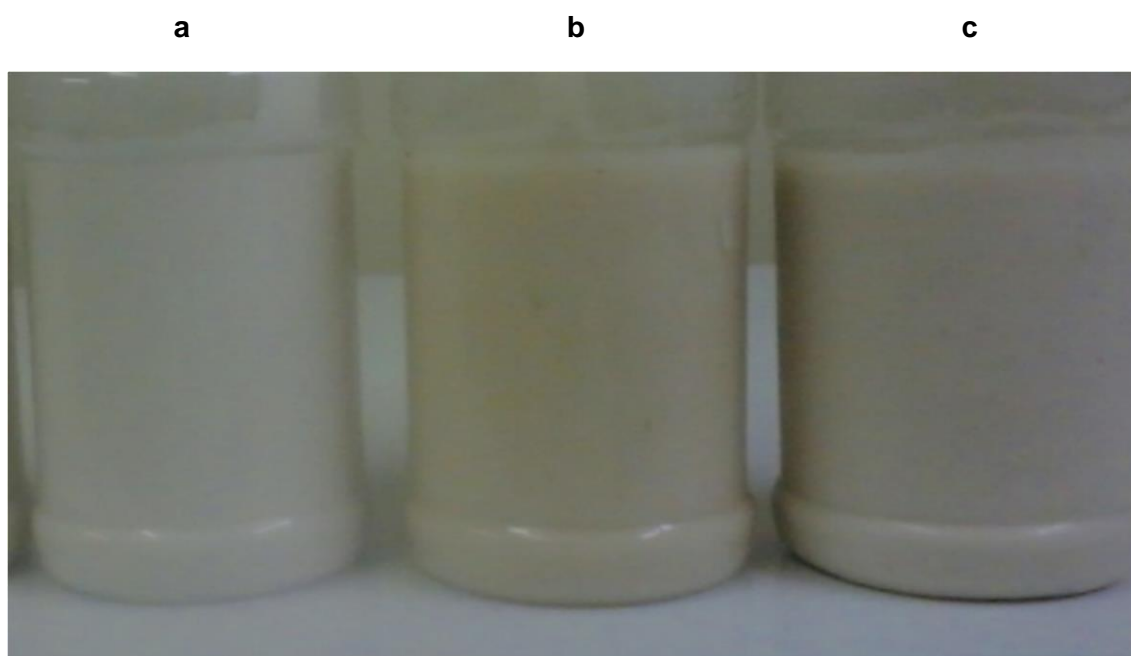


Figure 6.2 Bambara groundnut starch-soluble dietary fibre nanocomposite (STASOL) stabilised emulsions stored at (a) 5°C, (b) 20°C and (c) 45°C on day 3.

The emulsions stored at 20 and 45°C had started discolouring on day 3, while no colour change was observed on the emulsion stored at 5°C.

1. *Turbiscan stability of STASOL stabilised emulsions*

Figures 6.3 show the effect of time (20 days) and temperature (5, 20 and 45°C) on the physical stability of STASOL stabilised emulsions. For all emulsions, scans did not overlay perfectly indicating destabilisation over time. The backscattering profile of the emulsions stored at 5°C showed the least separation between scans during the storage period as shown in Figure 6.3a. The low refrigeration temperatures slowed down the rate of microbial activity and chemical reactions in food products. As such, the emulsions maintained their stability more than the ones stored at room temperature (20°C) and elevated temperature (45°C). The destabilisation of emulsions was attributed to phenomena involving droplet aggregation such as coalescence and flocculation. These phenomena manifest as a continuous increase or decrease in backscattering in the middle of the Turbiscan tube, in the 20-40 mm zone.

The extent of destabilisation is dependent on the size of oil droplets within an emulsion. When oil droplets are larger than the wavelength of the light source, there is a larger distance between oil droplets therefore backscattering decreases due to the increase in the mean path of photons (Adeyi, 2014). Sedimentation and creaming were excluded as possible destabilisation mechanisms of STASOL stabilised emulsions because the separation was not observed in the lower (0-20 mm) and top (50-60 mm) regions of the Turbiscan tube. The behaviour displayed by the emulsions stored at 5°C was in agreement with the results reported by Kiokias *et al.* (2004) where high stability of whey-protein-stabilised emulsions held at 5°C was observed.

Emulsions stored at 20°C showed noticeable disintegration with storage time as shown by visibly separated scans in Figure 6.3b. Destabilisation was observed on day 3 and it progressed throughout the storage time. The increased deterioration compared to emulsions stored at 5°C could be attributed to the fact that room temperature is conducive for the proliferation of mesophiles and the progression of chemical reactions (Tortora *et al.*, 2016). These factors could be mostly responsible for the destabilisation observed in the emulsions.

Emulsions stored at 45°C showed the most destabilisation as shown by the scans in Figure 6.3c. The noticeable separation between scans was observed from day 3, symbolising more destabilisation with increasing storage time. Elevated temperatures accelerate the rate of chemical reactions and the kinetic energy of oil droplets within emulsion systems. As a result, the migration speed of oil droplets increased and coalescence, as well as flocculation, occur at a faster rate, subsequently resulting in the loss of stability.

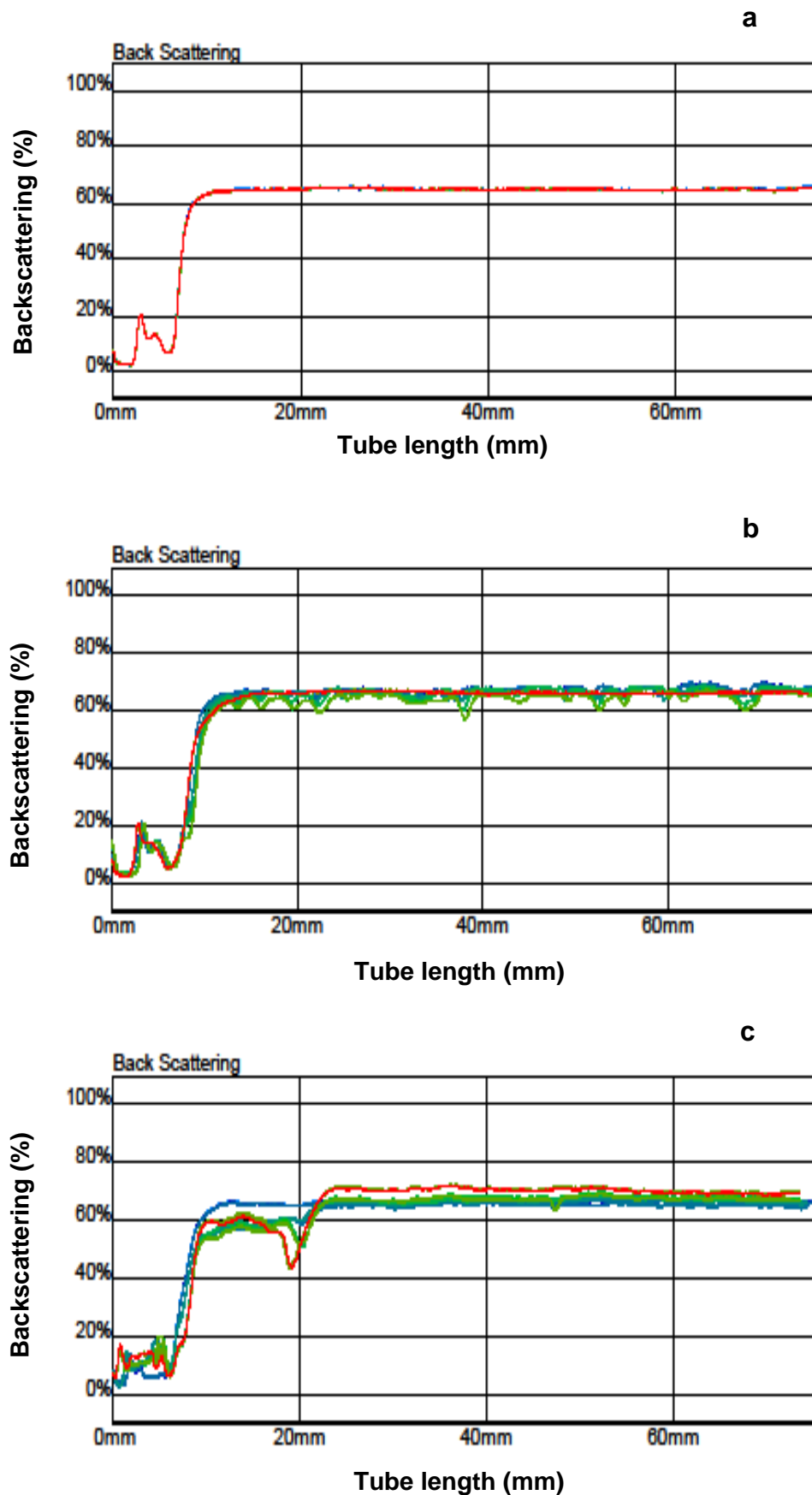


Figure 6.3 Changes in the backscattering profile as a function of sample height of emulsions stored at a) 5°C, b) 20°C and c) 45°C for 20 days.

The elevated storage temperature could have also contributed to the breakdown of the structure of STASOL, leading to a less viscous system. With decreased viscosity, droplet migration increases and destabilisation is accelerated (Goncalves & Campos, 2009). Furthermore, the oxidation of orange oil could have contributed to the destabilisation of emulsions. Orange oil contains high amounts of limonene (94%), a thermally unstable compound that is easily oxidised to a brownish colour (Ren *et al.*, 2018). The backscattering results in this study were in agreement with the literature. Adeyi (2014) studied the stability of oil-in-water emulsions stored at different temperatures over 20 days and reported the highest and least physical stability for emulsions stored at 5 and 45°C, respectively.

Figure 6.4 shows the variation in oil droplet aggregation kinetics in the middle of the Turbiscan tube (20-40 mm zone) monitored over 20 days for samples stored at 5, 20 and 45°C.

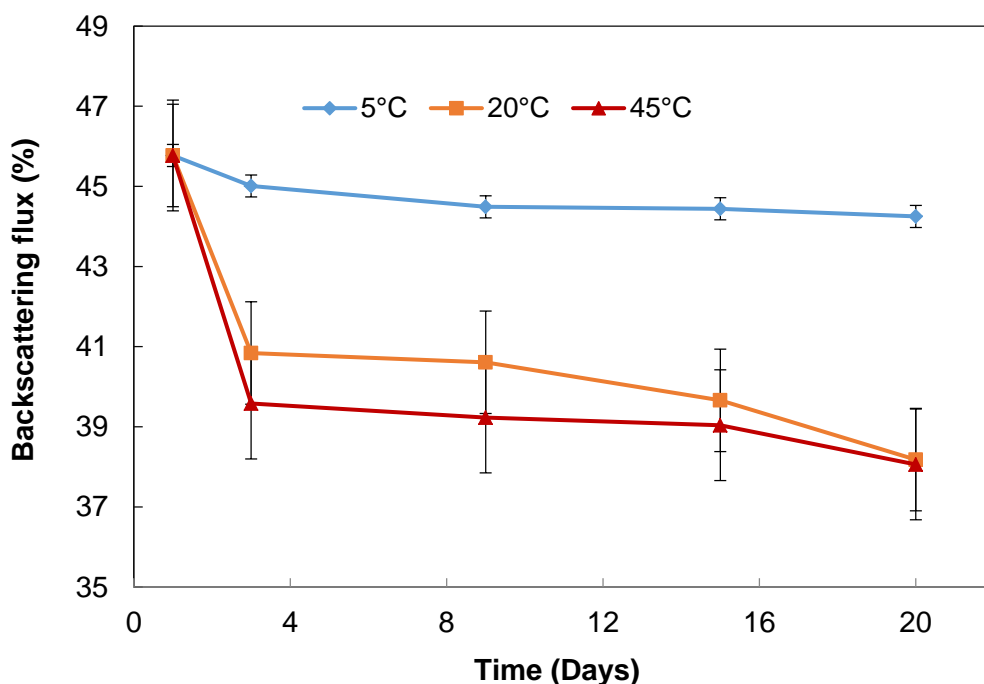


Figure 6.4 Variation in backscattering in the 20-40 mm zone monitored over 20 days for samples stored at 5, 20 and 45°C.

These reference graphs provide information necessary to predict the stability of emulsions over a very long time such as during storage and distribution in the industry. It was observed that both temperature and time affected the extent of destabilisation, with emulsions stored at 5 and 45°C showing the least and most destabilisation with increasing time, respectively. For all emulsions, there was a decrease in backscattering with increasing storage time.

By day 3, all the emulsions had begun destabilising with the emulsions stored at 45°C showing the most destabilisation. Throughout the storage period, emulsion destabilisation proceeded to increase, as shown by the decrease in backscattering flux percentage. The emulsion stored at 5°C maintained its stability the most throughout the 20 day storage period, which concurred with the results illustrated in Figure 6.3a.

It was presumed that low temperatures, apart from inhibiting microbial growth, thickened the emulsion system and therefore retarded the agglomeration of oil droplets hence maintaining stability over time (Adeyi, 2014). STASOL was the stabilising component in all emulsion systems. Stabilisers are defined by Maphosa (2016) as macromolecules that retard droplet migration by thickening the continuous phase. The structural integrity of STASOL was hugely affected by the temperature of storage. The physical stability of emulsions depends on the low chemical and microbial activity with lower temperatures decreasing the rate of both reactions (Dickinson, 2009). Several literature studies were in agreement with the results of this study. Adeyi (2014) reported a high destabilisation rate of BGN flour stabilised oil-in-water emulsions stored at 45°C compared to similar emulsions stored at 5 and 20°C. Kiokias *et al.* (2004) reported high stability of whey-protein-stabilised oil-in-water emulsions stored at 5°C.

2. Creaming stability of STASOL stabilised emulsions

The creaming index is an indirect indicator of the extent of droplet aggregation, with a smaller value indicating a smaller amount of agglomerated droplets (Onsaard *et al.*, 2006; Garcia *et al.*, 2012). Creaming in emulsions is observed as a transparent layer (serum) at the bottom and an opaque layer (cream) at the top of the tube (Maphosa & Jideani, 2018). The creaming indexes of STASOL stabilised emulsions stored at 5, 20 and 45°C for 20 days are presented in Table 6.1.

Table 6.1 Creaming stability of STASOL* stabilised emulsions

Days	Creaming index (%)		
	5°C	20°C	45°C
1	0 ± 0 ^a	0 ± 0 ^a	0 ± 0 ^a
3	0 ± 0 ^a	0 ± 0 ^a	27 ± 0 ^b
9	2 ± 0 ^a	10 ± 0 ^a	73 ± 0 ^c
15	5 ± 0 ^a	20 ± 0 ^a	73 ± 0 ^c
20	5 ± 0 ^a	63 ± 0 ^b	73 ± 0 ^c

*STASOL: Bambara groundnut starch-soluble dietary fibre nanocomposite. Values are mean ± standard deviation. Means within a column followed by different superscripts are significantly [$p \leq 0.05$] different.

There was no significant difference in the creaming indexes of emulsions stored at 5°C throughout the storage period. The creaming index of emulsions stored at 20°C increased significantly ($p = 0.000$) on day 20 while that of emulsions stored at 45°C increased significantly ($p = 0.000$) on day 3. On day 20, the creaming indexes of emulsions stored at 5, 20 and 45°C differed significantly ($p = 0.000$) and were 5, 63 and 73%, respectively. The least separation between layers was observed in the emulsions stored at 5°C compared to those stored at 20 and 45°C. Therefore, refrigeration effectively slowed down the destabilisation of emulsions. This was in agreement with Turbiscan studies discussed in section 6.3.1. Clear separation in emulsions stored at 20°C was observed on day 9 with a creaming index of 10% (Table 6.1). This observation was in fair agreement with the results of Moschakis *et al.* (2010) and Kuhn & Cuhna (2012). The former reported lack of creaming in Gum Arabic stabilised sunflower oil emulsions stored for 7 days at 20°C and the latter reported lack of creaming in whey-protein-isolate stabilised flaxseed oil emulsions stored for 9 days at 20°C. The higher destabilisation rates of emulsions stored at room temperature than refrigeration temperature could be attributed to chemical degradation such as the oxidation and breakdown of citric acids of orange oil droplets (Ren *et al.*, 2018).

Emulsions stored at 45°C had a creaming index of 27% on day 3 and 73% on day 9. The relatively fast destabilisation rate could be due to the thermal structural damage of STASOL molecules, resulting in the breakage of the long STASOL chains into shorter ones (Juttulapa *et al.*, 2016). Consequently, the emulsion system would be less viscous, oil droplets would quickly migrate to the top of the tube owing to buoyancy and biopolymer stabilising properties would be reduced (Choi *et al.*, 2014). The separation of layers as observed in Figures 6.2-6.4 and the creaming indexes (Table 6.1) of all emulsions increased with increasing storage time. At the end of the study (day 20), the emulsions stored at 5°C showed the least separation of phases while those stored at 45°C had completely separated into two distinct layers, with a creaming index of 73%. It was concluded that all the oil in the emulsions stored at 45°C had completely separated because by day 9, the creaming index was 73% and remained constant until the end of the storage period. STASOL stabilised emulsions contained 30% orange oil; therefore a creaming index of 73% suggested complete separation of phases.

The results of this study corresponded with the reports of Juttulapa *et al.* (2016) who reported increased creaming indexes for zein and pectin stabilised emulsions exposed to 40°C compared to those kept at room temperature. Furthermore, the creaming stability results of this study were in agreement with physical stability measurements [section 6.3.1 (1)] where it was established that emulsions stored at 5 and 45°C had the highest and lowest stability with increased storage time, respectively.

6.3.2 Turbidity loss of STASOL stabilised emulsions

Turbidity loss rate assesses the changes in cloud stability of emulsions in diluted form (Mirhosseini *et al.*, 2008). A higher amount of turbidity loss indicates higher instability and suggests that the emulsion in question would quickly lose its cloudiness in storage (Gharibzahedi *et al.*, 2012). Cloudiness is consumer acceptable in beverage emulsion products such as soft drinks (Homayoonfal *et al.*, 2015). Figure 6.5 shows the logarithm plots (Ln) of absorbance as an indicator of turbidity loss in STASOL stabilised emulsions stored at 5, 20 and 45°C for 20 days.

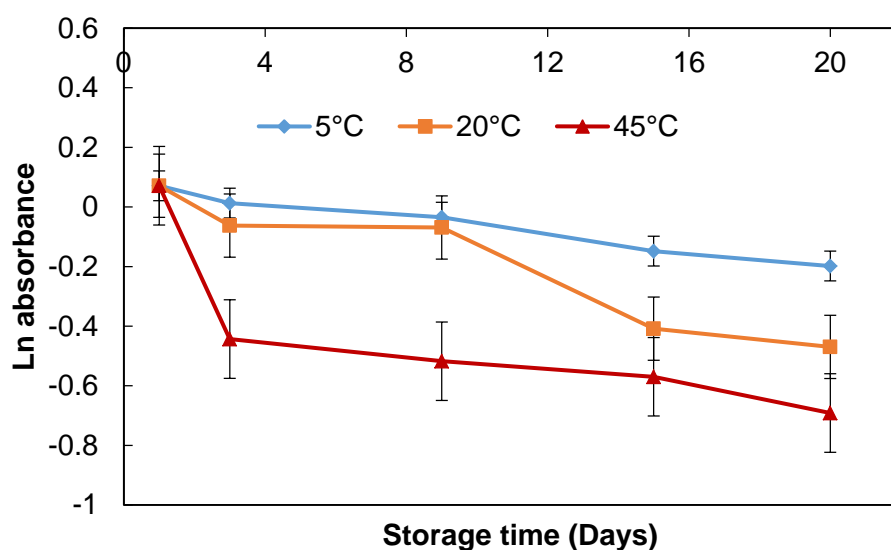


Figure 6.5 Turbidity loss of Bambara groundnut starch-soluble dietary fibre nanocomposite (STASOL) stabilised emulsions stored at 5, 20 and 45°C for 20 days.

Emulsions were diluted to a ratio of 1:400 (w/w), emulsion:sugar solution for easy analysis. In the food industry, concentrated beverage emulsions are diluted, with the finished product having about 20 mg/L oil phase (Reiner *et al.*, 2010). The absorbance of STASOL stabilised emulsions stored at 5, 20 and 45°C was 1.0737 at the beginning of the study and 0.8203, 0.6253 and 0.5009, respectively, on day 20. All emulsions showed a decrease in turbidity with increasing storage time as evidenced by the negative slopes. On the first 9 days, there was no significant difference in the turbidity of emulsions stored at 5 and 20°C. After the ninth day, the turbidity of the emulsions stored at 5°C decreased significantly ($p = 0.000$). There was no significant difference in the turbidity of emulsions stored at 20 and 45°C on days 15-20 while both were significantly ($p = 0.000$) different from the turbidity of the emulsions stored at 5°C. The loss of turbidity showed that the cloudiness of STASOL

stabilised emulsions decreased over time, and this was in agreement with the reports of several researchers (Gharibzahedi *et al.*, 2012).

The loss of turbidity in emulsions during storage can be attributed to the loss of STASOL around the film layers formed at the interfacial surface rendering STASOL weak hence reducing its stabilising efficiency. Turbidity loss could also be attributed to flocculation, coalescence and droplet aggregation which cause an increase in average droplet size which leads to destabilisation of emulsions (Mirhosseini *et al.*, 2008; Maphosa, 2016; Homayoonfal *et al.*, 2015). The observed turbidity loss concurred with the results of physical and creaming stability analyses (Section 6.3.1) where emulsions stored at 5°C exhibited the highest stability while emulsions stored at 45°C exhibited the least.

6.3.3 Effect of storage time and temperature on the pH of STASOL stabilised emulsions

Figure 6.6 shows the changes in the pH of STASOL stabilised emulsions stored at 5, 20 and 45°C for 20 days. The initial pH of all emulsions was 3.47 and on day 20, the pH of the emulsions stored at 5, 20 and 45°C had increased to 3.68, 3.77 and 4.05, respectively.

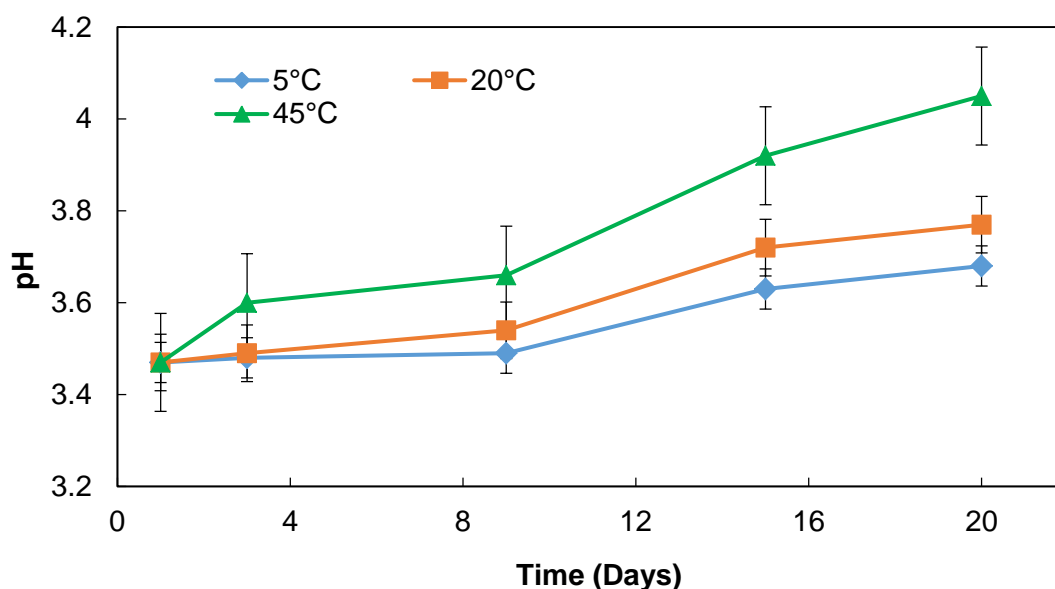


Figure 6.6 Change in pH of emulsions stored at 5, 20 and 45°C for 20 days.

The pH of all emulsions had significantly ($p = 0.000$) increased at the end of storage time (day 20). The pH on day 20 for the emulsions stored at 5 and 20°C did not differ significantly and both differed significantly ($p = 0.000$) from the pH on day 20 of the emulsions stored at 45°C. Food emulsions generally have pH between 2.5 and 7.5. Changes in pH indicate

chemical changes within a system (Campelo *et al.*, 2017). The pH of the studied emulsions increased with increasing storage time. For the first 9 days, the pH of emulsions stored at 5°C did not change significantly, increasing only by 0.02 (Figure 6.6) due to low storage temperatures significantly slowing down chemical reactions. On day 9, the pH of emulsions stored at 20 and 45°C had significantly ($p = 0.000$) increased to 3.60 and 4.05, respectively. Orange oil beverage emulsions are expected to have a pH lower than 4.5 (Tan, 1990), therefore the reported pH values in this study were desirable. Mirhosseini *et al.* (2008) reported the pH of orange oil emulsions stabilised with Gum Arabic and xanthan gum in the range 3.83-4.04. The cited values were related to those reported in the present study. Lower pH of orange oil emulsions are desirable as they result in reduced particle sizes, therefore increased stability (Zhao *et al.*, 2018).

The increase in pH of the emulsions with increasing storage time can be attributed to factors such as the breakdown of citric acid and acid hydrolysis of STASOL resulting in decreased acidity (Alaka *et al.* 2003; Rehman *et al.* 2014). An increase in pH of fruit juices over 30 days of storage was attributed to the acid hydrolysis of polysaccharides to monomers by Rehman *et al.* (2014). Furthermore, Alaka *et al.* (2003) reported an increase in the pH of guava juice with time which was in agreement with observations made in this study.

STASOL stabilised emulsions are orange-oil beverage emulsions and their end products include ready-to-drink beverages. Such drinks are generally acidic (Qian *et al.*, 2010). Higher pH values in the range 4-6 were reported for Gum Arabic stabilised lime essential oils emulsions (Campelo *et al.*, 2017). The differences of these values to those reported in this study could be attributed to different stabilisers and oil. The microorganisms that could have been responsible for any microbial breakdown in emulsions during storage are acidophiles. Some neutrophiles would still have been able to survive and proliferate but at a very slow rate because of the acidic pH (Tortora *et al.*, 2016).

6.3.4 Effect of STASOL and orange oil on droplet size and microstructure of STASOL stabilised emulsions

Figure 6.7 shows micrographs of STASOL stabilised emulsions stored at different temperatures for 20 days. The small droplets observed in the images represent orange oil droplets, the empty spaces represent the continuous phase and the strand-like clusters observed in some of the images possibly represent STASOL dispersed within the emulsion system. Small droplet sizes in emulsions are an indication of higher stability (Mirhosseini *et al.*, 2008). As storage time increased, the emulsions stored at 5°C maintained a relatively small droplet size compared to emulsions stored at 20 and 45°C. Low temperatures prolonged emulsion stability and agreed with stability and turbidity loss studies in sections 6.3.1 and 6.3.2, respectively.

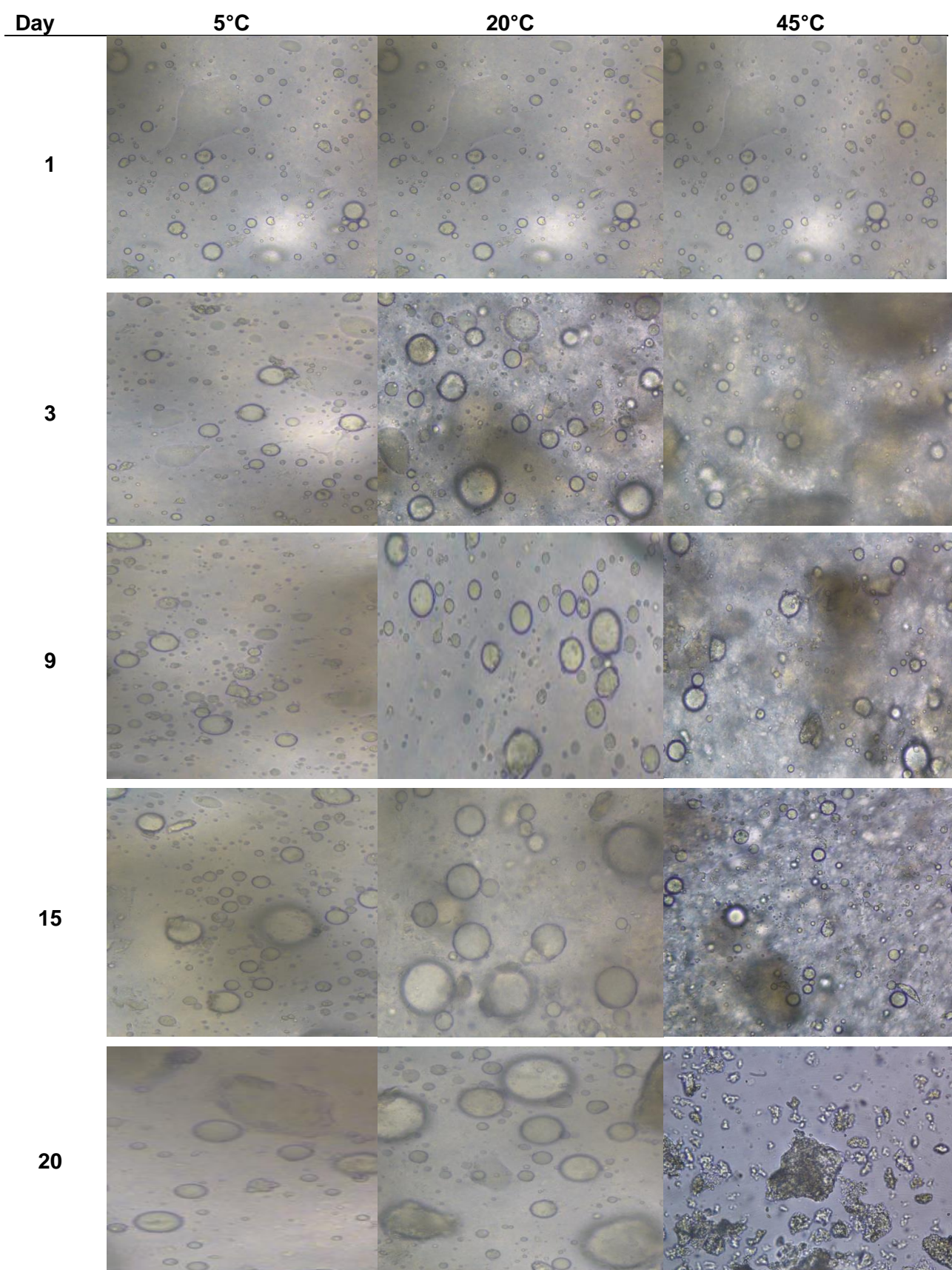


Figure 6.7 Microstructures of Bambara groundnut starch-soluble dietary fibre nanocomposite (STASOL) stabilised emulsions stored at 5, 20 and 45°C for 20 days.

With increasing storage time, coalescence and flocculation were observed. The former was observed as small oil droplets adsorbed on the surface of larger ones and the latter was observed as groups of oil droplets clumped together (Maphosa, 2016). This observation confirmed the physical stability results in section 6.3.2 (1) where the destabilisation phenomenon of STASOL stabilised emulsions was predicted to be droplet aggregation (flocculation and/or coalescence). At the end of the storage period (day 20), no droplets were observed in the micrograph of the emulsion stored at 45°C, confirming that oil had completely separated from the aqueous phase. The emulsion appeared burnt, and that could have been the reason for the appearance observed. This observation was in agreement with the creaming index results reported in section 6.3.1 (2) where the emulsions stored at 45°C had turned brown on day 20 due to possible caramelisation of sugars.

In chapter 4 (section 4.3.6) STASOL was reported to have a desirable oil binding capacity (OBC) and high solubility. Oil binding and solubility indexes of biopolymers affect their emulsion stabilising properties with higher OBCs binding the oil phase better (Adeyi, 2014) and those with higher solubility indexes binding the aqueous phase better. Stabilisers cover the temporary interface in emulsions preventing oil droplets from aggregating and therefore resulting in a lower droplet volume-surface mean diameter (Aveyard *et al.*, 2002). It was therefore concluded that STASOL adequately covered the temporary interface of orange oil droplets after manufacture and gradually disintegrated with time.

Figure 6.8 shows the mean diameters of droplets in STASOL stabilised emulsions stored at 5, 20 and 45°C.

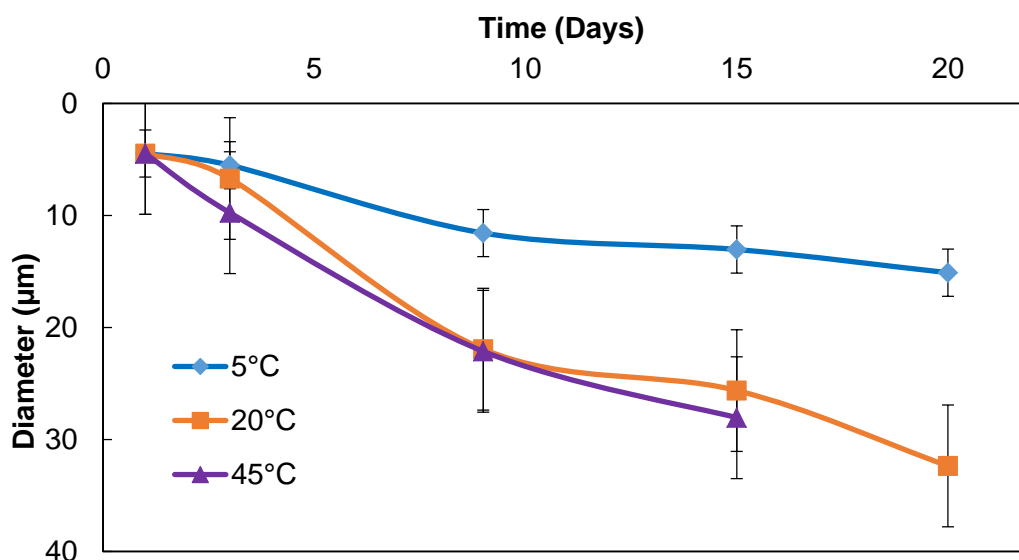


Figure 6.8 Droplet sizes of Bambara groundnut starch-soluble dietary fibre nanocomposite (STASOL) stabilised emulsions stored at 5, 20 and 45°C for 20 days.

The initial mean droplet size of emulsions stored at 5 and 20°C was 4.47 µm on day 1 and 15.11 and 32.36 µm, respectively, on day 20. The mean droplet sizes of all emulsions increased with increasing storage time. The emulsions stored at 5 and 45°C had the lowest and highest mean diameters throughout the 20 day storage period. Emulsions stored at 5 and 45°C for 20 days were the most and least stable, respectively. This indicated that the highest droplet volume characterised emulsions stored at 5°C because of their lowest droplet size (Chanamai *et al.*, 2000). The mean droplet size of emulsions stored at 45°C was 28.05 µm on day 15 and could not be determined on day 20 as the emulsion had burned, as shown in Figure 6.5. The mean droplet size of all emulsions had significantly ($p = 0.000$) increased at the end of storage time. From day 9, the mean droplet size of emulsions stored at 5°C differed significantly ($p = 0.000$) from those of the emulsions stored at 20 and 45°C. There was no significant difference between the mean droplet sizes of emulsions stored at 20 and 45°C throughout the storage period.

The addition of stabilisers to emulsions reduces their droplet sizes (Behrend *et al.*, 2000). Emulsions with smaller droplet sizes have relatively high strength and stable matrices. Among the three emulsions, those stored at 45°C would be expected to show the highest coalescence rate. Emulsions with larger droplet sizes exhibit a higher tendency to coalescence due to higher impact during the collision (Behrend *et al.*, 2000; Adeyi, 2014). These observations agreed with the results reported in the previous sections where emulsions stored at 5°C showed more stability over time while those at 45°C destabilised at a faster rate. It was evident that both storage time and temperature largely affected the stability of STASOL stabilised orange-oil beverage emulsions.

6.3.5 Effect of storage time and temperature on the hysteresis loop area of STASOL stabilised emulsions

Table 6.2 shows the Power Law model parameters of STASOL stabilised emulsions stored 5, 20 and 45°C for 20 days. The Power Law model was used to describe the flow behaviour of the emulsions over the storage period. Power Law consists of two parameters, namely the consistency coefficient (K) which describes the viscosity of a system and the flow behaviour index (n) which measures the reluctance of a fluid to flow and describes shear rate against shear stress (Maphosa, 2016). Low values of the consistency coefficient (K) indicate a low viscous solution and values of flow behaviour index (n) less than 1 indicate shear thinning behaviour (Rezvani *et al.*, 2011; Lim *et al.*, 2011; Adeyi, 2014).

At the beginning of the study, the consistency coefficient (K) and flow behaviour indexes (n) of the upward flow of all emulsions were 1.3943 Pa.s ^{n} and 0.1406, respectively, and at the end of the study (day 20), the consistency coefficient (K) and flow behaviour index (n) of all emulsions were 1.3958 Pa.s ^{n} and 0.0143, 11.4460 Pa.s ^{n} and 0.0269, 53.1800 Pa.s ^{n} and 0.0061 for 5, 20 and 45°C, respectively.

Table 6.2 Effect of storage time and temperature on Power law parameters and hysteresis loop area of the most stable emulsion

Day	K (Pas ⁿ)	n	R ²	K' (Pas ⁿ)	n'	R ²	HLA (Pas ⁻¹)
5°C							
1	1.3943 ± 0.14	0.1406 ± 0.08	0.7715	1.1338 ± 0.88	0.1307 ± 0.07	0.5848	8.09 ± 0.37
3	5.3512 ± 1.64	0.0398 ± 0.02	0.3890	4.7971 ± 2.78	0.0599 ± 0.03	0.5921	9.11 ± 1.20
9	9.3932 ± 3.09	0.0279 ± 0.01	0.4434	7.9657 ± 3.23	0.0323 ± 0.01	0.3541	35.72 ± 8.26
15	11.0991 ± 1.11	0.0242 ± 0.02	0.4371	10.237 ± 1.23	0.0259 ± 0.02	0.4401	22.32 ± 5.58
20	13.9580 ± 4.37	0.0143 ± 0.01	0.2800	11.9410 ± 4.21	0.0232 ± 0.01	0.3441	48.37 ± 4.71
20°C							
1	1.3943 ± 0.14	0.1406 ± 0.01	0.7715	1.1340 ± 0.88	0.1307 ± 0.01	0.5848	8.09 ± 0.37
3	2.4011 ± 1.15	0.0955 ± 0.05	0.6995	2.0562 ± 1.00	0.0893 ± 0.01	0.5333	10.03 ± 1.37
9	5.2990 ± 2.50	0.0516 ± 0.04	0.6160	3.9864 ± 1.70	0.0572 ± 0.03	0.4725	34.94 ± 1.16
15	8.4283 ± 1.42	0.0351 ± 0.02	0.5761	8.3879 ± 1.10	0.0308 ± 0.02	0.4464	77.52 ± 1.88
20	11.4460 ± 7.00	0.0269 ± 0.02	0.5572	10.6020 ± 3.09	0.0226 ± 0.01	0.4250	80.15 ± 2.05
45°C							
1	1.3943 ± 0.14	0.1406 ± 0.01	0.7715	1.1340 ± 0.88	0.1307 ± 0.07	0.5848	8.09 ± 0.37
3	14.0230 ± 6.59	0.0251 ± 0.02	0.5638	13.633 ± 5.42	0.0226 ± 0.01	0.5128	11.49 ± 1.89
9	26.8510 ± 4.41	0.0105 ± 0.00	0.6161	24.8830 ± 9.23	0.0108 ± 0.01	0.4092	51.18 ± 1.98
15	34.8370 ± 2.91	0.0101 ± 0.00	0.5561	30.8930 ± 1.57	0.0122 ± 0.00	0.3201	100.38 ± 3.02
20	53.1800 ± 9.12	0.0061 ± 0.00	0.5325	50.8580 ± 7.87	0.0073 ± 0.00	0.5132	58.54 ± 5.23

Values are mean ± standard deviation. K: Consistency coefficient; n: Flow behaviour index; R²: Coefficient of determination; HLA: Hysteresis loop area.

At the beginning of the study, the consistency coefficient (K) and flow behaviour index (n) of the downward flow of all emulsions were 1.1338 Pa.sⁿ and 0.1307, respectively, and at the end of the study (day 20), the consistency coefficient (K) and flow behaviour index (n) of all emulsions were 11.9410 Pa.sⁿ and 0.0232, 10.6020 Pa.sⁿ and 0.0226, 50.8580 Pa.sⁿ and 0.0073 for 5, 20 and 45°C, respectively. The consistency coefficient (K) of all emulsions decreased with increasing storage time. All emulsions were shear thinning as indicated by flow behaviour indexes (n) having values less than 1. According to Guillon & Champ (2000), the viscosities of polysaccharides are dependent on temperature, with higher temperatures resulting in lower viscosities.

Figure 6.9 shows the hysteresis loop curves of STASOL stabilised emulsions stored at 5, 20 and 45°C for 20 days. The hysteresis loop area is an indication of structural breakdown with increasing shearing time and it provides information on the structure and behaviour of emulsions over prolonged periods of mixing (shear) and storage time (Adeyi, 2014).. The presence of space between the forward and backward curves of all emulsions indicated structural damage in all emulsions (Maphosa *et al.*, 2017). The rheograms in Figure 6.9 indicated that structural damage occurred at an accelerated rate at elevated temperatures than refrigeration temperatures which were in agreement with stability and microstructural studies.

6.3.6 Effect of storage time and temperature on the minimum apparent viscosity of STASOL stabilised emulsions

Figure 6.10 shows the change in the minimum apparent viscosity of STASOL stabilised emulsions stored at 5, 20 and 45°C for 20 days. Both time and temperature affected the viscosities of the emulsions. The initial apparent viscosity of the emulsions stored at 5, 20 and 45°C ranged from 0.51-0.36, 0.51-0.18 and 0.51-0.12 Pas, respectively, for days 1 and 20. All emulsions showed a decrease in viscosity with storage time with the emulsions stored at 5°C preserving their characteristics the most. The viscosity of emulsions stored at 5°C started significantly ($p = 0.000$) decreasing after day 9 while that of emulsions stored at 20 and 45°C significantly ($p = 0.000$) decreased after day 3. On all days, the viscosity of the emulsions stored at 5°C was highest and those stored at 45°C was the lowest. Elevated temperatures decrease the viscosity of the continuous phase by breaking down the stabiliser hence the viscosity of emulsions stored at 45°C decreased at a faster rate than those stored at lower temperatures (Goncalves & Maia Camos, 2009). However, thermal studies (Chapter 3, section 3.3.9) indicated high thermal stability of STASOL. This disconnect could be because thermal studies in Chapter 3 only evaluated the stability of STASOL once-off, immediately after production and not within an emulsion system. As such, it could be a possibility that STASOL disintegrated with time at lower temperatures than reported by the thermal studies.

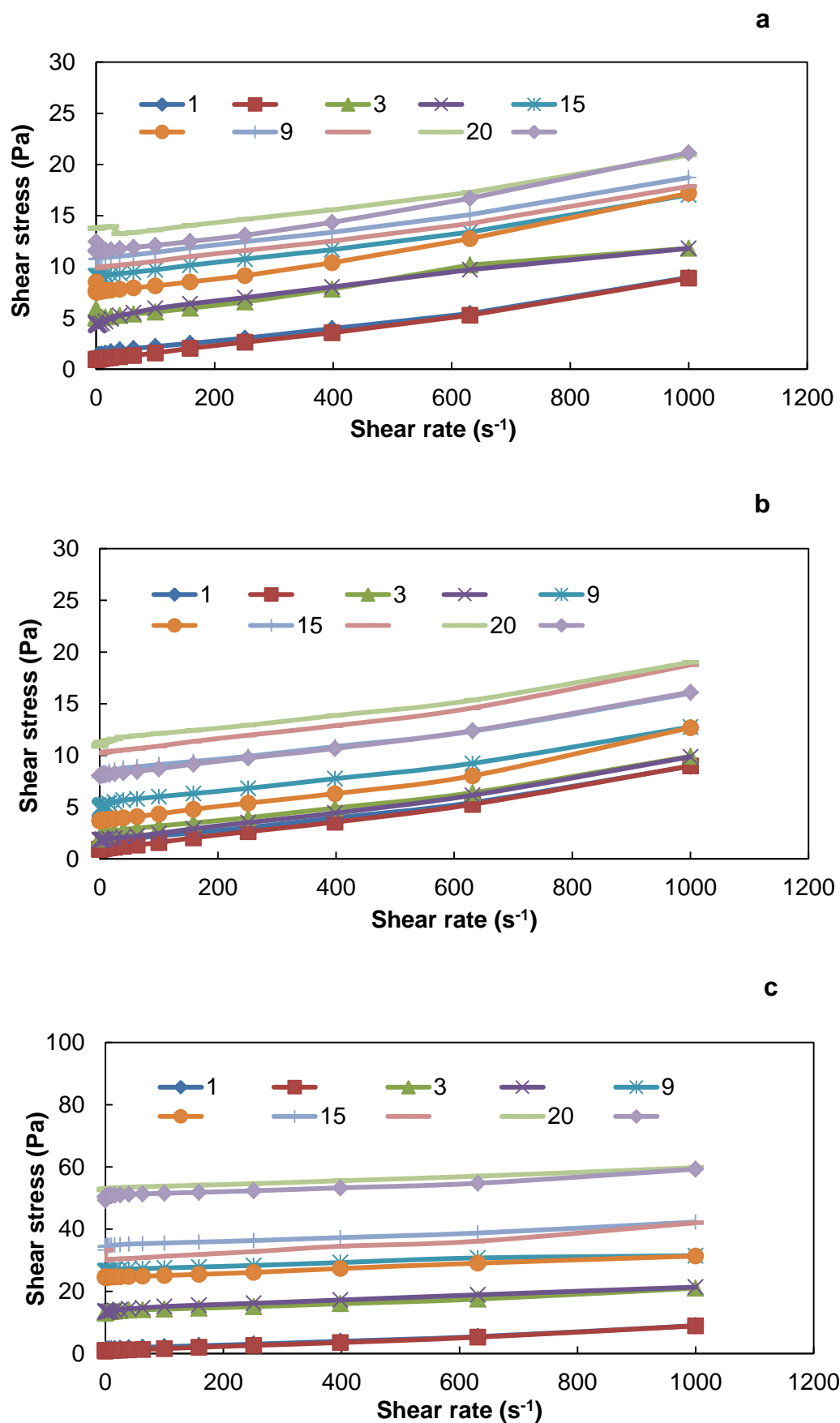


Figure 6.9 Hysteresis loop areas of Bambara groundnut starch-soluble dietary fibre nanocomposite (STASOL) stabilised emulsions stored at (a) 5°C, (b) 20°C and (c) 45°C for 20 days.

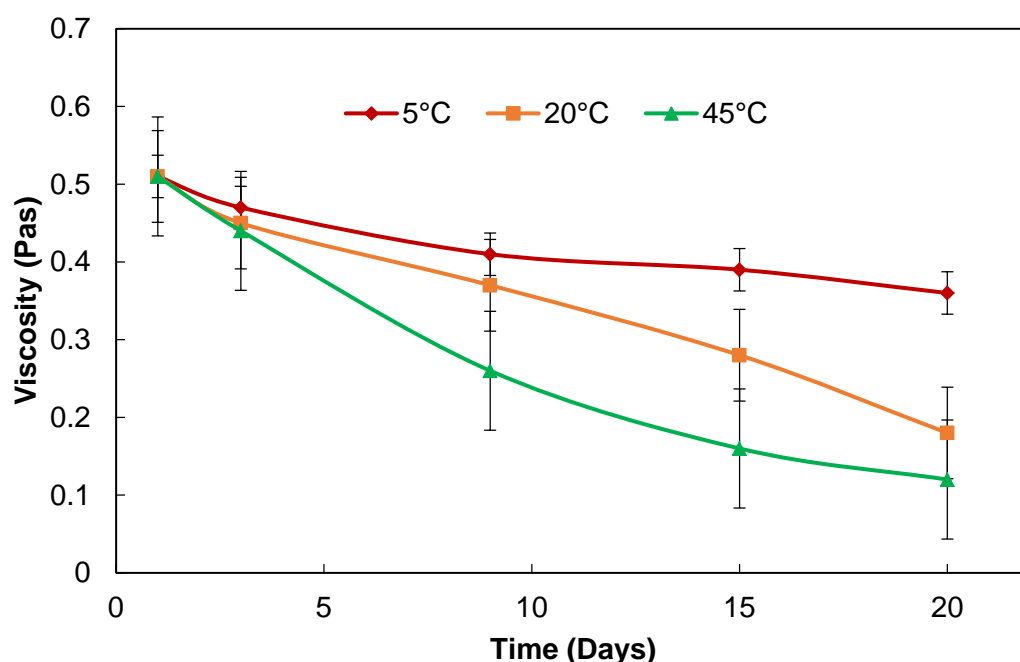


Figure 6.10 Apparent viscosity of STASOL stabilised emulsions stored at 5, 20 and 45°C for 20 days.

The decrease in viscosity of emulsions stored at 20°C could be assumed to be mainly due to microbial action as room temperature is the optimum growth temperature of many microorganisms (Tortora *et al.*, 2016). Microorganisms would have weakened the structure of the emulsion systems by breaking down STASOL thus weakening the matrix, reducing the resistance to flow.

6.4 Conclusions

The effect of storage time and temperature on the rheological and stability properties of STASOL stabilised emulsions was successfully investigated. The rate of disintegration of STASOL and the subsequent loss of stability increased with increasing temperature and storage time for all emulsions. By the third day, all emulsions had started to destabilise, with emulsions stored at 5°C exhibiting minimal destabilisation and maintaining superior rheological properties than those stored at 20 and 45°C. This was attributed to the reduction in kinetic energy of droplets at low temperatures thereby decreasing their migration rate through the emulsion and consequently reducing their rate of coalescence and flocculation. The decrease in viscosity of emulsions stored at 20°C was due to room temperature being conducive for chemical reactions and the proliferation of many microorganisms. Hence, at 20°C, microbial degradation of the structure of STASOL resulted in decreased viscosity and

loss of stability. The emulsion stored at 45°C showed the most destabilisation throughout the storage period, attributed to the elevated storage temperature. As temperature increases, the excitement of molecules also increases, resulting in higher kinetic energy of molecules. Therefore, at 45°C the increasing mobility of droplets within the emulsion system coupled with the thermal disintegration of STASOL led to the decrease in viscosity of the continuous phase and the subsequent destabilisation. Emulsions stabilised with STASOL would have a longer shelf life when stored at low temperatures. Therefore, refrigeration storage of these emulsions is highly recommended. The inclusion of preservatives in STASOL stabilised emulsions is expected to further increase their shelf life. As such, future studies could look into the storage stability of STASOL stabilised emulsions across a wide range of low temperatures, including frozen storage, as well as with different preservatives, to determine their best storage temperature.

References

- Adeyi, O. (2014). Effect of Bambara Groundnut flour on the stability and rheological properties of oil-in-water emulsion. PhD Thesis, Cape Peninsula University of Technology.
- Alaka, O.O., Aina, J. O. & Falade, K.O. (2003). Effect of storage conditions on the chemical attributes of ogbomoso mango juice. *European Food Research Technology*, **37(6)**, 213-217.
- Aveyard, R., Bink, B.P. & Clint, J.H. (2002). Emulsions stabilised solely by colloidal particles. *Advances in Colloid and Interface Science*, **100-102**, 503-546.
- Campelo, P.H., Junqueira, L.A., de Resende, J.V., Zacarias, R.D., de Barros Fernandes, R.V., Botrel, D.A. & Borges, S.V. (2017). Stability of lime essential oil emulsion prepared using biopolymers and ultrasound treatment. *International Journal of Food Properties*, **20(1)**, S564-S579.
- Cha, Y., Shi, X., Wu, F., Zou, H., Chang, C., Guo, Y., Yuan, M. & Yu, C. (2019). Improving the stability of oil-in-water emulsions by using mussel myofibrillar proteins and lecithin as emulsifiers and high-pressure homogenization. *Journal of Food Engineering*, **258**, 1-8.
- Chanamai, R. & McClements, D.J. (2000). Impact of weighting agents and sucrose on gravitational separation of beverage emulsions. *Journal of Agricultural and Food Chemistry*, **48**, 5561-5565.
- Choi, S.J., Decker, A.E., Henson, L., Popplewell, M., Xiao, H. & McClements, D.J. (2011). Formulation and properties of model beverage emulsions stabilized by sucrose onopalmitate: Influence of pH and lyso-lecithin addition. *Food Research International*, **44(9)**, 3006-3012.

- Choi, S.J., Won, J.W., Park, K.M. & Chang, P. (2014). A new method for determining the emulsion stability index by backscattering light detection. *Journal of Food Process Engineering*, **37**(3), 229-236.
- Dickinson, E. (2001). Milk protein interfacial layers and the relationship to emulsion stability and rheology. *Colloids and Surfaces B: Biointerfaces*, **20**(3), 197-210.
- Dickinson, E. (2009). Hydrocolloids as emulsifiers and emulsion stabilizers. *Food Hydrocolloids*, **23**, 1473-1482.
- Fujisawa, S., Togawa, E. & Kuroda, K. (2017). Facile Route to Transparent, Strong, and Thermally Stable Nanocellulose/Polymer Nanocomposites from an Aqueous Pickering Emulsion. *Biomacromolecules*, **18**(1), 266-271.
- Garcia, L.C., Tonon, R.V. & Hubinger, M.D. (2012). Effect of homogenization pressure and oil load on the emulsion properties and the oil retention of microencapsulated basil essential oil (*Ocimumbasilicum* L.). *Drying Technology*, **30**(13), 1413-1421.
- Gharibzahedi, S.M.T., Mousavi, S.M., Hamed, M. & Ghasemlou, M. (2012). Response surface modeling for optimization of formulation variables and physical stability assessment of walnut oil-in-water beverage emulsions. *Food Hydrocolloids*, **26**, 293-301.
- Gomez-Romero, J., Garcia-Pena, I., Ramirez-Munos, J. & Torres, L.G. (2014). Rheological characterisation of a mixed fruit/vegetable puree feedstock for hydrogen production by dark fermentation. *Advances in Chemical Engineering and Science*, **4**(1), 81-88.
- Goncalves, G.M.S. & Maia Camos, P.M.B.G. (2009). Shelf life and rheology of emulsions containing vitamin C and its derivatives. *Journal of Basic and Applied Pharmaceutical Sciences*, **30**(2), 89-94.
- Guillon, F. & Champ, M. (2002). Structural and physical properties of dietary fibres, and consequences of processing on human physiology. *Food Research International*, **33**, 233-245.
- Homayoonfal, M., Khodaiyan, F. & Mousavi, M. (2015). Modelling and optimising of physicochemical features of walnut-oil beverage emulsions by implementation of response surface methodology: Effect of preparation conditions on emulsion stability. *Food Chemistry*, **174**, 649-659.
- IBM Corp. (2016). IBM Statistical Package for the Social Science (SPSS), Statistics for Windows, Version 22.0. Armonk, NY: IBM Corp.
- Jiao, J. & Burgess, D.J. (2003). Ostwald ripening of water-in-hydrocarbon emulsions. *Journal of Colloid and Interface Science*, **264**(2), 509-516.
- Juttulapa, M., Piriyaprasarth, S., Takeuchic, H. & Sriamornsak, P. (2017). Effect of high-pressure homogenization on stability of emulsions containing zein and pectin. *Asian Journal of Pharmaceutical Sciences*, **12**(1), 21-27.

- Kerkhofs, S., Lipkens, H., Velghe, F., Verlooy, P., Martens, J.A. (2011). Mayonnaise production in batch and continuous process exploiting magnetohydrodynamic force. *Journal of Food Engineering*, **106(1)**, 35-39.
- Kiokias, S., Reiffers-Magnani, C.K. & Bot, A. (2004). Stability of whey-protein-stabilised oil-in-water emulsions during chilled storage and temperature cycling. *Journal of agriculture and food chemistry*, **52(12)**, 3823-3830.
- Kuhn, K.R. & Cunha, R.L. (2012). Flaxseed oil - whey protein isolate emulsions: effect of high pressure homogenization. *Journal of Food Engineering*, **111(2)**, 449-457.
- Lim, S.S., Baik, M.Y., Decker, E.A., Henson, L., Michael Popplewell, L., McClements, D.J. & Choi, S.J. (2011). Stabilization of orange oil-in-water emulsions: A new role for ester gum as an Ostwald ripening inhibitor. *Food Chemistry*, **128(4)**, 1023-1028.
- Mao, L. & Miao, S. (2015). Structuring food emulsions to improve nutrient delivery during digestion. *Food Engineering Reviews*, **7**, 439-451.
- Maphosa, Y. (2016). Characterisation of Bambara groundnut (*Vigna Subterranea* (L) Verdc.) non-starch polysaccharides from wet milling as prebiotics. Master of Technology Thesis, Cape Peninsula University of Technology.
- Maphosa, Y., Jideani, V.A. & Adeyi, O. (2017). Effect of soluble dietary fibres from Bambara groundnut varieties on the stability of orange oil beverage emulsion. *African Journal of Science, Technology, Innovation and Development*, **9**, 69-76.
- Maphosa, Y. & Jideani, V. A. (2018). Factors Affecting the Stability of Emulsions Stabilised by Biopolymers, Chapter 5 in Science and Technology Behind Nanoemulsions. (Editor: Selcan Karakuş). DOI: 10.5772/intechopen. 75308.
- McClements, D.J. (2005). Emulsions. In: *Food Emulsions Principles, Practices, and Techniques*. 2nd Ed. Boca Raton: CRC Press.
- Mirhosseinia, H., Tan, C.P., Hamid, N.S.A. & Yusof, S. (2008). Effect of Arabic gum, xanthan gum and orange oil contents on ζ -potential, conductivity, stability, size index and pH of orange beverage emulsion. *Colloids and Surfaces A Physicochemical and Engineering Aspects*. **315(1-3)**, 47-56.
- Molet-Rodríguez, A., Salvia-Trujillo, L. & Martín-Belloso, O. (2018). Beverage emulsions: key aspects of their formulation and physicochemical stability. *Beverages*, **4(70)**, 1-10.
- Moschakis, T., Murray, B.S. & Biliaderis, C.G. (2010). Modifications in stability and structure of whey protein-coated o/w emulsions by interacting chitosan and gum arabic mixed dispersions. *Food Hydrocolloids*, **24(1)**, 8-17.
- Onsaard, E., Vittayanont, M., Srigam, S. & McClements, D.J. (2006). Comparison of properties of oil-in-water emulsions stabilized by coconut cream proteins with those stabilized by whey protein isolate. *Food Research International*, **39(1)**, 78-86.
- Payet, L. & Terentjev, E.M. (2008). Emulsification and stabilization mechanisms of O/W emulsions in the presence of chitosan. *Langmuir*, **24(21)**, 12247-12252.

- Qian, C., Decker, E.A., Xiao, H. & McClements, D.J. (2011). Comparison of biopolymer emulsifier performance in formation and stabilization of orange oil-in-water emulsions. *Journal of the American Oil Chemists' Society*, **88**, 47-55.
- Rehman, M.A., Khan, M.R., Sharif, M.K., Shabbir, A. & Shah, F. (2014). Study on the storage stability of fruit juice concentrates. *Pakistan Journal of Food Sciences*, **24(2)**, 101-107.
- Reiner, S.J., Reineccius, G.A. & Peppard, T.L. (2010). A Comparison of the stability of beverage cloud emulsions formulated with different Gum Acacia- and starch-based emulsifiers. *Journal of Food Science*, **75**, 236-246.
- Ren, J.N., Zhang, Y., Fan, G., Wang, M.P., Zhang, L.L., Yang, Z.Y. & Pan, S.Y. (2018). Study on the optimization of the decolorization of orange essential oil. *Food Science and Biochemistry*, **27(4)**, 929-938.
- Sjoblom, J. (2006). Emulsion and emulsion stability. In: *Surfactant Science Series*. 2nd Edition Pp. 185-223.
- Tadros, T. (2004). Application of rheology for assessment and prediction of the long-term physical stability of emulsions. *Advances in Colloid and Interface Science*, **108-109**, 227-258.
- Tadros, T.F. (2013). Emulsion Formation, Stability, and Rheology. In: *Emulsion Formation and Stability*. Wiley Online. Pp. 1-76.
- Tan, C. (1990). Beverage Emulsions. In: *Food Emulsions*. 2nd Edition. Eds. K. Larsson & S.E. Friberg. New York: Marcel Dekker. Pp. 445-478.
- Tortora, G.J. Berdell R., Funke, B.R. & Case, C.L. (2016). In: *Microbiology: An Introduction*, 12th Ed. Global Edition. Pearson (Intl).
- Zhang, J. (2011). Novel emulsion-based delivery systems. PhD Thesis, University of Minnesota.
- Zhao, S., Gao, W., Tian, G., Zhao, C., DiMarco-Crook, C., Fan, B., Li, C., Xiao, H., Lian, Y. & Zheng, J. (2018). Citrus oil emulsions stabilized by citrus pectin: the influence mechanism of citrus variety and acid treatment. *Journal of Agricultural and Food Chemistry*, **66(49)**, 12978-12988.

CHAPTER SEVEN

GENERAL SUMMARY, CONCLUSIONS AND RECOMMENDATIONS

7.1 General Summary and Conclusions

This thesis reported the behaviour and properties of Bambara groundnut (BGN) (*Vigna subterranea* (L.) Verdc) starch-soluble dietary fibre nanocomposite (STASOL) and its capacity to deliver active compounds in food systems. This study aimed to assess the effect of STASOL on the rheological, functional and physicochemical properties of beverage emulsion systems. The objectives of the study were to synthesise and characterise the physicochemical, nutritional and functional properties of STASOL extracted from the BGN black-eye variety as well as establish the optimum quantity of STASOL for a stable orange oil beverage emulsion. Further objectives were to characterise and model the rheological and stability properties of STASOL stabilised orange oil beverage emulsions, establish the relationship between emulsion stability and rheological properties, and investigate the effect of different storage temperatures and time on the stability and rheological properties of the emulsions.

Soluble dietary fibre and starch were extracted from the BGN black-eye variety. The study was divided into four research chapters, chapters three to six. The first objective of chapter three was to manufacture and verify STASOL from BGN-SDF and BGNS using an ascorbic acid-hydrogen peroxide redox pair. Phase behaviour studies were used to determine the optimum ratio of BGNS and BGN-SDF for a stable nanocomposite. STASOL was successfully produced and was verified as a new compound with different properties from its parent compounds. The particle size (Zetasizer), conductivity (Zeta potential), functional groups (Fourier transform infrared), crystallinity (powder X-ray diffraction), morphology (scanning electron microscopy) and thermal properties (differential scanning calorimetry and thermogravimetric analysis) were evaluated. These analyses confirmed the successful formation of a new complex from BGNS and BGN-SDF. STASOL had a mean particle size of 74.01 nm which qualified it as a nanocomposite. STASOL and BGN-SDF exhibited irregular, polygonal morphologies and were amorphous suggesting high solubility in water, while BGNS had smooth, oval morphologies and was crystalline, suggesting high insolubility in water. STASOL was thermally stable indicating that it could withstand elevated processing temperatures, such as those applied in baking, in the food industry. STASOL had superior functional properties compared to its parent compounds BGNS and BGN-SDF. The hypothesis that BGNS and BGN-SDF would be successfully complexed to form STASOL, a nanocomposite with desirable physicochemical and functional properties, was accepted.

The objective of Chapter 4 was to characterise the antioxidant, nutritional, physicochemical and functional properties of STASOL, BGNS and BGN-SDF. The pasting

properties (rapid visco analysis), colour, chemical composition (nutritional properties), hydration properties [solubility index and water holding capacity (WAC)], oil binding capacity (OBC), emulsion activity index (EAI), emulsion stability index (ESI), glucose, phenolic profile and total antioxidant properties were studied. Pasting properties measured peak, trough, breakdown and final viscosities as well as setback, pasting temperature and peak time. STASOL possessed antioxidant properties and had a low glycemic index (GI) therefore it was concluded to be desirable for health-conscious consumers. The superior physicochemical and functional properties of STASOL would make it valuable to the food industry as a potential fortifier, thickening agent, stabiliser and fat binder. Similarities in functional and antioxidant characteristics between STASOL and other commercial modified starches were observed demonstrating the suitability of STASOL as an alternative to these starches. As such, STASOL is expected to compete successfully with other modified starches and composites in the market.

The broad objective of chapter five was to study the main emulsion components (STASOL, orange oil, water) to identify the combination that would give the most stable orange oil beverage emulsion. The emulsion formulations were designed using randomised D-optimal exchange mixture design and parameters (stability and rheology) were modelled as a function of emulsion components (STASOL, orange oil and water) using empirical models, rheological models and response surface methodology. Eleven formulations of different ratios of STASOL (8-20%), orange oil (30-42%) and water (50-62%) were studied. Emulsion stability properties are important in predicting shelf life and rheological properties predict the behaviour of emulsions under processing, handling and distribution conditions. The first objective of chapter five was to investigate the effect of emulsion components on the stability of the emulsions. Emulsion stability parameters were studied using the Turbiscan MA 2000 and expressed as initial backscattering, backscattering profiles and Turbiscan stability index. The mean initial backscattering values, Turbiscan profiles representations and Turbiscan stability indexes revealed emulsions formulated with combinations of 20% STASOL and 30% orange oil as the most stable. The second objective of chapter five was to assess the effect of different ratios of STASOL (8-20%), orange oil (30-42%) and water (50-62%) on the rheological properties of eleven beverage emulsion systems. Rheological analyses investigated the time-dependent and independent parameters of the emulsions using an MCR 300 Paar physical rheometer. All STASOL stabilised emulsions were shear-thinning (pseudoplastic) and thixotropic. This is of importance in food systems as STASOL stabilised emulsions would be expected to exhibit 'short' flow and be non-slimy in the mouth to have a positive effect on their sensory properties. Combinations of higher concentrations of STASOL and lower concentrations of orange oil had higher viscosities signifying that where thickness is desired in food systems, higher concentrations of STASOL would be required. The presence of hysteresis loop areas showed the structural breakdown of

STASOL stabilised emulsions. The time-dependent behaviour of the emulsions was fitted to the first-order stress decay with a zero equilibrium stress value and Weltman models, with the former found more suitable for describing the data because of relatively higher R^2 and lower RMSE and SSE values. The data obtained from time-independent rheological studies were fitted to Power law, Casson, Bingham plastic and Herschel-Bulkley models. The Bingham plastic and the Power law models were the best and least describers, respectively, of the flow behaviour of STASOL stabilised emulsions.

The most stable combinations as determined by the stability and rheological studies were formulated with 20:30:50 (STASOL:oil:water). This may be a result of more STASOL molecules present in the system resulting in increased viscosity and the subsequently reduced oil droplet migration rate. Low oil concentration meant that few oil droplets were available hence there was a decreased chance of flocculation and/or coalescence. The hypothesis that STASOL would significantly affect the rheological and stability properties of orange oil beverage emulsions was accepted. The hypothesis that the rheological behaviour of STASOL stabilised orange oil beverage emulsions would be effectively described using rheological models was also accepted. All emulsion systems were non-Newtonian, time-dependent, thixotropic, pseudoplastic fluids that possessed yield stress.

The objective of chapter six was to investigate the effect of storage temperature and time on the stability and rheological properties of the most stable STASOL stabilised emulsion. Emulsions were stored at 5, 20 and 45°C for 20 days and analyses were carried out on days 1, 3, 9, 15 and 20. Emulsions stored at 5 and 45°C showed the most and least stability, respectively, throughout the storage period. The study of different storage times and temperatures of emulsions is important in finding the most suitable temperature that would preserve emulsion characteristics as well as allow for the prediction of the behaviour of emulsions over time. Low temperatures significantly slow down the rate of microbial and chemical storage while elevated temperatures have an opposite effect. Emulsions remained thixotropic and shear thinning at all storage temperatures over time, with emulsions stored at lower temperatures showing improved stability and exhibiting more desirable rheological properties than the ones at higher temperatures. The study of turbidity loss allows for the calculation of the rate at which emulsions will destabilise while creaming stability studies give a visual representation as well as an index of the separation of emulsion phases. Emulsions separate into the oil and aqueous phases over time due to different phenomena. It was concluded that storing STASOL stabilised emulsions in the refrigerator would increase their shelf life. The inclusion of preservatives in STASOL stabilised emulsions would further increase their shelf life. The hypothesis that STASOL stabilised orange oil beverage emulsions would have a desirable shelf life and exhibit desirable rheological properties was accepted.

STASOL is considered cost-effective as only 20% is required to stabilise an orange oil beverage emulsion compared to 30% BGN-SDF previously reported by Maphosa (2016). BGN-SDF is costly to obtain while the extraction process of BGNS is relatively cheap. Complexing these two polysaccharides to form a robust nanocomposite did not only provide a novel ingredient and emulsion stabiliser but also mitigated the limitations associated with native starch and allowed for the use of lower amounts of BGN-SDF. As such, the use of 30% STASOL was more cost-effective than the use of 30% BGN-SDF. STASOL contains 1.95:15 (BGN-SDF:BGNS), meaning a small fraction of BGN-SDF in STASOL is required to stabilise emulsions but still contribute desirable active compounds such as antioxidants.

The application of STASOL in a beverage emulsion will not only increase the utilisation and market value of BGN but will also be significant in improving the overall quality of the emulsion systems. The inclusion of starch in food increases the energy value of that system. A beverage emulsion stabilised with STASOL would find an important role in feeding programmes and subsequently in alleviating malnutrition and poverty. As such,

Several studies have looked into the application of starch, dietary fibres, proteins and flour from BGN as emulsion stabilisers and emulsifiers in food systems and reported high concentrations of the mentioned BGN components to attain desirable stability. Complexing polysaccharides from underutilised legumes with other polysaccharides or biopolymers like proteins would ensure the use of lower concentrations of polysaccharides while attaining robust complexes with desirable emulsifying and stabilising properties. As such, composites, particularly nanocomposites, can also be used as alternatives to widely utilised stabilisers.

The following conclusions can therefore be drawn from this study:

1. STASOL is a nanocomposite produced from BGNS and BGN-SDF.
2. The physicochemical, antioxidant and functional properties of STASOL are more superior and at times similar to those of BGN-SDF.
 - 2.1. In the food industry, STASOL can be used as a fortifier, thickener, stabiliser and fat binder, amongst other functions.
 - 2.2. STASOL can be used in high temperature food processes.
 - 2.3. STASOL possesses antioxidant properties and has a low glycemic index therefore it is desirable for health-conscious consumers.
3. The rheological and stability properties of STASOL stabilised beverage emulsions is dependent on STASOL, water and oil concentrations.
4. STASOL can stabilise both concentrated and diluted orange oil beverage emulsions.
5. STASOL stabilised emulsions are stable to creaming and destabilise mainly by flocculation and/or coalescence.
6. STASOL is a cost-effective, natural emulsion stabiliser that will be invaluable as an alternative to synthetic stabilisers and other commonly used starches.

7. STASOL stabilised emulsions should be stored at refrigeration temperature (5°C).

7.2 Future Studies and Recommendations

Future studies could look into the application of different polysaccharide-polysaccharide and polysaccharide-protein complexes as delivery vehicles for nutrients and bioactive compounds in food products. Research is also required to determine the application and behaviour of STASOL in different food systems such as frozen, baked and meat products. Research into the nanoencapsulation of therapeutic metabolites using biopolymers as encapsulating agents should also be considered. Studies would then look into the physical, chemical, rheological, functional and nutritional properties of these complexes as well as their interaction with various emulsion media. Furthermore, biopolymers from other underutilised, orphan and climate smart crops such as pigeon pea, yam bean, morama bean and grass pea need to be studied. Lesser crops thrive in adverse weather conditions and are nutritionally rich, making them suitable alternatives, in the face of global climate changes.

7.3 Research Outputs

Outputs from this study include the following:

1. **Maphosa, Y.**, Jideani, V. A. & Ikhu-Omoregbe, D.I. (2021). Functional properties of starch-soluble dietary fibre nanocomposite. South African Association for Food Science and Technology. 24th Biennial International Virtual Congress. 20-22 September 2021. (Poster presentation).
2. Jideani, V. A., **Maphosa, Y.**, Ikhu-Omoregbe, D.I. & Gulu, N.B. (2021). Bambara groundnut starch and soluble dietary fibre (STASOL). *Patent* (Pending).
3. **Maphosa, Y.** & Jideani, V. A. (2019). Phase behaviour of Bambara Groundnut starch-soluble dietary fibre nanocomposite. 13th International Congress on Engineering and Food (ICEF13), Melbourne, Australia, 23-26 September 2019. (Paper presentation).
4. **Maphosa, Y.** & Jideani, V. A. (2018). Factors Affecting the Stability of Emulsions Stabilised by Biopolymers, Chapter 5 in Science and Technology Behind Nanoemulsions. (Editor: Selcan Karakuş). DOI: 10.5772/intechopen.75308.
5. **Maphosa, Y.** & Jideani, V.A. (2017). The Role of Legumes in Human Nutrition. In: *Functional Food - Improve Health through Adequate Food*. Edited by Maria Chavarri Hueda. DOI: 10.5772/intechopen.69127
6. **Maphosa, Y.** & Jideani, V. A. (2021). *Vigna Subterranea* [L.] Verdc Starch -Soluble Dietary Fibre Nanocomposite: Thermal Behaviour, Morphology and Crystallinity. *Processes*. (Submitted for publication).

References

Maphosa, Y. (2016). Characterisation of Bambara groundnut (*Vigna Subterranea* (L) Verdc.) non-starch polysaccharides from wet milling as prebiotics. Master of Technology Thesis, Cape Peninsula University of Technology.